

**A phage display study of interacting peptide
binding partners of malarial
S-Adenosylmethionine
decarboxylase/Ornithine decarboxylase**

by

**Jandeli Niemand
21001953**

**Submitted in partial fulfillment of the requirements for the degree MSc.
Biochemistry in the Faculty of Natural and Agricultural Science**

**University of Pretoria
Pretoria**

June 2007

Acknowledgements

- ❖ Prof A. I. Louw, my supervisor for teaching me how to think outside of the box.
- ❖ Dr Lyn-Marie Birkholtz, my co-supervisor, for her innovative ideas, encouragement and leadership
- ❖ The NRF for the Scarce skills bursary that enabled me to pursue post-graduate studies
- ❖ Dr Christine Maritz-Olivier, Katherine Clark and Gordon Wells for many helpful discussions
- ❖ My fellow postgraduate students for their support and encouragement.
- ❖ My family and friends. Thank you for believing in me.
- ❖ God, for giving me the strength and wisdom to see this through. All glory be unto You.

Contents

I. List of Figures	iv
II. List of Tables	vii
III. List of Abbreviations.....	viii
Chapter 1: Literature review	1
1.1 Pathogenesis of malaria	1
1.2 The burden of malaria.....	5
1.3 Malaria control.....	7
1.3.1 Vaccine development.....	7
1.3.2 Anti-malarial therapy	9
1.3.3 Vector control	13
1.4 Protein interactions	14
1.4.1 Nature of protein-protein interactions.....	15
1.4.2 Protein-protein interactions as drug targets	15
1.5 Polyamine metabolism	20
1.5.1 Polyamine metabolism in humans	21
1.5.2 Polyamine metabolism in <i>P. falciparum</i>	23
1.5.3 Polyamine metabolism as an anti-malarial target.....	24
1.6 Research aims	27
Chapter 2: Optimisation of the heterologous expression and isolation of PfAdoMetDC/ODC	28
2.1 Introduction	28
2.1.1 S-Adenosylmethionine decarboxylase/Ornithine decarboxylase.....	28
2.2 Materials and methods.....	32
2.2.1 Isolation and cloning of <i>PfAdoMetDC/ODC</i> (PlasmoDB accession number Pf10_0322).....	32
2.2.2 Plasmid isolation	32
2.2.3 Quantification of nucleic acids: (Sambrook et al., 1989).....	33
2.2.4 Preparation of Heat-shock competent cells (Hanahan et al., 1991).....	33
2.2.5 Transformation of cells using heat shock method	34
2.2.6 Subcloning of <i>PfAdoMetDC/ODC</i> into pASK-IBA43+	34
2.2.7 Agarose gel electrophoresis of PCR products.....	35

2.2.8	Purification of PCR products.....	35
2.2.9	Cloning protocols	35
2.2.10	Subcloning of <i>PfAdoMetDC/ODC</i> into pASK-IBA43+	37
2.2.11	Recombinant protein expression and isolation of <i>PfAdoMetDC/ODC</i>	39
2.2.12	Protein concentration determination (Bradford, 1976)	41
2.2.13	Electrophoretic analysis	42
2.2.14	Western Blotting	43
2.2.15	Enzyme activity assays of <i>AdoMetDC</i> and <i>ODC</i>	44
2.2.16	Sized exclusion-based purification of recombinantly expressed <i>PfAdoMetDC/ODC</i>	45
2.2.17	Mass-Spectrometry Analysis of contaminating bands	45
2.3	Results.....	46
2.3.1	Recombinant expression and isolation of <i>PfAdoMetDC/ODC</i>	46
2.3.2	Determination of the origin of the contaminating fragments.....	46
2.3.3	Optimization of recombinant expression and isolation of <i>PfAdoMetDC/ODC</i>	48
2.3.4	Tandem affinity purification (TAP)	48
2.3.5	Comparison of the subcloned <i>PfAdoMetDC/ODC</i> to the original construct and tandem affinity purification (TAP).....	51
2.3.6	Explanatory investigations	56
2.3.7	Purification of <i>PfAdoMetDC/ODC</i> from <i>E. coli</i> heat shock proteins.....	60
2.4	Discussion	62

Chapter 3: Identification of peptide binding partners to <i>PfAdoMetDC/ODC</i> through the use of a <i>P. falciparum</i> phage display library.....		71
3.1	Introduction	71
3.1.1	Identification of protein-protein interactions.....	71
3.1.2	Phage display.....	72
3.1.3	Phage display for the study of protein-protein interactions.....	76
3.1.4	Phage display in the fight against malaria	78
3.2	Materials and methods	80
3.2.1	<i>P. falciparum</i> cDNA phage display library	80
3.2.2	Titer determination via plaque assay	80
3.2.3	Biopanning of <i>P. falciparum</i> cDNA phage display library against recombinant <i>PfAdoMetDC/ODC</i>	81
3.2.4	Screening of <i>P. falciparum</i> cDNA inserts	83
3.2.5	Sequence analysis	86

3.2.6	Verification of binding partners to PfAdoMetDC/ODC	87
3.3	Results.....	90
3.3.1	Biopanning of <i>P. falciparum</i> cDNA phage display library against recombinant PfAdoMetDC/ODC to create Library A	90
3.3.2	Screening of <i>P. falciparum</i> cDNA inserts by PCR amplification and gel electrophoresis of Library A.....	92
3.3.3	Identification of <i>P. falciparum</i> cDNA inserts with nucleic sequencing.....	92
3.3.4	Verification of size distribution of original phage starting library used for biopanning against PfAdoMetDC/ODC.....	94
3.3.5	Modification of the biopanning procedure for the identification of T7 phage particles containing <i>P. falciparum</i> cDNA inserts that encodes for peptides with affinity to PfAdoMetDC/ODC.....	95
3.3.6	Screening of insert cDNA by PCR amplification and gel electrophoresis of Libraries B,C,D,E and F following round 3 of biopanning	98
3.3.7	Sequencing of cDNA inserts	100
3.3.8	Verification of the specific interaction between the isolated phage clones and PfAdoMetDC/ODC.....	104
3.4	Discussion	106
 Chapter 4: Concluding discussion		113
Summary		122
References		124
Appendix A		A
Appendix B: Screened phage clones		A

I. List of figures

Figure 1.1: The life cycle of the <i>Plasmodium</i> parasite (Young and Winzeler, 2005). Details in text.	2
Figure 1.2: Effects of malaria infection (Breman et al., 2004).....	3
Figure 1.3: Sequestration of parasitised erythrocytes via PfEMP1 (Miller et al., 2002).	4
Figure 1.4: Global spread of malaria according to the World Malaria Report 2005 from the WHO (http://www.rbm.who.int).	6
Figure 1.5: Malarial protein targets under vaccine development (Greenwood et al., 2005).	8
Figure 1.6: Chemical structures of some of the major antimalarial agents (Ridley, 2002).	10
Figure 1.7: Current and possible drug targets for anti-malarial therapy (Ridley, 2002).....	12
Figure 1.8: Traditional versus functional genomic view of protein function. Adapted from (Eisenberg et al., 2000).	14
Figure 1.9: The role of proteomics in the identification of proteins involved in a specific metabolic pathway or disease process.	16
Figure 1.10: Schematic representation of a bifunctional blocker (Way, 2000).....	18
Figure 1.11: The structures of putrescine, spermidine and spermine (Seiler et al., 1996).	20
Figure 1.12: Polyamine metabolism in humans (Wallace et al., 2003).	21
Figure 1.13: Schematic representation of polyamine metabolism in <i>P. falciparum</i> . Created from (Casero and Woster, 2001; Haider et al., 2005; Molitor et al., 2004; Müller et al., 2001; Schramm et al., 1996).....	24
Figure 2.1: Schematic organization of the various domains and parasite-specific inserts of the bifunctional PfAdoMetDC/ODC. Adapted from (Birkholtz, 2002).	28
Figure 2.2: Model of A: the homodimeric form of PfAdoMetDC and B: the dimeric form of PfODC, as viewed from beneath (Birkholtz et al., 2003; Wells et al., 2006).	29
Figure 2.3: Schematic representation of the various parasite-specific inserts of PfAdoMetDC/ODC.	30
Figure 2.4: A: SDS-PAGE analysis of recombinantly expressed PfAdoMetDC/ODC with C-terminal <i>Strep</i> -tag; B: Calibration curve of Rf values.....	46
Figure 2.5: A: SDS-PAGE analysis of recombinantly expressed and affinity purified pASK-IBA3 and PfAdoMetDC/ODC; B: Western blot of recombinantly expressed and affinity purified pASK-IBA3 and PfAdoMetDC/ODC.	47
Figure 2.6: SPS-PAGE analysis of affinity purified PfAdoMetDC/ODC after blocking of <i>Strep</i> -tactin Sepharose.....	48
Figure 2.7: A: Optimisation of amount of template for amplification of <i>PfAdoMetDC/ODC</i> ; B: large-scale amplification of <i>PfAdoMetDC/ODC</i>	49

Figure 2.8: A: Fragments obtained after cutting <i>PfAdoMetDC/ODC</i> cloned into pGem [®] -T Easy with <i>Eco</i> RI. B: Screening for positive clones after ligating <i>PfAdoMetDC/ODC</i> into pGem [®] -T Easy.....	50
Figure 2.9: Gel electrophoresis of colony screening PCR of <i>PfAdoMetDC/ODC</i> cloned into pASK-IBA43+.....	50
Figure 2.10: A: Vector map indicating the fragments obtained after digesting <i>PfAdoMetDC/ODC</i> cloned into pASK-IBA43+ with <i>Hind</i> III. B: Restriction enzyme digestion screening for positive clones after ligating <i>PfAdoMetDC/ODC</i> into pASK-IBA 43+.....	51
Figure 2.11: Comparison of expression and isolation of <i>PfAdoMetDC/ODC</i> from pASK-IBA3 and pASK-IBA43+ using affinity purification and TAP.....	52
Figure 2.12: Activity assay of A: AdoMetDC and B: ODC activity.....	52
Figure 2.13: SDS-PAGE analysis of samples obtained following ultracentrifugation.	53
Figure 2.14: Size-exclusion HPLC of the recombinant <i>PfAdoMetDC/ODC</i> purified with affinity chromatography.	54
Figure 2.15: SDS-PAGE of fractions collected with SEC-HPLC of affinity-purified <i>PfAdoMetDC/ODC</i>	55
Figure 2.16: Native-PAGE of <i>PfAdoMetDC/ODC</i>	55
Figure 2.17: Effect of protease inhibitor cocktail on degradation of <i>PfAdoMetDC/ODC</i>	56
Figure 2.18: Western blot using A: anti- <i>Strep</i> -Tag II and B: anti-His-tag antibodies.	57
Figure 2.19: Preparative SDS-PAGE for MS analysis.....	58
Figure 2.20: MS results and analysis. A: Matched peptides for the ~112 kDa fragment after comparison with <i>PfAdoMetDC/ODC</i> (peptides indicated in red). B: Sequence analysis of <i>PfAdoMetDC/ODC</i> showing possible internal Shine Dalgarno and internal AUG codons as well as the number of base-pairs located in-between.....	59
Figure 2.21: Effect of the addition of ATP on the purification of recombinant <i>PfAdoMetDC/ODC</i>	60
Figure 2.22: Western blot using A: anti- <i>Strep</i> -tag II antibody and B: anti-DnaK antibody on <i>PfAdoMetDC/ODC</i> isolated in the absence and presence of ATP.....	61
Figure 2.23: Schematic representation of ribosomal slippage on mRNA secondary structures, leading to various sized fragments. (With the help of Jaco de Ridder).....	66
Figure 2.24: The GroEL/GroES chaperone cycle of <i>E. coli</i> . Adapted from (Walter and Buchner, 2002).	68
Figure 2.25: DnaK/DnaJ/GrpE chaperone system in <i>E. coli</i> . Adapted from (Walter and Buchner, 2002).	69
Figure 3.1: Different types of phage libraries. Adapted from (Willats, 2002).....	73

Figure 3.2: Genetic map and structural elements of T7. Adapted from (Rosenberg et al., 1996).	74
Figure 3.3: Identification of protein ligands by the phage display cycle (Willats, 2002).	76
Figure 3.4: The concept of convergent evolution, where affinity peptides may have sequence similarity to the natural binding partners of a protein. Adapted from (Willats, 2002).	77
Figure 3.5: Example of typical results following titer of phage sample.....	90
Figure 3.6: A: SDS-PAGE and B: dot blot Western analysis of recombinant PfAdoMetDC/ODC used as bait in biopanning.	91
Figure 3.7: A: Representative sample of PCR amplification and subsequent gel electrophoretic analysis of <i>P. falciparum</i> cDNA inserts, B: Representative example of restriction mapping of cDNA inserts using <i>Hind</i> III.....	92
Figure 3.8: Large-scale amplification of cDNA inserts for sequencing	93
Figure 3.9: Representative samples of screening for positive clones with A: colony screening PCR and B: Restriction enzyme digestion.	93
Figure 3.10: Representative sample of screening of <i>P. falciparum</i> cDNA inserts of Library A, Biopanning 3 with PCR amplification and gel electrophoresis.	94
Figure 3.11: Size distribution of cDNA inserts in the starting library.	95
Figure 3.12: SDS-PAGE analysis of the expression of recombinant PfAdoMetDC/ODC used as bait in biopanning.	96
Figure 3.13: Investigation of the size distribution of the <i>P. falciparum</i> cDNA inserts of the various libraries, following the first and second round of biopanning.....	97
Figure 3.14: Representative sample of the PCR amplification and gel electrophoresis analysis of the various libraries following the third round of biopanning, prior to sequencing	98
Figure 3.15: Example of restriction enzyme digestions of similarly sized <i>P. falciparum</i> cDNA inserts to differentiate between different clones.	99
Figure 3.16: Possible consensus sequences in the identified peptides with affinity to PfAdoMetDC/ODC, identified by the MEME Motif discovery tool.	104
Figure 3.17: Verification of the recombinant expression of PfAdoMetDC/ODC and <i>E. coli</i> DnaK for verification experiments.	105
Figure 3.18: ELISA results using PfAdoMetDC/ODC and <i>E. coli</i> DnaK as bait.	105
Figure 3.19: Possible sites of phage binding. Adapted from (Howell et al., 2006).	111
Figure I.1: T7Select 10-3b cloning region (Novagen, USA).....	A

II. List of Tables

Table 1.1: Limitations of currently used anti-malarial drugs.	9
Table 2.1: Sequence and T _m of sequencing primers used for the sequencing of <i>PfAdoMetDC/ODC</i> (Birkholtz, 2002; Roux, 2006).	39
Table 2.2: Characteristics of the primers designed for subcloning of <i>PfAdoMetDC/ODC</i> into pASK-IBA43+	49
Table 3.1: Description and methodology of different libraries created by biopanning with affinity to <i>PfAdoMetDC/ODC</i>	82
Table 3.2: Sequences and T _m of primers used for the sequencing of the cDNA inserts from phages with affinity to <i>PfAdoMetDC/ODC</i>	86
Table 3.3: Phage titers obtained following each round of biopanning (BP) of Library A.	90
Table 3.4: Phage titers obtained following each round of biopanning (BP) for the different libraries (Library B-F).	96
Table 3.5: Number of phage plaques screened from each library and the number of phage cDNA inserts suitable for further screening (See appendix B).	99
Table 3.6: Identity of cDNA inserts in the various phage clones.	101
Table 3.7: Analysis of the physical characteristics of the various peptides identified through phage display with affinity to <i>PfAdoMetDC/ODC</i>	103
Table 4.1: Comparison between the rate-limiting enzymes of human and <i>Plasmodium</i> polyamine biosynthesis.	114
Table II.1: The various screened phage clones of the different libraries.	A

III. List of abbreviations

AHT	anhydrotetracycline
AMA1	Apical membrane antigen 1
AZ	Antizyme
BP	Biopanning
BSA	Bovine serum albumin
CR1	complement receptor 1
CSA	chondroitin sulphate A
CSP	circumsporozoite protein
DDT	dichlorodiphenyltrichloroethane
EBA	erythrocyte-binding antigen
EBL-1	Erythrocyte binding ligand 1
ELAM-1	endothelial/leukocyte adhesion molecule 1
EPM	Erythrocyte plasma membrane
EXP	exported antigen
FRET	fluorescence resonance energy transfer
GDP	Gross domestic product
GLURP	glutamine-rich protein
GO	Gene Ontology
GPI	glycosylphosphatidylinositol
Ha	hyaluronic acid
HRP	Horseradish peroxidase
HS-like GAGs	heparin sulphate-like glycosaminoglycans
ICAM-1	intercellular adhesion molecule 1
IL-1	Interleukin 1
IMAC	Immobilized Metal Affinity Chromatography
iNOS	inducible nitric oxide synthase
LB-Broth	Luria-Bertani liquid medium
LSA	liver stage antigen
ME	multiple-epitope string based on T-cell and B-cell epitopes of pre-erythrocytic stage antigens
MMV	Medicines for Malaria Venture
MS	Mass spectrometry
MSP	Merozoite surface protein
MVI	Malaria Vaccine Initiative
NO	Nitric oxide
ODC	Ornithine decarboxylase
Pam	pregnancy-associated malaria
PCA	Protein fragment complementation assay
PECAM	platelet endothelial cell adhesion molecule 1
<i>Pf</i>	<i>Plasmodium falciparum</i>
PfAdoMetDC/ODC	<i>Plasmodium falciparum</i> S-adenosylmethionine decarboxylase/ornithine decarboxylase
<i>pfCRT</i>	<i>P. falciparum</i> chloroquine-resistance transporter
PfEMP1	<i>P. falciparum</i> erythrocyte membrane protein-1
<i>pfmdr1</i>	<i>P. falciparum</i> multidrug resistance 1 transporter
Pfs 230 and Pfs 48/45	surface antigens of <i>P. falciparum</i> gametocytes
Pfs 25/Pfs 28 and Pvs 25/Pvs 28	surface antigens of ookinetes of <i>P. falciparum</i> and <i>P. vivax</i>
PfSpdSyn	<i>P. falciparum</i> spermidine synthase
pfu	Plaque forming units
PPM	Parasite plasma membrane

P-sel	P-selectin
PTM	Post translational modification
PTMs	Post translational modifications
PVM	Parasitophorous vacuolar membrane
RESA	ring-infected erythrocyte surface antigen
SAMI	South African malaria Initiative
SAP	Shrimp Alkaline Phosphatase
TAP	Tandem affinity purification
TBS	Tris buffered saline
TEMED	N,N,N',N'-Tetramethyl ethylenediamine
TNF	Tumour necrosis factor
TRAP	thrombospondin-related adhesion protein
TSP	thrombospondin
UNICEF	United Nations Children's fund
VCAM-1	vascular adhesion molecule 1
WHO	World Health Organization

Chapter 1: Literature review

'The time has come to close the book on infectious diseases'

This is what the then U.S. Surgeon General, W.H. Steward, told the United States Congress in 1967. Unfortunately, this statement has proven to be overly optimistic, especially in view of the failure of the 1950s mosquito eradication campaign in third world countries by the World Health Organization (WHO). Due to the lack of an effective vaccine and escalating drug resistance, malaria is currently a greater crisis than in any previous era (Kooij et al., 2006). It has been suggested that malaria has caused more fatalities than all the plagues and wars of human history combined (<http://www.botgard.ucla.edu/html>). Malaria has been known to man since the dawn of time and is thought to have come into existence during the early Holocene or late Pleistocene periods (Joy et al., 2003; Su et al., 2003). It evolved with our primate ancestors into the modern form, and has been spread with human migrations. The blood borne parasites were first identified in 1880 by Alphonse Laveran, and Ronald Ross identified the mosquito vector in 1897. Henry Shortt and Cyril Garnham identified the hepatic stages in 1947 (Cox, 2002).

1.1 Pathogenesis of malaria

Malaria is caused by infection with unicellular, eukaryotic protozoan parasites of the genus *Plasmodium*. There are four different *Plasmodium* species that can infect humans, namely *Plasmodium falciparum*, which causes the most deaths, as well as *P. malariae*, *P. vivax* and *P. ovale* (Kirk, 2001).

The lifecycle of the *P. falciparum* parasite consists of a sexual stage inside the female members of the *Anopheline* species and an asexual stage inside the human host (Fig 1.1). When the mosquito takes a blood meal, sporozoites are injected subcutaneously with the saliva (Fig 1.1 a), from where they move to the liver through the bloodstream. Inside the liver, the sporozoites infect the hepatocytes and develop into schizonts (Fig 1.1 b). Each schizont develops into thousands of merozoites that are released into the blood, which then proceed to infect the erythrocytes of the host (Fig 1.1 c). It is within the erythrocyte that the subsequent asexual replication through various stages (ring (Fig 1.1 d), trophozoite (Fig 1.1 e) and schizont (Fig 1.1 f)), takes place. The mature schizonts can then release merozoites that will proceed to infect healthy erythrocytes (Fig 1.1 g). A few of the parasites do not undergo asexual replication, but develop into male and female gametocytes (Fig 1.1 h). After these gametocytes have infected a

mosquito taking a blood meal, they develop into gametes in the midgut (Fig 1.1 i), a process dependent on host Gametocyte Activating Factors (GAF). A diploid zygote (Fig 1.1 j) is produced after fertilisation. The zygote develops into a motile ookinete (Fig 1.1 k) that travels to the mosquito body cavity (haemocoel), where it forms the oocyst (Fig 1.1 l). This in turn gives rise to thousands of motile sporozoites (Fig 1.1 m) that migrate to the salivary glands via the haemolymph (Fig 1.1 n) (Frevert, 2004; Ghosh et al., 2002; Khan and Waters, 2004; Miller et al., 2002).

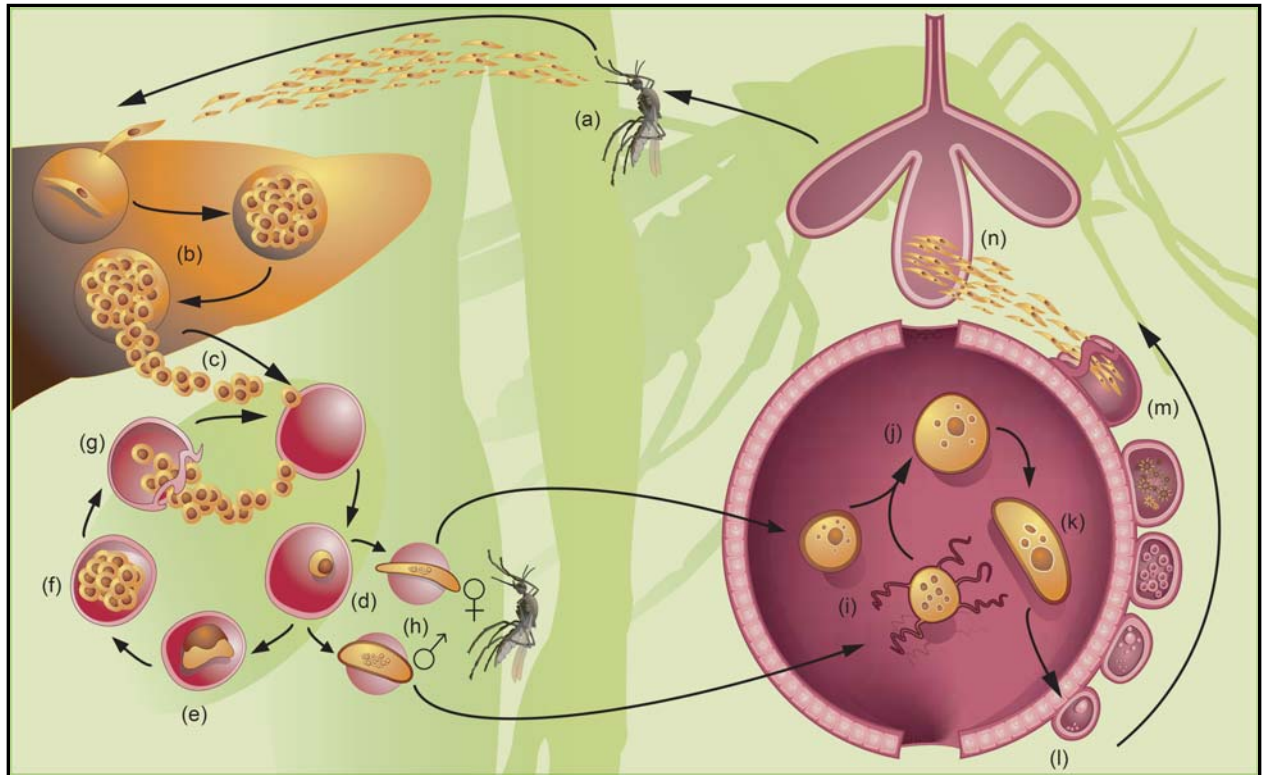


Figure 1.1: The life cycle of the *Plasmodium* parasite (Young and Winzeler, 2005). Details in text.

Malaria infection can lead to mortality, severe malaria, clinical malaria, or asymptomatic parasitemia, as well as several pregnancy-associated effects, as summarised in Fig 1.2 (Bremar, 2001). Severe malaria can be defined by the occurrence of parasites in the blood plus at least one of several clinical features such as coagulopathies, multi-organ failure, circulatory collapse, acidosis, hypoglycaemia, anaemia and neurological impairment. It is caused by the destruction and sequestration of infected erythrocytes, leading to decreased or loss of local blood flow. This can have a multitude of effects such as anaemia, acidosis and organ damage, as well as the stimulation of host cytokine release by parasite compounds like glycosylphosphatidylinositol (GPI). Several different factors can cause malarial associated anaemia, such as the destruction of infected red blood cells during schizogony, the destruction of uninfected red blood cells by the immune system and dyserythropoiesis due to cytokine imbalances. Metabolic acidosis,

usually lactic acidosis, which may lead to respiratory distress, can be caused by increased parasitic lactic acid production, decreased liver clearance in infected individuals or reduced oxygen delivery to tissues (Greenwood et al., 2005; Heddini, 2002; Miller et al., 2002). Severe malarial infection can also lead to long term neurocognitive sequelae such as visual, aural, language and cognitive impairment, epilepsy, learning difficulties and severe motor deficits (Breman et al., 2004).

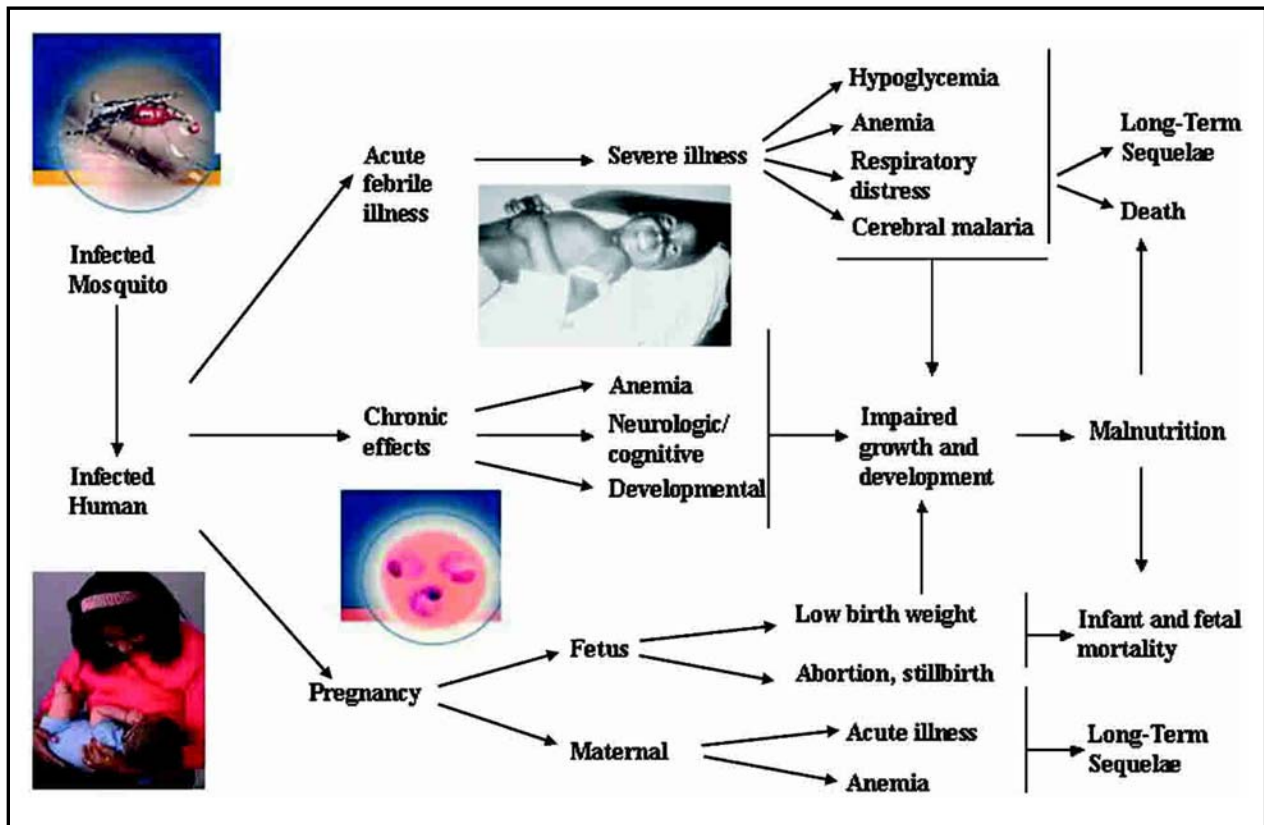


Figure 1.2: Effects of malaria infection (Breman et al., 2004).

Parasitised red blood cells can also adhere to the vascular endothelium of various organs, including the placenta and brain, due to the interaction between various host-receptors and parasite proteins expressed on the surface of an infected red blood cell. This process of sequestration protects the parasite from clearance in the spleen via the immune system and is a key virulence factor in cerebral malaria. Sequestration can lead to organ dysfunction, as well as reduced blood flow and oxygen provision, which may cause acidosis, hypoxia and inflammatory responses, which is mediated by cytokines. The interaction between the vascular endothelium and the infected red cells are localised at knob-like, electron dense structures, which is dependent on the expression of various parasite proteins. These include the knob-associated histidine-rich protein (KAHRP) that is found on the cytoplasmic side of the red cell plasma membrane as well as *P. falciparum* erythrocyte membrane protein-1 (PfEMP1), encoded by the *var* gene family, that also play a role in antigenic variation. PfEMP1 has a highly conserved C-

terminal domain located in the cytoplasm of the host erythrocyte and a vastly variable N-terminal ectodomain that mediates the adhesion of the infected erythrocyte to various endothelial cell receptors such as CD36, intercellular adhesion molecule 1 (ICAM-1) and chondroitin sulphate A (CSA). With chronic malaria infection, every consecutive incidence of parasitaemia express a different variant of PfEMP1, thereby circumventing the antibodies produced against the previous wave of parasites (Fig 1.3) (Heddini, 2002; Miller et al., 2002; Oh et al., 2000; Richie and Saul, 2002; Waller et al., 1999).

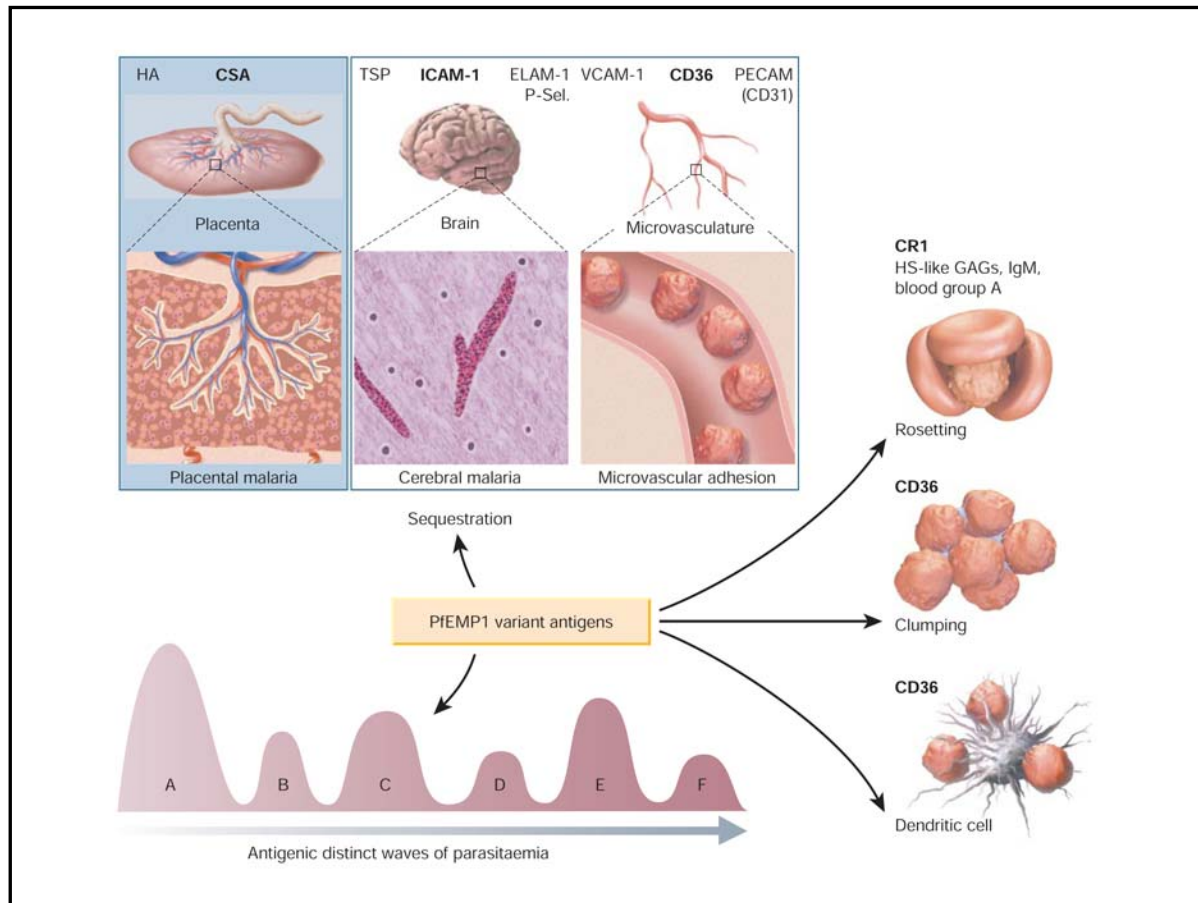


Figure 1.3: Sequestration of parasitised erythrocytes via PfEMP1 (Miller et al., 2002).

Ha: hyaluronic acid; CSA: chondroitin sulphate A; TSP: thrombospondin; ICAM-1: intercellular adhesion molecule 1; ELAM-1: endothelial/leukocyte adhesion molecule 1; VCAM-1: vascular adhesion molecule 1; PECAM: platelet endothelial cell adhesion molecule 1 P-sel: P-selectin; CR1: complement receptor 1; HS-like GAGs: heparin sulphate-like glycosaminoglycans.

Due to the adhesive properties of infected red blood cells, they can also bind to uninfected erythrocytes (rosetting), which may aid in the infection of new red blood cells following schizogony. Alternatively, it has been suggested that this phenomenon shields the parasites from the immune system. Infected erythrocytes can also adhere to one another (clumping) or to cells of the immune system (Fig 1.3) (Heddini, 2002; Miller et al., 2002). During pregnancy, parasites expressing a specific form of PfEMP1 also adhere to CSA in the placenta. Although this prevents the foetus from becoming infected, it also leads to low birth weight, premature delivery and mortality, as well as maternal anaemia. Malaria during pregnancy could be responsible for

50% of the mortality and morbidity of African children under the age of 5, due to low birth weight and anaemia (Breman, 2001; Miller et al., 2002).

Nitric oxide (NO) has been associated with malaria pathogenesis, but its precise role remains unclear. On the one hand, the release of host cytokines (such as Tumour necrosis factor (TNF), Interleukin 1 (IL-1) and lymphotoxin), which is mediated by the release of malarial GPI and sequestration, leads to the production of NO due to the induction of inducible nitric oxide synthase (iNOS). This may lead to the depletion of cellular energy due to the production of peroxynitrite that damages DNA. The subsequent need for NAD⁺ and ATP can inhibit aerobic respiration, thus leading to host acidosis. On the other hand, it has been shown that NO down-regulates the production of TNF and IL-1 and prevents the adhesion of infected erythrocytes to the microvasculature. As such, NO may be involved in host defence mechanisms (Clark et al., 2004; Sobelowski et al., 2005).

P. falciparum is the most virulent of the malarial species that infects humans, due to the additional manifestations that may lead to cerebral malaria. This is mediated by the cytoadherence of infected red blood cells to endothelial cells, caused by interactions of PfEMP1. While both *P. falciparum* and *P. vivax* may cause anaemia, only the former cause metabolic acidosis with the accompanying respiratory distress, hypoglycaemia and cerebral malaria. *P. vivax* and *P. ovale* causes recrudescence and renal complications are common during infections with *P. malariae* (Breman, 2001; Greenwood et al., 2005; Miller et al., 2002).

1.2 The burden of malaria

Every year, more than 300 million severe cases of malaria infection occurs worldwide, which results in more than a million deaths. In Africa, these deaths occur mostly among children, and according to the WHO there is a malaria-induced death of a child every 30 seconds (<http://www.rbm.who.int>). These figures are however based on passive national reporting. Snow and colleagues have suggested that the actual number of clinical episodes of malaria may be as much as 50% higher (Snow et al., 2005). Disability adjusted life years (DALYs), which is a cumulative measurement of disability, morbidity and mortality, show that Africa carries more than 90% of the malaria induced burden, whilst South-East Asia shoulders approximately 9% of the burden (Fig 1.4). Some figures show that, while Africa experiences the most deaths from malaria, the Asian malaria-induced morbidity has been vastly underestimated (Greenwood et al., 2005). It is estimated that malaria-induced mortality accounts for more than 2% of the global DALYs (Breman et al., 2004).

Unfortunately, the impact of malaria is not limited to the number of fatalities per year. Malarial infections, especially cerebral malaria, have also been implicated in impaired development. Due to reduced work attendance and productivity as well as healthcare costs, the economic burden of malaria on an endemic country is immense (Greenwood et al., 2005). Countries where malaria is endemic have lower economic growth rates and more than a five-fold difference in per-capita gross domestic product (GDP) in comparison to non-endemic areas. These economic burdens are not solely due to the cost of healthcare and lost income due to illness, but also due to the impact of malaria on tourism, foreign investment and trade (Sachs and Malaney, 2002).

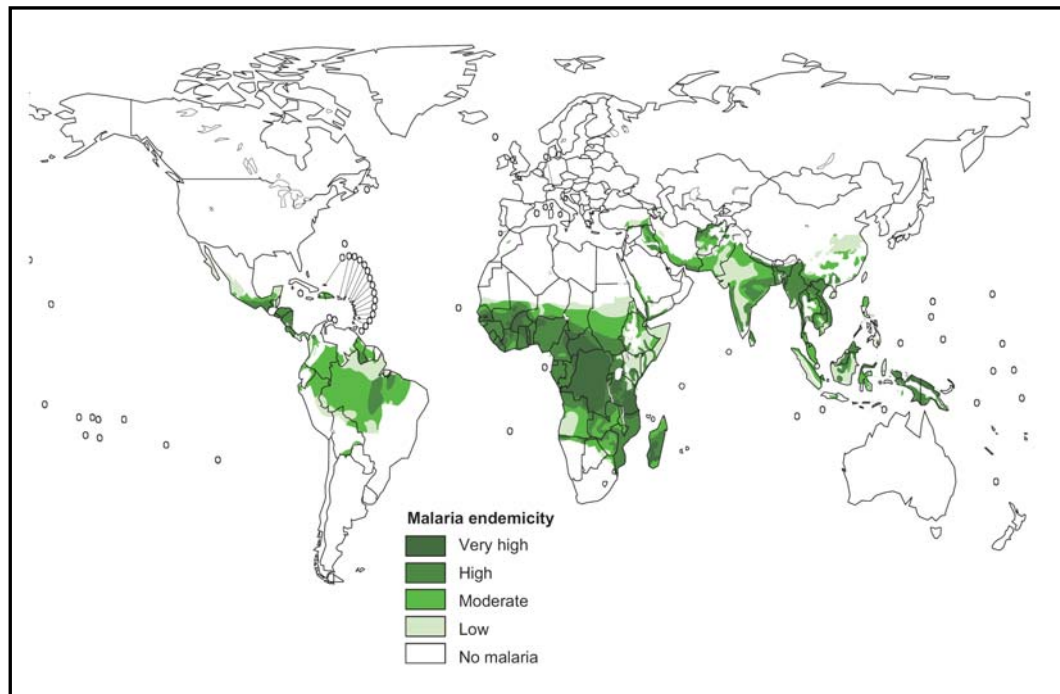


Figure 1.4: Global spread of malaria according to the World Malaria Report 2005 from the WHO (<http://www.rbm.who.int>).

There are both intrinsic and extrinsic determinants for the burden of malaria on a country. Intrinsic factors include: genetic susceptibility for example the Duffy blood factor, which is necessary for infection with *P. vivax*, the sickle cell trait that restricts parasite reproduction within affected red blood cells, and immune status such as maternally-derived protection in children. The species of *Plasmodium* prevalent in a specific area and the spread and insecticide resistance of the various *Anopheline* vectors are all also intrinsic factors that determine the impact that malaria has on a community in a certain area. Among extrinsic determinants, the environment plays a large role, since wet, tropical areas are conducive to mosquito breeding. Economic, social and educational factors also have an impact on the ability of a country to deal with malarial infections. The political stability of regions can also influence the spread of malaria, since there is often a high occurrence of tropical diseases caused by the high numbers of people and inadequate healthcare in refugee camps (Bremner, 2001).

Between 1975 and 1997, 1223 new chemical entities were commercialised for therapeutic applications, of which less than 0.4 % were for the treatment of malaria. These 4 drugs are Artemether IM, Atavaquone/proguanil, Halofantrine hydrochloride and Mefloquine (Pécoul et al., 1999). The abandonment of tropical diseases by the pharmaceutical companies underscores the need for academic research to find a solution to this devastating disease. All, however is not lost. The last couple of years have seen an upsurge in strategic, political and financial support for fighting the scourge of malaria. These include several public-private partnerships such as the Gates Malaria Partnership, the Malaria Vaccine Initiative (MVI), Medicines for Malaria Venture (MMV) and the South African Malaria Initiative (SAMI). Increased funding has also been received from institutions such as the Wellcome Trust, the Bill and Melinda Gates foundation and the United Nations Children's fund (UNICEF) (Breman et al., 2004). This increase in public awareness of the burden of malaria brings the goal of global malaria eradication almost within reach.

1.3 Malaria control

Various strategies have been and are currently employed in an effort to control this devastating disease. These include vaccine development, drug treatment and vector control as discussed in the following sections.

1.3.1 Vaccine development

Due to the complicated lifecycle of the malaria parasite, three different strategies for vaccine development have evolved, namely pre-erythrocytic stage vaccines, blood stage vaccines and transmission blocking vaccines (Fig 1.5). The pre-erythrocytic stage vaccines are directed against schizont-infected liver cells or sporozoites, thus preventing merozoite release and infection. Examples of this type of vaccine include RTS,S/AS02A, which is a chimera based on the circumsporozoite protein of *P. falciparum* and a hepatitis-B surface antigen, and portions of thrombospondin-related adhesion protein (TRAP) encoded by a modified vaccinia virus. While the RTS,S/AS02A vaccine did reduce severe disease and clinical malaria in the vaccinees, the immunity obtained was transient (Greenwood et al., 2005). Preliminary Phase IIb trials of the vaccine based on TRAP were disappointing, but this vaccine is still under investigation. However, it has to be noted that a pre-erythrocytic stage vaccine has to be 100% effective, since the survival of even one sporozoite can lead to thousands of merozoites. For this reason, it has been suggested that this type of vaccine has to be used in conjunction with a blood stage vaccine. Blood stage vaccines aspire to reduce or eradicate the blood-borne forms of the parasite, thus reducing the severity of infection (Greenwood et al., 2005; Matuschewski, 2006). A major focus of this work is on the parasite proteins involved in the invasion of red blood cells by merozoites,

namely merozoite surface protein (MSP) MSP1, MSP2, MSP3 and apical membrane antigen 1 (AMA-1) as well as other rhoptry proteins (Breman et al., 2004; Greenwood et al., 2005; Matuschewski, 2006; Richie and Saul, 2002). Studies focused on PfEMP1 are also underway, although these are hampered by the extreme diversity of the members encoded by the *var* gene family. It has been suggested that a vaccine cocktail of multiple antigenic elements would have to be employed to deal with the extreme antigenic polymorphism of the parasite (Young and Winzeler, 2005). One area of malaria infection where a vaccine against PfEMP1 would be effective is during pregnancy-associated malaria (PAM). This is due to the fact that a single variant of PfEMP1, namely VAR2CSA is thought to interact with CSA, leading to the sequestration of the parasites in the placenta. Although a vaccine based on this interaction will not protect the general public, it may reduce the negative effects and mortality associated with PAM (Matuschewski, 2006).

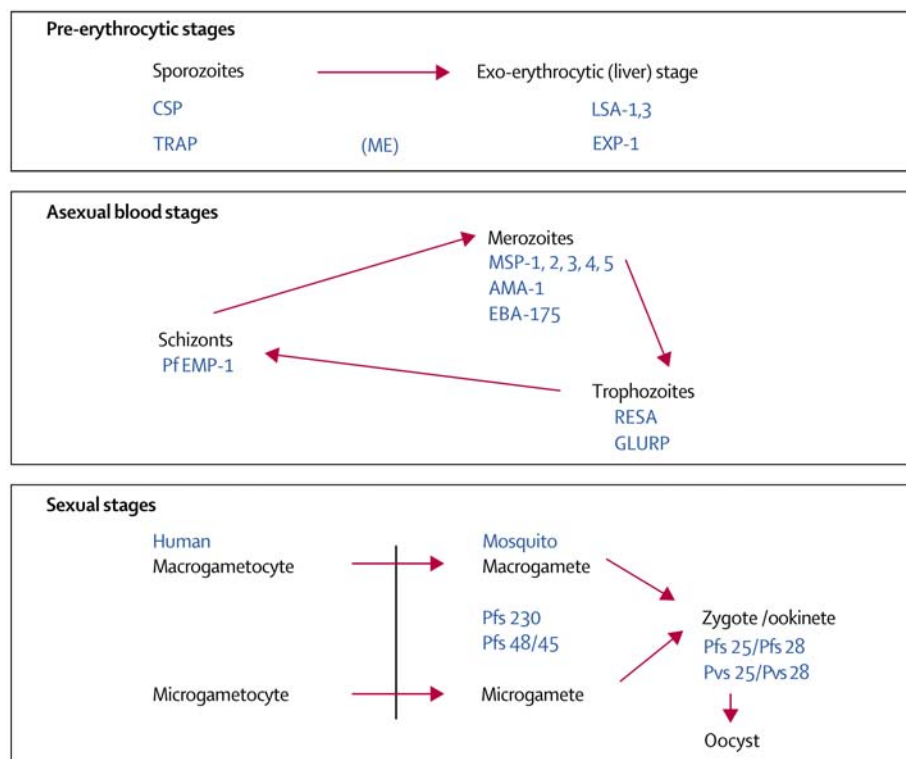


Figure 1.5: Malarial protein targets under vaccine development (Greenwood et al., 2005).

CSP: circumsporozoite protein; TRAP: thrombospondin-related adhesion protein; LSA: liver stage antigen; EXP: exported antigen; ME: multiple-epitope string based on T-cell and B-cell epitopes of pre-erythrocytic stage antigens; MSP: Merozoite surface protein; AMA: apical merozoite antigen; EBA: erythrocyte-binding antigen; RESA: ring-infected erythrocyte surface antigen; GLURP: glutamine-rich protein; PfEMP: *P. falciparum* erythrocyte membrane protein; Pfs 230 and Pfs 48/45: antigens located on the surface of *P. falciparum* gametocytes; Pfs 25/Pfs 28 and Pvs 25/Pvs 28 antigens located on the surface of ookinetes of *P. falciparum* and *P. vivax* (Greenwood et al., 2005).

Transmission blocking vaccines are so-called altruistic vaccines, since they do not protect an individual but rather the community at large. These vaccines are based on the fact that the proteins expressed during the sexual stage of the parasite lifecycle did not evolve to circumvent

the human immune system. As such, antibodies taken up by the mosquito during a blood meal can act against these parasites, thereby preventing re-infection of the population. To date, ookinete secretory protein WARP, the chitinase CHT1 and the invasin CTRP, and gametocyte-specific surface antigens such as P25 and P28 have undergone further study in this regard (Bremant et al., 2004; Greenwood et al., 2005; Matuschewski, 2006; Richie and Saul, 2002).

1.3.2 Anti-malarial therapy

Although malarial infections can be reduced by the use of insecticide-treated bed nets and vector control, the absence of an efficient vaccine means that life-threatening infections, which can only be treated by drugs, still occur at an alarming rate (Bathurst and Hentschel, 2006). Although there are several different drugs available for the treatment of malarial infections, they do have limitations such as the development of resistance and questions about their safety (Table 1.1). Some of the more common drugs will be discussed below.

Table 1.1: Limitations of currently used anti-malarial drugs.

Compiled from (Arav-Boger and Shapiro, 2005; Bathurst and Hentschel, 2006; Edwards and Biagini, 2006; Jambou et al., 2005; Kremsner and Krishna, 2004; Ridley, 2002).

Anti-malarial drug	Year launched	Resistance	Limitations
Quinolines and related antimalarials			
Quinine	19 th century	1910	Compliance (3 times a day, 7 days) Safety
Chloroquine	1945	1957	None
Amodiaquine	1975	None	Safety (occasional agranulocytosis, hepatotoxicity) Possible resistance
Mefloquine	1977	1982	Safety (Neuropsychiatric disturbances) Cost
Halofantrine	1988	1992	Safety (contra-indicated for people with heart disease) Cost
Artemisinin			
Artemisinin derivatives	1970	<i>In vitro</i> to field isolates from French Guiana	Compliance (5-7 days of treatment) Cost Possible safety issues (neuronopathy in lab animals, sporadic allergic reactions)
Other antimalarials			
Proguanil	1948	1949	Possible resistance, Cost
Primaquine	1950	None	Safety
Sulfadoxine-pyrimethamine	1967	1967	None
Atovaquone	1996	1996	High cost due to complexity of synthesis
Lapdap™ (combination of dapsone and chlorproguanil)	2003	None	Possible resistance

Hemoglobin degradation by metallo-, cysteine and aspartic proteases is a major source of nutrients for intraerythrocytic parasites. During this process, Fe (II) haeme is released, which is sequestered as the pigment haemozoin following oxidation to Fe (III) haematin. Quinolines and related anti-malarials (Fig 1.6) such as chloroquine, amodiaquine, mefloquine, the bisquinoline

piperazine, halofantrine and the halofantrine analogue lumefantrine cause haeme-induced toxicity to the parasite by preventing the formation of haemozoin through disrupting the stacking of the planar aromatic structures (Fig 1.7). This is mediated by the accumulation of host chloroquine to much higher levels in the parasite acidic digestive vacuole than in the plasma. Chloroquine-resistant parasites do not accumulate chloroquine due to the action of *pfcr1* (*P. falciparum* chloroquine-resistance transporter) and *pfmdr1* (*P. falciparum* multidrug resistance 1 transporter). A K76T mutation in *pfcr1* allows the diprotonated form of chloroquine that usually accumulates in the acidic food vacuole to exit the organelle, thus leading to chloroquine-resistant parasites (Arav-Boger and Shapiro, 2005; Hyde, 2005; Kremsner and Krishna, 2004; Ridley, 2002).

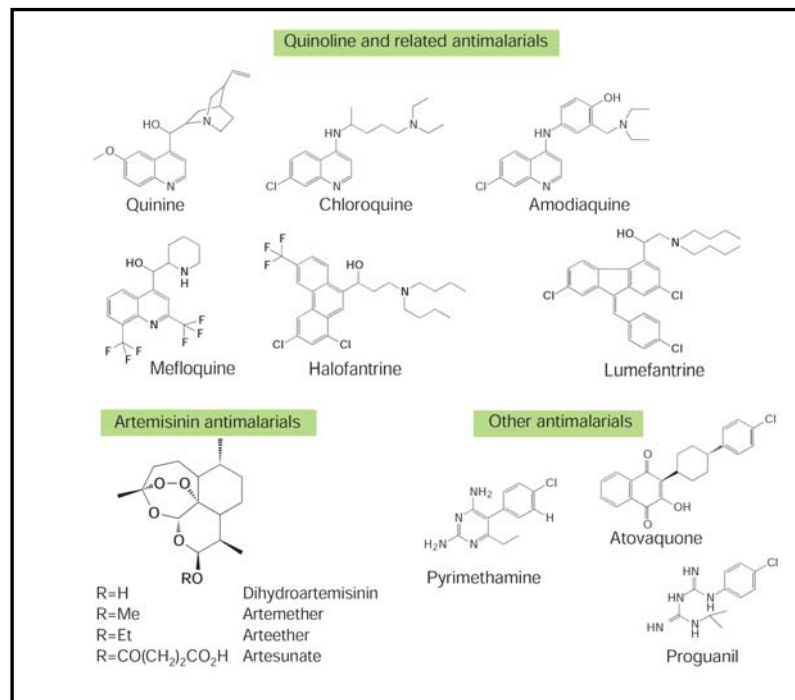


Figure 1.6: Chemical structures of some of the major antimalarial agents (Ridley, 2002).

Nucleic acid and protein biosynthesis require monomers that are generated by methyl transfer reactions. The Plasmodial folate biosynthesis pathways that generate the tetrahydrofolate used as a cofactor in these reactions differ from that of the human host, making it an attractive drug target. Both dihydrofolic acid and *para*-aminobenzoic acid can be procured by *de novo* synthesis as well as by uptake from the human host. Several of the biosynthetic enzymes also have a bifunctional arrangement, such as dihydro-6-hydroxymethylpterin pyrophosphokinase and dihydropteroate synthase, as well as dihydrofolate reductase and thymidylate synthase (DHFR-TS). It has been suggested that the bifunctional arrangement of these enzyme allow for substrate channelling, thereby providing more efficient biosynthesis. Pyrimethamine (Fig 1.6) inhibits dihydrofolate reductase, while the sulphonamide, sulfadoxine, inhibits dihydropteroate

synthase. As such, the combination of sulfadoxine-pyrimethamine has been used for the synergistic inhibition of folate metabolism. However, due to point mutations in the targeted enzymes, resistance to these drugs are widespread. This has led to targeting the production of tetrahydrofolate through alternate pathways such as the shikimate pathway (Arav-Boger and Shapiro, 2005; Ridley, 2002).

Mitochondrial electron transport can be targeted by the ubiquinone analog atovaquone (Fig 1.6), which destroys the mitochondrial membrane potential by preventing respiration at the cytochrome bc_1 complex. A point mutation in cytochrome c reductase led to rapid resistance against this drug. However, it was found that combining atovaquone with the antifolate proguanil, increases its anti-malarial activity by synergism (Arav-Boger and Shapiro, 2005; Hyde, 2005; Ridley, 2002).

Artemisinin, isolated from *Artemisia annua*, and its derivatives, especially artemether, arteether and artesunate have been increasingly used to combat malaria. The various derivatives are all metabolised to the active agent dihydro-artemisinin, which contains an endoperoxide bridge that is involved in the production of toxic free radicals. It has been suggested that the intracellular calcium stores and ATPase activities can be altered by this drug. It also has gametocytocidal activity, thus preventing re-infection of the vector (Arav-Boger and Shapiro, 2005; Ridley, 2002). However, artemisinin-based therapies have been contra-indicated in the first trimester of pregnancy, due to neuronal degradation and neurotoxicity seen in animals (Bathurst and Hentschel, 2006). The WHO does however state that in the absence of alternative therapies, artemisinin can be used in the second and third trimester of pregnancy (Dellicour et al., 2007). *In vitro* resistance by field isolates from French Guiana were detected against this drug in 2005, leading to fears that *in vivo* resistance could become widespread (Jambou et al., 2005).

Several other targets are also being investigated for anti-malarial therapy, based on the biochemical and metabolic knowledge of the parasite (Fig 1.7). These include lactate dehydrogenase, since the parasite is dependent on anaerobic glycolysis for ATP production due to the apparent lack of a functional citric acid cycle during the asexual stage of the lifecycle. Although bioinformatics analyses have identified *Plasmodium* homologues to most of the enzymes involved in oxidative phosphorylation, mitochondrial pyruvate dehydrogenase has yet to be found (van Dooren et al., 2006; Wiesner et al., 2003). *Plasmodium* parasites contain a plastid-like organelle that is thought to have been obtained through endosymbiosis with algae. This prokaryotic-like apicoplast has its own genome that encodes the various cellular machineries responsible for the replication of this organelle (Wiesner et al., 2003). Various

aspects of apicoplast metabolism have come under the spotlight, such as type II fatty acid biosynthesis mediated by enoyl-acyl carrier protein reductase (FabI), which can be inhibited by the antibiotic triclosan, as well as protein farnesyltransferase. The prokaryotic characteristics of the apicoplast have led to the investigation of the antimalarial activity of various antibiotics, with varying success (Arav-Boger and Shapiro, 2005; Bathurst and Hentschel, 2006; Ridley, 2002). In infected erythrocytes, hemoglobin degradation by various proteases is the source of amino acids for Plasmodial protein synthesis, as well as a method to preserve the correct osmotic stability of the parasite. One of the proteases involved in hemoglobinase activity is falcipain-2 (FP2), a member of the papain family of cysteine proteases. Since inhibitors of FP2 have been shown to inhibit hemoglobin degradation and subsequently parasite development, this protein has been considered as a possible target for anti-malarial therapy (Pandey et al., 2005). Inhibitors of another protease, plasmepsin, have also been shown to have anti-malarial activity (Ridley, 2002). Phosphatidylcholine synthesis for the formation of new biological membranes is dependent on choline uptake from the blood. It has been shown that inhibitors of choline transport have anti-malarial activity (Wiesner et al., 2003).

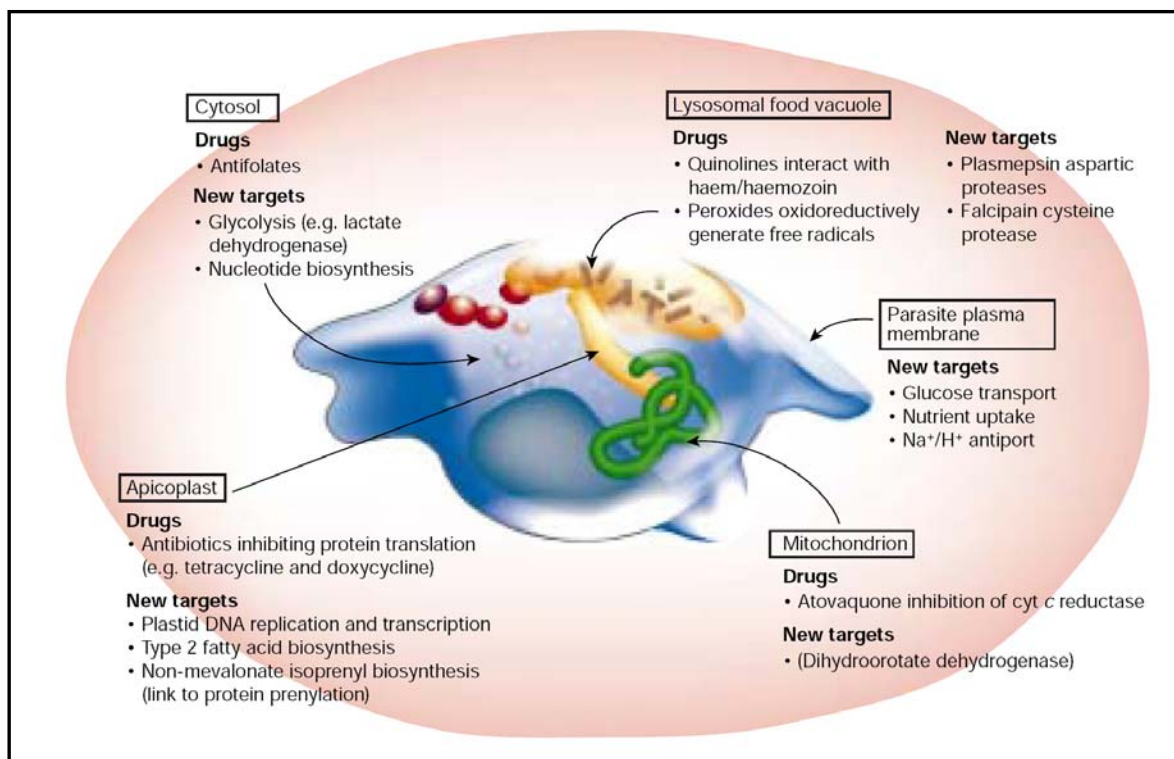


Figure 1.7: Current and possible drug targets for anti-malarial therapy (Ridley, 2002).

Due to the prevalence of multidrug-resistant *P. falciparum*, the WHO is recommending drug combinations as first-line treatment (Jambou et al., 2005). There are however different schools of thought on the requirements for the effective combinations of anti-malarial drugs. Some authors state that the parasite biomass must be adequately reduced by one of the drug

components to reduce chances of resistant mutations to the other component to occur. This implies that one of the components must have a much longer half-life than the other one (Davis et al., 2005; Edwards and Biagini, 2006). Others believe that the pharmacokinetics of the component drugs must be similar to prevent the onset of resistance to a single drug present in declining concentrations (Edwards and Biagini, 2006; Kremsner and Krishna, 2004). There are several combination therapies currently in use, such as Lapdap™, which is a combination of dapsone, a sulphone, which inhibits dihydropteroate synthetase and chlorproguanil that inhibits dihydrofolate reductase; Co-artem™ which consists of a combination of lumefantrine and artemether and Artekin™, which is a mixture of dihydroartemisinin and piperazine (Edwards and Biagini, 2006).

There are several factors that complicate malarial therapy. The large number of people that can be infected at a given time in an endemic population, often without access to proper healthcare; the harshness of the disease in pregnant women and children; as well as the need to protect healthy travellers in an endemic area implies that any anti-malarial drug must meet considerable requirements for safety. In addition, the complicated nature of the malarial lifecycle may necessitate the use of a variety of drugs (Arav-Boger and Shapiro, 2005). The successful treatment of infection often depends on exploiting the metabolic differences between the human host and the responsible pathogen (Macreadie et al., 2000). Ideally, both the asexual forms and gametocytes should be targeted to treat both the infection and to block transmission to the rest of the population (Bathurst and Hentschel, 2006). Although there are several drugs currently in use (see Table 1.1) increasing resistance against the currently used drugs highlights the urgent need for alternative therapies in the near future (Ridley, 2002).

1.3.3 Vector control

During the 1930s to the 1950s, malaria was eliminated from countries such as Spain, Greece, Italy and the United States by strategies such as indoor spraying of dichlorodiphenyltrichloroethane (DDT), a residual insecticide and the elimination of potential breeding grounds of the *Anopheline* vectors by the draining of swampland (Sachs and Malaney, 2002). While indoor spraying of DDT, pyrethroids and carbamates has improved malaria control in certain regions of Africa, it has not succeeded in eradicating the disease. This has led to the use of insecticide-treated bed nets that, while not a permanent cure for the malaria problem, has led to a decrease of overall child mortality in the areas of use. Several other strategies including modified house design and zooprophylaxis (biological control) such as the use of larvivorous fish have been successful in certain areas, but further studies on these approaches are needed (Greenwood et al., 2005).

1.4 Protein interactions

A cell can be viewed as an intricate network of interacting molecules. Historically, scientists have studied only the specific sections of the cell involved in a certain process or function, which gave rise to the concept of “pathways” in which proteins play a major role (Apic et al., 2005). Proteins are the workhorses of the cell and function as the primary structural elements, catalysts and molecular machines (Eisenberg et al., 2000). Although knowledge of the pathways in which proteins function is the logical starting point for the validation of a specific protein as a drug target, these pathways have to be known in their entirety i.e. not only the up- and downstream reactions and the proteins that catalyse them, but also the various interconnections that a protein may have in a cell (Apic et al., 2005).

Traditionally, a protein’s function was defined by a single reaction, such as the binding of a molecule or the catalysis of a certain reaction. This can be viewed as the molecular function of a protein (Fig 1.8) (Eisenberg et al., 2000). Currently, the functional genomics view indicates that proteins function as nodes in an extensive network of interacting molecules and, as such, a protein’s function should be characterized in relation to the interactions formed with other proteins in the cell (Eisenberg et al., 2000).

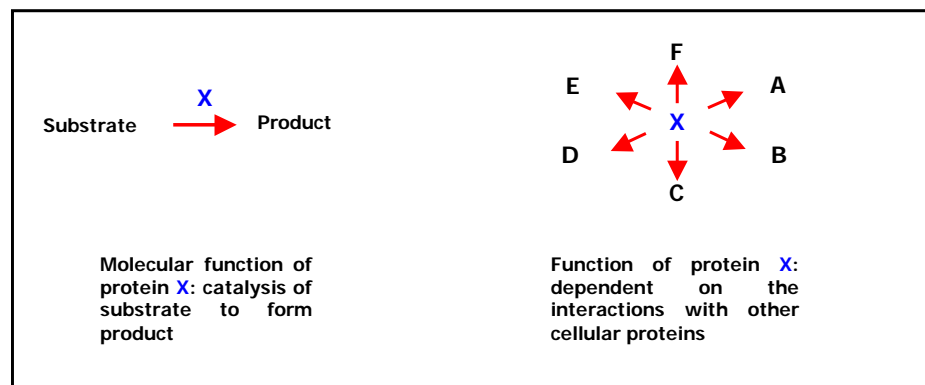


Figure 1.8: Traditional versus functional genomic view of protein function. Adapted from (Eisenberg et al., 2000).

Protein-protein interactions refer to any of a number of encounters between proteins, ranging from transient interactions to the formation of stable complexes (Kluger and Alagic, 2004). Protein-protein interactions play pivotal roles in the functional and structural ordering of the cell (Ito et al., 2000) ranging from antibody-antigen interactions (Buckingham, 2004) to signal transduction cascades (Pawson and Nash, 2000) to the degradation of a protein by the proteasome (Fischer and Lane, 2004). Such interactions often illuminate the molecular mechanisms that form the core of biological processes and can take place with various

specificities and affinities. The interactions between proteins can also be influenced by a variety of other factors, such as the concentration and oligomeric state of the respective proteins, as well as the ionic strength, pH and type of counter ions of the solvent (Howell et al., 2006).

Protein-protein interactions cause various effects inside a cell: 1) the kinetic properties or stability of proteins can be altered, which can lead to differences in substrate affinity, catalytic activity or allosteric properties of the proteins; 2) substrate channelling is often effected by protein-protein interactions; 3) the interaction can reveal a new binding site or 4) can inactivate a protein and 5) substrate specificity can also be altered by protein-protein interactions (Kluger and Alagic, 2004; Phizicky and Fields, 1995).

1.4.1 Nature of protein-protein interactions

The most important factors responsible for the interactions between various protein surfaces are steric considerations, van der Waals, electrostatic and hydrophobic interactions as well as the presence of hydrogen bonds. There are between 1-50 water molecules present at the protein-protein interface, which, through the formation of hydrogen bonds with various amino acids, result in an aqueous network that can stabilise the protein-protein interface (Archakov et al., 2003). Site-directed mutagenesis studies of protein-protein interfaces have shown that only a few residues in the interface have a strong contribution to the energy of the interaction. These so called 'hot spots' of high-energy interactions contain high levels of Trp, Arg and Tyr, and to a lesser extent, Asp and Ile (Arkin and Wells, 2004; Bogan and Thorn, 1998; Pérez-Montfort et al., 2002). These hot spots are often quite complementary to each other in both their shape and the composition of the amino acids, where hydrophobic amino acids from one surface are positioned into indentations in the surface of the opposite surface and the negative electronic character of one amino acid is countered by a positively charged amino acid on the opposite face (Arkin and Wells, 2004; Gadek and Nicholas, 2003).

1.4.2 Protein-protein interactions as drug targets

The identification of a suitable drug target is the first step in the design of a new, physiologically active compound, followed by the elucidation of this target enzyme, metabolic pathway or transport process properties and the design of an appropriate inhibitory ligand (Archakov et al., 2003). Of the 4 types of biological macromolecules, namely nucleic acids, lipids, polysaccharides and proteins, that can be targeted in therapeutic interventions, the majority of successful drugs target proteins (Hopkins and Groom, 2002). Proteomics is a system-wide attempt to elucidate the modification, function, localization, interaction and regulation of all the proteins transcribed by a cell (Piggott and Karuso, 2004). Proteomics has been involved in various areas of the drug discovery pipeline and may have the potential to increase the effectiveness of the drug

development procedure. Proteomics encompass various techniques, which can be classified in two groups: differential expression analysis or interaction analysis (Fig 1.9). While both types of techniques have the potential to connect specific proteins to a diseased state or process, interaction analysis is an extremely focused approach to finding proteins that are of significance in a metabolic pathway or disease process. In situations where a specific pathway has already been identified as a possible drug target, the use of interaction analysis to find proteins that are either directly or indirectly involved in this metabolic pathway can be extremely relevant to the drug target discovery process (Peltier et al., 2004).

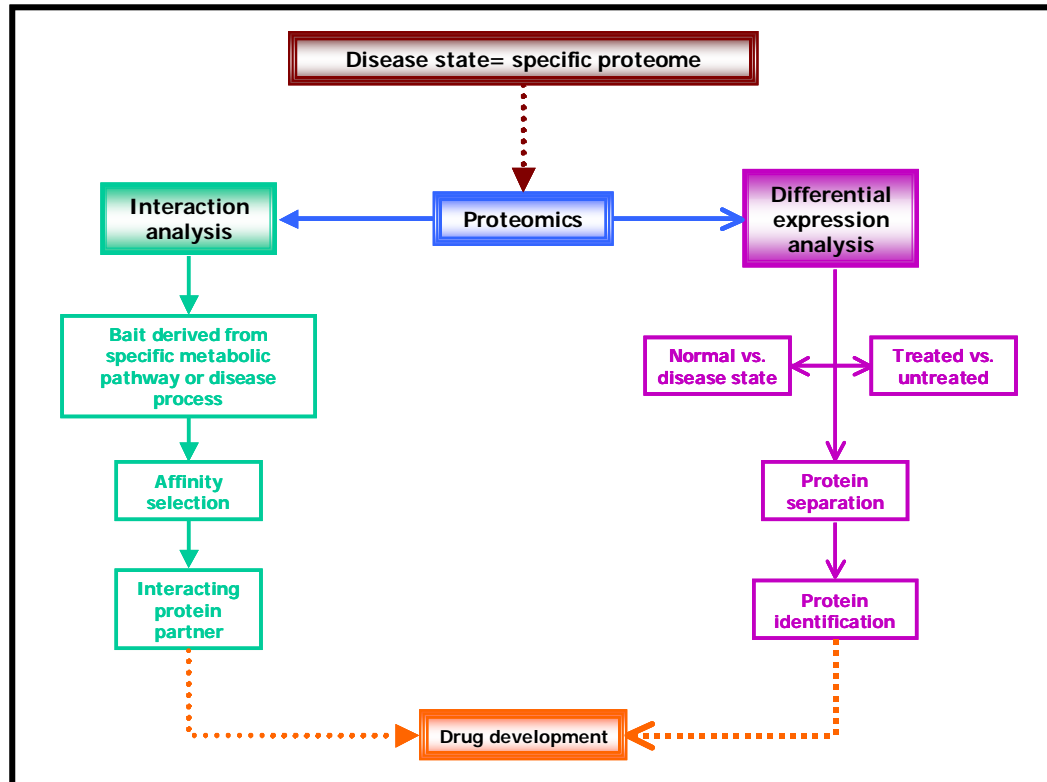


Figure 1.9: The role of proteomics in the identification of proteins involved in a specific metabolic pathway or disease process.

Generally, an identified enzyme or metabolic pathway is targeted by designing molecules that target the catalytic site of the enzyme, mainly because there is often structural data available on the catalytic site of an enzyme and because the activity of an enzyme will certainly be affected by the insertion of a foreign molecule (Pérez-Montfort et al., 2002). Enzymes are “drug friendly” since their substrates can act as a scaffold in the design of antagonistic molecules (Arkin and Wells, 2004). The effect that a drug has on an enzyme is also readily determined by detecting the differences in enzyme activity (Yin and Hamilton, 2005).

Protein-protein interactions are viable drug targets due to the fact that protein-protein interactions mediate a large number of physiological and pathological processes (Falciani et al., 2005). The advantage of targeting a specific metabolic pathway through a protein-protein

interaction instead of the catalytic site of an enzyme is that the active site of an enzyme often has high structural similarity to that of the human host, while there is greater structural variability in the protein-protein interfaces between different organisms. This can lead to more effective differentiation between the parasite and host proteins (Archakov et al., 2003). It has been shown that protein-protein interfaces of enzymes differ in composition between different species, possibly due to the insertions, deletions or substitutions of amino acids during evolution (Pérez-Montfort et al., 2002). Resistance against chemotherapeutic agents is also often achieved by point mutations, which can have a small effect on the enzyme activity, but cause a decreased affinity to the chemotherapeutic agent. In contrast, the important amino acids responsible for the protein-protein interface of a specific organism are often invariable and even one amino acid mutation can lead to the dissociation of the complex (Archakov et al., 2003). This implies that resistance to agents that target protein-protein interfaces should be slower to appear, since a functional mutation at both protein interfaces is necessary for effective resistance to occur (Buendía-Orozco et al., 2005).

One objection raised against targeting protein-protein interactions, instead of enzyme active sites, is that the catalytic sites of enzymes are accessible to the medium, since the substrate has to be able to diffuse into the catalytic pocket. In contrast, the crystal structures of protein-protein interactions show an impregnable barrier that will prevent therapeutic agents from disrupting protein interfaces. However, it has to be remembered that in solution, protein-protein interactions are continually undergoing fluctuations, which could allow the diffusion of therapeutic agents into binding sites that are not apparent from crystallographic data (Pérez-Montfort et al., 2002). Another problem encountered when targeting protein-protein interfaces is the flatness of these targets when compared to the substrate-cavities of enzymes (Buendía-Orozco et al., 2005) and the fact that there are often too many contacts between the two surfaces for a small-molecule to inhibit (Way, 2000). The drug industry face three major problems when it comes to the design of inhibitors of protein-protein interactions: 1) knowledge of the structural characteristics of the binding interfaces is limited; 2) the size of protein-protein interfaces is such that there is a large thermodynamic barrier to disrupting these interfaces with a single small molecule; and 3) molecules that can overcome these thermodynamic challenges are not readily found in the current available chemical libraries (Watt, 2006).

One possible method to overcome these problems is the use of bifunctional blockers that contain both a highly specific specificity group and a poorly reactive bonding group (Fig 1.10). By highly specific, non-covalent interaction with the target protein, the specificity group positions the poorly reactive bonding group near its target amino acid. Due to the high local

concentration of the bonding group, a covalent interaction between the amino acid and bonding group can form quite easily, thereby preventing subsequent protein-protein interactions (Way, 2000).

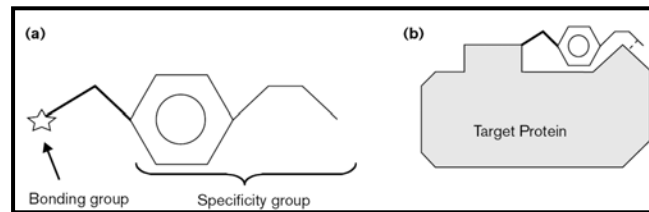


Figure 1.10: Schematic representation of a bifunctional blocker (Way, 2000).

Another possible strategy for the inhibition of protein-protein interactions is to use peptides that reproduce the essential characteristics of one of the partner proteins to interfere with the formation of the protein complexes (Cochran, 2000). These peptides can range between 2 to 5 kDa (10 to 40 amino acids) and can be used since they have the same binding effect as the whole protein (Meloan et al., 2004). Peptides can be very useful as drugs since they are extremely variable and have the ability to recognise other molecules. Peptides can also be synthesised chemically with a large array of modifications and functional groups (Falciani et al., 2005). However, there are several problems associated with the therapeutic use of peptides, such as rapid proteolytic degradation, reduced bioavailability and propensity to cause immunogenic reactions (Pollina, 1996; Ripka and Rich, 1998). One method to circumvent these problems is the design of peptidomimetics based on the original parent peptide. Peptidomimetics are small peptide analogs that imitate the function and structure of bioactive peptides, but with chemical modifications that improve their drug-like characteristics (Pollina, 1996). The use of D-peptides instead of L-peptides has also been suggested to improve stability (Szardenings, 2003). Alternatively, credit card libraries consisting of small, planar, aromatic molecules that can bind selectively to the hot-spots mediating the protein-protein interactions, can also be used as interaction inhibitors (Xu et al., 2006).

Although the targeting of protein-protein interactions for therapeutic treatment is a relatively new field, there are several examples where such a strategy was viable for target inhibition. These include the interaction between MDM2 and p53 in cancerous cells (Vassilev et al., 2004) (Fischer and Lane, 2004), the dimerization of HIV-1 protease (Schramm et al., 1996) and the prevention of polymerisation of α - β tubulin by vinblastine during the formation of the mitotic spindle, which has been used for almost 50 years for the treatment of cancer (Gadek and Nicholas, 2003).

1.4.2.1 Protein-protein interactions as drug targets in the fight against pathogenic parasites

Based on these reports, protein-protein interactions in pathogenic parasites can be considered as drug targets (Pérez-Montfort et al., 2002). Examples of the successes of this strategy include peptidomimetic protein farnesyltransferase inhibitors with activity against *Trypanosoma brucei* and *P. falciparum* (Carrico et al., 2004; Ohkanda et al., 2004) as well as inhibitory interface peptides of *P. falciparum* triosephosphate isomerase (TIM) (Singh et al., 2001). Due to the increasing resistance against the currently used anti-malarial drugs, novel chemotherapeutic agents for the treatment of malarial infections are urgently needed. This can be achieved both by targeting validated targets in novel ways, thereby generating new drug candidates and by investigating the biochemical and metabolic processes of the malaria parasite to identify new drug targets (Olliaro and Yuthavong, 1999). The rational design of drugs based on the function and structure of vital parasitic protein-protein interactions should lead to slower drug resistance development.

Several protein-protein interaction analyses that can aid in the design of mechanistically novel drugs that target Plasmodial protein-protein interactions have recently been published. Approximately a year after the commencement of this study, LaCount and co-workers published an extensive protein-protein interaction network of *P. falciparum* obtained from Two-Hybrid screens in *Saccharomyces cerevisiae*. This identified 2 846 distinctive pairwise interactions, which was then grouped in a vastly interconnected network linking 1 267 proteins by 2 823 interactions. Small groups of one or two interactions linked an additional 41 proteins. Clusters of interacting proteins were grouped together by using gene ontology (GO) annotations, determination of the enrichment of certain protein domains and by co-expression studies. This led to the identification of interacting groups involved in host cell invasion, mRNA stability, transcription, chromatin modification and ubiquitination (LaCount et al., 2005). When this network was compared with the protein interaction networks of *S. cerevisiae*, *Drosophila melanogaster*, *Caenorhabditis elegans* and *Helicobacter pylori*, it was found that the *P. falciparum* network had very little conservation with the protein networks of the other organisms and contained 29 parasite-specific protein interaction networks. Only the protein networks involved in endocytosis, the unfolded protein response and the MCM complex/heat shock proteins showed conservation between *P. falciparum* and *S. cerevisiae*. Apart from *S. cerevisiae*, *P. falciparum* did not show any conservation with the protein networks of the other organisms examined in the study (Suthram et al., 2005).

More recently, bioinformatics-based predictions of the Plasmodial interactome have been published. Date and co-workers created a genome wide computational model of the interactome

of *P. falciparum* (Date and Stoeckert Jr, 2006). Approximately 68% of the genome was covered by integrating experimental functional genomics and *in silico* data, thereby generating almost 400 000 linkages between 3667 proteins. Although approximately 60% of the proteins in the interaction map are hypothetical, 95% of these could be linked to known proteins, thus giving an indication of the possible functions of these hypothetical proteins. Additionally, since 107 of the hypothetical proteins were only linked to other hypothetical proteins, the interaction map can give an indication of possible new biochemical targets that can be exploited for drug development (Date and Stoeckert Jr, 2006). Recently, Wuchty and co-workers published a combined draft of the network of *P. falciparum* protein interactions. This network was derived from three autonomous data sources, namely known protein domain interactions, experimentally measured protein interactions and evolutionary conserved interactions in other organisms, based on orthologous proteins involved in these interactions being present in *P. falciparum*. Utilising these methods, 19 979 interactions between 2321 proteins were determined, notably clustering in the ribosomal and proteosomal activities (Wuchty and Ipsaro, 2007).

According to Peltier et al., using interaction analysis to find proteins that are either directly or indirectly involved in a specific metabolic pathway can be extremely relevant to the drug discovery process (Peltier et al., 2004). One such pathway that is a possible drug target in *P. falciparum* is polyamine metabolism.

1.5 Polyamine metabolism

Polyamines are aliphatic, low-molecular weight nitrogenous bases, which carry a positive charge on each nitrogen atom at physiological pH (Fig 1.11) (Birkholtz, 2002; Wallace et al., 2003).

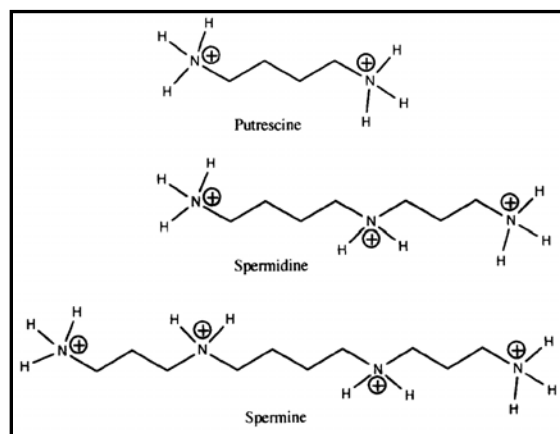


Figure 1.11: The structures of putrescine, spermidine and spermine (Seiler et al., 1996).

These organic cations can react with negatively charged macromolecules within cells, such as phospholipids and nucleic acids. However, there are two basic differences between the

polyamines and normal bivalent cations such as Ca^{2+} and Mg^{2+} . Firstly, the positive charge on the polyamines is dispersed along the entire length of the flexible backbone chain and as such, the electrostatic interactions between the polyamines and the macromolecules are more flexible than that of the point charges of the bivalent cations. Secondly, polyamine homeostasis is controlled by an intricate metabolic machinery (Jänne et al., 2004; Wallace et al., 2003).

The four physiologically important polyamines are the primary diamines, cadaverine (1,5-diaminopropane, which only occurs in prokaryotes), and putrescine (1,4-diaminobutane), as well as the triamine putrescine derivative spermidine (N-(3-aminopropyl)-1,4-diaminobutane) and the tetra-amine putrescine derivative spermine (N, N1-bis (3-aminopropyl)-1,4-butanediamine) (Fig 1.11) (Cohen, 1998). Polyamines occur in all species, except two orders of Archaea, namely the Halobacteriales and Methanobacteriales. This emphasizes the importance of polyamines for cell survival (Wallace et al., 2003).

1.5.1 Polyamine metabolism in humans

The polyamine levels in cells are regulated by several pathways such as *de novo* synthesis, various uptake mechanisms that recover polyamines from e.g. intestinal microorganisms and the diet as well as catabolism and export (Fig 1.12) (Thomas and Thomas, 2001).

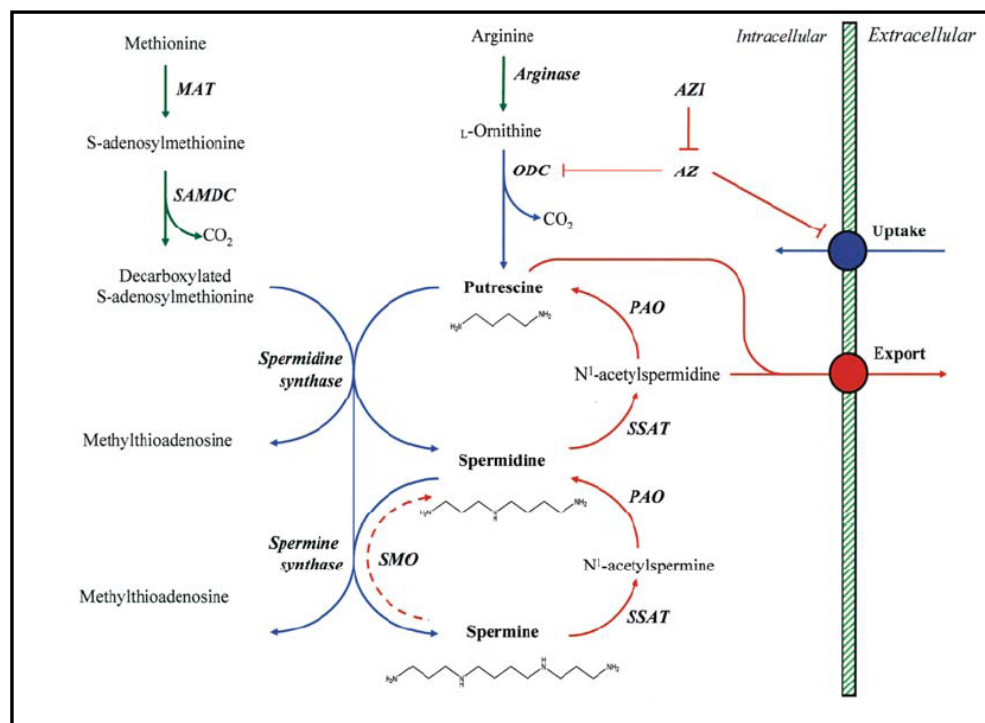


Figure 1.12: Polyamine metabolism in humans (Wallace et al., 2003).

The primary precursors of polyamines are the amino acids L-ornithine and L-methionine. L-ornithine is obtained from the diet, or cleaved from L-arginine by mitochondrial arginase II and then decarboxylated by the rate-limiting enzyme ornithine decarboxylase (ODC) (EC 4.1.1.17) to

yield putrescine. L-methionine is converted to S-adenosyl-L-methionine (AdoMet) and then decarboxylated by another rate-limiting enzyme, S-adenosylmethionine decarboxylase (AdoMetDC) (EC 4.1.1.50) to form decarboxylated S-adenosylmethionine (dcAdoMet). dcAdoMet then operates as an aminopropyl donor and donates its aminopropyl moiety to putrescine to form spermidine in a reaction catalyzed by spermidine synthase (EC 2.5.1.16). Another aminopropyltransferase reaction transfers a second aminopropyl moiety to spermidine to form spermine in a reaction catalyzed by spermine synthase (Jänne et al., 2004; Schipper et al., 2000; Wallace et al., 2003). The activities and levels of the two rate-limiting enzymes in the polyamine pathway, ODC and AdoMetDC, are independently controlled on the transcriptional, translational and post-translational levels (Müller et al., 2000).

ODC is a cytosolic, inducible subunit enzyme with an extremely short half-life (10 min –1 h) that utilize pyridoxal phosphate as co-factor. The active enzyme is in the form of a homodimer, where the active site is formed at the interface of the two subunits. ODC is regulated by both negative and positive feedback regulation, as well as by the action of a polyamine-induced protein called antizyme (AZ) (Wallace et al., 2003). The C-terminal PEST (proline-, glutamate-, serine- and threonine-rich) region in the enzyme is essential for degradation. ODC does not require ubiquitination for degradation, but instead is targeted to the 26S proteasome by interaction with AZ. AZ mRNA encodes a stop codon situated close to the initiation codon. High concentrations of polyamines cause a translational frameshift, which subverts the ribosome from its original reading frame to a new reading frame by a +1 frameshift on the mRNA, resulting in the translation of complete AZ (Gandre et al., 2002; Wallace et al., 2003). AZ subsequently binds to an ODC subunit, and since antizyme has a higher affinity for ODC than the subunits of ODC have for each other, enzymatically inactive heterodimers are formed. Thus, ODC is inactivated and is targeted for degradation by the 26S proteasome, possibly due to the exposure of the PEST regions on the C-terminus. Antizyme also mediates polyamine-induced regulation of transport. Antizyme inhibitor (AZI) is a protein that occurs in mammalian cells with homology to ODC and with a higher binding affinity to antizyme than ODC, which can bind to AZ to release functional ODC. AZ is also degraded by the 26S proteasome, but this degradation is ODC independent and ubiquitin dependent (Gandre et al., 2002).

Since the decarboxylation and aminopropyl transferase reactions are almost irreversible, there are distinct pathways for retro-conversion. Spermidine and spermine are first acetylated by cytosolic spermidine/spermine *N*¹-acetyltransferase (SSAT) (EC 2.3.1.57) using acetyl-CoA as a source of the acetyl group, to form *N*¹-acetylspermidine and spermine that can then be exported from the cell. This acetylation reaction occurs specifically at primary amino groups. Compared to

free polyamines, these acetylated polyamines have decreased affinity to RNA and DNA due to the decrease in positive charge. Alternatively, these molecules can be oxidized by the peroxisomal FAD-dependant polyamine oxidase (PAO) (EC 1.5.3.11) to spermidine and putrescine in a reaction that also yields H₂O₂ and 3-acetamidopropanal. With every acetylation and oxidation cycle, H₂O₂ is produced, which leads to the continuation of this cycle, since H₂O₂ is an inducer of SSAT activity (Wallace et al., 2003).

Towards the end of 2002, it was discovered that spermine could also be converted back to spermidine by spermine oxidase (SMO), which prefers spermine as substrate to the acetylated form and does not use spermidine as substrate at all. Spermidine also serves as a precursor for the amino acid hypusine that is derived from the aminobutyl moiety of spermidine and forms an integral part of the eukaryotic initiation factor 5A (eIF5A) (Jänne et al., 2004; Wallace et al., 2003). Copper-containing amine oxidases can also irrevocably degrade polyamines by oxidative deamination. The products thus produced are toxic and unstable and are further degraded to water, carbon dioxide and urea (Schipper et al., 2000).

Polyamine uptake is regulated by the intracellular concentrations of the polyamines. Mammalian cells can transport polyamines by energy-dependant, carrier-mediated mechanisms. Although most cells have a single transporter for putrescine, spermidine and spermine, certain cells do have separate transporters for putrescine and spermidine. The transporters are not very specific and polyamine analogues as well as compounds with little structural resemblance to the polyamines, like paraquat, can be transported (Seiler et al., 1996).

1.5.2 Polyamine metabolism in *P. falciparum*

Polyamine synthesis in the human malaria parasite is much simpler than that of the human host and differ in several ways (Fig 1.13). A single open reading frame encodes both ODC and AdoMetDC in a protein consisting of 1419 amino acids with three domains: residues 1-529 (N-terminal region) is the AdoMetDC region, residues 530-804 forms a linker peptide and residues 805-1419 (C-terminal) is homologous to known ODC sequences (Müller et al., 2000). This bifunctional protein decarboxylates both ornithine and S-adenosylmethionine to form putrescine and dcAdoMet, from which spermidine is formed by spermidine synthase (SpdSyn). It has been suggested that the low levels of spermine present in the parasite is due to the fact that this enzyme can also transfer an aminopropyl moiety to spermidine to form spermine (Burger et al., 2007; Haider et al., 2005). The 5'-methylthioadenosine (MTA) that is also formed by this reaction enters the methionine recycling pathway (MR) (Müller et al., 2001). While mammalian ODC is barely inhibited by putrescine, the ODC activity of the bifunctional malarial protein is susceptible to feedback inhibition by putrescine (Krause et al., 2000). In addition,

PfAdoMetDC/ODC has a half-life of more than two hours, in contrast to the exceptionally short half-lives of the mammalian AdoMetDC and ODC (Müller et al., 2001). The advantage of having the bifunctional PfAdoMetDC/ODC is that polyamine synthesis can be controlled by the regulation of a single protein (Wrenger et al., 2001), since there is synchronized transcription and translation of the rate-limiting enzymes of the polyamine metabolic pathway (Müller et al., 2001).

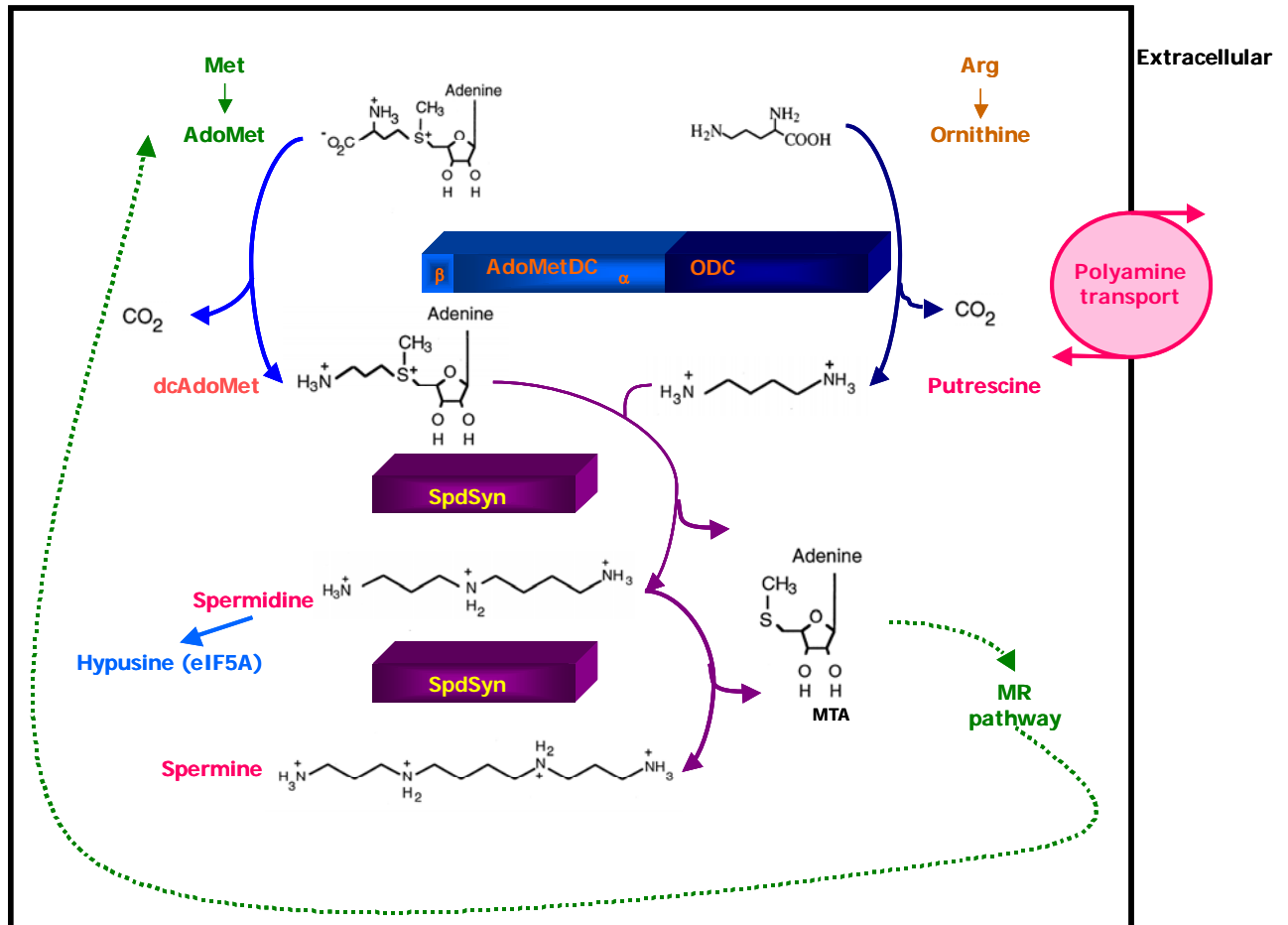


Figure 1.13: Schematic representation of polyamine metabolism in *P. falciparum*. Created from (Casero and Woster, 2001; Haider et al., 2005; Molitor et al., 2004; Müller et al., 2001; Schramm et al., 1996).

1.5.3 Polyamine metabolism as an anti-malarial target

Polyamines and their biosynthetic enzymes occur in increased concentrations in proliferating cells, which includes cancerous cells as well as parasitic organisms. As such, it is clear that inhibition of polyamine metabolism is a rational approach for the development of anti-parasitic drugs (Birkholtz, 2002; Heby et al., 2003).

Merrell Dow synthesized the putrescine analogue DL- α -difluoromethylornithine (DFMO) in the late 1970s, which acts as a suicide inhibitor of ODC (Wallace and Fraser, 2003), since it causes irreversible alkylation of the enzyme near or at the active site (Krause et al., 2000). Due to the fact that DFMO is effective in the treatment of West African trypanosomiasis (Marton and Pegg,

1995), it was also tested as a possible chemotherapeutic agent for malarial infection (Müller et al., 2001). The decrease in putrescine and spermidine levels caused by DFMO blocked the transformation from trophozoites to schizonts (Assaraf et al., 1987b). DFMO didn't have an effect on the spermine levels, which was postulated at the time to be due to the fact that spermine synthesis is absent in *P. falciparum*. However, it is possible that the parasite compensates for decreased polyamine synthesis by increased uptake. The inhibition of polyamine synthesis caused specific protein inhibition, which led to limited inhibition of RNA levels and total inhibition of DNA synthesis (Assaraf et al., 1987a). Polyamine analogues in combination with DFMO have also been shown to cure rodent malaria (Bitonti et al., 1989). Chokepoint reactions either produce or use a unique substrate. Since the inhibition of the enzymes that catalyse these reactions would thus either lead to the accumulation or depletion of a specific substrate, they can be possible drug targets. One such enzyme is AdoMetDC, since the dcAdoMet produced is only used for polyamine biosynthesis (Yeh et al., 2004). The ODC inhibitor 3-aminooxy-1-aminopropane and its derivatives and the AdoMetDC inhibitors CGP52622A and CGP 54169A have been shown to arrest the parasite lifecycle at the trophozoite stage *in vitro* (Das Gupta et al., 2005). It has also been shown that the prevention of spermidine biosynthesis with MDL73811, which inhibits AdoMetDC irreversibly, prevents the *in vitro* growth of the parasites (Wright et al., 1991). Recent ODC gene knock-out experiments indicated that parasite growth can not be revived by the end products of polyamine biosynthesis, which quintessentially validates this pathway as a drug target (unpublished results of international collaborators C Wrenger and RD Walter, Bernhard Nocht Institute for Tropical Medicine, Hamburg, Germany). The inhibition of spermidine metabolism prevents the formation of the amino acid hypusine, which occurs in the eukaryotic translation initiation factor (eIF-5a). Due to the fact that hypusinilation is necessary to convert the inactive precursor to the biologically active eIF-5a, it is possible that the cytostatic effect of polyamine depletion is due to the decrease in hypusine levels and thus the decrease in active eIF5a (Molitor et al., 2004). However, the use of DFMO and other polyamine analogues have had limited success against clinical cases of *P. falciparum* infections. This is possibly due to limited uptake of the drug, since it has to cross three membrane systems, namely the parasite plasma membrane (PPM), the parasitophorous vacuolar membrane (PVM) and the erythrocyte plasma membrane (EPM) (Kirk, 2001), as well as the increased transport of polyamines in the absence of biosynthesis (Müller et al., 2001). As such it is clear that, while the polyamine metabolic pathway of *P. falciparum* is a viable drug target, a different targeting strategy may have to be considered than was previously used.

The bifunctional PfAdoMetDC/ODC has several parasite-specific inserts, and it has been suggested that they play a part in interactions with unknown regulatory proteins. Although it has been shown that these stretches of amino acids are involved in various inter- and intra-domain interactions that are important for both decarboxylase activities and bifunctional complex formation (Birkholtz et al., 2004), the possibility that these inserts are also involved in interactions with other proteins can not be discarded. Linear motifs that mediate protein-protein interactions often occur within such regions of low complexity (Neduva et al., 2005). There are various reasons why the identification of the protein binding partners of the bifunctional PfAdoMetDC/ODC can be important for drug development. The dual nature of bifunctional proteins such as the PfDHFR-TS has been suggested to mediate substrate channelling. In the polyamine pathway, the activity of a third enzyme, spermidine synthase is needed to form spermidine. As such, it was thought that the bifunctional arrangement of PfAdoMetDC/ODC is not to facilitate substrate channelling, but so that the rate-limiting enzymes in the pathway can be regulated in a single step (Müller et al., 2000). However, if spermidine synthase binds to the heterotetrameric enzyme, substrate channelling can be achieved. Alternatively, as was shown with malarial TIM, peptide inhibitors of endogenous protein-protein interactions derived from the interprotein interface are viable as lead sequences for the design of antiparasitic agents (Singh et al., 2001). Since the activity of especially the ODC domain of the bifunctional enzyme is dependent on dimerization (Wrenger et al., 2001), it is possible that interface peptides or peptidomimetics can inhibit its activity (Birkholtz et al., 2004), as was the case with the Plasmodial TIM (Singh et al., 2001). Due to the high degree of structural conservation between the active sites of the human and parasite AdoMetDC and ODC enzymes (Birkholtz et al., 2003; Wells et al., 2006), the design of parasite-specific active site inhibitors is not presently feasible. As such, the accumulating evidence of the importance of protein-protein interactions for the activities of the Plasmodial polyamine biosynthetic enzymes indicate that the inhibition of the bifunctional protein's protein-protein interactions is a viable starting point for non-active site inhibition strategies.

1.6 Research aims

This study was aimed at identifying possible peptide binding partners for PfAdoMetDC/ODC. These peptides could be part of native, endogenous malarial proteins, thus giving an indication of other malarial proteins with which PfAdoMetDC/ODC have protein-protein interactions. Alternatively, peptides with affinity to PfAdoMetDC/ODC that can be used as possible lead molecules for drug development can be isolated.

- **Chapter 2: Optimisation of the heterologous expression and isolation of PfAdoMetDC/ODC.** Various experimental strategies were executed in an attempt to purify PfAdoMetDC/ODC from contaminating proteins that are present following affinity purification. The identity of these contaminating proteins and their possible origins were investigated.
- **Chapter 3: Identification of peptide binding partners to PfAdoMetDC/ODC through the use of a *P. falciparum* phage display library.** Phage display was performed to identify possible peptide binding partners to PfAdoMetDC/ODC. A *P. falciparum* cDNA library cloned into the lytic T7 phage was employed.
- **Chapter 4: Concluding Discussion**

Chapter 2: Optimisation of the heterologous expression and isolation of PfAdoMetDC/ODC

2.1 Introduction

2.1.1 S-Adenosylmethionine decarboxylase/Ornithine decarboxylase

Polyamines and their biosynthetic enzymes occur in increased concentrations in proliferating cells, which includes cancerous cells as well as parasitic organisms. As such, the inhibition of polyamine metabolism is considered to be a rational approach for the development of anti-parasitic drugs (Heby et al., 2003). Polyamine synthesis in *P. falciparum* is facilitated by a single open reading frame that encodes both rate-limiting enzymes in the polyamine pathway, namely ornithine decarboxylase (ODC) and S-adenosylmethionine decarboxylase (AdoMetDC) (Müller et al., 2000). This bifunctional protein decarboxylates both ornithine and S-adenosylmethionine to form putrescine and decarboxylated S-adenosylmethionine, from which spermidine is formed by spermidine synthase (Müller et al., 2001).

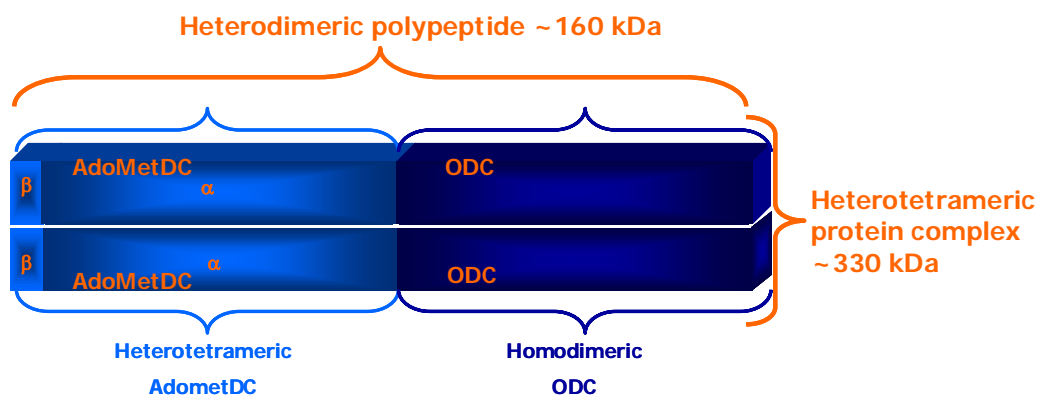


Figure 2.1: Schematic organization of the various domains and parasite-specific inserts of the bifunctional PfAdoMetDC/ODC. Adapted from (Birkholtz, 2002).

In the bifunctional enzyme, the AdoMetDC/ODC domains are assembled in a heterotetramer of approximately 330 kDa that is formed by the ~150 kDa heterotetrameric AdoMetDC (α and β subunits) and the ~180 kDa homodimeric ODC (Birkholtz et al., 2004) (Fig 2.1). The N-terminal AdoMetDC is a pro-enzyme that cleaves itself between the putative cleavage sites Glu-72 and Ser-73 into a large α subunit, generating a catalytically indispensable pyruvoyl residue, which is derived from the serine residue at the new N-terminal, and a small β subunit of approximately 9 kDa. The functional heterotetrameric complex thus consists of two subunits each of the 160 kDa α -AdoMetDC/ODC and the 9 kDa β -AdoMetDC (Heby et al., 2003; Müller et al., 2000; Wells et al., 2006; Wrenger et al., 2001).

The AdoMetDC domain appears at the N-terminus of the bifunctional peptide, from residues 1-529. Like the human enzyme, it consists of an $(\alpha\beta)_2$ dimer, but unlike other AdoMetDC enzymes, the Plasmodial enzyme is not stimulated by putrescine (Ekstrom et al., 1999; Wells et al., 2006; Wrenger et al., 2001). Although Plasmodial AdoMetDC domains differ significantly from other eukaryotic enzymes, the active site and surrounding surface contain only four substitutions. As can be seen in Fig 2.2 A, the active site is located between the two β -sheets comprised of eight β -strands each in the homodimeric model of the enzyme. These β -sheets are surrounded by eleven α -helices (Wells et al., 2006).

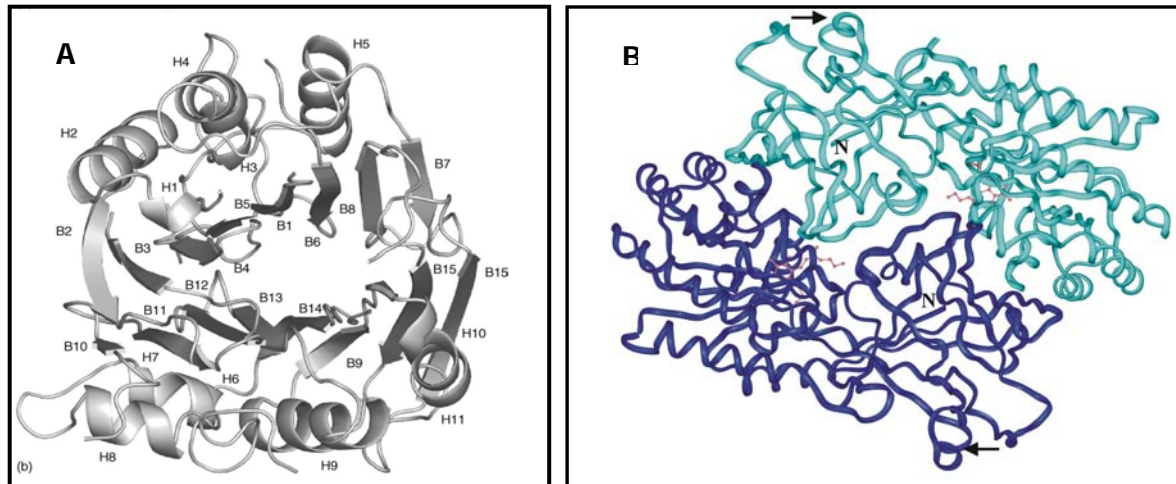


Figure 2.2: Model of A: the homodimeric form of PfAdoMetDC and B: the dimeric form of PfODC, as viewed from beneath (Birkholtz et al., 2003; Wells et al., 2006).

The ODC domain occurs at the C terminus of the bifunctional peptide, from residues 805-1419. It contains regions of homology to the mammalian ODC, especially concerning the residues involved with co-factor binding, structural features and catalytic activity, although these regions are interspersed with parasite-specific inserts (Birkholtz et al., 2004; Müller et al., 2000). As in other eukaryotes, the activity of the *P. falciparum* ODC is dependent on the formation of a homodimer, with two active sites that is formed by residues from both monomers occurring at the interface formed by the two monomers (Fig 2.2 B). This interface is distinguished by an aromatic amino acid zipper, formed by the head-to tail association of the two ODC monomers, which places the C-terminal area of one of the ODC monomers vertical to the N-terminal area of the other monomer (Birkholtz et al., 2003). In contrast to mammalian ODC, there is no clearly defined C-terminal PEST region, although this region does contain a high occurrence of Pro, Glu and Ser (Müller et al., 2000).

Both the ODC and AdoMetDC domains contain parasite-specific inserts that disrupt the regions of homology (Müller et al., 2000) (Fig 2.3). There are six parasite-specific areas that vary in size, from 7-274 residues. These areas contain a high percentage of charged residues like Asn and

Lys, are not significantly antigenic and have a distinct hydrophilic nature. Low complexity regions have been predicted for all the inserts, with the exception of O₁ (Birkholtz et al., 2004). It has been hypothesised that such low complexity regions in proteins may promote protein-protein interactions (Karlin et al., 2002). This hypothesis is further supported by the fact that protein areas high in glutamine/asparagine residues, so-called 'prion domains', have been implicated in mediating protein-protein interactions (Michelitsch and Weissman, 2000).



Figure 2.3: Schematic representation of the various parasite-specific inserts of PfAdoMetDC/ODC.

Initially, it was thought that AdoMetDC contains only 1 insert. The original insert A₁ consisted of 197 residues in the AdoMetDC region (residues 214-410) with significant α -helical areas. It is necessary for the decarboxylase activity of both domains, as seen in the loss of activity after deletion of this insert. Although it appears that this insert is not directly involved in the physical interactions that is important for the formation of the bifunctional complex, the interactions between the domains was disrupted by the conformational changes induced by the loss of this insert (Birkholtz et al., 2004). However, recently published results showed that there are indeed three parasite-specific inserts in the AdoMetDC domain, namely insert A₁ (residues 55-62), A₂ (residues 110-137) and A₃ (residues 260-407) (Wells et al., 2006). Mutational analysis to determine the effect of these inserts on the dimerization and decarboxylase activities of the bifunctional enzyme is currently underway.

A hinge region of 274 amino acids, from residue 530-804 connects the AdoMetDC and ODC regions (Müller et al., 2000). Several secondary structures occur in this region, notably 2 α -helices and 1 β -sheet (Birkholtz et al., 2004; Roux, 2006). It has been shown that the α -helices have an indirect effect on the catalytic activities of both enzyme domains due to contributions to interdomain interactions. Deletion of the β -sheet appeared to result in multiple conformations of the bifunctional enzyme, with variable catalytic activity, suggesting that this secondary structure is essential for the stabilization of the entire protein (Roux, 2006).

There are two inserts in the ODC domain of PfAdoMetDC/ODC, a smaller, 39 amino acids insert O₁ from residues 1047-1085, and a larger 147 amino acids insert O₂ from residues 1156-1302. The O₁ insert has considerable secondary structure, with four anti-parallel β -sheets and an α -

helix. Mutational analyses showed that the mobility of this insert is vital for the decarboxylase activities of both domains since the correct positioning of the α -helix mediates physical contacts between the two domains. The O₂ insert forms no significant secondary structures and is more important for ODC activity than for AdoMetDC activity since it is spatially removed from the N-terminal (Birkholtz et al., 2004). However, this insert contains several (NND)_x-repeats that is thought to play an important role in the formation of the ODC homodimer through the formation of a polar zipper (Birkholtz et al., 2004; Roux, 2006). This is not unusual for a *P. falciparum* protein, as it has been shown that ~35% of these proteins contain amino acid repeats, with asparagines occurring the most. It has been suggested that these repeats form structures that extend out from the folded protein core (Singh et al., 2004).

It is clear that these parasite-specific inserts mediate the essential protein-protein interactions necessary for the formation of the heterotetrameric complex and as such, the activity of the bifunctional protein. It has been suggested that by targeting interdomain interactions, one could obtain non-active site inhibition of the enzyme (Birkholtz et al., 2004).

Since the activity of especially the ODC domain of the bifunctional enzyme is dependent on dimerization (Wrenger et al., 2001) that is mediated by the parasite specific inserts (Birkholtz et al., 2004), it is possible that interface peptides or peptidomimetics can inhibit its activity, as was the case with the Plasmodial triosephosphate isomerase (Singh et al., 2001). It has also been shown that for *T. brucei* ODC, mutations far removed from the active site had an impact on activity, which could imply that therapeutic agents that target non-active site residues could have an effect on the activity of the enzyme (Myers et al., 2001). However, since no crystal structure exists to date for this enzyme and the exact residues involved in the interactions are not known, direct design of molecules that disrupt the protein-protein interactions is not possible. One approach to finding peptides that bind to this protein is through the use of high-throughput systems such as phage display (See Chapter 3). Peptides thus identified could ultimately lead to novel chemotherapeutic drugs in the fight against this deadly disease. However, the use of phage display requires pure bait protein. This chapter deals with the purification of recombinant PfAdoMetDC/ODC for use as bait protein.

A part of this work was presented at the SASBMB XXth Conference 2006.

2.2 Materials and methods

2.2.1 Isolation and cloning of *PfAdoMetDC/ODC* (PlasmoDB accession number Pf10_0322)

The complete coding region of *PfAdoMetDC/ODC* was amplified and cloned into the expression vector pASK-IBA3 (IBA GmbH, Germany) by Sylke Müller and co-workers. In short, genomic DNA from *P. falciparum* 3D7 cultures was used as template during the amplification reaction using *Pfu* DNA polymerase (Stratagene, USA), together with the sense oligonucleotide (5'-GCGCGCGGTCTCCAATGAACGGAATTTTTGAAGG-3') and the antisense oligonucleotide (5'-GCGCGCGGTCTCCGCGCTCCAATGTTTGTGGTTGCCCC-3'). Both the PCR product and expression vector was digested with the restriction enzyme *Bsa*I and ligated to form the final construct, hereafter referred to as pIBA3-PfA/O (Müller et al., 2000).

2.2.2 Plasmid isolation

Plasmids were isolated using either the High Pure Plasmid Isolation kit (Roche Diagnostics, Germany) or the E.Z.N.A.[®] Plasmid Miniprep Kit I (Pierce and Warriner, Germany). Both these isolation kits make use of alkaline lysis to release the DNA from the cells, with the removal of the RNA with RNase. Plasmid DNA is completely re-annealed by a high salt, low pH buffer but due to its size the genomic DNA does not anneal fully. The genomic DNA can thus be removed together with the proteins and other cellular debris by centrifugation. Plasmid DNA binds to glass fibres in the presence of the chaotropic salt guanidine-HCl through the formation of salt-bridges, and is purified by a series of wash steps. Elution of the plasmid DNA is achieved by low ionic strength conditions. The procedure used for High Pure Plasmid Isolation kit is explained below. The composition of the E.Z.N.A.[®] Plasmid Miniprep Kit I is proprietary and the kit was used as per manufacturers instructions.

E. coli cells, transformed with the appropriate plasmid, were grown overnight with agitation (250 rpm) at either 30°C or 37°C (depending on the availability of incubators) in 5 ml Luria-Bertani liquid medium (LB-Broth) (1% w/v tryptone, 1% w/v NaCl and 0.5 % w/v yeast extract, pH 7.5) containing 50 µg/ml ampicillin (Roche Diagnostics, Germany). The cultures were centrifuged at 1 600xg for 30 sec in a Hermle z232M centrifuge (Hermle Labortechnik GmbH, Germany) and the pellet resuspended in 250 µl Suspension buffer (50 mM Tris-HCl, 10 mM EDTA, pH 8.0) containing 0.1 mg/ml RNase. 250 µl Lysis Buffer (0.2 M NaOH, 1% w/v SDS) was added and the solution incubated for 5 min at room temperature. After the addition of 350 µl ice-cold Binding Buffer (4 M guanidine hydrochloride, 0.5 M potassium acetate, pH 4.2) and a 5 min incubation on ice, the sample was centrifuged for 10 min at 16 100xg in a Hermle z232M centrifuge. The supernatant was transferred to a High Pure filter tube and centrifuged for 1 min at 16 100xg

after which the flow-through was discarded. 500 μ l Wash buffer I (5 M guanidine hydrochloride, 20 mM Tris-HCl, 37% v/v ethanol, pH 6.6) was added and the column centrifuged for 1 min at 16 100xg. The flow-through was discarded and 700 μ l Wash Buffer II (20 mM NaCl 2 mM Tris-HCl, 80% v/v ethanol, pH 7.5) was added and the column centrifuged as above. The column was centrifuged for a second time to remove any residual Wash buffer II and the DNA eluted with 100 μ l Elution Buffer (10 mM Tris-HCl, pH 8.5) by centrifugation for 30 sec at 16 100xg. The concentrations of the plasmid DNA were determined spectrophotometrically as described below.

2.2.3 Quantification of nucleic acids: (Sambrook et al., 1989)

The concentrations of the oligonucleotides and DNA were calculated from the absorbance at 260 nm (A_{260}) obtained with the GeneQuant Pro Spectrophotometer (Amersham Biosciences, England) using the following equation:

$$\text{Concentration} = A_{260} \times 1 \text{ absorption unit at } A_{260} \times \text{dilution factor}$$

One absorbance unit at 260 nm is equal to 50 ng/ μ l double stranded DNA and 33 ng/ μ l single stranded DNA. Due to the fact that pure double stranded DNA should have an absorbency ratio of 260 nm to 280 nm of 1.7-1.9, the $A_{260/280}$ ratio was used as an indication of protein contamination and thus purity.

2.2.4 Preparation of Heat-shock competent cells (Hanahan et al., 1991)

Heat-shock competent *E. coli* cells were prepared as follows: the cells were inoculated from -70°C stock in 500 μ l LB-Broth and grown with agitation (250 rpm) at 37°C for 2 ½ hrs. The culture was plated onto LB-agar (LB-Broth, 1% w/v agar) plates and grown overnight at 37°C. A single colony was inoculated in 5 ml SOB (2% w/v tryptone, 0.5% w/v yeast extract, 0.05% w/v NaCl, 10 mM MgCl₂ and 10 mM MgSO₄) and grown overnight at 37°C with agitation. Alternatively, 5 ml of SOB was inoculated directly from frozen *E. coli* cell stocks and grown overnight at 37°C with agitation. The entire 5 ml of culture was added to 50 ml LB-Broth and incubated with agitation at 30°C until an OD₆₀₀ = 0.3 was reached. Subsequently, the cells were incubated on ice for 10 min, after which they were centrifuged for 15 min at 1000xg at 4°C in a Beckman model J-6 centrifuge (Beckman, USA). The pellet was dissolved in 16.7 ml ice-cold CCMB 80 medium (80 mM CaCl₂.2H₂O, 20 mM MnCl₂.4H₂O, 10 mM K⁺CH₃COO⁻, 10 mM MgCl₂.6H₂O, 10% v/v glycerol, pH 6.4) and incubated on ice for 20 min. After centrifugation, the pellet was dissolved in 8.4 ml ice-cold CCMB 80 medium. The cells were aliquotted in 200 μ l amounts in Eppendorf tubes and stored at -70°C.

2.2.5 Transformation of cells using heat shock method

The prepared competent cells in Eppendorf tubes were thawed from -70°C on ice. After the plasmid was added to 100 μl cells the reaction was incubated on ice for 30 min, followed by heat shock for 90 sec at 42°C . Subsequently, the reaction was incubated on ice for 2 min, after which 900 μl prewarmed LB-glucose (LB-Broth, 20 mM glucose) or SOC (SOB, 20 mM glucose) was added. The cells were incubated for 1 hr with agitation at 37°C . The transformation mix (50-100 μl) was plated onto LB-agar plates containing ampicillin (100 $\mu\text{g/ml}$). The plates were incubated overnight at 37°C .

2.2.6 Subcloning of *PfAdoMetDC/ODC* into pASK-IBA43+

The complete coding region of *PfAdoMetDC/ODC* was cloned into the expression vector pASK-IBA43+ (IBA GmbH, Germany) that encodes a N-terminal hexahistidine tag and a C-terminal *Strep*-tag II to allow tandem affinity purification of the recombinant protein.

2.2.6.1 Subcloning Primer design

Sequence specific forward (Forward 43+) and reverse (Reverse 43+) primers were designed with *Bsa*I recognition (5' GGTCTC(N)₁↓ 3') (3' CCAGAG(N)₅↓ 5') sites to adapt the *PfAdoMetADC/ODC* gene for the precise insertion into the expression vector pASK-IBA43+ according to specifications given by the manufacturer. The internal stability, self-complementary, primer pair compatibility and composition of all primer sequences were investigated with the oligonucleotide-designing program OLIGO V4.0 (National Biosciences, USA). The annealing temperature was calculated according to the following formula:

$$T_m = 69.3 + 0.41(\%GC) - 650/\text{length}.$$

The primers were dissolved in 10 mM Tris-HCl (pH 8) and the concentration was determined spectroscopically (section 2.2.3).

2.2.6.2 Optimisation of amplification of *PfAdoMetDC/ODC*

All PCR reactions were performed in 200 μl thin walled tubes (Quality Scientific Plastics, USA) in either a Perkin Elmer GeneAmp PCR system 2400 or system 9700 (PE Applied Biosystems, USA). The 25 μl reactions contained 1x Takara ExTaq Reaction Buffer™ (2 mM Mg^{2+} , proprietary solution) (Takara, Japan), 0.2 mM each dNTP (Takara, Japan), 5 pmol each of the primers Forward 43+ and Reverse 43+ and 1 U of Takara ExTaq™ (Takara, Japan), which is a high fidelity DNA polymerase mixture of *Pfu* DNA polymerase and *Taq* DNA polymerase. 0.7-2.8 μg pIBA3-PfA/O as described in section 2.2.1 and isolated as in section 2.2.2 was used to optimise the amount of template needed. The cycling reaction was performed as follows: an initial denaturation step was executed at 94°C for 3 min, incubation at 80°C for 2 min during which the enzyme was added as a hot-start, followed by 24 cycles of denaturation at 94°C for 30 sec, annealing at 60°C for 30 sec, extension at 65°C for 4 min, followed by a final incubation of 65°C

for 7 min. 65°C was used as extension temperature since it has been shown that large A+T rich Plasmidial sequences are amplified more efficiently using lower extension temperatures (Su et al., 1996). The above reaction was increased to ten 25µl reactions (0.695 pg template each) to obtain sufficient DNA for further reactions.

2.2.7 Agarose gel electrophoresis of PCR products

All PCR reactions were analyzed on 1% w/v agarose (Promega, USA)/TAE (0.04 M Tris-acetate, 1mM EDTA, pH 8) gels in TAE running buffer at 4-10 V/cm in a Hoefer HE 33 mini submarine electrophoresis unit (Amersham Biosciences, England). Each sample was loaded in 1x loading dye (0.025% w/v bromophenol blue and 30% v/v glycerol). GeneRuler™ 1 kb DNA ladder (Fermentas, USA) was used as molecular marker. The agarose/TAE gels either contained EtBr (50 µg) or were stained in a 10 µg/ml EtBr solution for approximately 30 min. The DNA bands were visualized under UV-light with a Spectroline TC-312 AV transilluminator (Spectronics Corporation, USA) at 312 nm. A CCD camera coupled to IC Capture software (The Imaging Source Europe, Germany) was used to capture the image.

2.2.8 Purification of PCR products

The Nucleospin® Extract II (Macherey-Nagel GmbH & Co.KG, Germany) method is based on the binding of DNA to silica in the presence of chaotropic salts. The buffers in the kit are proprietary, but buffer NT contains chaotropic salts, buffer NT3 is ethanolic and elution occurs under low ionic strength conditions with the slightly alkaline NE buffer (5 mM Tris-HCl, pH 8.5). After amplification, PCR reactions were pooled and 2 volumes of buffer NT were added for each 1 volume of sample. Alternatively, if the DNA sample was purified from an agarose gel, 200 µl NT buffer was added for each 100 mg of agarose gel and the sample incubated at 50°C for 10 min to completely dissolve the gel. The sample was pipetted onto a NucleoSpin® Extraction column and centrifuged for 1 min at 11 000xg, after which the flow-through was discarded. 600 µl of buffer NT3 was added and the column centrifuged for 1 min at 11 000xg. To facilitate complete removal of the ethanolic buffer NT3, the column was centrifuged for 2 min at 11 000xg. 15-50 µl of elution buffer NE was added and the column incubated for 1 min at room temperature before centrifugation for 1 min at 11 000xg. The DNA concentration was determined by spectrophotometry (section 2.2.3).

2.2.9 Cloning protocols

2.2.9.1 Ligation of *PfAdoMetDC/ODC* into the pGem®-T Easy vector (Promega, USA.)

During PCR amplification *Taq* polymerase adds a non-template dependent adenosine residue at the 3' end of each strand synthesized. Since the pGem®-T Easy vector has a 3' T overhang in the multiple cloning site, *PfAdoMetDC/ODC* amplified with ExTaq™ can be cloned into the vector

using A/T cloning. The 3' T overhang also prevents recircularization of the vector. pGem[®]-T Easy vector contains T7 and SP6 RNA polymerase promoters, an ampicillin resistance gene for primary selection, as well as the *LacZ* gene which codes for the β-galactosidase α-peptide for secondary selection using blue-white selection. This works on the basis of insertional deletion: if the ligation reaction is unsuccessful, the gene is intact and β-galactosidase is produced. This enzyme cleaves 5-bromo-4-chloro-3-indolyl galactoside (Xgal), to give a blue product. Isopropyl-D-galactoside (IPTG) is added as inducer of the *lac* operon, which controls the production of the β-galactosidase α-peptide. White colonies indicate the absence of the enzyme and thus positive clones. Since the vector: insert molar ratio must be 3:1 for optimal sticky end ligation (Sambrook et al., 1989), the amount of DNA needed for the reaction was calculated from the following formula:

$$\frac{(\text{ratio of insert: vector}) \times \text{ng vector} \times \text{kb size of insert}}{\text{kb size of vector}} = \text{ng insert required}$$

The ligation reaction (20 μl final volume) contained 208 ng insert, 1x Rapid ligation Buffer (20 mM Tris-HCl (pH7.8), 20 mM MgCl₂, 20 mM DTT, 2 mM ATP, and 10% v/v polyethylene glycol), 50 ng pGem[®]-T Easy vector and 3 Weiss units T4 DNA ligase. 1 Weiss unit is defined by the manufacturer as the amount of enzyme needed at 16°C to catalyse the ligation of more than 95% of 100 μg Lambda DNA digested with *HindIII*, in 20 min. The reaction was incubated at 4°C for at least 16 hrs prior to transformation.

2.2.9.2 Transformation of ligation reaction

Heat shock competent DH5α (Gibco BRL Life Technologies, USA) *E. coli* cells were prepared as in section 2.2.3 and transformed with 5 μl of the ligation reaction as described in section 2.2.4. Transformation mix (50–100 μl) was plated onto LB-agar plates supplemented with 100 μg/ml ampicillin which were previously coated with 20μl Xgal (50 mg/ml) and 100 μl IPTG (100 mM) according to the manufacturers instructions for blue-white selection. The plates were incubated overnight at 37°C. White colonies indicated possible positive clones.

2.2.9.3 Screening for positive clones: Restriction enzyme digestion

Five possible positive clones (pGem-PfA/O) were picked and grown overnight in LB-Broth containing 50 μg/ml ampicillin as a means of selection, since the positive clones should contain the pGem[®]-T Easy vector with the ampicillin resistance gene. Stocks were made of these clones and frozen away at –70°C in LB-Broth containing 15% v/v glycerol. Plasmids were isolated from the overnight cultures using the High Pure Plasmid Isolation Kit (Roche Diagnostics, Germany) (section 2.2.2) according to the manufacture's specifications.

The restriction enzyme digestions were set up as follows: plasmid DNA isolated with the High Pure Plasmid Isolation kit (between ~0.5-1.2 μg) was digested overnight at 37°C with 12 U *EcoRI* (Promega, USA) in Buffer H (90 mM Tris-HCl, 10 mM MgCl_2 , 50 mM NaCl, pH 7.5). The reaction was terminated when the digestions were electrophoresed on a 1% w/v agarose/TAE gel at 4-10 v/cm. The gel was stained in a 10 $\mu\text{g}/\text{ml}$ EtBr solution for approximately 30 min and the DNA bands were visualized under UV-light.

2.2.10 Subcloning of *PfAdoMetDC/ODC* into pASK-IBA43+

PfAdoMetDC/ODC was amplified from pIBA3-PfA/O using primers that inserted *BsaI* recognition sites for precise cloning into pASK-IBA 43+ and cloned into pGem[®]-T Easy for more efficient subcloning (see section 2.2.9). Saturated cultures of DH5 α cells containing pGem-PfA/O and pASK-IBA43+ were used for plasmid isolation according to section 2.2.2.

pGem-PfA/O (~1.6 μg) and the pASK-IBA43+ vector (~1.4 μg) were digested with 20 U of *BsaI* (New England Biolabs, UK) for 1 h at 50°C to generate the sticky ends needed for ligation. After restriction enzyme digestion, pASK-IBA43+ was incubated with 1 U of Shrimp Alkaline Phosphatase (SAP, Promega, USA) for 45 min at 37°C. SAP catalyses the dephosphorylation of 5' phosphate groups from DNA, thereby preventing the recircularization of the vector. The *BsaI* and SAP were heat-inactivated by incubation at 65°C for 20 min. Both the digested vector and insert reactions were run on a 1% agarose/TAE gel as described in section 2.2.7. The correctly sized bands were excised and purified with the Nucleospin[®] Extract II (Macherey-Nagel GmbH & Co.KG, Germany) purification kit (see section 2.2.8).

The amount of plasmid and insert required for efficient ligation was calculated as explained in section 2.2.9. Ligation reaction was performed using the rapid ligation system from Promega, USA: The ligation reaction (20 μl final volume) contained 96 ng insert, 1x Rapid ligation Buffer (20 mM Tris-HCl, pH7.8, 20 mM MgCl_2 , 20 mM DTT, 2 mM ATP, 10% polyethylene glycol), 25 ng pASK-IBA43+ and 3 Weiss units T4 DNA ligase.

Heat shock competent DH5 α *E. coli* cells (Gibco BRL Life Technologies, USA) were prepared as in section 2.2.4 and transformed with 5 μl of the ligation reaction as described in section 2.2.5. Transformation mix (50 –100 μl) was plated onto LB-agar plates supplemented with 100 $\mu\text{g}/\text{ml}$ ampicillin and incubated overnight at 37°C.

2.2.10.1 Screening for positive clones

2.2.10.1.1 Colony screening PCR

In order to identify positive clones, 16 colonies were randomly picked and grown overnight in LB-Broth supplemented with 50 µg/ml ampicillin. Colony screening PCR was used to identify clones with the correct insert cloned into pASK-IBA43+ (pIBA43+-PfA/O). The 25 µl reactions contained 1x Takara ExTaq Reaction Buffer, 0.2 mM each dNTP, 5 pmol each of Forward 43+ and Reverse 43+ and 1 U of Takara ExTaq™ (Takara, Shuzo, Japan). As template, 1 µl of bacterial culture was used. The cycling reaction was run as follows: 94°C for 7 min to lyse the cells, 80°C for 2 min during which the enzyme was added as a hot-start, followed by 30 cycles of denaturation at 94°C for 30 sec, annealing at 50°C for 30 sec, extension at 65°C for 4 min, and a final incubation of 65°C for 7 min. The PCR products were analysed by running on a 1% w/v agarose/TAE gel and checked for the correctly sized product as described in section 2.2.7.

2.2.10.1.2 Restriction enzyme digestion

Plasmid isolation (section 2.2.2) was done on the clones that gave the correctly sized band with colony screening PCR, followed by restriction enzyme digestion using *Hind*III (Promega, USA) in Buffer E (6 mM Tris-HCl, 6 mM MgCl₂, 100 mM NaCl, pH 7.5) overnight at 37°C. The samples were analysed using a 1% w/v agarose/TAE gel to verify possible positive clones.

2.2.10.2 Automated nucleotide sequencing

The nucleotide sequence of the subcloned *PfAdoMetDC/ODC* as well as the original construct was determined with an automated ABI PRISM® 3100 Genetic Analyzer (PE Applied Biosystems, California, USA) based on the Sanger-dideoxy method. Automated sequencing uses dideoxynucleotide chain terminators where the incorporation of a labelled nucleotide cause chain termination at different stages of strand synthesis. Each type of nucleotide is coupled to a different fluorophore and the wavelength-specific light emitted by the dyes after excitation is used to determine the sequence in a single sequencing run. The sequencing reactions were done with BigDye® Terminator v3.1 Cycle Sequencing kit (Applied Biosystems, USA), the product precipitated and run on a denaturing electrophoresis gel.

The 20 µl sequencing reactions contained 4 µl Big Dye Ready Reaction mix version 3.1, 2 µl Big Dye Sequencing buffer (400 mM Tris-HCl pH 9.0, 10 mM MgCl₂), 5 pmol sequencing primer and as template 0.9-1.2 µg plasmid DNA. The cycle-sequencing reactions were run as follows: an initial denaturation step at 96°C for 1 min, followed by 25 cycles of denaturation at 96°C for 10 sec, the primer appropriate annealing temperature for 5 sec (see Table 2.1), extension at 60°C for 4 min and a final incubation of 60°C for 7 min. All sequencing reactions were run on either a Perkin Elmer GeneAmp PCR system 2400 or system 9700 (PE Applied Biosystems, USA). All the

truncated PCR products with incorporated chain terminators were precipitated to remove any un-incorporated labelled nucleotides, which can lead to high background readings. This was done by adding sodium acetate (final concentration of 83 mM, pH 4.6) and 2.5x the volume absolute ethanol to the entire sequencing mixture, followed by centrifugation for 30 min at 16 100xg at 4°C. The supernatant was aspirated and the pellets washed with 250 µl 70% v/v ethanol. After centrifugation for 15 min the supernatant was removed and the pellet dried *in vacuo*. The protocol outlined in the ABI PRISM® 3100 Genetic Analyzer user's manual was followed to analyse the samples, and the results confirmed by visual inspection of the electropherograms obtained.

Table 2.1: Sequence and T_m of sequencing primers used for the sequencing of PfAdoMetDC/ODC (Birkholtz, 2002; Roux, 2006).

Primer	Sequence	T _m °C
pASK-IBA 43+ forward	GAGTTATTTTACCACTCCCT	53
K215 A2 forward	GCTTCTACGTTTAAATTCTGTTCGG	63
ODCF1	GAATTTTTATAATGGAAAGTATATG	51.5
ODCR4	GTTTCGAATTAATAAATAAGTC	56
ODC seq 2	TATGAATTACATACATTTACCG	51
ODC R3	GAATTTATACAACTACTGATG	51
ODC seq 1	TATGGAGCTAATGAATATGAATG	53.5
ODC R1	GCTACTCATATCGAATACATCTCTAC	60
ODC seq 3	GAATTTAAAAGACCATTACGATCC	55
pASK-IBA 43+ reverse	CGCAGTAGCGGTAAACG	55

The sequences were aligned and a consensus sequences obtained with BioEdit v.5 (Hall, 1999). The consensus sequences were compared to the sequence of the original construct.

2.2.11 Recombinant protein expression and isolation of PfAdoMetDC/ODC

The ODC- and AdoMetDC- deficient *E. coli* cell line EWH331 (Hafner et al., 1979) made available by Dr H. Tabor (National Institutes of Health, MD, USA) was utilised for expression of PfAdoMetDC/ODC. pASK-IBA3 was used as the expression vector, since it allows for affinity purification of the recombinantly expressed proteins using the *Strep-tag*® purification system, which is derived from the interaction between biotin and streptavidin. The plasmid encodes for a C-terminally expressed *Strep-tag*® II (WSHPQFEK) that binds to the *Strep-Tactin* Sepharose with high affinity, allowing for the isolation of fusion protein under physiological conditions (IBA GmbH, Germany). Alternatively, the expression vector pASK-IBA43+ was used, since it encodes a N-terminal hexahistidine tag and a C-terminal *Strep-tag* II to allow tandem affinity purification

(TAP) of the recombinant protein. Immobilized Metal Affinity Chromatography (IMAC) was used for the first purification step, which entails purification using nickel-nitriloacetic acid chromatography with His-select Nickel Affinity gel (SIGMA, USA), based on the interaction between the hexahistidine tag and Ni^{2+} ion chelated on the agarose. Elution is effected by adding free imidazole. The eluted protein was then further purified using the *Strep-tag*[®] purification system.

pIBA3-PfA/O or pIBA43+-PfA/O (~ 15 ng each) was transformed into heat shock competent EWH331 cells (section 2.2.5). Transformed cells (50 μl) were plated onto LB-agar plates supplemented with 100 $\mu\text{g}/\text{ml}$ ampicillin and incubated overnight at 37°C. A positive colony was selected and grown overnight in LB-Broth containing 50 $\mu\text{g}/\text{ml}$ ampicillin. The saturated culture obtained was diluted 1:100 and grown at 37°C in a shaking incubator until optical density at $\text{OD}_{600} = 0.5$ units was reached. Protein expression is under the transcriptional control of the tetracycline operator/promotor. The tet promotor is highly regulated by the constitutive expression of the tet repressor, which gives rise to a balanced stoichiometry between the number of plasmids and the repressor molecules. Due to the fact that the tet operator/promoter is not functionally linked to the genetic background or other inherent bacterial regulation mechanisms, the expression of the recombinant protein only occurs after the chemical induction with anhydrotetracycline (AHT) which prevents 'leaky' expression. Protein expression was thus induced by the addition of 200 ng/ml AHT (IBA GmbH, Germany) and the cells were allowed to grow for a further 16 hrs at 22°C with agitation. The cells were harvested by centrifugation at 1 500xg for 30 min at 4°C in a Beckman model J-6 centrifuge. The resulting cell pellet was either frozen away at -20°C or used immediately. After thawing on ice, the frozen pellet was again centrifuged at 1 500xg for 15 min to remove any residual culture medium. All subsequent steps were performed either on ice or at 4°C.

The thawed or fresh cell pellet was resuspended in 8 ml cold Buffer W (100 mM Tris pH8, 1 mM EDTA, 150 mM NaCl, pH 8) containing 0.1 mM phenylmethylsulfonylfluoride (PMSF) (Roche Diagnostics, Germany), 1 $\mu\text{g}/\text{ml}$ aprotinin (Roche Diagnostics, Germany), both of which are serine protease inhibitors and 2.5 $\mu\text{g}/\text{ml}$ leupeptin (Roche Diagnostics, Germany), a serine and thiol protease inhibitor. Alternatively, Complete Mini Protease inhibitor cocktail tablets (Roche Diagnostics, Germany), which inhibit calpains as well as a variety of cysteine, serine and metalloproteases, were used. After a 30 min incubation on ice with 0.1 mg/ml lysozyme (Roche Diagnostics, Germany), the cells were sonicated for 6 cycles of 20 sec with a 40 sec rest interval. This was done with a Sonifier Cell Disruptor B-30 (Instrulab, South Africa) using a duty cycle of 90, an output control of 3 and a flat tip. The homogenized cells were ultracentrifuged at

100 000xg for 60 min at 4°C in a Beckman Avanti J-25 centrifuge (Beckman, USA) using a rotor with a fixed angle.

Affinity chromatography was performed at 4°C using a *Strep*-Tactin Sepharose (IBA GmbH, Germany) affinity column with a 1 cm³ bed volume. The soluble protein extract obtained after ultracentrifugation was run through the column thrice, followed by three washes with 10 column volumes buffer W. Elution was effected with 5 column volumes Buffer E (Buffer W containing 2.5 mM desthiobiotin, pH 8 (IBA GmbH, Germany)) since desthiobiotin, a biotin analogue, is a reversible competitor of the *Strep*-tag II. To remove the desthiobiotin, the column was regenerated with buffer R (Buffer W containing 1mM 4-hydroxy azobenzene-2-carboxylic acid (HABA), pH 8). 0.02% Brij 35, a non-ionic detergent, was added to the eluted protein to improve stability (Krause et al., 2000).

Alternatively, for tandem affinity purification, the following protocol was used: Following protein expression, the cell pellet was resuspended in 8 ml His Equilibration buffer (50 mM sodium phosphate, pH8, 0.3 M NaCl and 10 mM imidazole) containing 0.1 mM PMSF (Roche Diagnostics, Germany), 1 µg/ml aprotinin (Roche Diagnostics, Germany), and 2.5 µg/ml leupeptin (Roche Diagnostics, Germany). The cell suspension was then sonified and centrifuged as described above.

HIS-Select™ Nickel Affinity gel (SIGMA, USA) was used for either batch (500 µl) or column purification (1 ml, 1 cm³ bed volume). The protein extract was bound for either 30 min with rotation or run three times through the column, followed by 3 washes with 10 column volumes Wash/Equilibration buffer (50 mM sodium phosphate, pH 8, 0.3 M NaCl and 10 mM imidazole). The protein was eluted with 10 column volumes Elution buffer (50 mM sodium phosphate, pH 8, 0.3 M NaCl and 250 mM imidazole). The eluted protein was then further purified using the *Strep*-Tactin Sepharose column described above.

2.2.12 Protein concentration determination (Bradford, 1976)

The Bio-Rad Quick Start™ Bradford Protein assay (Bio-Rad Laboratories, USA) was used to determine the concentration of the purified recombinant proteins. It is based on the Bradford method of protein quantitation, where the electrostatic binding of the sulfonic groups of the Coomassie Brilliant Blue G-250 dye to basic and aromatic amino acids causes a shift in the absorbance of the dye from A₄₆₅ to A₅₉₅. 50 µl of the protein solutions was added to 150 µl Quick Start™ reagent, incubated for 15 min and the absorbance at 595 nm read with a Multiskan Ascent scanner (Thermo labsystems). A standard protein series ranging from 200

µg/ml to 6.25 µg/ml was prepared with Bovine serum albumin (BSA) and used to create a calibration curve.

2.2.13 Electrophoretic analysis

2.2.13.1 SDS-Polyacrylamide Gel Electrophoresis (SDS-PAGE) of proteins (Laemmli, 1970)

Denaturing SDS-PAGE was performed using a 4 % stacking gel (4% w/v acrylamide 0.13 M Tris-HCl, pH 6.8 and 0.1% w/v SDS) and a 7.5 % separating gel (7.5% w/v acrylamide, 0.375 M Tris-HCl, pH8.8 and 0.1% w/v SDS). The acrylamide (30% w/v acrylamide, 0.8% w/v N',N'-methylene bisacrylamide), Tris-HCl and SDS solutions were degassed for 15 min and polymerised by the addition of 50 µl 10% w/v ammonium persulphate (MP Biomedicals, France) and 5 µl TEMED (N,N,N',N'-Tetramethyl ethylenediamine, Merck, Germany).

The protein samples were diluted 4:1 in reducing sample buffer (0.0625 M Tris-HCl pH 6.8, 2% w/v SDS, 0.1% v/v glycerol, 0.05% v/v β-mercaptoethanol and 0.025% w/v Bromophenol Blue) and boiled for 5 min. PAGERULER Prestained Protein ladder or PAGERULER Protein ladder (Fermentas, USA) was used as molecular markers. Electrophoresis was carried out in Running buffer (25 mM Tris-HCl, 0.2 M glycine, 3.5 mM SDS buffer, pH 8.3) in a Biometra electrophoresis system (Biometra GmbH, Germany) with a preliminary voltage of 50 V until the separating gel was reached, followed by a voltage of 100 V until completion.

2.2.13.2 Native Polyacrylamide Gel Electrophoresis of proteins

Non-Denaturing SDS-PAGE was performed using a 4% stacking gel (4% w/v acrylamide 0.13 M Tris-HCl, pH 6.8) and a 7.5% separating gel (7.5 % w/v acrylamide, 0.375 M Tris-HCl pH8.8). The rest of the gel preparation was performed as above.

High Molecular weight Calibration kit (Pharmacia LKB Biotechnology Inc, USA) was used as a molecular marker. The protein samples and standards were diluted 4:1 in non-reducing sample buffer (0.0625 M Tris-HCl pH 6.8, 30 %v/v glycerol, and 0.1% w/v Bromophenol Blue) and boiled for 5 min or loaded as is. Electrophoresis was carried out as above in a 25 mM Tris-HCl, 0.2 M glycine buffer, (pH 8.3).

2.2.13.3 Visualization of protein gels

2.2.13.3.1 Silver staining (Merril et al., 1981)

Following SDS-Page, the proteins were visualised with a silver staining procedure with sensitivity in the nanogram range. The gels were fixed for at least 30 min in fixing solution (30% v/v ethanol, 10% v/v acetic acid) after which the gel was sensitised for 30 min in sensitising solution (30% v/v ethanol, 0.5 M sodium acetate, 0.5% v/v glutaraldehyde and 0.2% w/v

Na₂S₂O₃). Following three washes with dddH₂O for 10 min each, the gel was impregnated with silver for 30 min in silver solution (0.1% w/v AgNO₃, 0.25% v/v formaldehyde). Excess silver was removed from the surface by two brief washes with dddH₂O. The developing solution (2.5% w/v Na₂CO₃, 0.01% v/v formaldehyde) was used to reduce the silver ions to metallic silver, thereby visualising the protein bands. The reaction was terminated by the addition of 0.05 M EDTA.

2.2.13.3.2 Colloidal Coomassie (Neuhoff et al., 1988)

After SDS-PAGE, proteins were visualised with a staining method that utilise the colloidal properties of Coomassie Brilliant Blue G-250. It was found that the shifting of the dye from the colloidal form to the molecular dispersed form, as achieved by the addition of methanol, results in the complete diffusion of dye into the gel. This in turn results in complete protein staining with higher sensitivity (ng range) and less background staining. A 0.1% w/v Coomassie Brilliant Blue G-250 solution was prepared, (10% w/v ammoniumsulphate, 2% v/v phosphoric acid), which was diluted 4:1 with methanol and used to stain the protein gel for at least 24 hrs. After staining the gel was washed quickly in a 25% v/v methanol and 10% v/v acetic acid solution and destained in a 25% v/v methanol solution.

2.2.14 Western Blotting

Following SDS-PAGE of the affinity purified recombinant PfAdoMetDC/ODC, the gel was equilibrated in 10 mM CAPS (3-(cyclohexylamino)-1-propanesulfonic acid, pH >9 Sigma, USA) for 5 min to ensure that all proteins are positively charged. PolyScreen PVDF Transfer Membrane (Nen™ Life Science Products, USA) was prepared by wetting in methanol for 15 sec and then equilibrated in 10 mM CAPS (pH >9). The proteins were electrophoretically transferred to the PVDF membrane at 10 V for 45 min with a Trans-Blot® SD Semi-Dry Electrophoretic Transfer Cell (Bio-Rad Laboratories, CA). The membranes were blocked overnight at 4°C in blocking buffer (PBS with 3% w/v BSA, 0.5% v/v Tween-20, pH 7.4).

For immunodetection of the *Strep*-tag II, the membrane was incubated with gentle agitation in a 1:4000 dilution of monospecific, polyclonal *Strep*-tag II antibodies (IBA GmbH, Germany) in wash buffer (PBS with 1% w/v BSA, 0.5% v/v Tween-20, pH 7.4) for 1 hr at 37°C. The *Strep*-tag II peptide (WSHPQFEK), coupled to keyhole limpet hemocyanin, was used to produce these antibodies in rabbits. For the detection of His-tags, mouse anti-His antibody from mouse ascites fluid (Amersham Biosciences, UK) at a dilution of 1:700 was used. For the detection of DnaK, a 1:4000 dilution of mouse anti-DnaK was used. The DnaK antibodies were a kind gift from Prof G. Blatch, Rhodes University. The difference in the concentration of the primary antibodies was due to experimentally observed difference in activity.

The membranes were washed 3 times with wash buffer for 15 min at 37°C followed by incubation with horseradish peroxidase (HRP) conjugated goat anti-rabbit (Cappel™ Research Products, USA) or anti-mouse (Promega, USA) IgG at 1:10 000 or 1:1000 dilutions respectively in wash buffer for 45 min at 37°C. For the detection of anti-DnaK antibodies sheep anti-mouse HRP conjugated antibodies (SIGMA, USA) diluted 1:1000 in wash buffer was utilised. The membranes were washed 6 times with wash buffer for 10 min at 37°C to remove excessive background signal.

SuperSignal® West Pico Chemiluminescent Substrate (Pierce, USA) was used for chemiluminescent detection of the protein bands. The washed membranes were incubated for 5 min in equal volumes of the Luminol/Enhancer Solution and Stable Peroxidase Solution and encapsulated in plastic. The horseradish peroxidase enzyme conjugated to the secondary antibody generate a hydroxide ion that gives rise to the transition of luminol to 3' aminophthalate, with the concurrent emission of light.

Hyperfilm High Performance chemiluminescence film (Amersham Biosciences, England) was exposed to the membrane in an X-ray film cassette for 5 sec-1min. The film was developed for 1 min in either Structurix G128 Developer (AGFA, SA) or ILFORD Universal Paper Developer (ILFORD Imaging UK limited, UK), rinsed with dddH₂O and fixed for 3 min with either G333c Rapid Fixer (AGFA, SA) or ILFORD Rapid Fixer (ILFORD Imaging UK limited, UK).

2.2.15 Enzyme activity assays of AdoMetDC and ODC

The decarboxylase activities of the recombinantly expressed AdoMetDC and ODC were determined by measuring the amount of ¹⁴CO₂ released by the decarboxylation of S-adenosyl-(methyl-¹⁴C)methionine (60.7 mCi/mmol, Amersham) and L-(1-¹⁴C)ornithine (55 mCi/mmol, Amersham Biosciences, England) as described (Birkholtz et al., 2004; Müller et al., 2000; Wrenger et al., 2001). The results are reported as the specific activity (nmol/min/mg) and are the mean of 2 independent experiments performed in duplicate. The following formula was used to calculate the specific activity:

$$\text{Specific activity} = \frac{\text{CPM} \times \text{nmol substrate}}{(\text{mg protein}) \times \text{min} \times \text{total CPM}}$$

2.2.16 Sized exclusion-based purification of recombinantly expressed PfAdoMetDC/ODC

2.2.16.1 Ultracentrifugation size exclusion

Further purification of the affinity purified recombinant proteins was attempted using Nanosep 100 K Omega ultracentrifuge size exclusion columns (with a 100 kDa cut-off, Pall Corporation, USA). The columns were prepared by washing with dddH₂O at 4°C for 3 min at 1000xg in an Eppendorf Centrifuge 5415R (Eppendorf AG, Germany). 500 µl aliquots of the protein sample were applied to the column and centrifuged at 10 000xg at 4°C in an Eppendorf Centrifuge 5415R. After centrifugation the eluate was discarded and the sample resuspended in cold Buffer W.

2.2.16.2 Size-exclusion high pressure liquid chromatography (SEC-HPLC)

After affinity purification of the *Strep*-tagged PfAdoMetDC/ODC, further purification was attempted with SEC-HPLC using the Phenomenex Biosep-Sec-S-3000 column installed on a Millenium HPLC system. The silica based Biosep-Sec-S-3000 gel filtration column has an exclusion range of 5-700 kDa. All buffers were filtered through a 0.22 µm cellulose acetate filter (Sartorius, Germany) and degassed in a sonic waterbath prior to use. The eluted proteins from the *Strep*-Tactin affinity column in Buffer E was concentrated as in 2.2.9.1 and filtered through a 0.22 µm filter prior to application to the column. Using isocratic conditions and a flow speed of 0.5 ml/min, the column was equilibrated with Buffer W (100 mM Tris pH8, 1 mM EDTA/150 mM NaCl pH 7) and calibrated with a mixture of 1 mg/ml lysozyme (14.4 kDa), BSA (69 kDa) and thyroglobulin (670 kDa). The affinity-purified proteins were injected into the column and collected in 0.5 ml fractions. SDS-PAGE (section 2.2.5) was used to analyse the collected fractions.

2.2.17 Mass-Spectrometry Analysis of contaminating bands

Recombinant PfAdoMetDC/ODC expressed as described in section 2.2.4 was separated using a 7.5% SDS-PAGE gel, stained with colloidal coomassie (section 2.2.6) and sent to Prof John Hyde and Dr. Paul Sims, University of Manchester, UK for Mass Spectrometry-analysis.

2.3 Results

2.3.1 Recombinant expression and isolation of PfAdoMetDC/ODC

PfAdoMetDC/ODC was recombinantly expressed and purified using affinity chromatography. This was done in preparation for its use as bait protein in the search for peptide binding partners using a *P. falciparum* phage display library.

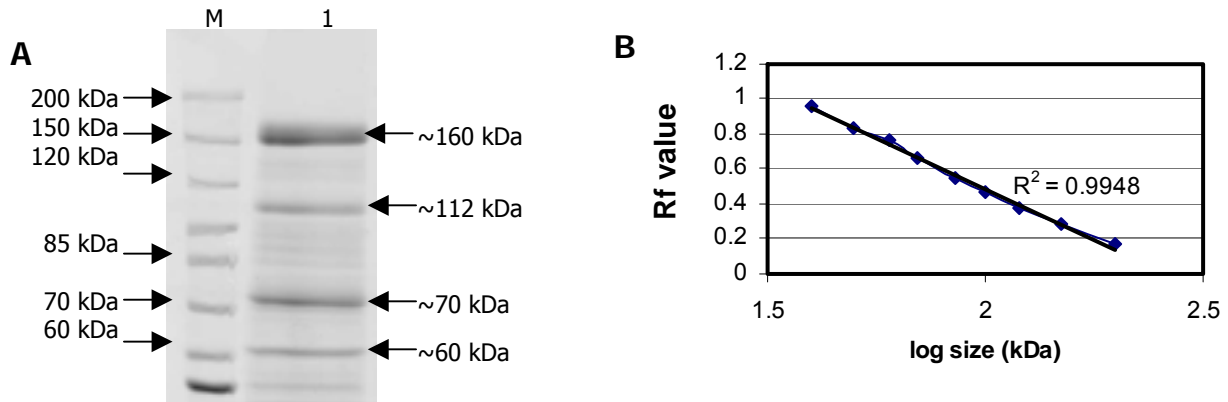


Figure 2.4: A: SDS-PAGE analysis of recombinantly expressed PfAdoMetDC/ODC with C-terminal *Strep*-tag; B: Calibration curve of Rf values.

Lane M: PageRuler™ Protein ladder used as molecular marker. Lane 1: *Strep*-tag purified PfAdoMetDC/ODC. The protein eluate was analysed on a 7.5% SDS-PAGE gel and visualised with silver staining.

As can be seen in Fig 2.4 A, affinity purification using *Strep*-Tactin Sepharose (IBA GmbH, Germany) of the recombinantly expressed protein with a C-terminal *Strep*-tag does not result in a homogenous protein solution, as visualised by silver staining. Instead, four major protein bands are obtained: the correctly sized ~160 kDa PfAdoMetDC/ODC, and three other protein bands at ~112 kDa, ~70 kDa and ~60 kDa (based on their Rf values, Fig 2.4 B). The origin of these smaller bands was subsequently investigated.

2.3.2 Determination of the origin of the contaminating fragments

PfAdoMetDC/ODC was produced using a recombinant bacterial expression system. This implies that these contaminating fragments could either be of heterologous origin (i.e. vector derived, or fragments of PfAdoMetDC/ODC) or *E. coli* proteins. If these proteins are of heterologous origin, they should carry the *Strep*-tag II encoded by the expression vector and can thus be identified using anti-*Strep*-tag II antibodies. Proteins originating from the bacterial host would not carry the *Strep*-Tag II and as such should not be detected with anti-*Strep*-tag II antibodies. If the contaminating proteins are of *E. coli* origin, their co-elution with PfAdoMetDC/ODC could be either due to the complex formation with the recombinant *Plasmodium* protein or due to non-specific binding with the Sepharose.

SDS-PAGE analysis of the eluate obtained after recombinant expression and affinity isolation of both the empty pASK-IBA3 expression vector and PfAdoMetDC/ODC cloned in to the pASK-IBA3 expression vector was performed to determine the origin of the contaminating fragments. As can be seen in Fig 2.5 A, affinity purification of the empty pASK-IBA3 did lead to the non-specific isolation of some proteins. However, these isolated proteins' sizes do not correlate exactly to the ~112 kDa, ~70 kDa and ~60 kDa bands previously seen. In addition, there are two large proteins respectively larger and smaller than the full-length PfAdoMetDC/ODC protein. Western blot analysis (section 2.2.14) using antibodies directed against *Strep*-tag II was performed to test whether these contaminating fragments are recombinantly produced with a C-terminal *Strep*-tag II, thus indicating their heterologous origin.

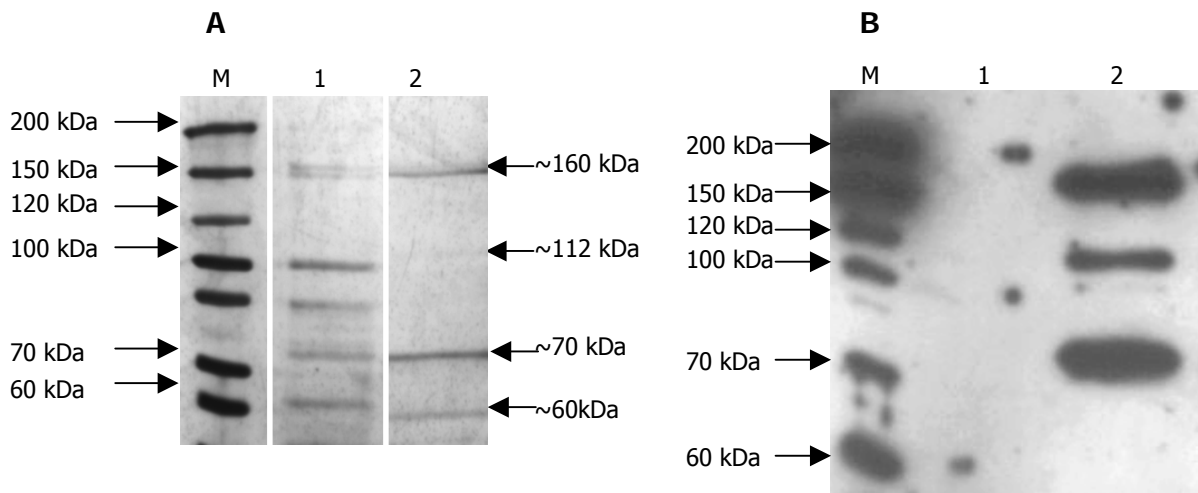


Figure 2.5: A: SDS-PAGE analysis of recombinantly expressed and affinity purified pASK-IBA3 and PfAdoMetDC/ODC; B: Western blot of recombinantly expressed and affinity purified pASK-IBA3 and PfAdoMetDC/ODC.

Lane M: PageRuler™ Protein ladder used as molecular marker. Each band contains an inherent *Strep*-tag II sequence and can thus be detected with anti *Strep*-tag II antibody. Lane 1: *Strep*-tag purified isolate from empty pASK-IBA3. Lane 2: *Strep*-tag purified PfAdoMetDC/ODC. The proteins were separated using 7.5% SDS-PAGE before Western blotting.

As can be seen from Fig 2.5 B lane 1, the 3 strongly contaminating proteins arise from the recombinant expression of the C-terminally tagged PfAdoMetDC/ODC itself and not from the expression vector, since on the Western blot no bands appear in the lane loaded with the expression product of empty pASK-IBA3. This implies that the bands seen with SDS-PAGE analysis (Fig 2.5 A lane 2), which does not correlate with the 3 strongly contaminating bands, may be due to background binding of *E. coli* proteins to the Sepharose. However, these bands are not routinely seen following the expression and isolation of PfAdoMetDC/ODC in pASK-IBA3 (Fig 2.4 and 2.5 A lane 2). The full-length protein (~160 kDa) as well as the contaminating fragments at ~112 kDa and ~70 kDa are strongly identified by the anti-*Strep*-Tag II antibody. These results show that these protein fragments carry the *Strep*-Tag II and are indeed of heterologous origin. Interestingly enough, the ~60 kDa band is not identified by the antibody,

indicating that this protein is of *E. coli* origin. Various methods were subsequently employed in an attempt to further purify the recombinantly expressed PfAdoMetDC/ODC to homogeneity.

2.3.3 Optimization of recombinant expression and isolation of PfAdoMetDC/ODC

2.3.3.1 Blocking of *Strep*-Tactin Sepharose

It is possible that these contaminating bands arise from non-specific binding of *E. coli* proteins to the *Strep*-Tactin Sepharose. Alternatively *E. coli* proteins may bind to the recombinant protein, thus leading to co-purification. To ascertain if this is the case, the *Strep*-Tactin Sepharose was blocked by incubating the Sepharose for 1 hr at 4°C with rotation in Buffer W containing 1% w/v casein to coat the Sepharose with protein and 0.5% v/v Tween-20 to prevent any non-specific hydrophobic binding of *E. coli* proteins to the Sepharose. The recombinantly expressed proteins were then purified as described in section 2.2.11, however, Buffer W was supplemented with 0.5% Tween-20 to prevent non-specific hydrophobic interactions. As can be seen in Fig 2.6, lane 2, the blocking of the resin did not succeed in preventing the co-purification of contaminating proteins, nor did the Tween-20 in the wash buffer prevent possible non-specific hydrophobic interactions with recombinant PfAdoMetDC/ODC itself, since the same contaminating bands appeared in both lane 1 (control) and lane 2. It is thus unlikely that the 3 strongly contaminating proteins are co-eluted due to non-specific interactions with either the Sepharose or the bifunctional protein.

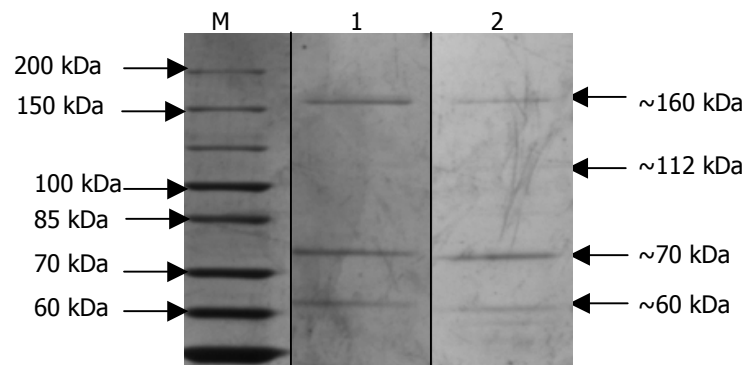


Figure 2.6: SDS-PAGE analysis of affinity purified PfAdoMetDC/ODC after blocking of *Strep*-tactin Sepharose.

Lane M: PageRuler™ Protein ladder used as molecular marker. Lane 1: *Strep*-tag purified PfAdoMetDC/ODC. Lane 2: Purified PfAdoMetDC/ODC using casein blocked *Strep*-tactin Sepharose and 0.5% Tween-20 in Buffer W. The proteins were analysed on a 7.5% SDS-PAGE gel and visualised with silver staining.

2.3.4 Tandem affinity purification (TAP)

2.3.4.1 Subcloning of PfAdoMetDC/ODC into pASK-IBA 43+

The complete coding region of PfAdoMetDC/ODC was subcloned into the expression vector pASK-IBA43+ (IBA GmbH, Germany) that encodes a N-terminal hexahistidine tag and a C-terminal *Strep*-tag II to allow TAP of the recombinant protein. By first isolating the recombinant

protein using Immobilised Metal Affinity Chromatography (IMAC) via a N-terminal His-tag, followed by isolation using the C-terminal *Strep*-tag II, a purer protein isolate may be obtained under physiological conditions (Legrain et al., 2000). Forward and reverse primers (see Table 2.2) were designed to amplify *PfAdoMetDC/ODC* prior to subcloning into pASK-IBA 43+.

Table 2.2: Characteristics of the primers designed for subcloning of *PfAdoMetDC/ODC* into pASK-IBA43+.

Blue: *Bsa*I recognition site, Pink: sequence prescribed by manufacturer for efficient subcloning, Green: gene specific sequence

Characteristic	Forward 43+	Reverse 43+
Sequence	GT CAT AGG TCT CAG GGCC ATG AAC GGA ATT TTT GAA GGA	GAT CTC GGT CTC TGC GCT CCA ATG TTT GTT TGG TTG CCC
Composition: A+T / C+G	55.3% 44.7%	46.2% 53.8%
Tm	70.5°C	74.7°C
MW g/mol	11 781.7	11 913.7
ΔG 3' end (kcal /mol)	-1.9	-4.3

These primers were used to amplify *PfAdoMetDC/ODC*. The amplification was optimised for the amount of template used in the amplification reaction.

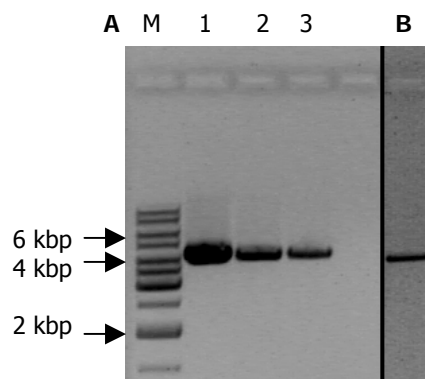


Figure 2.7: A: Optimisation of amount of template for amplification of *PfAdoMetDC/ODC*; B: large-scale amplification of *PfAdoMetDC/ODC*.

A: Lane M: GeneRuler 1 kbp DNA ladder used as molecular marker. Lane 1: Amplification of *PfAdoMetDC/ODC* using 2.8 pg template, Lane 2: 1.4 pg template and Lane 3: 0.7 pg template. B: Sample of the pooled large-scale amplification of *PfAdoMetDC/ODC* using 0.7 pg template. The DNA was analysed on a 1% agarose/TAE gel and visualised with EtBr.

Based on Fig 2.7 A lane 3, it was decided to use 0.7 pg template for the large scale amplification of the gene. After amplification, the PCR reactions were pooled and a 15 μ l sample of the pooled large-scale PCR products analysed on a 1 % agarose/TAE gel to verify the identity of the product obtained before purification (Fig 2.7 B).

2.3.4.2 Cloning of *PfAdoMetDC/ODC* in the pGem[®]-T Easy vector

Purified *PfAdoMetDC/ODC* PCR product was ligated into the pGem[®]-T Easy vector (Promega, USA) using A/T cloning and transformed into heat shock competent DH5 α *E. coli* cells. Positive clones were screened with *Eco*RI digestion, thus giving four DNA fragments, namely 3004 bp, 2167 bp, 1718bp and 418 bp (Fig 2.8).

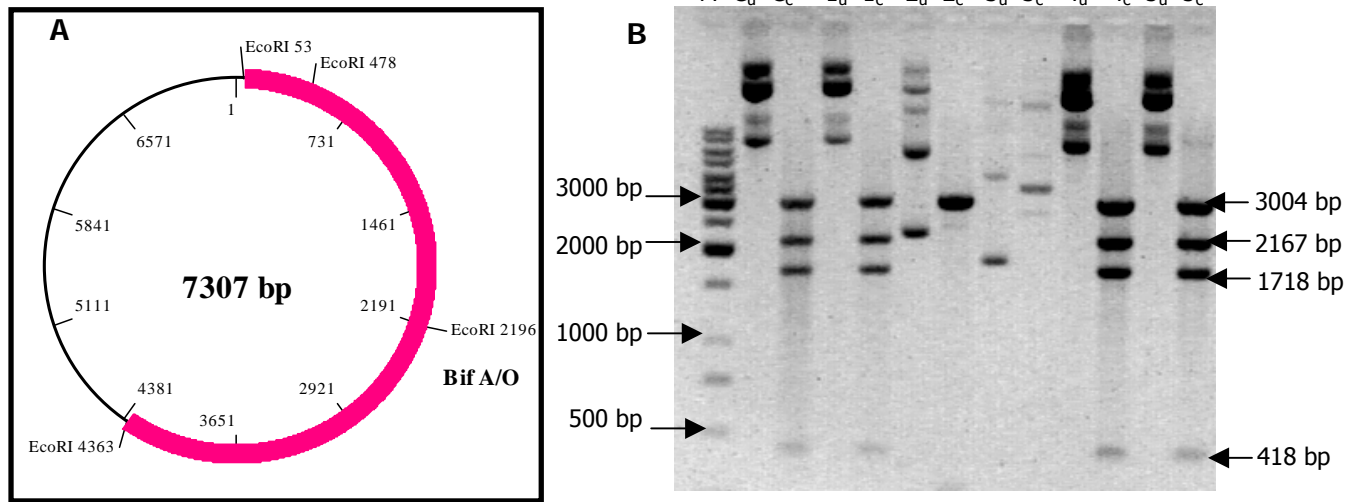


Figure 2.8: A: Fragments obtained after cutting *PfAdoMetDC/ODC* cloned into pGem[®]-T Easy with *EcoRI*. B: Screening for positive clones after ligating *PfAdoMetDC/ODC* into pGem[®]-T Easy.

Lane M: GeneRuler 1 kbp DNA ladder used as molecular marker. Lanes C_u, C_c is the positive control prior and following digestion with *EcoRI*. Lanes 1-5: The various positive candidates. The subscript u indicates uncut plasmid and the subscript c indicates digested plasmid. The DNA was analysed on a 1% agarose/TAE gel and visualised with EtBr.

From figure 2.8 it can be seen that 3 of the 5 plasmids were positive for the *PfAdoMetDC/ODC* insert, namely clones 1, 4 and 5. Subsequently, the complete coding region of *PfAdoMetDC/ODC* was excised with *BsaI* and subcloned into the expression vector pASK-IBA43+, transformed into DH5 α cells and screened with colony-screening PCR to determine the presence of positive clones (Fig 2.9).

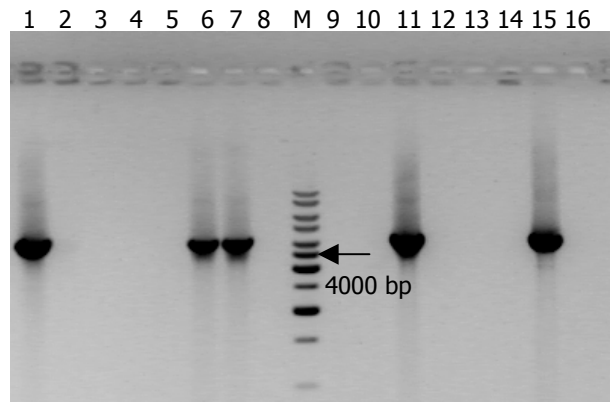


Figure 2.9: Gel electrophoresis of colony screening PCR of *PfAdoMetDC/ODC* cloned into pASK-IBA43+.

Lane M: GeneRuler 1 kbp DNA ladder used as molecular marker. Lanes 1-16: Amplification of *PfAdoMetDC/ODC* from possible positive clones. The DNA was analysed on a 1% agarose/TAE gel and visualised with EtBr.

5 clones gave the correctly sized band (~4257 bp) after PCR amplification using gene specific primers. Subsequently, plasmids were isolated from these clones and digested with *HindIII* to confirm the presence of the correct insert. As can be seen from Fig 2.10, *HindIII* digestion of positive clones should give fragments of 3942 bp, 3074 bp and 452 bp.

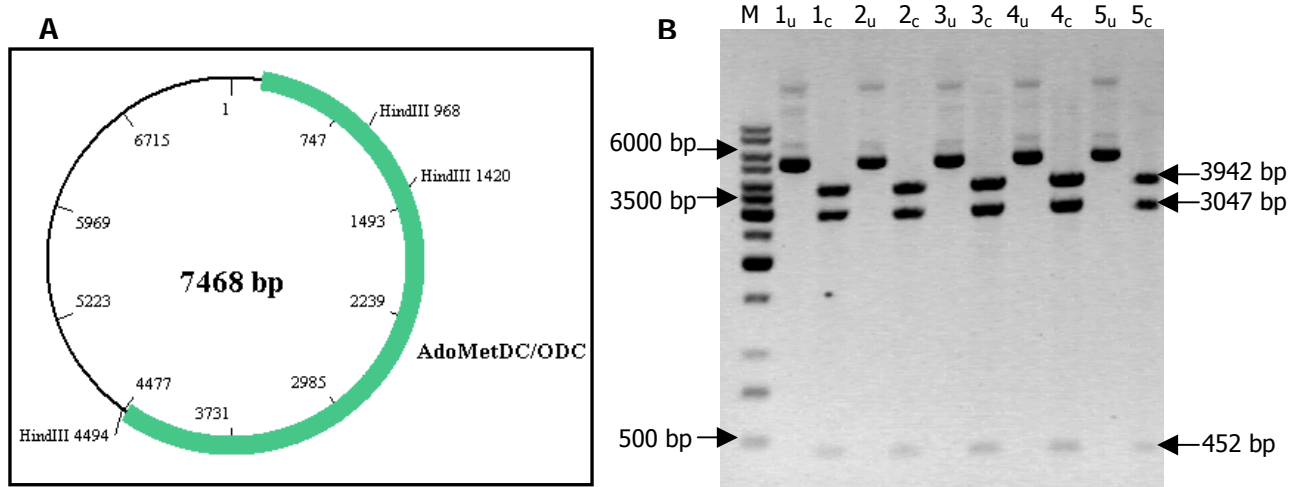


Figure 2.10: A: Vector map indicating the fragments obtained after digesting *PfAdoMetDC/ODC* cloned into pASK-IBA43+ with *HindIII*. B: Restriction enzyme digestion screening for positive clones after ligating *PfAdoMetDC/ODC* into pASK-IBA 43+.

Lane M: GeneRuler 1 kbp DNA ladder used as molecular marker. Lanes 1-5: The various positive candidates. The subscript u indicates uncut plasmid and the subscript c indicates digested plasmid. The DNA was analysed on a 1% agarose/TAE gel and visualised with EtBr.

These results show that *PfAdoMetDC/ODC* was successfully subcloned into pASK-IBA43+. The correct insertion of the gene into the vector was confirmed with sequencing (results not shown).

2.3.5 Comparison of the subcloned *PfAdoMetDC/ODC* to the original construct and tandem affinity purification (TAP)

2.3.5.1 SDS-Page analysis

PfAdoMetDC/ODC was recombinantly expressed with a N-terminal His-tag and a C-terminal *Strep*-tag II. To compare the expression of the double-tagged construct to that of the original one, the differently tagged *PfAdoMetDC/ODC* proteins were isolated using *Strep*-Tactin Sepharose and analysed using SDS-PAGE (Fig 2.11 lanes 1 and 2). The same pattern of protein bands following SDS-PAGE analysis was obtained for both the single and double-tagged *PfAdoMetDC/ODC* when isolated using only the interaction between the C-terminal *Strep*-tag II and the *Strep*-Tactin Sepharose. To test whether TAP succeeds in providing pure full-length protein, *PfAdoMetDC/ODC* in pASK-IBA43+ was expressed as in section 2.2.11 and isolated with TAP, first by Immobilized Metal Affinity Chromatography (IMAC) via the N-terminal His tag, followed by isolation through the C-terminal *Strep*-Tag II with *Strep*-Tactin Sepharose. As can be seen from Fig 2.11 lane 3, TAP of recombinantly expressed *PfAdoMetDC/ODC* with IMAC followed by the *Strep*-tag® purification system did not succeed in providing pure, full-length protein.

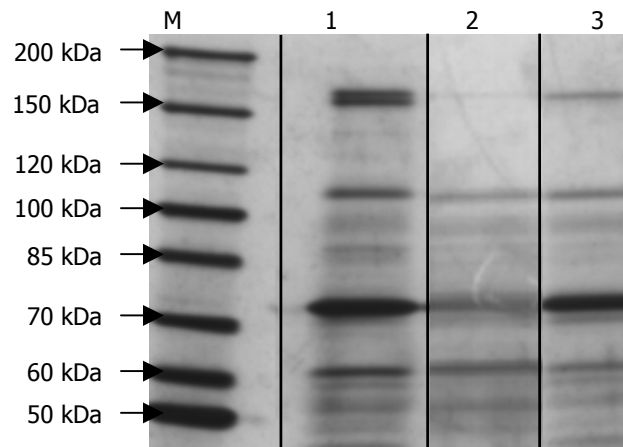


Figure 2.11: Comparison of expression and isolation of PfAdoMetDC/ODC from pASK-IBA3 and pASK-IBA43+ using affinity purification and TAP.

Lane M: PageRuler™ Protein ladder used as molecular marker. Lane 1: *Strep*-tag purified PfAdoMetDC/ODC expressed from pASK-IBA 3. Lane 2: *Strep*-tag purified PfAdoMetDC/ODC expressed from pASK-IBA 43+. Lane 3: TAP purified PfAdoMetDC/ODC expressed from pASK-IBA 43+. The proteins were analysed on a 7.5% SDS-PAGE gel and visualised with silver staining.

2.3.5.2 Activity assays

To verify that the double-tagged protein still attains the correct conformation, the decarboxylase activities of the new construct was compared to the original construct by measuring the release of $^{14}\text{CO}_2$ (section 2.2.8). The results of two independent experiments performed in duplicate were normalized against the specific activity (nmol/min/mg protein) of the original construct. These assays were performed in parallel. Figure 2.12 shows the difference in activity between the original construct with a C-terminal *Strep*-Tag II and the construct with both the N-terminal His-tag and C-terminal *Strep*-Tag II.

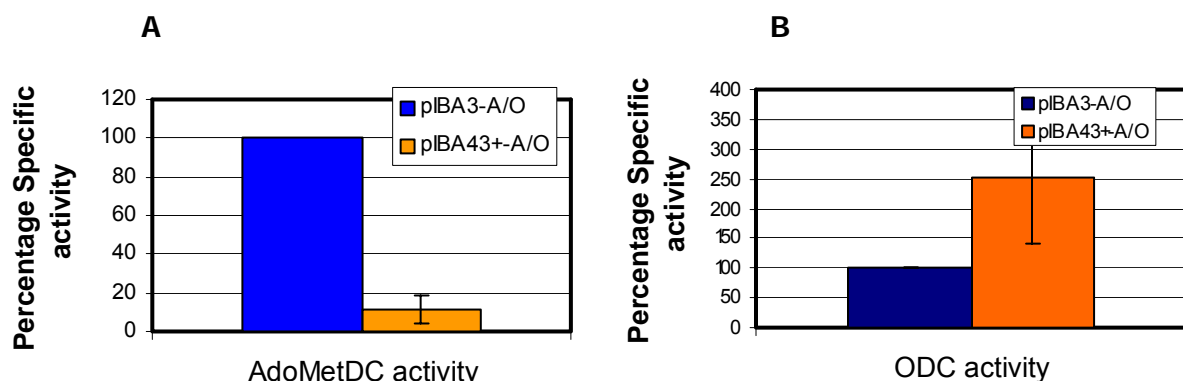


Figure 2.12: Activity assay of A: AdoMetDC and B: ODC activity.

The protein activity of PfAdoMetDC/ODC in pASK-IBA43+ was normalised against the wild type activity and given as a percentage.

From these results it can be seen that the His-tag interfered with both the AdoMetDC and ODC activities of the bifunctional protein. The AdoMetDC activity is almost abolished with only ~ 12%

of the original activity left. In contrast, the ODC activity of the double tag construct is $\sim 250\%$ of that of the original construct, possibly due to stabilisation of the protein.

In conclusion, the subcloning of *PfAdoMetDC/ODC* into pASK-IBA43+ did not have the positive effects envisioned, since the tandem affinity purification of the protein using two tags did not succeed in providing pure, full length *PfAdoMetDC/ODC*. Additionally *PfAdoMetDC/ODC* in the double tag vector expresses at lower concentrations than the original construct. This is surprising since the pASK-IBA43+ vector is a modification of pASK-IBA3 and carries the same promoter. The N-terminal His-tag also influences both decarboxylase activities of the protein. As such, it was decided to use the original construct for further purification studies.

2.3.5.3 Sized-based purification of recombinant *PfAdoMetDC/ODC*

2.3.5.3.1 Ultracentrifugation size exclusion

Further purification of the affinity purified recombinant protein was attempted using Nanosep 100 K Omega ultracentrifuge size exclusion columns (Pall Corporation, USA). Centrifugal force is used to drive the sample through a low adhesion membrane with a specific molecular cut-off size, thereby purifying samples based on size. Since the columns have a cut-off of 100 kDa, the ~ 70 kDa and ~ 60 kDa proteins should be removed from the full-length protein (~ 330 kDa heterotetrameric complex). However, it was expected that the ~ 112 kDa peptide would be isolated with the full-length protein due to the fact that it is larger than the specific cut-off value of the membrane. SDS-PAGE analysis of the retained solution however showed that the proteins were only concentrated and no separation of the different proteins was achieved (Fig 2.13).

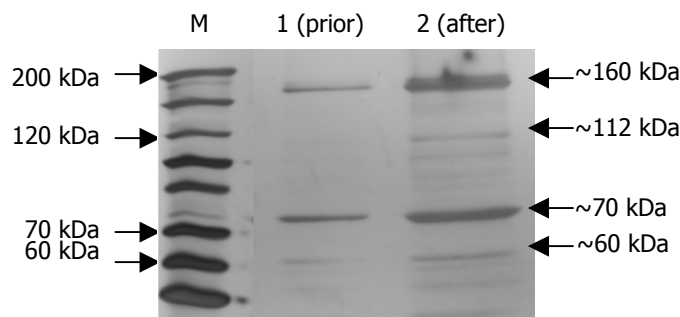


Figure 2.13: SDS-PAGE analysis of samples obtained following ultracentrifugation.

Lane M: PageRuler™ Protein ladder used as molecular marker. Lane 1: *Strep*-tag purified *PfAdoMetDC/ODC* prior to ultracentrifugation. Lane 2: *Strep*-tag purified *PfAdoMetDC/ODC* after ultracentrifugation. The proteins were analysed on a 7.5% SDS-PAGE gel and visualised with silver staining.

2.3.5.3.2 Size-exclusion high pressure liquid chromatography (SEC-HPLC)

Following affinity purification of the *Strep*-tagged *PfAdoMetDC/ODC*, further purification was attempted with a calibrated Phenomenex Biosep-Sec-S-3000 column (Fig 2.14, B). As can be seen in Fig 2.14, A, 3 peaks were obtained for the affinity purified recombinant protein following

SEC-HPLC. Comparison with the calibration curve indicates that these peaks correlate to ~600 kDa, ~50 kDa and ~7 kDa. This is surprising since the ~330 kDa heterotetrameric complex was expected. The collected fractions surrounding these peaks were subsequently analysed with SDS-PAGE.

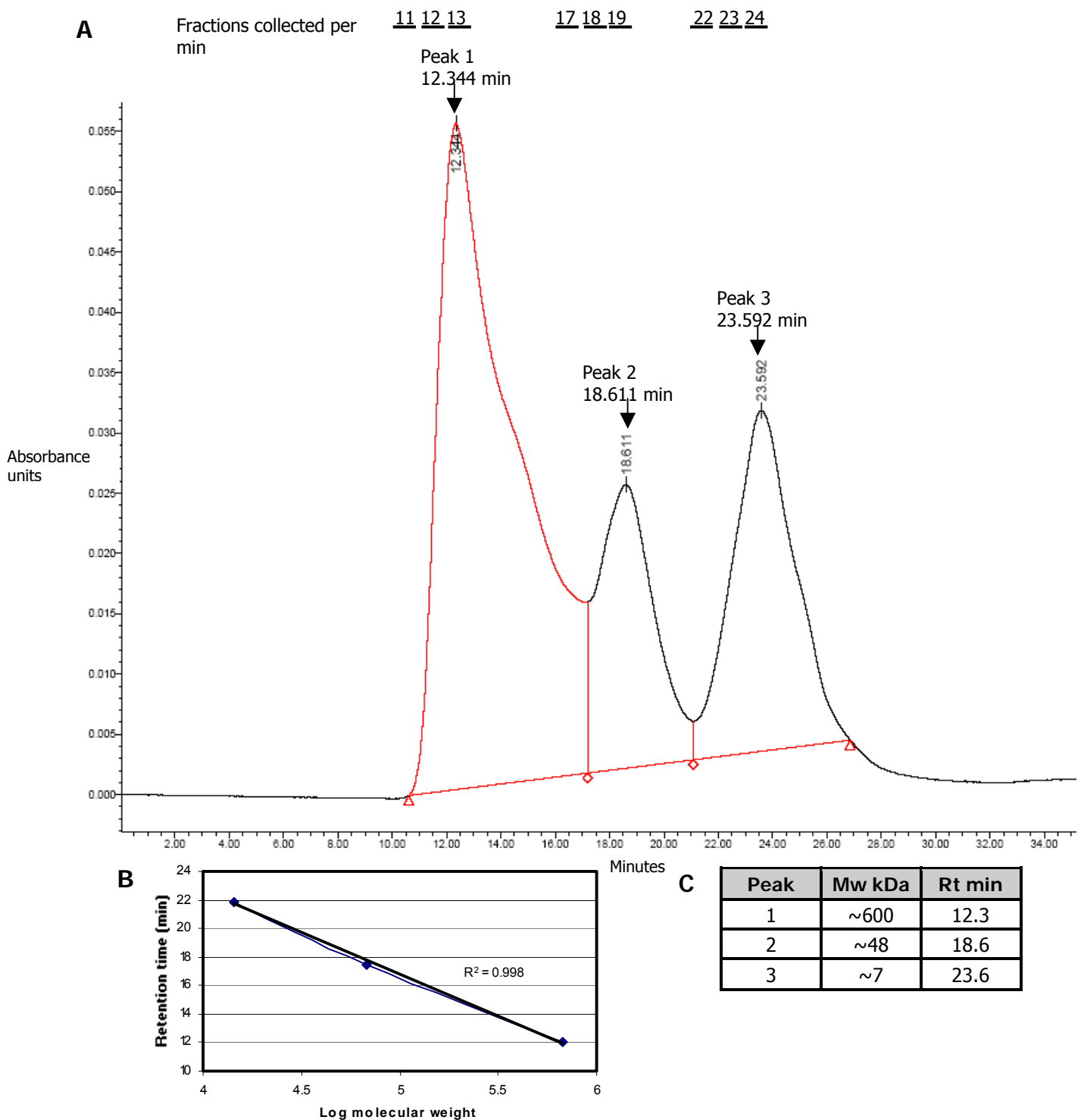


Figure 2.14: Size-exclusion HPLC of the recombinant PfAdoMetDC/ODC purified with affinity chromatography.

A: Elution profile of *Strep*-tag purified PfAdoMetDC/ODC. The three protein-containing peaks are indicated with arrows. **B:** Calibration curve for the size-exclusion HPLC. **C:** Retention times and calculated molecular weight of the 3 peaks

As can be seen in Fig 2.15, size-based purification of the affinity purified PfAdoMetDC/ODC did not succeed in purifying the protein to homogeneity, since the 4 strong protein bands still appeared following SDS-PAGE analysis, namely the ~ 160 kDa PfAdoMetDC/ODC and the 3 contaminating bands at ~ 112 kDa ~ 70 kDa and 60 kDa. However, comparison of the fractions eluted around peak 1 and 2 indicate that some of the ~ 70 kDa band is removed by SEC-HPLC, implying that this band could consist of two different proteins. Based on the calculated sizes of the eluted fractions, it appears as if the contaminating proteins adhere to the full-length PfAdoMetDC/ODC, thus eluting as a complex after SEC-HPLC.

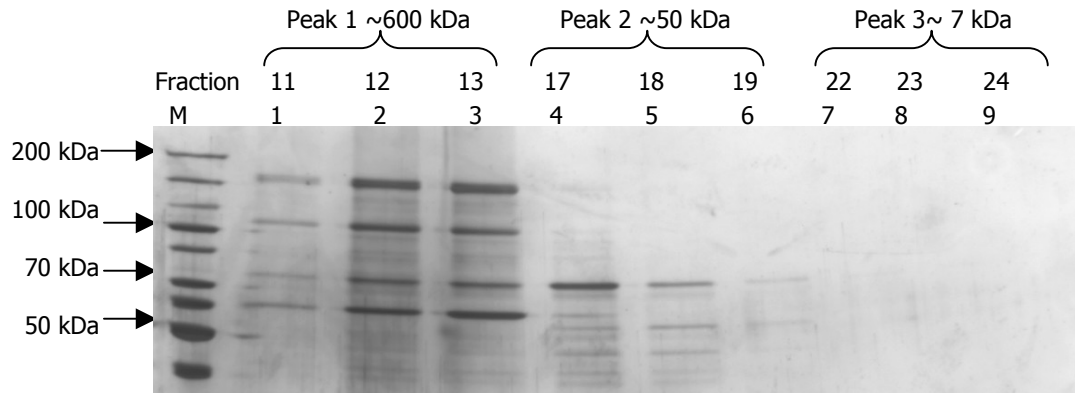


Figure 2.15: SDS-PAGE of fractions collected with SEC-HPLC of affinity-purified PfAdoMetDC/ODC.

Lane M: PageRuler™ Protein ladder used as molecular marker. Lane 2-9: SDS-PAGE analysis of the fractions corresponding to protein peaks obtained for *Strep*-tag purified PfAdoMetDC/ODC following SEC-HPLC. The fractions were analysed on a 7.5% SDS-PAGE gel and visualised with silver staining.

To verify the calculated sizes (based on the SEC-HPLC) of the complexes formed, PfAdoMetDC/ODC was expressed and isolated as described in section 2.2.4 and analysed using non-reducing native gel electrophoresis (Fig 2.16).

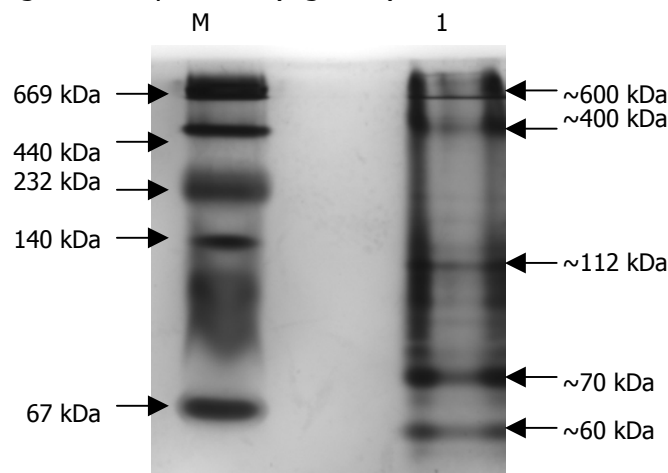


Figure 2.16: Native-PAGE of PfAdoMetDC/ODC.

Lane M: High Molecular Weight Electrophoresis calibration kit used as molecular marker. Lane 1: *Strep*-tag purified PfAdoMetDC/ODC. The proteins were analysed on a 7.5% Native-PAGE gel and visualised with silver staining.

As can be seen from Fig 2.16, it appears as if there is indeed a large protein complex formed that could correlate to ~ 600 kDa and one in the region of ~ 400 kDa. There are also bands that could be the ~ 112 kDa, ~ 70 kDa and ~ 60 kDa proteins. This could imply that the contaminating bands do indeed adhere to the full-length protein, thus explaining the lack of success in isolating pure protein.

2.3.6 Explanatory investigations

Since various attempts to purify the recombinant PfAdoMetDC/ODC to homogeneity did not succeed in providing pure protein, it was decided to investigate the identities of these contaminating proteins. While the ~ 60 kDa band appears to be an *E. coli* protein, the presence of the *Strep*-Tag II implies that the ~ 112 kDa and ~ 70 kDa proteins are smaller versions of the bifunctional protein (see section 2.3.2). There are several possible explanations for the occurrence of smaller peptides with the C-terminal tag, including post-translational degradation, ribosomal slippage on internal mRNA secondary structures and faulty translation initiation at AUG codons downstream of the start codon.

2.3.6.1 Post-translational degradation

In an effort to prevent the degradation, complete protease inhibitor cocktail tablets that inhibit a broad spectrum of proteases were added during the isolation steps.

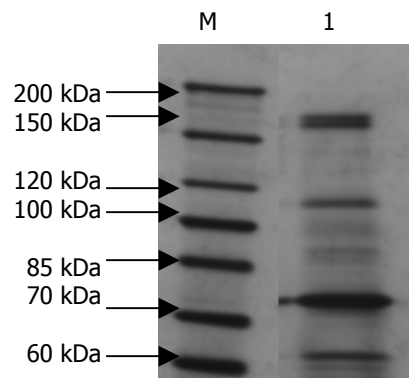


Figure 2.17: Effect of protease inhibitor cocktail on degradation of PfAdoMetDC/ODC.

Lane M: PageRuler™ Protein ladder used as molecular marker. Lane 1: *Strep*-tag purified PfAdoMetDC/ODC isolated in the presence of complete protease inhibitors. The protein were analysed on a 7.5% SDS-PAGE gel and visualised with silver staining.

Figure 2.17 shows that the addition of a broad-spectrum protease inhibitor cocktail does not lead to a purer protein extract. This means that if these *Strep*-tag II tagged contaminating fragments are due to proteolytic degradation, it occurs in the bacterial cell during expression itself, and thus cannot be prevented by the addition of protease inhibitors.

2.3.6.2 Ribosomal slippage on internal mRNA secondary structures

Ribosomal slippage on mRNA secondary structures was investigated by Western blot analysis of the original (C-terminal *Strep*-tag II) and double-tagged (N-terminal His- and C-terminal *Strep*-

tag II) protein construct, using both an anti-*Strep*-tag II and anti-His-tag antibody. If the contaminating bands are due to in-frame ribosomal slippage, peptide fragments with both the N-terminal His- and C-terminal *Strep*-tag II should be produced and the Western blots using the two tag-specific antibodies should be identical. Alternatively, in-frame translation initiation at AUG codons downstream of the start codon would lead to N-terminally truncated protein fragments that carry the *Strep*-tag II but not the N-terminal His-tag. As can be seen from Fig 2.18, the banding pattern of the Western blot performed using anti-*Strep*-tag II antibody differs from that obtained when an anti-His-tag antibody was utilised. In lane 2 (PfAdoMetDC/ODC with both N-terminal His-tag and C-terminal *Strep*-tag II) of both the blots using anti-*Strep*-tag II antibody (Fig 2.18 A) and anti-His-tag antibody (Fig 2.18 B) there is a strong band present at ~161 kDa, which indicate that the full-length protein indeed have both tags as expected. That is however the only high concentration band identified using the anti-His tag antibody. Although smaller bands are identified, their intensity is much lower, indicating lower concentration. It is also possible that these faint bands below the full-length protein in Fig 2.18 B can be merely background proteins. The 3 strongly contaminating bands (~112 kDa, ~70 kDa and ~60 kDa) do not appear, indicating that they do not carry the His-tag (Fig 2.18 B).

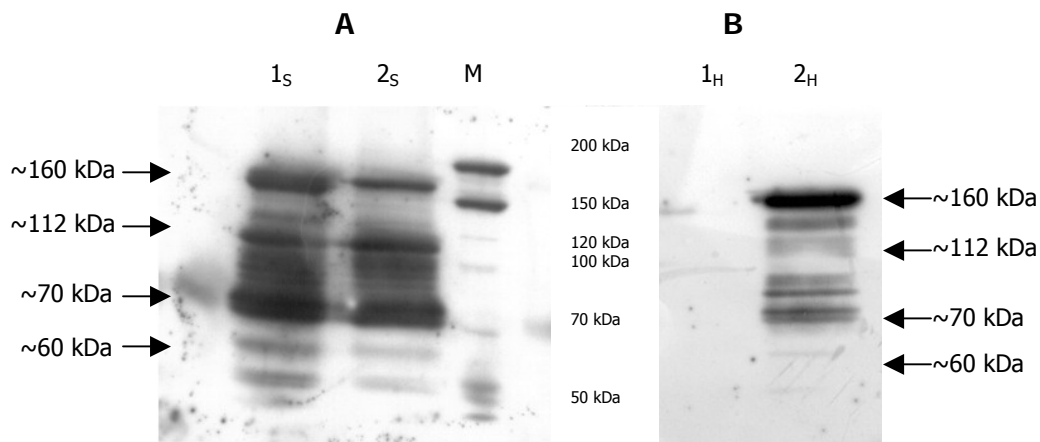


Figure 2.18: Western blot using A: anti-*Strep*-Tag II and B: anti-His-tag antibodies.

Lane M: PageRuler™ Protein ladder used as molecular marker. Lane 1: *Strep*-tag purified PfAdoMetDC/ODC from pASK-IBA3. Lane 2: *Strep*-tag purified PfAdoMetDC/ODC from pASK-IBA43+. The proteins were analysed on a 7.5% SDS-PAGE gel prior to Western blotting.

In contrast, the Western blot using an anti-*Strep*-tag II antibody (Fig 2.18 A) is identical for both constructs. The full-length PfAdoMetDC/ODC protein, ~112 kDa and ~70 kDa protein are all strongly identified. As in Fig 2.5, the ~60 kDa fragment is not identified above background by the anti-*Strep*-tag II antibodies. These results indicate that although there are some mRNA slippage as can be seen from the faint bands below the full-length protein on the His-tag Western blot, mRNA slippage do not account for the 2 strong *Strep*-tagged contaminating bands (~112 kDa and ~70 kDa) that are co-purified with the full-length protein. The fact that these

fragments carry the C-terminal *Strep*-Tag II imply that they either originate from N-terminally truncated proteins due to translation initiation at AUG codons downstream of the start codon or post translational degradation of PfAdoMetDC/ODC.

2.3.6.3 Translation initiation at AUG codons downstream of the start codon

As was seen from the previous experiments, the ~112 kDa and ~70 kDa contaminating fragments are of heterologous origin, since they carry the *Strep*-tag II. The ~60 kDa fragment is not identified by the anti-*Strep*-tag II antibody, indicating that it is an *E. coli* protein. These bands are not due to degradation during isolation (although post-translational degradation may occur in the bacterium prior to isolation) or ribosomal slippage on mRNA secondary structures. One possible explanation for the observed results is faulty translation initiation at AUG codons downstream of the start codon. To investigate the identity of the smaller contaminating fragments, recombinant PfAdoMetDC/ODC expressed as described in section 2.2.7 was separated using a 7.5% SDS-PAGE gel, stained with colloidal Coomassie (section 2.2.13.3) and sent to Prof John Hyde and Dr Paul Sims, University of Manchester for Mass Spectral-analysis, since their lab is proficient in the MS-analysis of *Plasmodium* proteins (Nirmalan, 2005; Nirmalan et al., 2004).

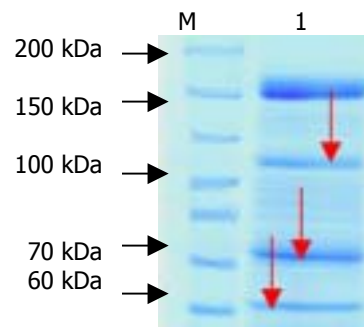


Figure 2.19: Preparative SDS-PAGE for MS analysis.

Lane M: PageRuler™ Protein ladder used as molecular marker. Lane 1: *Strep*-tag purified PfAdoMetDC/ODC. The protein were analysed using a 7.5% separating gel and stained with colloidal coomassie. The bands that were analysed are indicated with red arrows.

MS analysis indicated that the ~112 kDa protein is an N-terminally truncated version of the full-length protein, since that band contained no peptides prior to amino acid 525 (see Fig 2.20 A). The sequence of PfAdoMetDC/ODC upstream of amino acid 526 was analysed to determine possible reasons for the formation of a N-terminally truncated product. Two possible Shine-Dalgarno sequences were found upstream of an AUG, which could act as an initiation site (see Fig 2.20 B). It is possible that the *E. coli* ribosome recognise these sequences as false internal mRNA initiation sites, leading to fragmented expression of the protein.

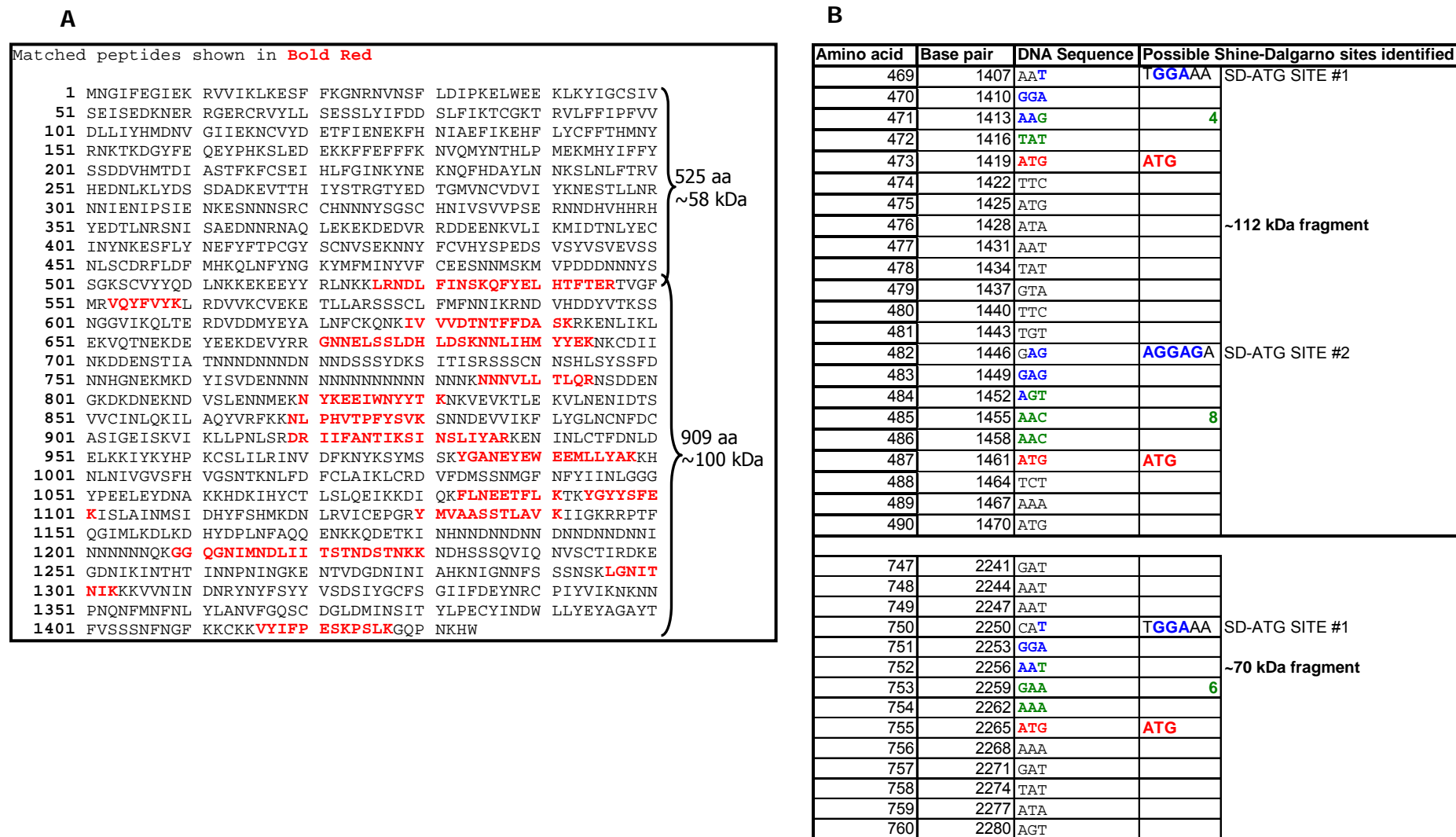


Figure 2.20: MS results and analysis. A: Matched peptides for the ~112 kDa fragment after comparison with PfAdoMetDC/ODC (peptides indicated in red). B: Sequence analysis of PfAdoMetDC/ODC showing possible internal Shine Dalgarno and internal AUG codons as well as the number of base-pairs located in-between.

Surprisingly, the ~70 kDa and ~60 kDa fragments were respectively identified as *E. coli* 70 kDa and 60 kDa heat shock proteins. However, the ~70 kDa fragment did contain traces of PfAdoMetDC/ODC. This is in correlation with the Western blot results obtained using anti *Strep*-tag II antibody, where the ~70 kDa fragment was identified, while the ~60 kDa band showed no reactivity with the antibody. A possible Shine-Dalgarno sequence was also found upstream of an AUG, which could act as an initiation site to generate the ~70 kDa band (see Fig 2.20 B).

2.3.7 Purification of PfAdoMetDC/ODC from *E. coli* heat shock proteins

Both *E. coli* DnaK (Hsp 70) and GroEL (Hsp 60) are ATP-binding proteins (Baneyx and Mujacic, 2004) and as such it was suggested that the addition of ATP during the isolation of the recombinant protein could help remove the contaminating chaperone proteins (G. Blatch, personal communication). PfAdoMetDC/ODC was recombinantly expressed and isolated as described in section 2.2.7, but with the addition of 2 mM ATP to Buffer W.

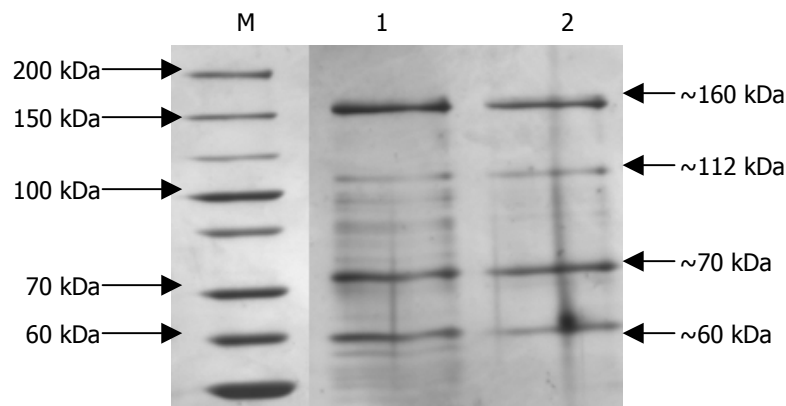


Figure 2.21: Effect of the addition of ATP on the purification of recombinant PfAdoMetDC/ODC

Lane M: PageRuler™ Protein ladder used as molecular marker. Lane 1: *Strep*-tag purified PfAdoMetDC/ODC. Lane 2: *Strep*-tag purified PfAdoMetDC/ODC isolated in the presence of 2 mM ATP. The protein were analysed on a 7.5% SDS-PAGE gel and visualised with silver staining

As can be seen from Fig 2.21, the addition of ATP to the purification procedure, while removing some very faint contaminating bands, did not succeed in preventing the co-purification of *E. coli* DnaK and GroEL. To confirm that the ~70 kDa band consists of both DnaK and the PfAdoMetDC/ODC fragment, even following the addition of ATP to the purification procedure, Western blot analysis using both anti-*Strep*-tag II and anti DnaK antibody was performed.

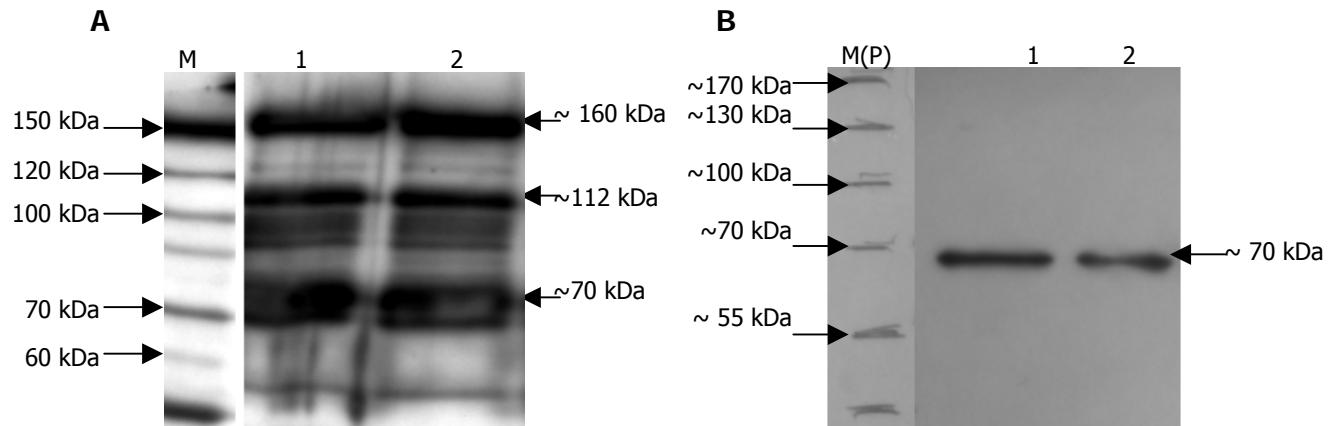


Figure 2.22: Western blot using A: anti-*Strep*-tag II antibody and B: anti-DnaK antibody on PfAdoMetDC/ODC isolated in the absence and presence of ATP.

Lane M: PageRuler™ Protein ladder used as molecular marker. Lane M (P): PageRuler™ Prestained Protein ladder used as molecular marker. The location of the marker bands was determined by comparison with the coloured bands on the PVDF membrane. Lane 1: *Strep*-tag purified PfAdoMetDC/ODC. Lane 2: *Strep*-tag purified PfAdoMetDC/ODC using ATP in the Wash buffer. The proteins were analysed on a 7.5% SDS-PAGE gel prior to Western blotting.

From Fig 2.22 A and B it can be seen that the addition of ATP to the isolation procedure did not succeed in providing pure recombinant protein. The ATP content was increased to 5 mM, with the same results (M. Williams, personal communication). These results indicate that it was not possible to isolate PfAdoMetDC/ODC to homogeneity. As such it was decided to use the protein as is for the identification of peptide binding partners.

2.4 Discussion

The heterologous expression and purification of *P. falciparum* proteins are notoriously difficult due to a variety of factors, such as the 80% A+T richness of the genome, RNA secondary structures and stability as well as the high occurrence of low-complexity regions and parasite specific inserts (Birkholtz et al., 2003; LaCount et al., 2005; Mehlin, 2005). In 2006, Christopher Mehlin and co-workers tested 1000 *P. falciparum* open reading frames for expression in *E. coli*. Of these, only 63 had soluble expression at levels sufficient for purification (at least 0.9 mg protein expressed from a litre of culture). Further investigation of the various proteins showed that protein size, disorder and pI are inversely correlated to effective expression. *P. falciparum* genes also contain stretches of A or T that frequently lead to frameshift mutations, as well as cryptic start sites that may result in truncated products. Given that *P. falciparum* proteins are frequently considerably larger than their homologues in other species, which is often due to the insertion of disordered parasite-specific inserts, it is not surprising that *Plasmodium* proteins are difficult to express in heterologous expression systems. Many *Plasmodium* proteins do not have *E. coli* homologues, which seems to further increase their difficulty of expression (Mehlin et al., 2006). However, new data suggests that the A+T richness of the genome does not have such a large effect on heterologous expression as previously suspected (Mehlin et al., 2006; Vedadi et al., 2007).

Bifunctional PfAdoMetDC/ODC was recombinantly expressed with a C-terminal *Strep*-tag II to allow affinity purification. Subsequent gel electrophoresis analysis showed the presence of 3 contaminating proteins (~60 kDa, ~70 kDa and ~112 kDa) that co-elute with the ~330 kDa PfAdoMetDC/ODC. Although the original publication on the bifunctional protein reported that silver staining following SDS-PAGE only revealed the ~160 kDa subunit corresponding to the heterodimeric PfAdoMetDC/ODC (Müller et al., 2000) these results could not be duplicated in either our lab or that of the original publishers (G. Wells, M. Williams, S. Roux, personal communication). Another publication published by the same group did refer to smaller protein bands and suggested that the smaller bands correspond to degradation products, since the ~70 kDa band were identified with antiserum raised against the ODC domain of the bifunctional protein (Krause et al., 2000). Western blot analysis showed that the ~112 kDa and ~70 kDa proteins were recombinantly produced with a *Strep*-tag II, indicating their heterologous origin. It was however shown that these fragments are not artefacts caused by the expression vector itself (section 2.3.2). It was therefore expected that these interacting proteins are smaller versions of the bifunctional protein. In contrast, the ~60 kDa protein appeared to be of *E. coli* origin.

It has been reported that affinity purification of recombinantly expressed proteins with a C-terminal *Strep*-tag does not necessarily lead to a homogenous protein preparation. For instance, when NI-Fr1 derived from the Nogo-A protein in oligodendrocytes was recombinantly expressed and purified using its C-terminal *Strep*-tag, it was found that only 50% of the purified protein corresponded to the full-length protein. The other 50% consisted of a succession of smaller polypeptides. It was suggested that these fragments are due to proteolytic degradation by a bacterial protease (Fiedler et al., 2002). In an attempt to obtain pure, full length PfAdoMetDC/ODC, the gene was subcloned into a double-tagged vector to allow for tandem affinity purification using both a His-tag and *Strep*-tag II. Previous publications have indicated that the combination of a His- and *Strep*-tag is fortuitous in providing pure recombinant protein, where His-tag purification serve to capture the recombinant protein from background expression, and subsequent *Strep*-tag purification providing pure protein (Lichty et al., 2005). By first isolating the recombinant protein using IMAC via a N-terminal His tag, followed by isolation using the *Strep*-tag II, the isolation of smaller polypeptide fragments carrying the C-terminal *Strep*-tag II was circumvented (Fiedler et al., 2002). Unfortunately, this strategy did not succeed in providing pure, full-length PfAdoMetDC/ODC, since the same contaminating polypeptides were obtained after tandem affinity purification (TAP). Additionally, when the decarboxylase activities of the original and subcloned proteins were compared it appeared as if the His-tag interfered with both the AdoMetDC and ODC activities of the bifunctional protein. The AdoMetDC activity was almost abolished with only ~12% of the original activity left. One possible explanation for this result is that the 6 His residues that comprised the tag folds over the active site of the enzyme, thereby preventing substrate access. Alternatively, as can be seen in Fig 2.11, the PfAdoMetDC/ODC expressed from the pASK-IBA43+ construct provides a slightly larger protein than the original construct. Mutational studies done by Wrenger et al. where Ser⁷³ was mutated into alanine, thereby preventing the post-translational cleavage of the AdoMetDC region (Wrenger et al., 2001), resulted in a protein with a size similar to the slightly larger band seen in Fig 2.11. It is possible that the His-tag interferes with the self-cleavage of PfAdoMetDC, resulting in a 9 kDa larger, inactive protein, similar to the mutation studies done by Wrenger et al., 2001. However, the observed size difference could merely be due to the presence of the hexahistidine tag. In contrast, the ODC activity of the double-tag construct is almost 250% of that of the original construct. It has been shown that the parasite-specific inserts of both the AdoMetDC and ODC domains have an effect on the adjacent domain (Birkholtz et al., 2004). It is possible that conformational changes in the AdoMetDC domain induced by the N-terminal His-tag causes stabilization of the ODC domain, with associated higher catalytic activity.

It was then attempted to further purify the protein based on size, using both ultracentrifuge size exclusion columns and SEC-HPLC. The ultracentrifuge size exclusion columns merely concentrated the protein and were not effective in purifying the smaller proteins from the large full-length protein. This was unexpected since the ~60 kDa and ~70 kDa proteins are smaller than the cut-off size and should have been removed. SEC-HPLC also did not succeed in purifying PfAdoMetDC/ODC from the contaminants, although some of the ~70 kDa band were removed, suggesting that this band could consist of more than one protein. Subsequent MS-analysis showed that the ~70 kDa band indeed does consist of an *E. coli* protein and the protein fragment of ODC that has previously been seen (Krause et al., 2000). This would explain why a part of the ~70 kDa band was not removed with HPLC analysis, since it correspond to at least a part of the ODC domain and can thus bind to the full-length protein through the interaction with the ODC monomer/dimer. Both these methods showed that there was a protein complex much larger than the expected ~330 kDa, indicating that the contaminating bands bind to the full-length protein. The results obtained after TAP supports this hypothesis, since only the full-length protein should carry the His-tag, and one would expect that the contaminating fragments would not be co-purified since the initial purification occurs using IMAC via the His-tag. Considering that ODC is responsible for the interaction of the bifunctional protein, it is possible that these peptides are fragments of ODC with the *Strep*-Tag II, which explains their co-purification using the *Strep*-Tactin Sepharose. Additionally, since ODC mediate the binding of the bifunctional complex (Birkholtz et al., 2004), these fragments will bind tightly to the full-length protein, with explains their co-purification with IMAC and the lack of success in trying to obtain pure, full-length AdoMetDC/ODC.

To verify this result, native PAGE analysis was performed, which showed that there was indeed a protein complex at ~600 kDa and another at ~400 kDa. The ~400 kDa complex could be the ~330 kDa bifunctional complex together with the ~70 kDa ODC fragment, while the ~600 kDa complex may consist of the ~330 kDa bifunctional complex and the ~112 kDa fragment, the ~70 kDa ODC fragment and and 1 copy of the ~60 kDa protein. Alternatively, the ~600 kDa complex may consist of the ~330 kDa bifunctional complex and either 2 copies of the ~70 kDa protein and 1 copy of the ~60 kDa protein or 1 copy of the ~70 kDa protein and 2 copies of the ~60 kDa protein.

Western blot analysis showed that the ~112 kDa and ~70 kDa proteins were recombinantly produced with a *Strep*-tag II, indicating their heterologous origin (section 2.3.2). This result, together with the unsuccessful application of size-exclusion techniques indicated that these interacting proteins are smaller versions of the bifunctional protein, which is co-purified due to

the formation of a large protein complex. Explanations for the presence of smaller proteins include post-translational degradation, ribosomal slippage on mRNA secondary structures or false translation initiation at AUG codons downstream of the start codon. However, if ribosomal slippage on mRNA secondary structures or false translation initiation at AUG codons downstream of the start codon is responsible for the appearance of these fragments, they would have to occur in-frame to account for the production of the C-terminal *Strep*-tag II. In contrast, the ~60 kDa protein appeared to be of *E. coli* origin.

Recombinant expression and isolation of NI-Fr1 derived from the Nogo-A protein in oligodendrocytes using a C-terminal *Strep*-tag led to the isolation of only 50% of the full-length protein. The other 50% consisted of a succession of smaller polypeptides. It was suggested that these fragments are due to proteolytic degradation by a bacterial protease (Fiedler et al., 2002). This hypothesis of post-translational degradation of the protein was tested by the addition of a complete protease inhibitor during the isolation steps. Since the addition of a complete protease inhibitor cocktail did not prevent the co-purification of these bands, it did not appear as if these bands occurred due to degradation during the isolation process. However, it is possible that post-translational degradation occurs in the cell itself during expression.

One possible explanation for these results is ribosomal slippage on mRNA secondary structures, leading to fragments with both the His-tag and *Strep*-tag II, but varying lengths of PfAdoMetDC/ODC protein inserted in-between (Fig 2.23). This would lead to the co-purification of smaller peptide fragments through TAP as seen in Fig 2.11, since these peptides would carry both the His-tag and the *Strep*-tag II. It has been shown that sequence elements that cause mRNA secondary structures through Watson and Crick base pairing can lead to differently expressed proteins in red clover mosaic dianthovirus (Kim and Lommel, 1998). From the Western blots done on the doubly-tagged protein, it could be inferred that the ~112 and ~70 kDa fragments are not due to ribosomal slippage on mRNA secondary structure, since only the C-terminal *Strep*-tag II was present in the contaminating fragments and not the N-terminal His tag (Fig 2.18). Although some fragments were identified that does contain both tags, these were at a very low concentration. The fact that the major contaminating fragments co-purified with IMAC (Fig 2.11) suggest that they bind to the full-length protein.

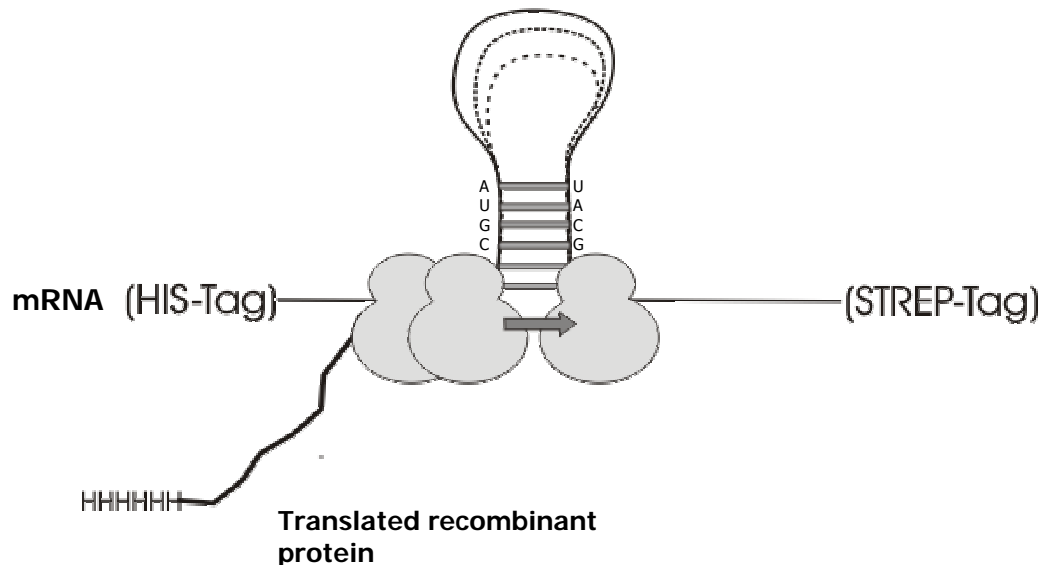


Figure 2.23: Schematic representation of ribosomal slippage on mRNA secondary structures, leading to various sized fragments. (With the help of Jaco de Ridder).

As was seen from the previous experiments, the ~ 112 kDa and ~ 70 kDa contaminating fragments are of heterologous origin, since they carry the *Strep*-Tag II. The ~ 60 kDa fragment is not identified by the anti-*Strep*-Tag II antibody. Since anti-His-tag antibody does not recognise these fragments, they are not due to ribosomal slippage on mRNA secondary structures. One possible explanation for the observed results is false translation initiation at AUG codons downstream of the start codon (Preibisch et al., 1988). The prokaryotic Shine-Dalgarno sequence plays a role in translation initiation, during which there is an interaction between the sequence and the 16S rRNA (Jana and Deb, 2005). If a heterologous gene encodes for a possible Shine-Dalgarno (AGGAGG) sequence preceding an ATG, it can lead to a protein being translated from false internal translation initiation sites on the transcribed mRNA. These internal sequences have no effect on the translation of the protein *in vivo*, since malaria is an eukaryotic organism, but does cause problems when using a prokaryotic expression system. This phenomenon, where N-terminally truncated proteins are due to internal Shine-Dalgarno sequences, has been seen in other malarial proteins, such as lactate dehydrogenase (Turgut-Balik et al., 2001). Recombinant expression of *P. falciparum* Liver-Stage Antigen 1 in *E. coli* also led to a mixture of proteins being produced, due to an ATG 62 codons downstream of the start site being recognised by the ribosome (Hillier et al., 2005). To ascertain if this was indeed the case, the bands were subjected to MS analysis.

It was shown that the ~ 112 kDa fragment is a N-terminally truncated form of PfAdoMetDC/ODC. Sequence analysis showed two possible Shine-Dalgarno (AGGAGG) sequences preceding an ATG, which may lead to the protein being translated from internal mRNA initiation sites, thus

producing a ~112 kDa N-terminally truncated protein. The location of these Shine-Dalgarno sequences is intriguing. The mascot searches showed that the ~112 kDa band contains no peptides prior to amino acid 525. This effectively means that that this fragment corresponds to the hinge and ODC domain of the protein (amino acid 530 onwards) (Müller et al., 2000). It has been suggested that the bifunctional nature of this protein is due to an exon-shuffling event during Plasmodia evolution, which, due to its advantageous nature, was incorporated (Birkholtz, 2002). If *P. falciparum* were of a pure prokaryotic origin, these Shine-Dalgarno sequences could have been relics of the time when these two proteins were still separate. However, since the parasite is in fact eukaryotic it is possible that these sequences appear purely by chance. Nevertheless, it is worth noting that malaria parasites contain plasmids of both plant and red algae origin (Vothknecht and Soll, 2005; Wilson, 2002). These results imply that it will not be possible to purify the full-length protein from the ~112 kDa protein, since the fragment will bind to PfAdoMetDC/ODC via the ODC domain. Since the dimerization of ODC is mediated by an aromatic amino acid zipper as well as several hydrophobic interactions and a salt bridge (Birkholtz et al., 2003), more stringent isolation procedures, for instance hydrophobic interaction chromatography, will probably dissociate the two monomers, thus inactivating the protein. For this reason, the ionic strength of the wash buffer was not increased, for fear of dissociating the protein. This implies that the most efficient way to prevent the co-purification of the ~112 kDa fragment is to induce silent mutations in the gene to remove the Shine-Dalgarno sequence, thereby completely preventing the expression of this fragment.

MS analysis of the ~60 kDa and ~ 70kDa fragments showed that they are endogenous *E. coli* proteins, namely *E. coli* hsp 60 and 70 respectively. The fact that these proteins co-purify with the full-length protein implies that these chaperones are bound to the protein, probably in an effort to correct the folding and expression of the heterologous protein. Molecular chaperones are a set of essential proteins that through controlled binding and release phases aid in the proper assemblage or folding of the substrate protein. This ensures that any newly translated polypeptide attains the properly folded conformation, as well as maintaining functional proteins in their active conformation, thereby ensuring cell viability (Houry, 2001). The heterologous expression of a foreign protein in *E. coli* often leads to cellular stress, with the concomitant upregulation of heat shock proteins and other chaperone systems (Baneyx and Mujacic, 2004; Sørensen and Mortensen, 2005).

The *E. coli* Hsp 60 protein, GroEL, is a 57 kDa ATP-dependent protein. *In vivo*, GroEL is a ~800 kDa oligomer consisting of 14 subunits arranged into two stacked homoheptameric rings, thus forming a cavity for protein folding. GroEL is an essential protein for *E. coli* and recognise

compact proteins with exposed hydrophobic residues, especially those with $\alpha\beta$ -folds. It functions together with a 10 kDa co-chaperone, GroES (Fig 2.24) (Baneyx and Mujacic, 2004; Hartl and Hayer-Hartl, 2002; Houry, 2001; Walter and Buchner, 2002).

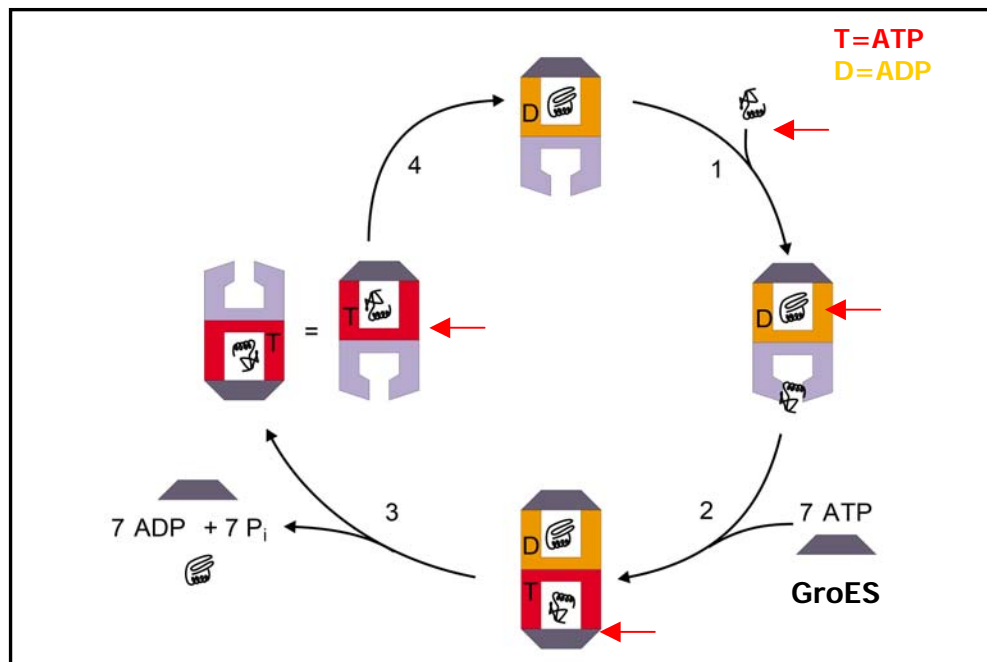


Figure 2.24: The GroEL/GroES chaperone cycle of *E. coli*. Adapted from (Walter and Buchner, 2002).

GroEL consist of two rings, its function is described for one ring, indicated with red arrows. 1) The nucleotide-free heptameric ring of GroEL (lilac) binds to a hydrophobic peptide. 2) ATP and GroES binds to this ring, causing structural changes that release the peptide into the folding cavity of GroEL. 3) The folded polypeptide, ADP and GroES that was bound to the top ring (orange) is also released by this conformational change, leading to a new available GroEL ring to be formed 4) The ATP is hydrolysed to ADP, starting the cycle anew. The folded polypeptide will only be released once a second peptide has bound to the GroEL cavity, leading to GroES binding and ATP hydrolysis (Houry, 2001; Walter and Buchner, 2002)

Due to size-restrictions of the cavity formed by GroEL, the substrate specificity of the GroEL/GroES chaperone system is constricted to proteins of 60 kDa or less (Hartl and Hayer-Hartl, 2002). It would then appear unlikely that this protein interacts with the ~ 330 kDa heterotetrameric PfAdoMetDC/ODC. It is possible that GroEL's propensity for binding to substrates with two or more $\alpha\beta$ domains (Houry, 2001) mediate the binding of the chaperone to the $\alpha\beta\beta\alpha$ -fold of the AdoMetDC domain (Wells et al., 2006) or the N-terminal α/β barrel of the ODC domain (Birkholtz et al., 2003). Due to size of the bifunctional protein, there are sterical constraints that prevent GroES from binding to GroEL; implying that no conformational change takes place, thus leading to the co-purification of GroEL with PfAdoMetDC/ODC.

The *E. coli* Hsp 70 protein, DnaK, consist of two domains, namely an ATPase domain (N-terminus) and a substrate-binding domain (C-terminus). It binds stretches of between four and

five hydrophobic residues, preferentially containing leucine and isoleucine in incompletely folded polypeptides, thereby preventing aggregation and misfolding. *In vivo*, the activity of DnaK is regulated by its co-chaperone, DnaJ (Hsp 40) and the nucleotide exchange factor GrpE (Fig 2.25) (Hartl and Hayer-Hartl, 2002; Houry, 2001; Szabo et al., 1994; Walter and Buchner, 2002).

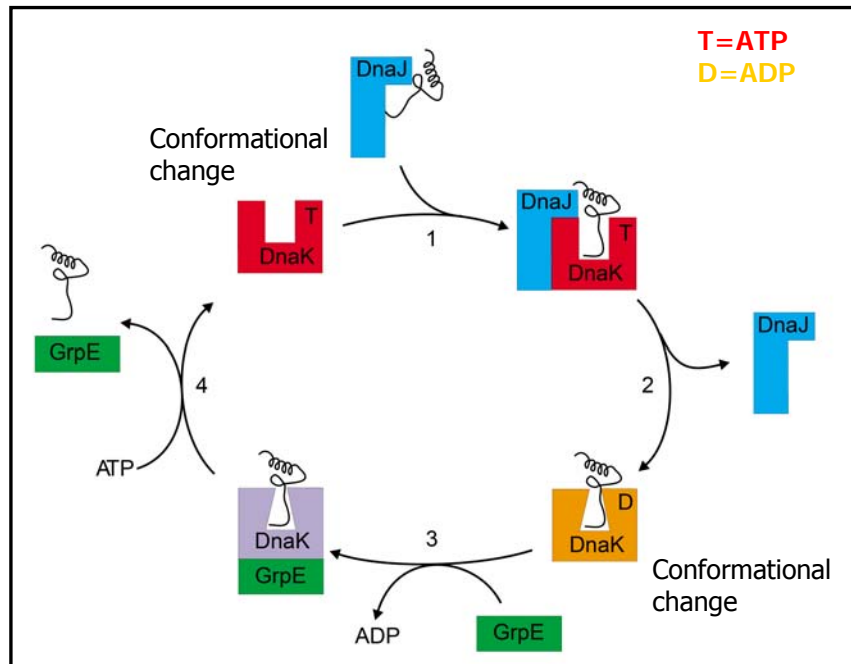


Figure 2.25: DnaK/DnaJ/GrpE chaperone system in *E. coli*. Adapted from (Walter and Buchner, 2002).

1) The co-chaperone DnaJ bind to a nascent, unfolded peptide, which is then transferred to the peptide-binding site of DnaK in its ATP-bound form. 2) The peptide and DnaJ stimulate the ATPase activity of DnaK, leading to the hydrolysis of ATP→ADP, the release of DnaJ and a conformational change to lead to the formation of a stable ADP-DnaK-substrate complex. 3) The binding of the nucleotide exchange factor GrpE to DnaK displaces the ADP from DnaK. 5) ATP binding to DnaK displaces GrpE and triggers a conformational change in DnaK that releases the bound peptide (Houry, 2001; Szabo et al., 1994; Walter and Buchner, 2002).

The unwanted co-purification of DnaK with recombinantly expressed proteins has been previously described and could not be removed by utilising low salt solutions, organic solvents, ion exchange chromatography or gel filtration. The authors did however find that the addition of ATP to the purification procedure did help in lessening the chaperone co-purification (Rial and Ceccarelli, 2002). However, as can be seen from Fig 2.21 and 2.22, the addition of ATP did not succeed in removing DnaK from PfAdoMetDC/ODC. One the other hand, it is possible that SEC-HPLC does indeed remove DnaK, since some of the ~70 kDa fragments were separated from the bifunctional complex (Fig 2.15). This would however have to be verified with Western blotting.

Additionally, a trace of PfAdoMetDC/ODC was identified in the ~ 70 kDa band by MS-analysis. This result is in agreement with the Western blots done using anti-*Strep*-tag II antibody where the ~ 70 kDa band was strongly identified but not the ~ 60 kDa band. The ~ 70 kDa band was also identified with antiserum raised against the ODC domain (Krause et al., 2000). Sequence analysis showed a possible Shine-Dalgarno sequence that could lead to the production of the ~ 70 kDa fragment (Fig 2.20). It has also been shown that *E. coli* can translate heterologous mRNA independent of a Shine-Dalgarno sequence (Roberts and Rabinowitz, 1989). Alternatively, this protein fragment could be due to post-translational degradation of the heterologous protein.

In conclusion, it was initially thought that there are three possible reasons for the presence of the smaller proteins, namely ribosomal slippage on mRNA secondary structures, internal mRNA initiation sites or post-translational degradation. It was shown that while ribosomal slippage on mRNA secondary structures are responsible for a small fraction of contaminating peptides and post-translational degradation may account for the appearance of an ~ 70 kDa fragment of the heterologous protein, they are not responsible for the 3 major contaminating bands. MS analysis showed that internal mRNA initiation sites account for two of the fragments, namely the ~ 112 kDa band and possibly the ~ 70 kDa band. Unexpectedly, the ~ 60 kDa and a fraction of the ~ 70 kDa band are *E. coli* chaperones produced due to the poor expression of the recombinant protein. These results prove that it is unlikely that the protein can be purified to homogeneity using conventional means. Instead, the PfAdoMetDC/ODC gene sequence may have to be re-synthesised in order to achieve better expression. Initially the work in this chapter was done in order to obtain pure protein for phage display. These results prove that at present this protein cannot be purified completely.

Since more than 50% of the protein eluate, namely the full-length protein, ~ 112 kDa protein and a part of the ~ 70 kDa protein are of PfAdoMetDC/ODC origin, it was decided to use the protein as is for phage display screening.

Chapter 3: Identification of peptide binding partners to PfAdoMetDC/ODC through the use of a *P. falciparum* phage display library

3.1 Introduction

3.1.1 Identification of protein-protein interactions

There are various experimental methods to identify protein-protein interactions, and they differ in the level of resolution, namely 1) atomic observation, through the use of X-ray structures, 2) direct interactions such as those identified by phage display and 3) determination of multiprotein complexes that only identify the proteins in a complex and not the binding sites, e.g. through mass-spectrometry (MS) analysis. Lastly, activity bioassays can identify the results of an interaction but does not provide information on the proteins involved in the interaction itself (Xenarios and Eisenberg, 2001).

Different methods can be used to determine direct interactions between proteins. These can be used either *in vitro* or *in vivo*, with various advantages and disadvantages. *In vivo* methods include Two-Hybrid based approaches, where the bait protein is typically fused to a DNA binding domain, whilst the prey (often proteins expressed from a cDNA library) forms a fusion protein with a DNA activation domain (Howell et al., 2006). Protein fragment complementation assay (PCA) or assisted protein reassembly can be used to detect protein-protein interactions *in vivo* and is based on the fact that several proteins such as Green Fluorescent Protein (GFP), ribonuclease and chymotrypsin inhibitor-2 can be reconstituted from their peptide fragments, if the correct dissection site is chosen (Ghosh et al., 2000). Upon protein-protein interaction, these two domains are brought into close enough proximity that a specific phenotypic effect can be observed. During PCA, cells that are concurrently expressing two different proteins that are fused to fragments of a reporter protein such as GFP, will fluoresce only if there is a physical interaction between the two proteins that can bring the fragments of the specific reporter protein into close enough proximity that refolding can take place (Remy and Michnick, 2004). Chemical crosslinking can be used both *in vivo* and *in vitro*, and entails the coupling of a specific bait protein with those in near proximity through the use of a crosslinking reagent. *In vitro*, co-immunoprecipitation studies, where prey proteins that adhere to a specific bait protein are co-precipitated by a bait-specific antibody, can be very useful if bait-specific antibodies are available. Affinity-tagged bait proteins are routinely used for the analysis of protein interactions in affinity purification of protein complexes (pull-down assays). Phage display is a high throughput method where prey proteins are fused to the viral coat proteins, leading to the

identification of proteins with affinity to the bait protein through the process of biopanning. Protein chip arrays, where the bait proteins are coupled to a chip surface and exposed to a plethora of possible prey proteins, followed by MS analysis, is another high-throughput method for the detection of protein-protein interactions. Several biophysical techniques such as fluorescence resonance energy transfer (FRET) or surface plasmon resonance can also be used to investigate protein-protein interactions (Howell et al., 2006; Phizicky and Fields, 1995).

3.1.2 Phage display

In 1985, G.P. Smith illustrated that fusion proteins can be expressed on the surface of *E. coli* filamentous phage, if the nucleotide sequence encoding the desired antibody fragment, peptide or protein is fused to the nucleotide sequence that encodes a phage coat protein (Phizicky and Fields, 1995; Smith, 1985; Willats, 2002). This process, called phage display, is used today as a straightforward functional genomics method for the identification of protein-ligand interactions (Mullen et al., 2006). This ranges from the identification of antibodies, (Bradbury and Marks, 2004), to interactions between peptides and various cellular proteins, (Szardenings, 2003; Uchiyama et al., 2005) to the identification of peptides with high binding affinity to inorganic compounds such as a diverse array of metals, (Kriplani and Kay, 2005). Phage display has even been used to identify peptides that bind to *Bacillus* spores, an application which may be used for the detection of biological weapons, such as anthrax that is caused by *B. anthracis* (Turnbough Jr, 2003).

Phage display is made possible by the fact that fusion proteins often have the same or similar biological effect as the original proteins from which they are derived (Uchiyama et al., 2005). It entails the fusion of foreign DNA sequences to one of the genes that encodes viral coat proteins, resulting in the expression of fusion peptides on the viral coat surface. There are basically two different types of libraries that are used in phage display, namely synthetic random libraries and natural peptide libraries (Fig 3.1). Synthetic random libraries are created using random peptides ranging from 5-20 amino acids, and it is possible to constrain the flexibility of these peptides by cyclisation (Uchiyama et al., 2005; Willats, 2002). The advantage of synthetic random libraries lies in the great diversity that can be generated (Mullen et al., 2006), as well as the fact that the library can be designed to include specific structural elements (Hoess, 2001). The process of biopanning with a synthetic random peptide library often leads to peptides with conserved consensus sequences, which can then be used as leads for synthetic peptide synthesis and further studies (Uchiyama et al., 2005). In contrast, natural peptide libraries are created from genome fragments of selected organisms, for example by fusing a cDNA library to one of the genes that encodes coat proteins. This implies that the peptides that are displayed should occur naturally in the organism, which is why this type of library is often used for the detection of *in*

in vivo protein-protein interactions. The disadvantage of this method is that theoretically only 1 in every 18 clones will be native peptides (only 1 in 3 will commence properly due to possible frameshifting, only 1 in 3 will finish correctly and only 1 clone in 2 will be the appropriate sense vs. antisense strand) (Mullen et al., 2006; Rodi et al., 2001). In this way, phage antibody libraries were created from the variable regions (V genes) of unimmunized or immunized organisms (Bradbury and Marks, 2004). However, it must be noted that certain authors regard phage antibody libraries as artificial ligands (Konthur and Crameri, 2003). Additionally, specific protein domains can be displayed on the surface of phage particles, thus allowing subsequent interaction studies with a specific bait protein (Willats, 2002).

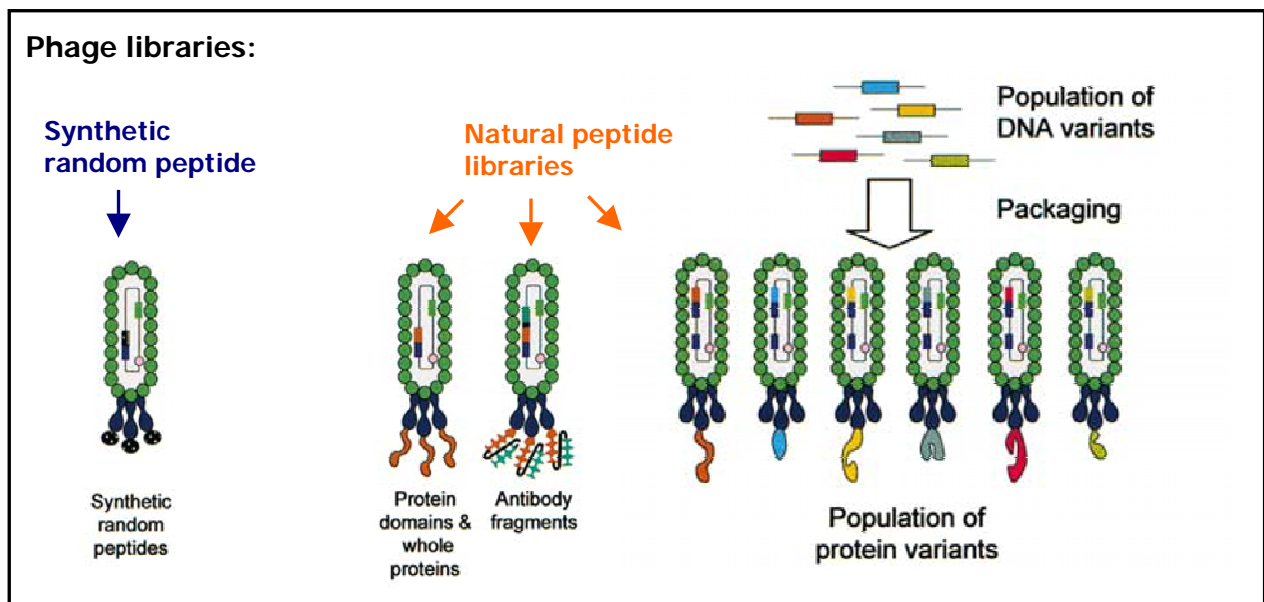


Figure 3.1: Different types of phage libraries. Adapted from (Willats, 2002).

Originally, the filamentous phage was used for polyvalent display where either the major capsid protein (g8p) encoded by gene VIII or the minor adsorption protein (g3p) encoded by gene III were involved in the cloning and expression of the fusion proteins (Azzazy and Highsmith, 2002; Smith, 1985). However, since all the g3p or g8p proteins were then expressed as recombinant proteins, severe limitations were imposed on the size of the fused protein to be displayed in order to maintain the viability of the phage particles. This problem was overcome with the development of a monovalent phagemid system. Phagemids are plasmids that contain both an *E. coli* and phage origin of replication, gene III, multiple cloning sites for the insertion of foreign DNA as well as a suitable antibiotic resistance gene. A helper phage that contains the majority of the genes needed for the construction of phage particles and wild-type copies of the coat protein are co-infected with the phagemid into the *E. coli* host. Thus, fusion coat proteins encoded by the phagemid and wild-type coat proteins provided by the helper phage are packaged in the *E. coli* host into phage particles capable of re-infection. (Azzazy and Highsmith,

2002; Baek et al., 2002; Fernández, 2004; Hoess, 2001; Mullen et al., 2006; Phizicky and Fields, 1995; Willats, 2002).

In spite of these advantages, the filamentous phages are severely restricted as display systems. The foreign DNA is fused to the N-terminal of gene III or gene VIII, making this system unsuitable for the expression of cDNA fragments that does not start with an initiation codon or that contain stop codons (Mullen et al., 2006). In addition, the non-lytic proliferation method of this type of phage imply that only peptides that can be exported through the bacterial inner membrane can be incorporated into the phage particle, since phage assembly takes place in the periplasm (Willats, 2002). It has also been shown that certain peptides and proteins are not effectively assembled on the virion capsid. The difference between the cytoplasmic and periplasmic chemical environments can also affect the stability and folding characteristics of the displayed protein (Castagnoli et al., 2001). These disadvantages led to the investigation of different phage systems that would not suffer from these limitations, such as lytic T7 phage.

T7 is a lytic phage consisting of double stranded DNA within an icosahedral capsid shell that consists of 415 copies of the capsid protein. Gene 10, which encodes for the capsid protein, undergoes a translational frameshift at amino acid 341 to produce two different proteins (based on the C-terminal sequence), namely gp10A (344aa) and gp10B (397aa) (Fig 3.2).

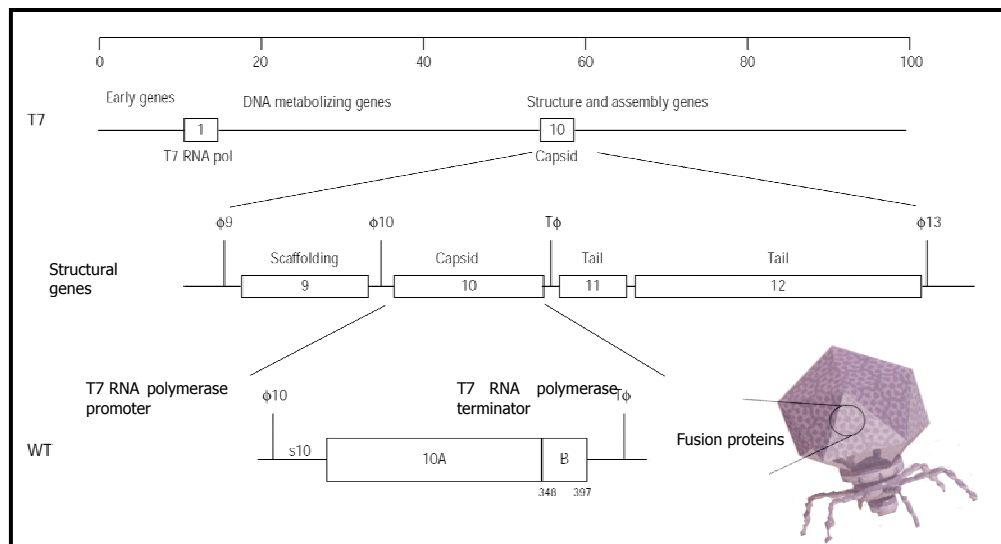


Figure 3.2: Genetic map and structural elements of T7. Adapted from (Rosenberg et al., 1996).

Due to the fact that functional phage particles contain capsids comprising of various ratios of these two capsid proteins, it was hypothesized that the T7 phage would tolerate fusion proteins on its surface, especially since it appeared as if the variable region of the capsid protein is

present on the surface of the phage. As a result, it was found that fusion proteins could be attached to the C-terminal end of the capsid protein, allowing for the display of cDNA libraries containing possible stop codons (Castagnoli et al., 2001; Condrón et al., 1991). The advantages of using T7 phage for phage display includes the display of recombinant hydrophobic or globular proteins that may not have been able to cross the bacterial membrane, since phage assembly occur inside the host cell and not inside the periplasm. Additionally, the T7 phages are resistant to extreme conditions and have a short lifecycle, thus reducing the time required for the several rounds of growth essential for selection. However, this system also have disadvantages, such as possible misfolding of the peptides due to lack of disulfide bond formation (Konthur and Cramer, 2003; Rosenberg et al., 1996).

The phage display cycle consists of 5 basic steps by which the large diversity in a library can be screened to obtain a manageable number of protein binding partners with affinity to the bait protein:

1. A diverse library such as a cDNA or a synthetic random peptide library is created and cloned into phagemid or phage genomes to produce phage particles that expresses the recombinant peptide fused to a surface protein (Fig 3.3, a and b).
2. The phage particles are brought into contact with the immobilised protein target (bait) for which a protein ligand (prey) is sought (Fig 3.3, c).
3. The non-binding phage particles are washed off (Fig 3.3, d).
4. The phage particles that bound to the immobilised protein are eluted, amplified by infection into host bacteria and screened again (Fig 3.3 e, f and g).
5. The phage particles are analysed to identify the binding proteins (Fig 3.3, h) (Willats, 2002).

The biopanning steps (steps 2-4) are repeated between three to five times to generate a library that is greatly enriched in the number of phage with binding affinity to the immobilised bait protein. However, since a library contains phages with a diverse range of avidity to the target protein, care must be taken to ensure a balance between the avidity and selectivity of the enriched clones. For instance, too little washing may lead to the enrichment of phage clones with high binding avidity, but low selectivity, while stringent washing may lead to the loss of phage clones with high selectivity, but weak binding (Willats, 2002).

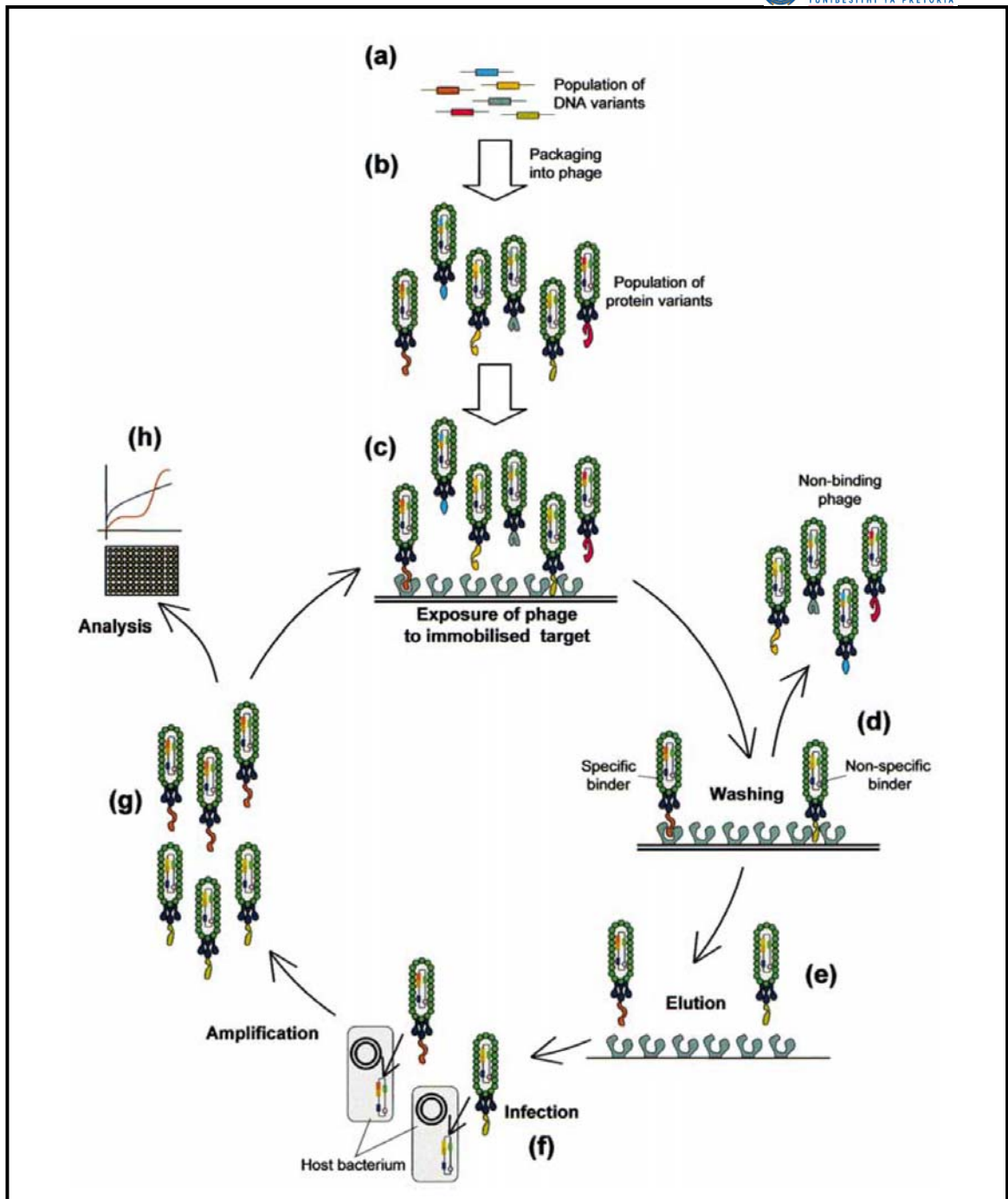


Figure 3.3: Identification of protein ligands by the phage display cycle (Willats, 2002).

3.1.3 Phage display for the study of protein-protein interactions

One major advantage of the phage display system for the study of protein-protein interactions is that a very large number of protein ligands can be screened in a short time. As such, phage display libraries with several billion variants can be used to study antibody and receptor binding sites, or the interaction between proteins and ligands in a matter of weeks (Azzazy and Highsmith, 2002; Rodi et al., 2001). There is also a genetic and phenotypic linkage due to the fact that the genetic information that encodes for the phenotypic effect is already cloned into the phage itself, which facilitates downstream reactions such as sequencing (Paschke, 2006). The peptide ligand identified during this process can also give an indication of the residues that

are involved in the binding of the bait and prey proteins, since only short peptides are expressed (Phizicky and Fields, 1995; Rodi et al., 2001; Willats, 2002). However, false negatives can occur due to the use of a bacterial expression system and the fact that a fusion protein is generated. It is possible that an *in vivo* ligand of the bait protein is not identified due to misfolding or a decrease in the accessibility of the relevant residues of the displayed recombinant protein (Phizicky and Fields, 1995).

Most proteins contain specific residues that are involved in binding to other proteins, over and above the active sites of enzymes that have evolved to allow the binding to specific small molecules (substrates). As such, proteins are viable targets for the identification of peptide ligands via phage display, since the binding of the displayed peptides usually occur at biologically relevant pockets, either at the active site or at other domains that have evolved to allow molecular interactions (Kay and Hamilton, 2001; Szardenings, 2003). It is worth noting that the concept of “convergent evolution” can play a role in the analysis of interacting peptides, where the sequences of synthetic random peptides that bind to a specific target may have homology to the *in vivo* protein partners of the bait protein. These *in vivo* partners can then be identified using similarity searches of the specific proteome (Fig 3.4) (Kay and Hamilton, 2001; Kay et al., 2000). As such, these isolated peptides can either inhibit the activity of the protein, aid in identifying the *in vivo* protein partners of a protein or elucidate the molecular basis (key residue ‘hot-spots’) of particular interactions between different protein binding partners (Kay and Hamilton, 2001). Phage display technology has already been used to identify peptide ligands to a diverse range of enzymes such as membrane dipeptidase (Rajotte and Ruoslahti, 1999), Enzyme I of the phosphoenolpyruvate-sugar phosphotransferase system (Mukhija and Erni, 1997) and Erm Methyltransferase (Giannattasia and Weisblum, 2000).

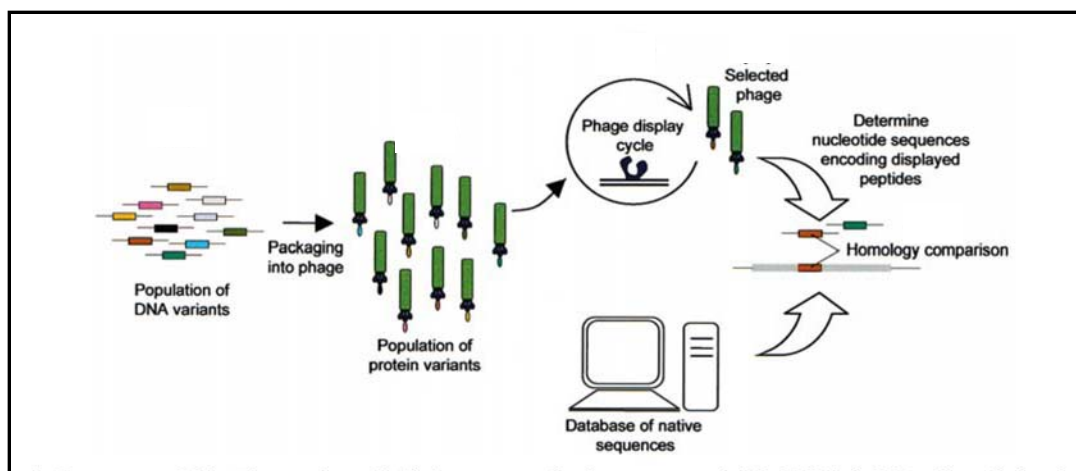


Figure 3.4: The concept of convergent evolution, where affinity peptides may have sequence similarity to the natural binding partners of a protein. Adapted from (Willats, 2002).

3.1.4 Phage display in the fight against malaria

Peptide ligands of a protein can be used in a drug-discovery process since, although peptides themselves do not generally make good drugs, they provide a backbone for the peptidomimetic design of efficient drugs. The large repertoire of possible applications of phage display has led to it being utilised in the fight against malaria in a variety of ways. These range from the identification of antibodies against *P. falciparum* merozoite surface protein-1 (Sowa et al., 2001) to the elucidation of the human antibody response to *P. falciparum* sporozoites (Chappel et al., 2004). Peptides that block the invasion of *P. falciparum* in *A. gambiae* (Ghosh et al., 2003; Ghosh et al., 2002), or merozoite invasion of erythrocytes (Keizer et al., 2003; Li et al., 2002) as well as those that targets infected erythrocytes, have been identified (Eda et al., 2004). Malarial proteins that may interact with host erythrocyte proteins have also been identified using a *P. falciparum* cDNA library cloned into T7 phage (Lanzillotti and Coetzer, 2004; Lauterbach et al., 2003).

The bifunctional PfAdoMetDC/ODC has several parasite-specific inserts, and it has been suggested that they play a part in interactions with unknown regulatory proteins. Although it has been shown that these stretches of amino acids are involved in various inter- and intra-domain interactions that is important for both decarboxylase activities and bifunctional complex formation (Birkholtz et al., 2004), the possibility that these inserts are also involved in interactions with other proteins can not be ignored. Linear motifs that mediate protein-protein interactions often occur within such regions of low complexity (Neduva et al., 2005). Since the activity of especially the ODC domain of the bifunctional enzyme is dependent on dimerization (Wrenger et al., 2001), it is possible that interface peptides or peptidomimetics can inhibit its activity (Birkholtz et al., 2004), as was the case with the plasmodial TIM (Singh et al., 2001). However, since no crystal structure exists to date for PfAdoMetDC/ODC and the exact residues involved in the interactions in the bifunctional complex have not been experimentally elucidated, structure-based design of molecules that disrupt the protein-protein interactions is not currently feasible. This necessitated the determination of protein-protein interactions of PfAdoMetDC/ODC through the use of a *P. falciparum* cDNA phage display library. There are three possible types of results that can be obtained through the use of such a library: Firstly, proteins that could have an interaction with PfAdoMetDC/ODC in the biological context due to co-expression at the correct location and lifecycle stage can be identified. Secondly, random peptides with affinity to PfAdoMetDC/ODC could be identified. Sequence alignment of these peptides could show conserved consensus regions that mediate the binding to PfAdoMetDC/ODC (Santonico et al., 2005). Synthetic peptides could then be produced based on these sequences and used as possible lead sequences in drug development. Lastly, fragments of PfAdoMetDC/ODC itself could

be obtained, which may prevent dimerization of the protein, as was the case with Plasmodial TIM (Singh et al., 2001). It has been shown that, under physiological conditions, the subunits of mammalian ODC voluntarily reassociate and dissociate (Coleman et al., 1994) and for *T. brucei*, a rapid equilibrium exists between the ODC subunits (Osterman et al., 1994). These results further support the hypothesis that fragments of ODC can be used to disrupt the formation of the bifunctional complex, thus preventing polyamine synthesis. This chapter aims to utilise phage display to identify peptide binding partners to PfAdoMetDC/ODC.

A part of this work was presented at the International Congress of Parasitology XI (ICOPA XI) in Glasgow, Scotland in August 2006.

3.2 Materials and methods

3.2.1 *P. falciparum* cDNA phage display library

A *P. falciparum* cDNA phage display library was created using the T7select Phage display system (Novagen, USA) by Sonja Lauterbach and co-workers (Lauterbach et al., 2003). In short, guanidinium isothiocyanate was used to extract total RNA from *P. falciparum* strain FCR-3 cultures, from which mRNA was isolated and used as template in cDNA synthesis. The cDNA thus obtained were end-modified for cloning into the T7Select10-3b vector system according to Novagen's specifications. Following cloning, the recombinant vectors were packaged into the T7 bacteriophage packaging extracts. The phages were proliferated in the *E. coli* strain BLT5403, which contains a plasmid encoding the 10A capsid protein (Rosenberg et al., 1996).

3.2.2 Titer determination via plaque assay

E. coli cells will grow to a lawn of bacteria with clear areas (plaques) corresponding to single phage infection incidences, mediated by single phage particles. To ascertain the number of phage particles present at a given time, serial dilutions of phage lysate (LB-broth containing the lysed BLT5403 cells and amplified phage particles) were combined with BLT5403 cells and molten agarose. The plaque assay was executed as follows: BLT5403 cells were inoculated from -70°C stock in 5 ml (LB-Broth) (1% w/v tryptone, 1% w/v NaCl and 0.5 % w/v yeast extract, pH 7.5) containing 50 µg/ml ampicillin (Roche Diagnostics, Germany) and grown with agitation (250 rpm) at 37°C for 4 hrs. The culture (20 µl) was plated onto LB-agar (LB-Broth, 1% w/v agar) plates containing ampicillin (100 µg/ml) and grown overnight at 37°C. A single colony was inoculated in LB-Broth containing 50 µg/ml ampicillin and grown to saturation overnight at 37°C with agitation. The overnight culture was diluted 1:100 with M9LB (LB-broth with 18.7 mM NH₄Cl, 22 mM KH₂PO₄, 22.4 mM Na₂HPO₄·7H₂O, 0.4% w/v glucose and 1 mM MgSO₄) and grown with agitation at 37°C until an OD₆₀₀=1 was reached. Subsequently, 100 µl of a serial dilution of phage lysate sample in sterile LB-broth (ranging from 10²-10¹² times dilution) and 5 ml of warm (~50°C) sterile molten top agarose (1% w/v tryptone, 0.5% w/v yeast extract, 0.5% w/v NaCl and 0.6% w/v agarose) were added to 250 µl of the cells. The samples were mixed and poured onto pre-warmed (37°C) LB-agar plates supplemented with 100 µg/ml ampicillin, swirled to ensure even distribution and incubated overnight at room temperature. The titer of the sample in plaque forming units (pfu) per unit volume was calculated according to the following equation:

$$\text{Titer (pfu/ml)} = \text{number of plaques} \times \text{dilution} \times 10$$

3.2.3 Biopanning of *P. falciparum* cDNA phage display library against recombinant PfAdoMetDC/ODC

A *P. falciparum* cDNA library displayed on the capsid protein of the lytic T7 phage was a kind gift from Professor Theresa L Coetzer, University of the Witwatersrand (Lauterbach et al., 2003). Two different libraries were created by Roberto Lanzillotti and Sonja B Lauterbach, respectively. The titer of each library was determined (section 3.2.2) and both libraries were diluted to 1×10^7 pfu/ml in Tris Buffered Saline (TBS, 50 mM Tris-HCl, 150 mM NaCl, pH 7.5) according to the manufacturer's specifications. Subsequently, equal volumes of each library were mixed to create a homogeneous starting library, which was used for subsequent biopanning procedures. The library thus obtained were pre-selected against *Strep*-Tactin Sepharose (IBA GmbH, Germany) to prevent non-specific background binding by incubating the diluted 1×10^7 pfu/ml starting library (500 μ l) with 100 μ l *Strep*-Tactin Sepharose overnight at 4°C. The pre-selection was repeated by incubating the diluted 1×10^7 pfu/ml starting library (500 μ l) with 100 μ l *Strep*-Tactin Sepharose at room temperature for 1 hr. The phage-*Strep*-Tactin Sepharose mixture was centrifuged at 16 100xg for 10 min at 4°C to separate the *Strep*-Tactin Sepharose from the phage library prior to biopanning.

PfAdoMetDC/ODC was expressed as described in section 2.2.11 with the following changes: Affinity chromatography was performed at 4°C using batch purification with 250 μ l *Strep*-Tactin Sepharose (IBA GmbH, Germany). The soluble protein extract obtained after ultracentrifugation was exposed to the Sepharose for 1 hr with rotation, followed by at least 6 washes with 4 volumes buffer W. 500 μ l of the pre-incubated phage was added to the immobilised protein and incubated overnight at 4°C with rotation. Following incubation, the *Strep*-Tactin Sepharose with immobilised PfAdoMetDC/ODC and bound phage were washed 3 times with 10 ml TBS containing 0.5 % (v/v) Tween-20 to remove any non-specific and unbound phage, followed by centrifugation at 100xg for 2 min in a Hermle z232M centrifuge (Hermle Labortechnik GmbH, Germany). Elution of the bound phage particles from the immobilised PfAdoMetDC/ODC was effected by a 15 min incubation with 200 μ l Phage elution buffer (TBS, 1% w/v SDS). PfAdoMetDC/ODC was eluted from the *Strep*-Tactin Sepharose with 2 volumes Buffer E (Buffer W containing 2.5 mM desthiobiotin, pH 8, IBA GmbH, Germany).

BLT5403 cells were inoculated from -70°C stock in 5 ml LB-Broth containing 50 μ g/ml ampicillin (Roche Diagnostics, Germany) and grown with agitation at 37°C, overnight. The culture was plated onto LB-agar (LB-Broth, 1% w/v agar) plates containing ampicillin (100 μ g/ml) and grown overnight at 37°C. A single colony was inoculated in LB-Broth containing 50 μ g/ml ampicillin and grown overnight at 37°C with agitation. 50 ml LB-Broth containing 50 μ g/ml ampicillin was inoculated with 500 μ l of this overnight culture and grown at 37°C until an

OD₆₀₀ = 0.5 was reached. The eluted phage particles from above were diluted 200-fold in TBS (pH 7.5) to prevent inhibition of bacterial growth by the SDS present in the phage elution buffer. Of this, 250 µl were added to the BLT5403 culture for amplification. The phage particles were amplified for approximately 6 hrs at 37°C, after which lysis of the BLT5403 cultures were observed. The phage lysates was prepared for storage by adding NaCl to a 0.5 M final concentration and cleared by centrifugation at 3 000xg for 20 min in a Hermle z232M centrifuge (Hermle Labortechnik GmbH, Germany) or at 1 500xg for 30 min in a Beckman model J-6 centrifuge. The titer was determined as described in section 3.2.2 and the lysate stored at 4°C until the next round of biopanning. This procedure was repeated for each biopanning round.

Six different phage libraries with affinity to PfAdoMetDC/ODC were created, based on different experimental conditions as described in Table 3.1. These include varying the Tween-20 concentrations in the TBS wash buffer to allow different selection stringencies, thus creating Libraries A and B. In an effort to prevent non-specific ionic interactions between poly-Lys encoding phages and the recombinant protein, PfAdoMetDC/ODC was blocked prior to biopanning using a poly-Lys solution. This was done prior to each round of biopanning to create Library C or for just the first two rounds of biopanning to create Library F (Library C and F were the same library initially, and only differed at round 3 of biopanning). It was also attempted to prevent non-specific ionic interactions by increasing the salt concentration in the wash buffer to 250 mM NaCl (Library D) or 500 mM NaCl (Library E).

Table 3.1: Description and methodology of different libraries created by biopanning with affinity to PfAdoMetDC/ODC.

Library	Name	Description
A	High Tween-20	Used 0.5% v/v Tween-20 in TBS wash buffer
B	Low Tween-20	Used 0.05% v/v Tween-20 in TBS wash buffer
C	Complete poly-Lys block	Blocked recombinant PfAdoMetDC/ODC with 3x molar excess of poly-L-Lysine hydrochloride (SIGMA, USA) (0.0014 % w/v in Buffer W) for 2 hrs at 4°C with rotation, followed by washing the beads with 4 volumes Buffer W prior to exposure to the phage library. Used 0.05% v/v Tween-20 in TBS wash buffer
D	Medium salt	Used 0.05% v/v Tween-20 in 50 mM Tris-HCl, 250 mM NaCl, pH7.5
E	High salt	Used 0.05% v/v Tween-20 in 50 mM Tris-HCl, 500 mM NaCl, pH7.5
F	Partial poly-Lys block	Blocked recombinant PfAdoMetDC/ODC with 3x molar excess of poly-L-Lysine hydrochloride (SIGMA, USA) (0.0014 % w/v in Buffer W) for 2 hrs at 4°C with rotation for the first two rounds of biopanning, followed by washing the beads with 4 volumes Buffer W prior to exposure to the phage library. Used 0.05% v/v Tween-20 in TBS wash buffer

The biopanning with the modifications as described in Table 3.1 were performed as discussed above.

3.2.3.1 Verification of the identity of the recombinant bait protein

The recombinant expression of PfAdoMetDC/ODC was verified with SDS-PAGE analysis (section 2.2.13.1) and dot blot Western analysis to ensure correct expression of the bait protein. PfAdoMetDC/ODC was recombinantly expressed and isolated as in section 2.2.11 and used as a positive control. Following SDS-PAGE, the proteins were visualised with silver staining (section 2.2.13.3.1). Protein concentration determination was performed as described in section 2.2.12.

The dot blot Western analysis was performed as follows: PolyScreen PVDF Transfer Membrane (Nen™ Life Science Products, USA) was prepared by wetting in methanol for 15 sec and then equilibrated in PBS, pH 7.4 for 5 min. 1 µl of each of the following entities were subsequently spotted onto the membrane: the starting phage library (1×10^7 pfu/ml) as negative control since no *Strep*-tag II should be present, affinity-purified PfAdoMetDC/ODC as positive control, the PfAdoMetDC/ODC containing eluate obtained with Phage elution buffer (TBS with 1% w/v SDS) and the eluate obtained with Buffer E following elution of the phage particles. The membranes were blocked overnight at 4°C or for 1 hr at 37°C in blocking buffer (PBS with 3% w/v BSA, 0.5% v/v Tween-20, pH 7.4). The *Strep*-tag II was immunodetected as described in section 2.2.14.

3.2.4 Screening of *P. falciparum* cDNA inserts

3.2.4.1 Determination of insert cDNA size by PCR amplification and gel electrophoresis

Following the final rounds of biopanning, the resulting libraries with affinity to PfAdoMetDC/ODC were plated out to obtain single plaques as described in section 3.2.2. After this, BLT5403 cells were inoculated from -70°C stock in LB-Broth containing 50 µg/ml ampicillin (Roche Diagnostics, Germany) and grown with agitation at 37°C overnight. The culture was plated onto LB-agar (LB-Broth, 1% w/v agar) plates containing ampicillin (100 µg/ml) and grown overnight at 37°C. A single colony was inoculated in LB-Broth containing 50 µg/ml ampicillin and grown overnight at 37°C with agitation. This was diluted 100-fold and grown at 37°C with agitation until $OD_{600} = 0.5$ was reached. This culture was inoculated with a single phage plaque, which was then allowed to amplify at 37°C for at least 3-4 hrs. Phage lysates were prepared for storage as in section 3.2.3. The phage DNA was released from the amplified phage particles by incubating 10 µl of phage lysate with 40 µl of 10 mM EDTA, pH 8.0 at 65°C for 10 min. The DNA was cleared from the cellular debris by centrifugation at 1000xg for 5 min at 4°C in a Beckman

model J-6 centrifuge and the DNA-containing supernatant used as template in a PCR amplification reaction.

All PCR reactions were performed in 200 μ l thin walled tubes (Quality Scientific Plastics, USA) in either a Perkin Elmer GeneAmp PCR system 2400 or system 9700 (PE Applied Biosystems, USA). The 25 μ l reactions contained 1 μ l of phage DNA prepared as above as template, 0.2 mM of each dNTP (Takara, Japan), 5 pmol each of the primers T7SelectUP and T7SelectDOWN (see Table 3.2) and 1 U of *Taq* DNA polymerase (Promega, USA) in 1 x buffer (10 mM Tris-HCl, pH 9.0, 50 mM KCl, 0.1% Triton[®]X-100 and 1.5 mM MgCl₂). The cycling reactions were performed as follows: an initial denaturation step at 94°C for 5 min, followed by 30 cycles of denaturation at 94°C for 50 sec, annealing at 55°C for 30 sec, extension at 72°C for 1 min, followed by a final incubation of 72°C for 6 min. The cycling reaction was later increased to 35 cycles as per Novagen's instructions for the amplification of phage inserts. Prior to sequencing, the reactions were increased to 5 x 25 μ l reactions to obtain sufficient DNA for further experiments.

All PCR reactions were analyzed on either 2% or 2.5% w/v agarose (Promega, USA)/TAE (0.04 M Tris-acetate, 1mM EDTA, pH 8) gels in TAE running buffer at 4-10 V/cm in a Hoefer HE 33 mini submarine electrophoresis unit (Amersham Biosciences, England). Each sample was loaded in 1x loading dye (0.025% w/v bromophenol blue and 30% v/v glycerol). GeneRuler™ 50 bp DNA ladder, the O' GeneRuler™ 50 bp DNA ladder (Fermentas, USA) or the 100 bp DNA ladder (Promega, USA) were used as molecular markers. The agarose/TAE gels either contained EtBr (50 μ g) or were stained in a 10 μ g/ml EtBr solution for approximately 30 min. The DNA bands were visualized under UV-light with a Spectroline TC-312 AV transilluminator (Spectronics corporation, USA) at 312 nm. A CCD camera coupled to IC Capture software (The Imaging Source Europe, Germany) was used to capture the image.

3.2.4.2 Differentiation between similar sized inserts with restriction mapping

The cDNA inserts that appeared to be of a similar size were amplified as above, followed by restriction enzyme digestion using 10 U *Hind*III (Promega, USA) in Buffer E (6 mM Tris-HCl, 6 mM MgCl₂, 100 mM NaCl, pH 7.5) or 12 U *Eco*RI (Promega, USA) in Buffer H (90 mM Tris-HCl, 10 mM MgCl₂, 50 mM NaCl, pH 7.5) for 3 hrs at 37°C. Alternatively, separate restriction enzyme digestions with 10 U *Nde*I (Promega, USA) in Buffer D (6 mM Tris-HCl, 6 mM MgCl₂ 150 mM NaCl and 1 mM DTT, pH 7.9) 10 U *Vsp*I (Fermentas, USA) in Buffer O (50 mM Tris-HCl, 10 mM MgCl₂ 100 mM NaCl and 0.1 mg/ml BSA, pH 7.5) or 10 U *Eam*1140I (Fermentas, USA) in Buffer Tango (33 mM Tris-acetate, 10 mM Mg-acetate, 66 mM K-acetate and 0.1 mg/ml BSA, pH 7.9) were performed overnight at 37°C. These enzymes were chosen due to the high A+T-content of their recognition sites, thus allowing for better differentiation between similarly sized DNA

inserts as mediated by the high frequency of cutting expected in the A+T rich malarial genome. The samples were analysed using either a 2% or 2.5% w/v agarose/TAE gel to differentiate between differently sized cDNA inserts.

3.2.4.3 Cloning protocols

The unique PCR products identified above were purified as described in section 2.2.8 with the Nucleospin[®] Extract II (Macherey-Nagel GmbH & Co.KG, Düren, Germany).

3.2.4.3.1 Ligation of cDNA inserts into the pGem[®]-T Easy vector (Promega, USA.)

See section 2.2.9.1 for details. The ligation reactions (10 µl final volume) contained 30.5-154 ng insert, 1x Rapid ligation Buffer (20 mM Tris-HCl, 20 mM MgCl₂, 20 mM DTT, 2 mM ATP, and 10% v/v polyethylene glycol, pH 7.8), 50 ng pGem[®]-T Easy vector and 3 Weiss units T4 DNA ligase. The reaction was incubated at 4°C for at least 16 hrs prior to transformation.

3.2.4.3.2 Transformation of ligation reaction

Heat shock competent DH5α (Gibco BRL Life Technologies, USA) *E. coli* cells were prepared as in section 2.2.3 and transformed with 5 µl of the ligation reaction as described in section 2.2.5. Transformation mix (50 –100 µl) was plated onto LB-agar plates supplemented with 100 µg/ml ampicillin that were previously coated with 20 µl Xgal (50 mg/ml) and 100 µl IPTG (100 mM) according to the manufacturer's instructions for blue-white selection. The plates were incubated overnight at 37°C. White colonies indicated possible positive clones.

3.2.4.3.3 Plasmid isolation

Possible positive clones were picked and grown overnight in LB-Broth containing 50 µg/ml ampicillin as a means of selection, since positive clones should contain the pGem[®]-T Easy vector with the ampicillin resistance gene. Plasmids were isolated from the overnight cultures using either the High Pure Plasmid Isolation Kit (Roche Diagnostics, Germany) or the E.Z.N.A.[®] Plasmid Miniprep Kit I (Pierce Biotechnology GmbH, Germany) (section 2.2.2) according to the manufacturer's specifications.

3.2.4.3.4 Screening for positive clones

Colony screening PCR was used to identify clones with the correct insert cloned into the pGem[®]-T Easy vector. 5 colonies of each clone were randomly picked and grown overnight to saturation in LB-Broth supplemented with 50 µg/ml ampicillin. The 25 µl reactions contained 1µl of bacterial culture as template, 0.2 mM of each dNTP (Takara, Japan), 5 pmol each of the primers T7SelectUP and T7SelectDOWN and 1 U of *Taq* DNA polymerase (Promega, USA) in 1 x buffer (10 mM Tris-HCl (pH 9.0), 50 mM KCl, 0.1% Triton[®]X-100 and 1.5 mM MgCl₂). The cycling reaction was performed as follows: an initial denaturation step at 94°C for 5 min, followed by either 30 or 35 cycles of denaturation at 94°C for 50 sec, annealing at 55°C for 30 sec,

extension at 72°C for 1 min, followed by a final incubation of 72°C for 6 min. The PCR products were analysed by running on either a 2% or a 2.5% w/v agarose/TAE gel and checking for the correctly sized product as described in section 2.2.7.

Alternatively, restriction enzyme digestion was performed on isolated plasmids to identify positive clones. The restriction enzyme digestions were set up as follows: plasmid DNA (between ~0.8-1.8 µg) was digested for 3 hrs at 37°C with 12 U *Eco*RI (Promega, USA) in Buffer H (90 mM Tris-HCl, 10 mM MgCl₂, 50 mM NaCl, pH 7.5). The reaction was terminated when the digestions were electrophoresed on either a 1.5% or a 2.5% w/v agarose/TAE gel at 4-10 v/cm. The gels were stained in a 10 µg/ml EtBr solution for approximately 30 min and the DNA bands were visualized under UV-light.

3.2.4.4 Automated nucleotide sequencing

The nucleotide sequences of the *P. falciparum* cDNA inserts were determined automatically with an automated ABI PRISM® 3100 Genetic Analyzer (PE Applied Biosystems, California, USA) based on the Sanger-dideoxy method (section 2.2.10.2). The 20 µl sequencing reactions contained 4 µl Big Dye Ready Reaction mix version 3.1, 2 µl Big Dye Sequencing buffer (400 mM Tris-HCl pH 9.0, 10 mM MgCl₂), 5 pmol sequencing primer and as template ~0.8-1.8 µg plasmid DNA or ~125-200 ng purified PCR product. The cycle-sequencing reactions were run as follows: an initial denaturation step at 96°C for 1 min, followed by 26 cycles of denaturation at 96°C for 10 sec, the primer appropriate annealing temperature for 10 sec (see Table 3.2), extension at 60°C for 4 min and a final incubation of 60°C for 7 min. This reaction was subsequently modified to an optimum annealing time of 15 sec and 28 cycles. All sequencing reactions were run on either a Perkin Elmer GeneAmp PCR system 2400 or system 9700 (PE Applied Biosystems, USA). All the truncated PCR products with incorporated chain terminators were precipitated and analysed as in section 2.2.10.2.

Table 3.2: Sequences and T_m of primers used for the sequencing of the cDNA inserts from phages with affinity to PfAdoMetDC/ODC.

Primer	Sequence	T _m °C
T7	5' GTA ATA CGA CTC ACT ATA GGG C 3'	58
SP6	5' ATT TAG GTG ACA CTA TAG AAT AC 3'	53.5
T7SelectUP	5' GGA GCT GTC GTA TTC CAG TC 3'	59
T7SelectDOWN	5' AAC CCC TCA AGA CCC GTT TA 3'	57

3.2.5 Sequence analysis

The identity of the *P. falciparum* cDNA inserts were determined using the Basic Local Alignment Search Tool (BLAST) (Altschul et al., 1990) using BLASTN (<http://www.plasmodb.org>) (Bahl et

al., 2002). The protein sequence encoded by the cDNA insert was determined by utilising the Translate tool accessed via the ExPASy interface (<http://au.expasy.org>) (Gasteiger et al., 2003). ProtParam (<http://au.expasy.org>) was used to determine the theoretical isoelectric point (pI), molecular mass, number of charged residues and instability index of the protein (Gasteiger et al., 2005). The percentage secondary structure motifs of the proteins were determined with the Predictprotein Server (<http://www.predictprotein.org>) (Rost et al., 2004). The proteins were also analysed for specific structural motifs and functional domains (PlasmoDB). Conserved domains were determined through Conserved Domains (Marchler-Bauer and Bryant, 2004) accessed through the NCBI website (www.ncbi.nlm.nih.gov). Consensus motifs between the various peptide sequences were determined with MEME, a motif discovery tool (Bailey and Elkan, 1994). Unless otherwise stated, all programs were run with the default parameters activated.

3.2.6 Verification of binding partners to PfAdoMetDC/ODC

3.2.6.1 Recombinant expression of PfAdoMetDC/ODC and *E. coli* DnaK

PfAdoMetDC/ODC was recombinantly expressed and purified as described in section 2.2.11. *E. coli* DnaK was cloned into the pQE-30 expression plasmid (Qiagen, USA), which encodes for a N-terminal His-tag (Dr Aileen Boshoff, Rhodes University). pQE-30-DnaK was transformed into 100 μ l XL2-Blue Ultracompetent Cells (Stratagene, USA) in an Eppendorf tube. Subsequent to thawing on ice, β -Mercaptoethanol was added to the cells (final concentration 24 mM) and incubated on ice for 10 min with occasional swirling. \sim 75 ng plasmid was added to the cells, followed by incubation on ice for 30 min. The cells were heat shocked at 42°C for 30 sec, followed by 2 min on ice. 900 μ l LB-glucose (LB-broth, 20 mM glucose) was added to the cells, followed by incubation at 37°C for 1 hr with agitation. Transformation mix (100 μ l) was plated onto LB-agar plates supplemented with 100 μ g/ml ampicillin and incubated overnight at 37°C. A positive colony was selected and grown overnight in 25 ml 2xYT broth (16% w/v tryptone, 10% w/v yeast extract and 5% w/v NaCl, pH7) containing 100 μ g/ml ampicillin. The saturated culture obtained was diluted 10-fold into fresh 2xYT broth containing 100 μ g/ml ampicillin (final volume 250 ml) and grown at 37°C with agitation until an optical density $OD_{600} = 0.3-0.4$ was reached. Protein expression is under the transcriptional control of the *lac* operator, which cause the inhibition of the T5 promoter due to the *lac* repressor protein. The addition of IPTG leads to the inactivation of the repressor protein and subsequent protein expression. Protein expression was induced by the addition of 1 mM IPTG and the culture incubated for a further 2 hrs.

The cells were harvested by centrifugation at 1 500xg for 30 min at 4°C in a Beckman model J-6 centrifuge. The resulting cell pellet was resuspended in Lysis buffer (50 mM sodium phosphate, 0.3 M NaCl and 10 mM imidazole, pH8) (1/100 of the culture volume) containing 0.1 mM

phenylmethylsulfonylfluoride (PMSF) (Roche Diagnostics, Germany) and frozen overnight at -20°C. After thawing on ice with 1 mg/ml added lysozyme (Roche Diagnostics, Germany), the cells were sonicated for 6 cycles of 20 sec with a 40 sec rest interval. This was done with a Sonifier Cell Disruptor B-30 (Instrulab, South Africa) using a duty cycle of 90, an output control of 3 and a flat tip. The disrupted cells were centrifuged at 16 000xg for 20 min at 4°C in an Eppendorf Centrifuge 5415R (Eppendorf AG, Germany) to clear the cellular debris.

HIS-Select™ Nickel Affinity gel (SIGMA, USA) was used for affinity purification (1 ml). The protein extract was bound for 2 hrs with rotation at 4°C. The sample was transferred to a column followed by 4 washes with 5 volumes wash/equilibration buffer (50 mM sodium phosphate, pH 8, 0.3 M NaCl and 10 mM imidazole). The protein was eluted with 5 volumes elution buffer (50 mM sodium phosphate, pH 8, 0.3 M NaCl and 250 mM imidazole). The protein concentration was measured as in section 2.2.12 and the expression verified with SDS-PAGE analysis (section 2.2.13.1) and visualised with silver staining (section 2.2.13.3.1).

3.2.6.2 ELISA

BLT5403 cells were inoculated from -70°C stocks in LB-Broth containing 50 µg/ml ampicillin (Roche Diagnostics, Germany) and grown with agitation at 37°C overnight. The culture was plated onto LB-agar (LB-Broth, 1% w/v agar) plates containing ampicillin (100 µg/ml) and grown overnight at 37°C. A single colony was inoculated in LB-Broth containing 50 µg/ml ampicillin and grown overnight at 37°C with agitation. LB-Broth containing 50 µg/ml ampicillin was inoculated with overnight culture (1:100 dilution) and grown at 37°C until OD₆₀₀= 0.5 was reached. This culture was inoculated with a single phage plaque, which was then allowed to amplify at 37°C for at least 3-4 hrs. The phage lysate was prepared for storage as in section 3.2.3.

The affinity purified recombinant proteins were concentrated using Nanosep 10 K or 100 K Omega ultracentrifuge size exclusion columns (with a 10 kDa or 100 kDa cut-off, Pall Corporation, USA) (section 2.2.16.1). The columns were prepared by washing with dddH₂O at 4°C for 3 min at 1000xg in an Eppendorf Centrifuge 5415R (Eppendorf AG, Germany). 500 µl aliquots of the protein samples were applied to the column and centrifuged at 16 000xg at 4°C in an Eppendorf Centrifuge 5415R.

The recombinant protein samples were placed in a 96-well microtiter plate (100 µl/well) and left to bind to the plate at 4°C overnight. Phage lysate (100 µl/well) was used as positive control and BSA was used as negative control. The adhesion of PfAdoMetDC/ODC and Dnak were verified with protein-specific antibodies as described below. The samples were removed and the

plate blocked with 200 μ l blocking buffer (TBS with 3% w/v BSA, 0.05% v/v Tween-20, pH 7.5) per well for 2 hrs at room temperature. The blocking buffer was replaced with 100 μ l of the phage lysate (diluted in blocking buffer to a concentration of approximately 10^9 pfu/ml) and incubated at room temperature for 1 hr. The plate was washed 6 times in wash buffer (TBS with 0.05% v/v Tween-20, pH 7.5) and incubated with 100 μ l of the appropriate primary antibody for 1 hr at room temperature: a 1:1000 dilution of monospecific, rabbit polyclonal anti-*Strep*-tag II antibody (IBA GmbH, Germany), a 1:1000 dilution of mouse anti-DnaK antibody and a 1:1300 dilution of mouse anti-T7 Tail Fiber Monoclonal antibody (Novagen, USA) in blocking buffer. The plate was washed three times, as above, and incubated with 100 μ l of the suitable secondary antibody for 1 hr at room temperature: 1:500 dilution of horseradish peroxidase (HRP) conjugated goat anti-rabbit (Cappel™ Research Products, USA) or sheep anti-mouse HRP conjugated antibodies (SIGMA, USA) in Block buffer. The plate was washed 6 times, as above, followed by the addition of 100 μ l developing Buffer (10 ml citrate, 0.1% w/v O-Phenylenediamine and 0.08% w/v H₂O₂). The development of a coloured substrate was monitored at 450 nm with a Multiskan Ascent scanner (Thermo labsystems).

3.3 Results

A *P. falciparum* cDNA library displayed on the capsid protein of the lytic T7 phage, was a kind gift from Professor Theresa L Coetzer, University of the Witwatersrand. Roberto Lanzillotti and Sonja B Lauterbach respectively created two different libraries (Lauterbach et al., 2003). The titer of each library was determined (section 3.2.2) (Fig 3.5) and both libraries were diluted to 1×10^7 pfu/ml in TBS, according to the manufacturer's specifications prior to biopanning. Equal volumes of each library were mixed to create a starting phage library, which was used for subsequent biopanning procedures.

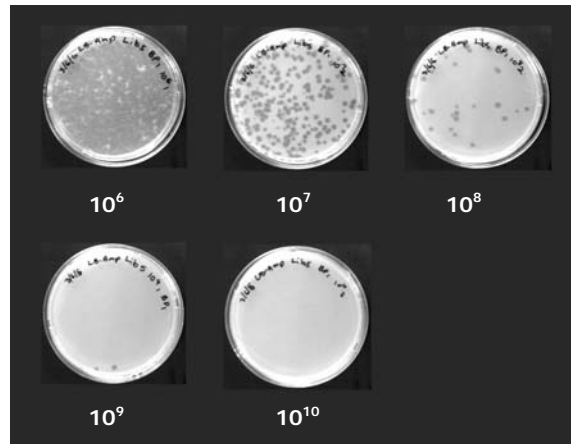


Figure 3.5: Example of typical results following titer of phage sample.

Serial dilutions of phage as indicated were combined with BLT5403 cells and grown overnight at room temperature. As can be seen from Fig 3.5, the number of phage plaques decrease with increasing dilution, leading to a change from almost complete lysis of bacteria (10^6 dilution) to a lawn of bacteria in the absence of phage plaques (10^{10} dilution).

3.3.1 Biopanning of *P. falciparum* cDNA phage display library against recombinant PfAdoMetDC/ODC to create Library A

The starting library was preincubated with *Strep*-Tactin Sepharose (IBA GmbH, Germany) to remove non-specific background interactions, after which four rounds of biopanning were performed to isolate phage particles with high affinity to PfAdoMetDC/ODC (Library A). Following each individual round of biopanning, the titer of the phage lysate was determined in duplicate (Table 3.3) prior to diluting the phages to 1×10^7 pfu/ml before the following round of biopanning.

Table 3.3: Phage titers obtained following each round of biopanning (BP) of Library A.

Phage titer (pfu/ml)			
BP1	BP2	BP3	BP4
4.8×10^{10}	1.8×10^{11}	5×10^{10}	5.1×10^{10}

The expression of recombinant PfAdoMetDC/ODC was verified following each round of biopanning by SDS-PAGE and dot blot Western analysis (Fig 3.6) to ensure the continuous presence and integrity of the recombinant bait protein.

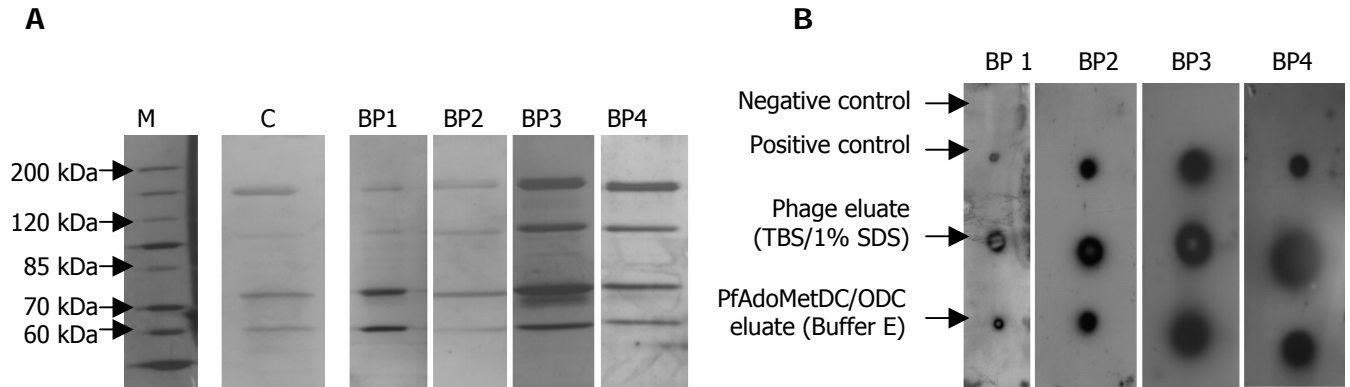


Figure 3.6: A: SDS-PAGE and B: dot blot Western analysis of recombinant PfAdoMetDC/ODC used as bait in biopanning.

A) Panel M: PageRuler™ Protein ladder used as molecular marker. Panel C: *Strep*-tag purified PfAdoMetDC/ODC used as control. Panel BP1: PfAdoMetDC/ODC used as bait for biopanning 1, Panel BP2: PfAdoMetDC/ODC used as bait for biopanning 2, Panel BP3: PfAdoMetDC/ODC used as bait for biopanning 3 and Panel BP4: PfAdoMetDC/ODC used as bait for biopanning 4. The proteins were analysed on a 7.5% SDS-PAGE gel and visualised with silver staining. **B)** The starting library (phage particles prior to biopanning) was used as negative control and recombinantly expressed PfAdoMetDC/ODC was used as positive control. The eluates obtained after elution with phage elution buffer (TBS with 1% SDS) and Buffer E following each biopanning were tested for the presence of the recombinantly expressed PfAdoMetDC/ODC.

As can be seen from Fig 3.6 A, PfAdoMetDC/ODC was successfully expressed for each biopanning procedure, with the same pattern of bands as was discussed in Chapter 2. Dot blot Western analysis using the *Strep*-tag epitope as marker confirmed this result. As can be seen in Fig 3.6 B (negative control), the phage particles themselves did not show reactivity with the anti-*Strep*-tag antibody. Both experimental spots (the phage eluate and the PfAdoMetDC/ODC eluate) showed reactivity to the antibody, due to the fact that the 1% SDS used to elute the binding phage, partially eluted some of the recombinant PfAdoMetDC/ODC as well. The *Strep*-tag/*Strep*-tactin interaction is only compatible with 0.1 % SDS (according to the manufacturer), thus leading to partial elution of the recombinant protein by the phage elution buffer (TBS, 1% w/v SDS).

Unfortunately, the concentration of the recombinant protein immobilised on the *Strep*-Tactin Sepharose could not be determined directly, since the amount of SDS in the solution is incompatible with the Bio-Rad Quick Start™ Bradford Protein assay (Bio-Rad Laboratories, USA) used, which can only tolerate 0.025% SDS. To obtain an indication of the amount of recombinant protein used as bait, control PfAdoMetDC/ODC was purified concomitantly as described in section 2.2.11 and used as an indication of protein concentration (section 2.2.12), as well as for a positive control during SDS-PAGE and dot blot Western analysis. It was found that approximately 140-265 µg recombinant protein was used as bait. This indicates that sufficient bait protein was used, since 120 µg of protein is sufficient to identify phages with high affinity to the bait protein (Lauterbach et al., 2003).

3.3.2 Screening of *P. falciparum* cDNA inserts by PCR amplification and gel electrophoresis of Library A

The T7SelectUP and T7SelectDown primers (Table 3.2) were used for the amplification of *P. falciparum* cDNA inserts released from the amplified phage particles. They anneal to the T7Select10-3b vector at locations just outside of the multiple cloning site, which implies that all PCR products contain an additional 107bp vector-derived sequence. 96 different phage clones from Library A were screened by PCR amplification and gel electrophoresis. Insert sizes ranging from ~150-250 bp were identified (Fig 3.7 A).

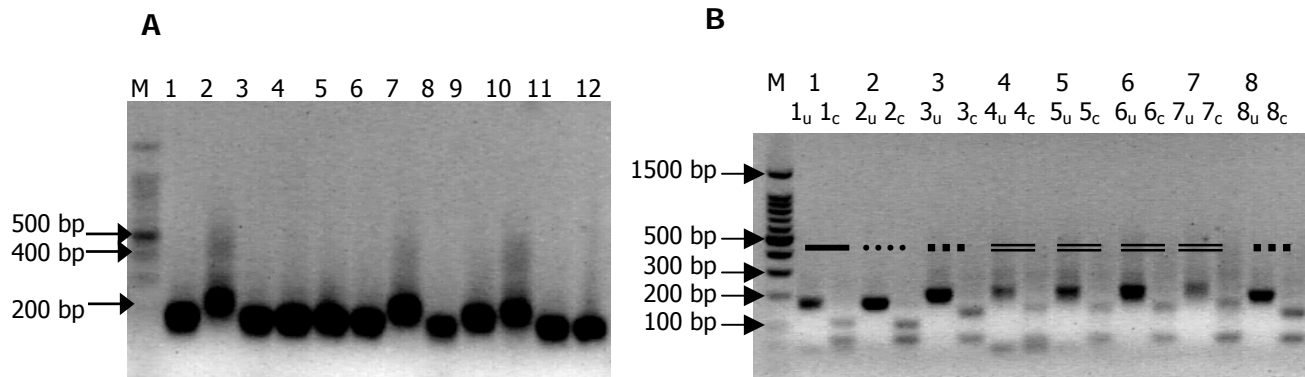


Figure 3.7: A: Representative sample of PCR amplification and subsequent gel electrophoretic analysis of *P. falciparum* cDNA inserts, B: Representative example of restriction mapping of cDNA inserts using *Hind* III.

A): Lane M: GeneRuler 50 bp DNA ladder used as molecular marker. Lane 1-12: Amplification of 12 different *P. falciparum* cDNA inserts cloned into T7 phage isolated with biopanning. The DNA was analysed on a 2.5% agarose/TAE gel and visualised with EtBr. **B):** Lane M: 100 bp DNA ladder used as molecular marker. Lanes 1-8: *P. falciparum* cDNA inserts analysed to determine if the clones are identical. The subscript u indicates uncut PCR product and the subscript c indicates digested PCR product. The DNA was analysed on a 2.5% agarose/TAE gel and visualised with EtBr. Different bars indicate identical clones based on restriction mapping.

Of the 96 clones screened, several were similar in size. For effective differentiation between the different *P. falciparum* cDNA inserts, 44 of those similar in size were chosen for amplification and restriction mapping. This resulted in slightly different banding patterns (Fig 3.7 B, indicated by different bars), indicating that some of these clones are not identical. Based on the restriction mapping patterns, 7 different phage clones were ultimately chosen from the original 96 for sequencing of the cDNA inserts.

3.3.3 Identification of *P. falciparum* cDNA inserts with nucleic sequencing

In order to determine the nucleic acid sequences of the *P. falciparum* cDNA inserts, the inserts were first cloned into the pGem[®]-T Easy vector to facilitate down-stream reactions. This strategy was due to sequencing facility constraints experienced at the time. After amplification, the PCR reactions were pooled and a 10 µl sample of the pooled large-scale amplification of the inserts from phage clones AA10, AB5, AB8, AB12, AC5, AC8 and AF2 analysed on a 2.5 % agarose/TAE gel to verify the identity of the product obtained before purification (Fig 3.8).

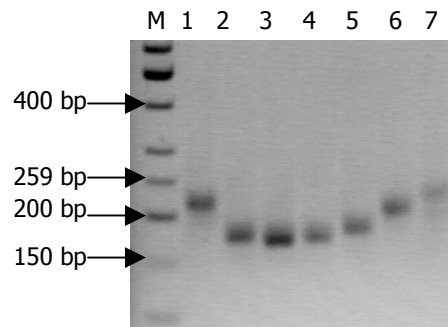


Figure 3.8: Large-scale amplification of cDNA inserts for sequencing.

Lane M: GeneRuler 50 bp DNA ladder used as molecular marker. Lanes 1: AA10, Lane 2: AB5, Lane 3: AB8, Lane 4: AB12, Lane 5: AC5, Lane 6: AC8 and Lane 7: AF2. The DNA was analysed on a 2.5% agarose/TAE gel and visualised with EtBr.

All the samples were purified directly, except for AF2 (Fig 3.8 lane 7), which was purified following separation on a 2% agarose/TAE gel since additional faint bands smaller than the main amplification product could be observed following gel electrophoresis. The inserts were cloned into the pGem[®]-T Easy vector and the presence of positive colonies verified with colony screening PCR and restriction enzyme digestion (Fig 3.9).

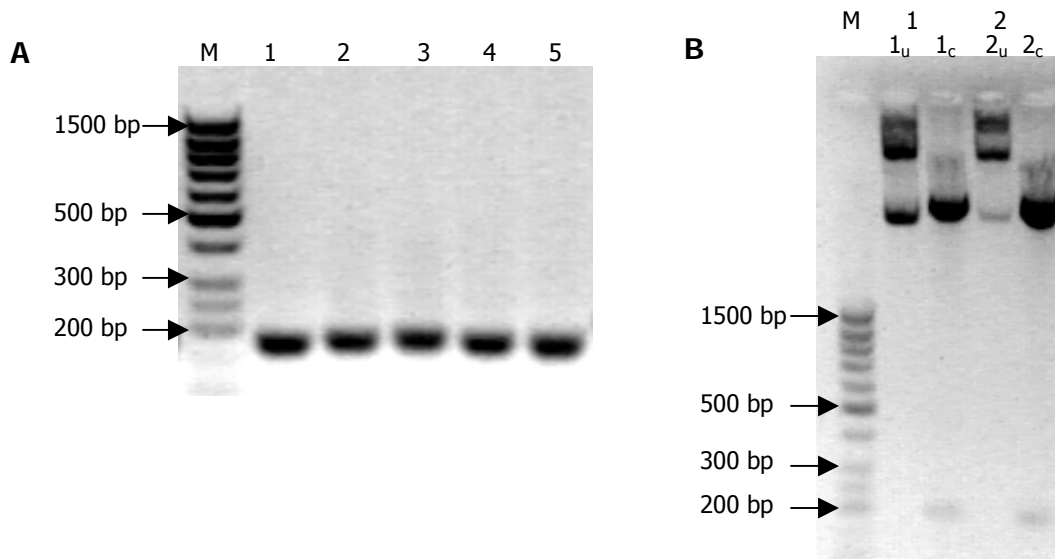


Figure 3.9: Representative samples of screening for positive clones with A: colony screening PCR and B: Restriction enzyme digestion.

A) Lane M: GeneRuler 50 bp DNA ladder used as molecular marker. Lanes 1-5: PCR amplification product of 5 different clones for AC5. **B)** Lane M: GeneRuler 50 bp DNA ladder used as molecular marker. Lanes 1-2: The various positive candidates for AA10 prior and following digestion with *Eco*RI. The subscript u indicates uncut plasmid and the subscript c indicates digested plasmid. The DNA was analysed on a 2.5% agarose/TAE gel and visualised with EtBr.

The positive clones were subsequently used to determine the nucleic sequence of the cDNA inserts using the T7/SP6 primers (Table 3.2), which anneals to the pGem[®]-T Easy vector. The obtained nucleic acid sequences of the *P. falciparum* cDNA inserts were analysed to determine the identity of the insert and if the cDNA was inserted in the correct reading frame. The *P. falciparum* cDNA inserts are cloned into the 10-3B protein gene on the phage coat using the

*Eco*RI and *Hind*III sites in the MCS, and as such have to be in frame after the Asn at position 351 to ensure correct expression of the peptide (see appendix A).

The sequence data showed that the inserts consisted of mainly poly-A stretches, varying between 46 and 108 adenine residues in length, thus coding for stretches of poly-Lys. This means that the inserts were not necessarily derived from any specific *P. falciparum* gene, but rather from poly-A stretches inside genes and those in the mRNA tail, as well as non-coding regions of the genome from contaminating genomic DNA (Sherman, 1998).

Library A, which was created by biopanning against recombinant PfAdoMetDC/ODC was subsequently screened following the third round of biopanning, in the hopes of identifying phage clones with *P. falciparum* cDNA inserts that do not consist of poly-A stretches.

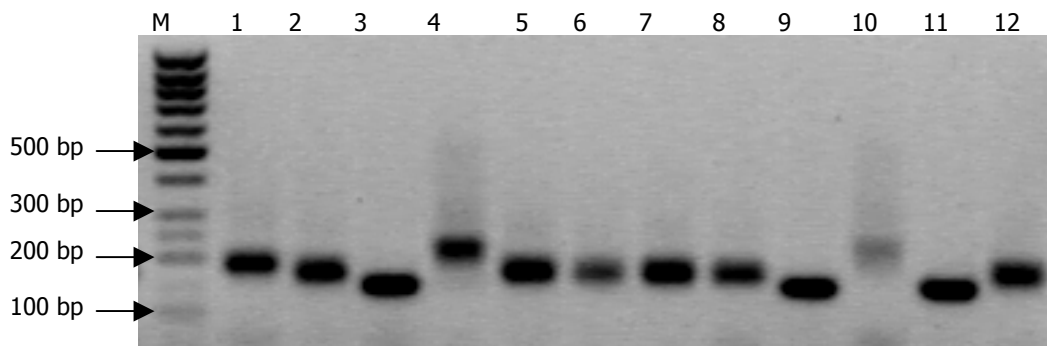


Figure 3.10: Representative sample of screening of *P. falciparum* cDNA inserts of Library A, Biopanning 3 with PCR amplification and gel electrophoresis.

Lane M: GeneRuler 50 bp DNA ladder used as molecular marker. Lanes 1-12: PCR amplification products of various *P. falciparum* cDNA inserts. The DNA was analysed on a 2.5% agarose/TAE gel and visualised with EtBr.

96 different phage clones were screened by PCR amplification and gel electrophoresis (Fig 3.10). Insert sizes ranging from ~150-250 bp were identified. Since this size distribution of inserts is the same as that obtained after screening of Library A, Biopanning 4, it was assumed that these fragments also encodes for poly-A stretches, and were not further investigated.

3.3.4 Verification of size distribution of original phage starting library used for biopanning against PfAdoMetDC/ODC

To verify that the distribution of *P. falciparum* cDNA insert sizes obtained from Library A is indeed a result of the biopanning against PfAdoMetDC/ODC and not inherent to the original library, the starting library was plated out to obtain single phage plaques (section 3.2.2) and the sizes of the inserts screened with PCR amplification and gel electrophoretic analysis (section 3.2.4.1).

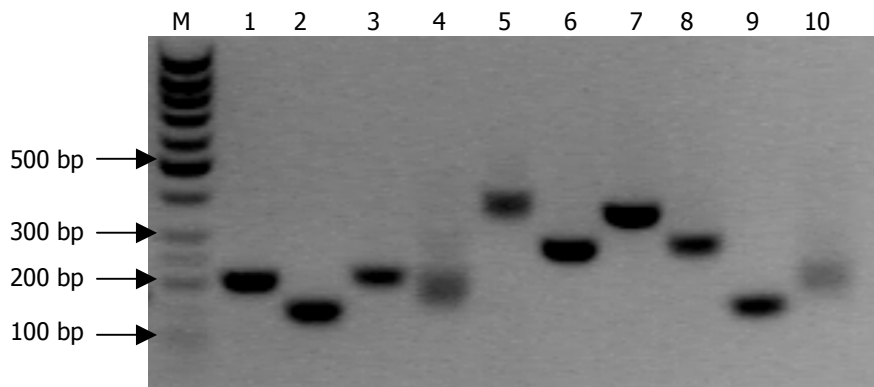


Figure 3.11: Size distribution of cDNA inserts in the starting library.

Lane M: GeneRuler 50 bp DNA ladder used as molecular marker. Lanes 1-10: PCR amplification products of various *P. falciparum* cDNA inserts from phage plaques chosen randomly. The DNA was analysed on a 2% agarose/TAE gel and visualised with EtBr.

As shown in Fig 3.11, the size distribution of randomly chosen phage plaques from the starting library has a size distribution of ~150-500 bp, which correlates well with the original publication on the *P. falciparum* cDNA T7 library (Lauterbach et al., 2003). This shows that the distribution of *P. falciparum* cDNA insert sizes obtained with Library A (~150-250 bp) is indeed a result of the biopanning against PfAdoMetDC/ODC and not inherent to the original library. By changing the biopanning procedure, it is possible that phage particles that display peptides other than poly-Lys stretches can be isolated from the original starting library.

3.3.5 Modification of the biopanning procedure for the identification of T7 phage particles containing *P. falciparum* cDNA inserts that encodes for peptides with affinity to PfAdoMetDC/ODC

In an effort to prevent the purification of singular phage clones that contains poly-A inserts and thus encode poly-Lys stretches, various different experimental strategies were followed (see Table 3.1). The percentage Tween-20 in the wash buffer was reduced to lessen the selection stringency, thus creating Library B. In an effort to prevent the non-specific ionic interactions between the poly-Lys encoding phages and the recombinant protein, PfAdoMetDC/ODC was blocked using commercial poly-Lys prior to each round of biopanning to create Library C or for just the first two rounds of biopanning, to create Library F. It was also attempted to prevent non-specific ionic interactions by increasing the salt concentration in the wash buffer to 250 mM NaCl (Library D) or 500 mM NaCl (Library E).

The number of biopanning rounds was also decreased from 4 rounds to 3, since there did not appear to be any difference between Biopanning 3 and Biopanning 4 of Library A. Following each individual biopanning round with the various libraries, the titer of the lysate was determined in duplicate (Table 3.4) so as to dilute the phages to 1×10^7 pfu/ml prior to the following round of biopanning.

Table 3.4: Phage titers obtained following each round of biopanning (BP) for the different libraries (Library B-F).

	Phage Titer (pfu/ml)		
	BP1	BP2	BP3
Library B	2.1×10^{10}	3.4×10^{10}	3.4×10^{10}
Library C	4.6×10^{10}	4.4×10^{10}	3×10^{10}
Library D	3.2×10^{10}	2.2×10^{10}	2.3×10^{10}
Library E	2.8×10^{10}	3.6×10^{10}	2.6×10^{10}
Library F	2.1×10^{10}	4.4×10^{10}	2.6×10^{10}

The expression of recombinant PfAdoMetDC/ODC was again verified by SDS-PAGE following each round of biopanning (Fig 3.12) to ensure the continuous presence and integrity of the recombinant bait protein.

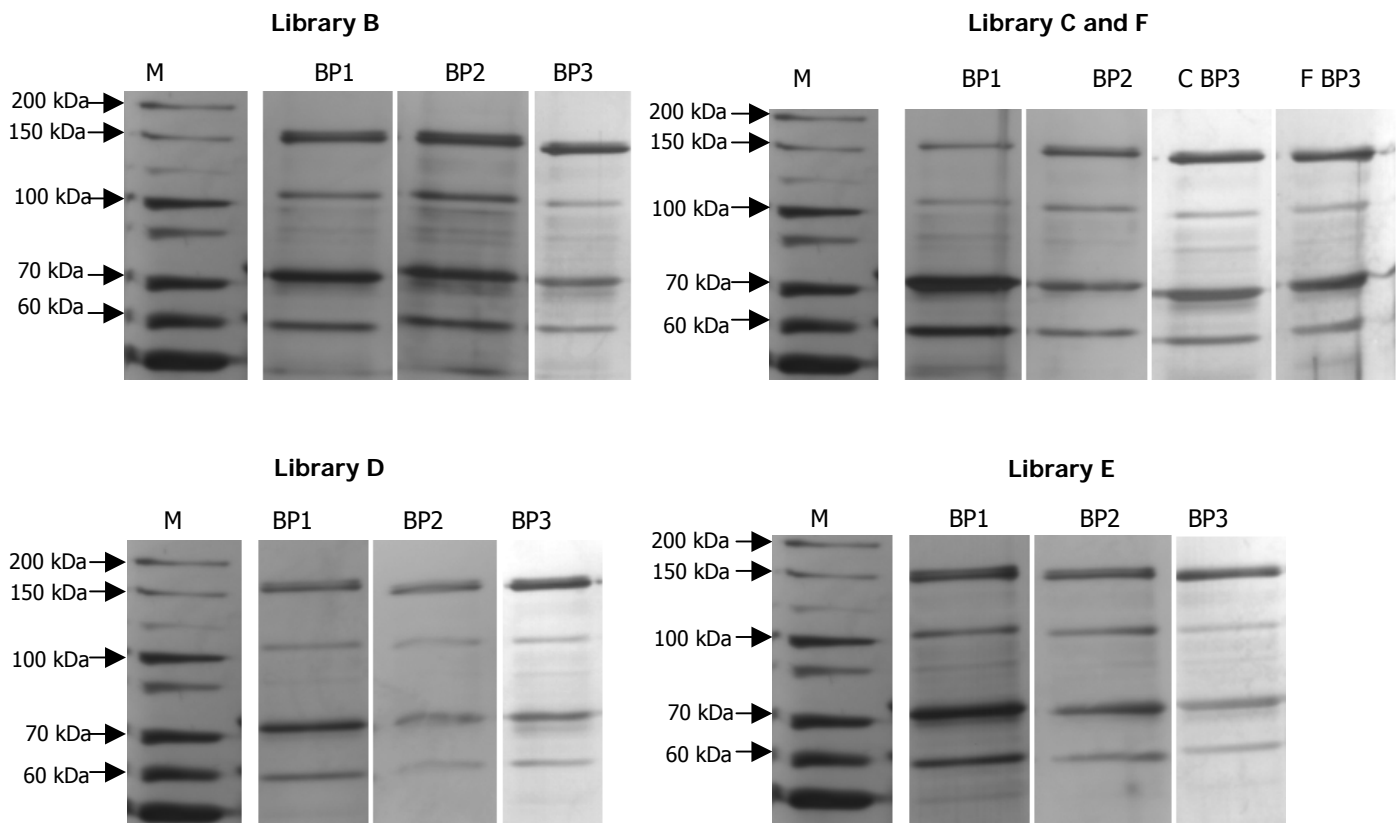


Figure 3.12: SDS-PAGE analysis of the expression of recombinant PfAdoMetDC/ODC used as bait in biopanning.

Lane M: PageRuler™ Protein ladder used as molecular marker. Lane BP1: PfAdoMetDC/ODC used as bait for biopanning 1, Lane BP2: PfAdoMetDC/ODC used as bait for biopanning 2 and Lane BP3: PfAdoMetDC/ODC used as bait for biopanning 3. Lane CBP3 and FBP3: PfAdoMetDC/ODC used as bait for biopanning 3 to generate Libraries C and F respectively. The proteins were analysed on a 7.5% SDS-PAGE gel and visualised with silver staining.

The sizes of the *P. falciparum* inserts were analysed after the first and second round of biopanning by randomly choosing 10 single plaques of each library for PCR amplification and gel electrophoresis analysis (section 3.2.4.1). This was done to monitor the enrichment of specific phages during the biopanning process, as well as to determine if only small inserts similar to Library A were isolated (Fig 3.13).

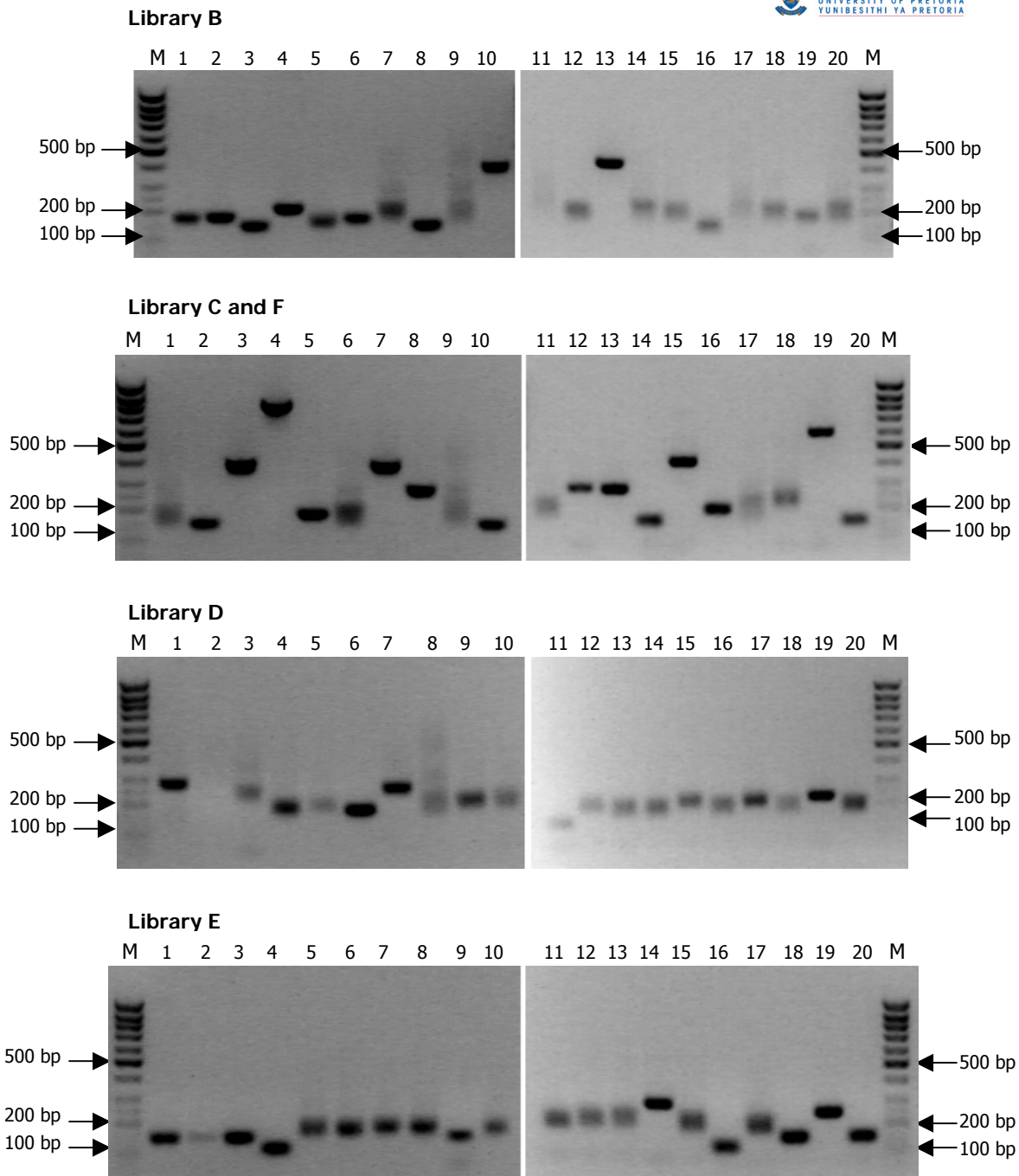


Figure 3.13: Investigation of the size distribution of the *P. falciparum* cDNA inserts of the various libraries, following the first and second round of biopanning.

Lane M: GeneRuler 50 bp DNA ladder used as molecular marker. Lanes 1-10: PCR amplification products of various cDNA inserts from phage plaques chosen at random from Biopanning 1. Lanes 11-20: PCR amplification products of various cDNA inserts from phage plaques chosen at random from Biopanning 2. The DNA was analysed on a 2% agarose/TAE gel and visualised with EtBr.

As shown in Fig 3.13, the size distribution of bands from some of the libraries differ from that of Library A, where bands of ~150-250 bp were obtained. Here, Library B had a size distribution of ~150-400 bp and Library C had a size distribution of ~150-800 bp. These results seem to indicate that the different experimental strategies succeeded in circumventing the enrichment of only the smaller sized poly-Lys encoding phage particles. It appeared as if Library C (and thus also Library F) had the greatest possibility to contain phages whose cDNA inserts encoded for

peptides with affinity to PfAdoMetDC/ODC, followed by Library B, since these libraries contained the largest inserts. Library D had a size distribution of ~150-200 bp and Library E had a size distribution of ~150-300 bp, similar to the size distribution of Library A.

3.3.6 Screening of insert cDNA by PCR amplification and gel electrophoresis of Libraries B,C,D,E and F following round 3 of biopanning

Due to the fact that the first and second rounds of biopanning of libraries B-F showed promising size distributions, it was decided to analyse the nucleic sequences of the *P. falciparum* cDNA inserts of the various libraries following the third round of biopanning. The libraries were titered (section 3.2.2) and single phage plaques amplified for PCR screening and gel electrophoresis (section 3.2.4.1). As shown in Fig 3.14, the *P. falciparum* cDNA insert sizes differed from those of Library A, indicating that it was possible that inserts other than poly-A stretches could be identified.

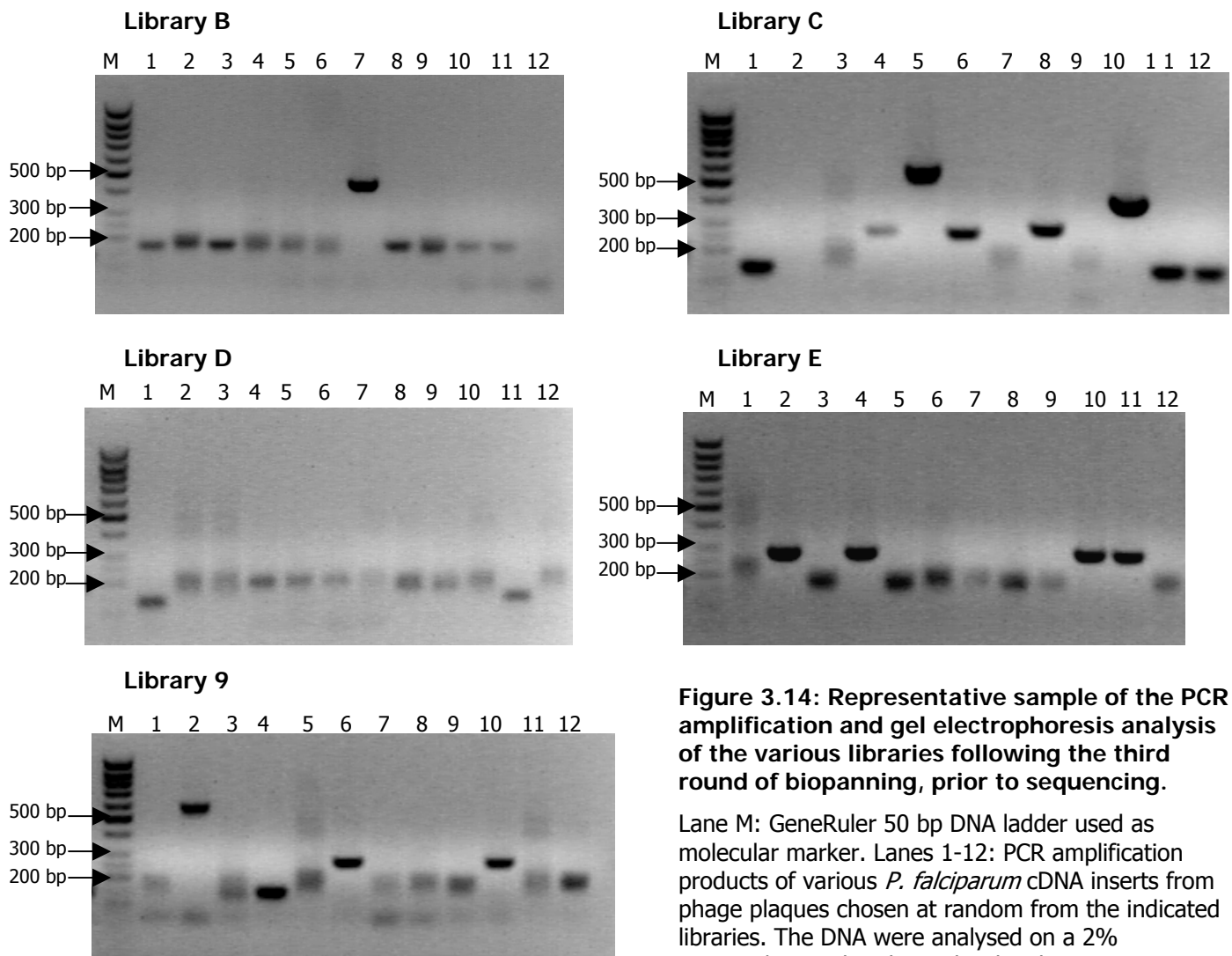


Figure 3.14: Representative sample of the PCR amplification and gel electrophoresis analysis of the various libraries following the third round of biopanning, prior to sequencing.

Lane M: GeneRuler 50 bp DNA ladder used as molecular marker. Lanes 1-12: PCR amplification products of various *P. falciparum* cDNA inserts from phage plaques chosen at random from the indicated libraries. The DNA were analysed on a 2% agarose/TAE gel and visualised with EtBr.

Those *P. falciparum* cDNA inserts bigger than 200 bp from each library were chosen for further analysis (Table 3.5) to circumvent the identification of only poly-A stretches.

Table 3.5: Number of phage plaques screened from each library and the number of phage cDNA inserts suitable for further screening (See appendix B).

Library	Number of plaques screened by PCR amplification and gel electrophoresis	Phage clones with cDNA inserts bigger than ~200 bp used for further screening	Number of cDNA inserts sequenced
B	48	2	2
C	96	33	22
D	24	0	0
E	24	6	5
F	96	9	2

The chosen phage clones were amplified as described in section 3.2.4.1 and digested with either *Hind*III or *Eco*RI. These enzymes could however not provide a clear differentiation between cDNA inserts of similar sizes (results not shown). Subsequently, *Nde*I, *Vsp*I and *Eam*1104I were chosen based on the high A+T-content of their recognition sites to differentiate between similar sized cDNA inserts. As can be seen from Fig 3.15, this resulted in more efficient differentiation between similarly sized fragments. For example, phage clones CC6 and CD2 or CD8 and CE8 contain different *P. falciparum* cDNA inserts, as shown by the differences in their respective restriction maps.

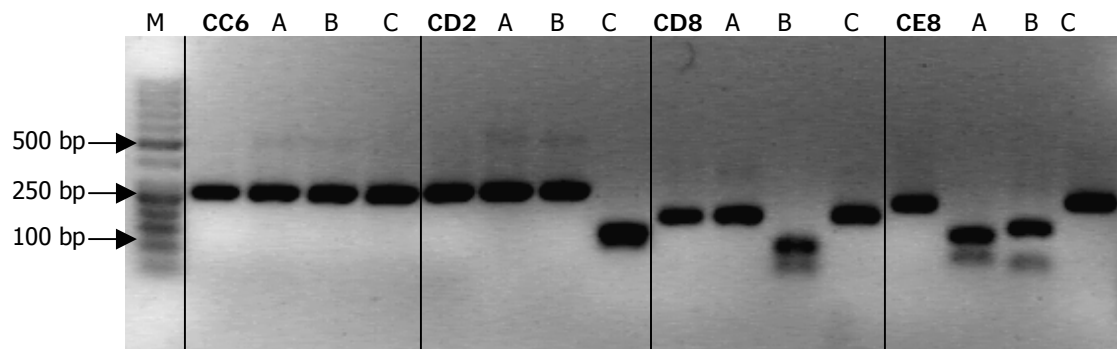


Figure 3.15: Example of restriction enzyme digestions of similarly sized *P. falciparum* cDNA inserts to differentiate between different clones.

Lane M: O' GeneRuler 50 bp DNA ladder used as molecular marker. Panel CC6: PCR amplification product of phage clone C6 from Library C, Panel CD2: PCR amplification product of phage clone D2 from Library C, Panel CD8: PCR amplification product of phage clone D8 from Library C and Panel CE8: PCR amplification product of phage clone E8 from Library C. A: Digested with *Nde*I, B; Digested with *Vsp*I and C: digested with *Eam*1104I. The DNA was analysed on a 2% agarose/TAE gel and visualised with EtBr.

Following large-scale amplification of the *P. falciparum* cDNA inserts chosen based on their restriction maps, the PCR products were pooled, analysed with gel electrophoresis (section 3.2.4.1), purified (section 3.2.4.3) and used either directly as template in a sequencing reaction

or ligated into pGem[®]-T Easy (section 3.2.4.4) (results not shown) prior to automated sequencing.

3.3.7 Sequencing of cDNA inserts

The sequences of the restriction mapped unique *P. falciparum* cDNA inserts were analysed to determine the identity of the cDNA inserts using BLASTN from PlasmDB, the *Plasmodium* genome database. These sequences were then translated to the encoded peptides and investigated to determine if the *P. falciparum* cDNA was inserted in-frame into the phage coat protein (see section 3.3.3), thus producing endogenous malarial peptides (native peptides that are part of malarial proteins). Alternatively, the cDNA inserts could have been cloned into the phage 10-3B protein gene out of frame, leading to the production of non-native peptides, i.e. peptides that do not occur as part of native malarial proteins (Table 3.6). Protein/peptide sequences longer than 10 amino acids (clones BB7, CA3, CE8, and CG2) were additionally analysed in terms of MW, pI, stability and overall secondary structure using the links provided by the ExPASy interface (Table 3.7). The secondary structures were determined with the PredictProtein server. Included in these analyses were two published *P. falciparum* protein fragments not identified by this study that were found to interact with PfAdoMetDC/ODC by a genome wide yeast Two-Hybrid analysis (LaCount et al., 2005).

Table 3.6: Identity of cDNA inserts in the various phage clones.

Phage clone	CDNA insert size	Gene of origin (BlastN)	Annotation	Peptide length	Peptide sequence Stop= stop codon	Native malarial peptide (correct reading frame)
CC8	191	PFI1475w	Merozoite surface protein 1, precursor	8	SSIRTQVF stop	X
CA2	179	PF14_0722	Hypothetical protein	19	FFFFCCISXIYFFIDLLNF stop	X
CA9	163	PFL2095w	Translation initiation factor SUI1, putative	9	SSETTLKSF stop	X
CC6	160					
CD10	160					
CH3	160					
FD10	160					
EE8	161					
FC12	159			5	SSEQR stop	
CG2	142	PFA0125c	Ebl-1 like protein, putative	47	SVVDRATDSMNLDPKVVHNNENMSD PNTNTEPDASLKDDKKEVDDAKK	√
CB10	102			34	SVVDRATDSMNLDPKVVHNNENMSD PNTNTEPDAS	
BB7	332	PF13_0197	Merozoite Surface Protein 7 precursor, MSP7	21	SSMNKKMKTRKNQNHFHYSKI stop	X
FC8	477	PF13_0073	Hypothetical protein	4	SSSK stop	X
CC1	451					
CF2	432					
FA8	477					
CC5	480					
CG3	444					
EF8	175	PFI0340c	Hypothetical protein	2	SS stop	X
EG8	175					
EH11	175					
EH10	175					

Chapter 3: Identification of peptide binding partners to PfAdoMetDC/ODC

CD2	185	PFF1225c	DNA polymerase1, putative	2	SS stop	X
C14	685	PF14_0510	Hypothetical protein	7	SSKKYKI stop	
CD4	308	MAL13P1.460	Conserved Hypothetical protein	6	SSRTIA stop	X
CE4	348			6	SSYIYI stop	X
CA11 CC2	189 191	PF14_0618 PFF1250w PF14_04277 PF14_0123	Hypothetical proteins	3	SSA stop	X
CC4	174	PF08_0130 PFF0755c PFE0055c PF14_0028 Mal13P1.234 Mal13P1.296	Wd repeat protein Hypothetical protein Heat shock protein, putative Hypothetical protein, conserved Hypothetical protein Hypothetical protein	5	SSIIL stop	X
CE8	161	PF14_0264 PF10260c PF08_0028	Hypothetical protein Hypothetical protein Hypothetical protein	12	SSFFFENAKDYI stop	X
CH6	142	-----	No identifiable gene sequence	4	SSIL stop	X
CF1	~49	Poly-A	Stretches of poly-A		Various stretches of Lys	
BA3	~64					
FB7	~45					
AA10	~100					
AB5	~54					
AB8	~50					
AB12	~50					
AC8	~90					
AF2	~80					

Table 3.7: Analysis of the physical characteristics of the various peptides identified through phage display with affinity to PfAdoMetDC/ODC.

Name	Sequence	Gene of Origin	Native peptide	MW kDa	pI	Overall Secondary structure	Stability	No of Charged Residues
Peptides identified with yeast Two-Hybrid analysis (LaCount, 2005)								
PF10_0212	GDENKQSGDENKQSGDENKQSGDENKQ TNNDIKQSDNDIKQSDDIYMNEDMNLFN DLNDRNFDNNEYFINNGDKDSHAEEMAI	PF10_0212 Hypothetical protein	√	10.3	3.9	Mixed	Unstable	- 25 + 8
Mal13P1.202	NEDIILTMNKEKEQEANQRINEYKNLIES YKKDKEKYNNEKVVAHNMNES	Mal13P1.202 Hypothetical protein	√	6.2	5.3	Mixed	Unstable	- 11 + 9
Peptides identified in this study with phage display								
BB7	SSMNKKMKTRKNQNHFHYSKI		X	2.6	10.6	Mixed	Unstable	- 1 + 6
CA3	SFFCCISXIYFFIDLLNF		X	2.4	3.8	All alpha (α -helix)	Stable	- 1 + 0
CE8	SSFFENAKDYI		X	1.4	4.37	*	Stable	-2 +1
CG2	SVVDRATDSMNLDPKQVHNENMSDPNT NTEPDASLKDDKKEVDDAKK	PFA0125c Ebl-1like protein, putative	√	5.3	4.4	Mixed	Stable	- 13 + 7

* The PredictProtein server used to determine secondary structures only accepts peptides longer than 17 amino acids in length

The stability of a protein in a test tube is estimated based on its instability index. The instability index of a peptide/protein is determined based on its size as well as the presence of certain dipeptides that have been shown to occur in higher numbers in unstable proteins (Gasteiger et al., 2005).

The presence of consensus motifs in the peptides/proteins with affinity to PfAdoMetDC/ODC that may possibly be used as lead sequences for drug development (Uchiyama et al., 2005) were investigated with the MEME Motif discovery tool (Bailey and Elkan, 1994).







Name	Combined p-value	Motifs
PF10_0212	5.78e-30	
MAL13P1.202	3.23e-23	
BB7	6.45e-08	
CA3	1.09e-05	
CE8	5.75e-03	
CG2	1.69e-25	

Figure 3.16: Possible consensus sequences in the identified peptides with affinity to PfAdoMetDC/ODC, identified by the MEME Motif discovery tool.

The p-value indicates the probability that a random string will have the same or higher match score (Bailey and Elkan, 1994).

As can be seen in Fig 3.16, there is no single consensus sequence/motif that occurs in all the peptides. Only motif 9 occurs more than twice, but this motif is not very specific, and contains a high degree of variability.

3.3.8 Verification of the specific interaction between the isolated phage clones and PfAdoMetDC/ODC

Due to the presence of *E. coli* chaperone proteins DnaK and GroEL in the purified PfAdoMetDC/ODC eluate (see Chapter 2), the interaction of the phage particles with PfAdoMetDC/ODC, instead of these co-eluting proteins, had to be verified. The anti-T7 Tail Fiber monoclonal antibody (Novagen, USA), which recognises the phage tail fiber protein, was used in an indirect ELISA protocol to detect whether the identified phage clones bind to immobilised *E. coli* DnaK or to PfAdoMetDC/ODC. Recombinant PfAdoMetDC/ODC and *E. coli* DnaK were used to determine the preference of binding of the phage particles. If the results indicate that the phage particles bind to both the test DnaK and purified PfAdoMetDC/ODC eluate, it would imply that the isolated phage particles bind in fact to DnaK and not to PfAdoMetDC/ODC, since the PfAdoMetDC/ODC eluate contain DnaK as well as GroEL. Alternatively, if there were no detection of phage particles binding to DnaK, it would imply that the phage particles have affinity to either PfAdoMetDC/ODC or to GroEL.

PfAdoMetDC/ODC and DnaK were recombinantly expressed (section 2.2.11 and 3.2.6.1.2) (Fig 3.17) and used to determine if the isolated phage particles bind to the malarial protein or to the co-eluting *E. coli* proteins. Between 3.3 and 5.5 μ g of the recombinant proteins were coated onto an ELISA plate as bait proteins. Phage clones BB7, CA3, CE8 and CG2 were then added in

triplicate to the plates to bind to the PfAdoMetDC/ODC or DnaK protein, washed and detected with anti-phage antibody.

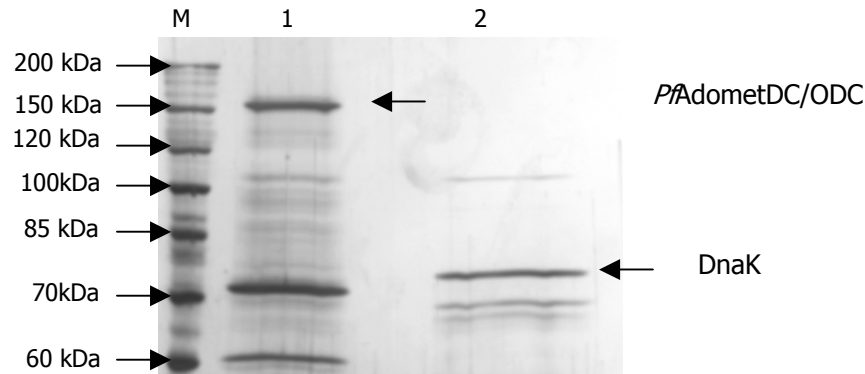


Figure 3.17: Verification of the recombinant expression of PfAdoMetDC/ODC and *E. coli* DnaK for verification experiments.

Lane M: PageRuler™ Protein ladder used as molecular marker. Lane 1: PfAdoMetDC/ODC. Lane 2: *E. coli* DnaK. The proteins were analysed on a 7.5% SDS-PAGE gel and visualised with silver staining. The difference in size between the co-eluted DnaK in lane 1 and the recombinant DnaK in lane 2 is presumably due to the presence of hexahistidine tag that adds approximately 1 kDa to the protein.

From Fig 3.18 it can be seen that a signal of binding to both *E. coli* DnaK and to the recombinant PfAdoMetDC/ODC eluate was obtained for all four phage clones. This implies that the fusion peptides encoded on the capsid protein probably have affinity to the co-purified *E. coli* proteins rather than to the recombinant malarial protein. The signal obtained for the PfAdoMetDC/ODC eluate is most probably due to the presence of DnaK in the preparation and not due to the binding of the phages to PfAdoMetDC/ODC itself. This suggests that no peptide binding partner specific to PfAdoMetDC/ODC was isolated in this study.

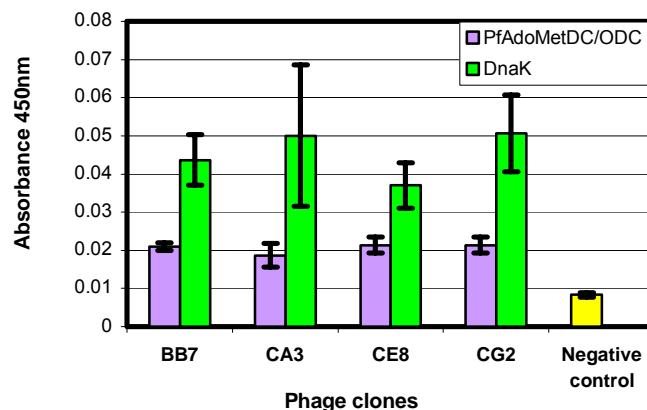


Figure 3.18: ELISA results using PfAdoMetDC/ODC and *E. coli* DnaK as bait.

Purple bars indicate the signal obtained for PfAdoMetDC/ODC and green bars the signal obtained for DnaK. The yellow bar indicates the negative control.

3.4 Discussion

The bifunctional PfAdoMetDC/ODC contains parasite-specific inserts with low complexity regions that has been suggested to play a part in interactions with unknown proteins (Birkholtz et al., 2004). It has been hypothesised that such low complexity regions and protein areas high in glutamine/asparagine content (so-called 'prion domains'), may promote protein-protein interactions (Karlin et al., 2002; Michelitsch and Weissman, 2000). Additionally, it has been shown that the parasite specific inserts in PfAdoMetDC/ODC are involved in various inter- and intra-domain interactions that is important for both decarboxylase activity and bifunctional complex formation (Birkholtz et al., 2004), which further emphasize their importance in protein-protein interactions. Most enzymes contain specific domains that have evolved to allow the binding of small molecules (i.e. the enzyme's active site) as well as specific residues involved in binding to other proteins. As such, enzymes are viable targets for the identification of peptide ligands via phage display, since the binding of displayed peptides usually occur either at the active site or at other domains that have evolved to allow molecular interactions (Kay and Hamilton, 2001; Szardenings, 2003).

Peptides identified through the use of phage display can be used in various ways. Due to convergent evolution, the primary structures of the identified peptides often have similarities to the primary structure of the biological interacting partner of the bait protein and can thus be used in similarity searches to identify such *in vivo* partners. These peptides can also be used to interfere with the binding of these two interacting proteins, which may have an effect on the biological activities of the targeted proteins. Alternatively, these peptides may also have an effect on the activity of enzymes, either through active site inhibition or long-range interactions (Kay et al., 2001).

It was decided to use a *P. falciparum* cDNA library cloned into the T7 lytic phage to identify peptide binding partners to PfAdoMetDC/ODC. A cDNA library was chosen instead of a synthetic random peptide library since the binding sequence originates from the organism of interest (*P. falciparum*) and as such had the potential to identify native binding partners to the protein. The bulk of peptide drugs that have been approved by the FDA have come from natural libraries, and not synthetic random peptide libraries. It is thought that this is due to the fact that natural libraries such as cDNA libraries encode peptides that have evolved to mediate protein-protein interactions, as opposed to the randomness of synthetic libraries (Watt, 2006). The disadvantage of this method is that non-native peptides originating from frameshifting events may be also identified. However, it was speculated that these may still encode for peptides with

affinity to the bait protein and that sequence alignment of these peptides could show a conserved consensus sequence that may be used for lead molecule development (Santonico et al., 2005; Uchiyama et al., 2005). Lytic T7 phage was chosen since cDNA libraries that can contain stop codons are tolerated due to the C-terminal fusion of the recombinant protein. In addition, T7 phage are quite robust and have a short life-cycle (Castagnoli et al., 2001), making them ideal for experimental conditions. Additionally, the T7Select system from Novagen allows for directional cloning of the cDNA inserts, ensuring that the inserts are in a sense orientation relative to the capsid protein. This means that a greater number of native peptides should be expressed.

Following four rounds of biopanning, Library A, theoretically consisting of phages with affinity to PfAdoMetDC/ODC, was created. Subsequent sequence analysis showed that the phages did not contain *P. falciparum* cDNA inserts that encode for endogenous malarial protein fragments or even random peptides, but contained stretches of adenine residues. Since AAA encodes for Lysine, this means that these phages display poly-Lys stretches on their capsid protein. Due to the high pKa value (10.53) and basic nature of the Lys side-chain, these stretches of poly-Lys should have a net positive charge. This implies that the interaction between these phages and PfAdoMetDC/ODC could be due to non-specific electrostatic interactions mediated by the negatively charged (NND)_x-repeats in the PfAdoMetDC/ODC inserts. The presence of these phages can be explained by the method in which the cDNA were created (as suggested by Novagen). Random primers with two dT at the 5' end of the primer anneal to complementary sequences to produce first strand cDNA with tandem 3'A to allow for directional cloning after end modification. However, due to the high A+T content of the malarial genome, these primers can anneal at stretches of poly-A sequences or at the poly-A tail of the mRNA, leading to the synthesis and subsequent insertion of cDNA molecules consisting almost entirely of poly-A stretches.

The cDNA inserts were amplified using an extension temperature of 72°C as suggested by the manufacturer of the display system. An extension temperature of 72°C was also used by the creators of the *P. falciparum* cDNA library (Lauterbach et al., 2003). Large A+T rich Plasmodial sequences are amplified more efficiently using lower extension temperatures (Su et al., 1996), but due to the small sizes of the cDNA inserts, a lower extension temperature was not necessary. Although no experimental difficulties were experienced in this study with amplifying the cDNA inserts with the higher extension temperature, it is possible that certain genes were lost during the construction of the original library due to the high extension temperature used for cDNA synthesis.

It was shown that 120 μg of protein is sufficient to identify phages with high affinity to the bait protein (Lauterbach et al., 2003). To ensure that enough recombinant PfAdoMetDC/ODC is used during the biopanning process, control PfAdoMetDC/ODC was purified concomitantly with the PfAdoMetDC/ODC used for biopanning to give an indication of protein concentration used. This was done since the concentration of the recombinant protein immobilised on the *Strep*-Tactin Sepharose could not be determined directly due to the fact that the SDS in the phage elution buffer interfered with the Bio-Rad Quick Start™ Bradford Protein assay (Bio-Rad Laboratories, USA). In addition, since some of the protein is already eluted with the phage elution buffer prior to elution with Buffer E, the correct concentration of the bifunctional protein immobilised on the Sepharose would be very difficult to measure. Since the exact amount of protein used is inconsequential as long as the Sepharose beads are adequately covered, this assay was chosen based on its ease of use and the short time required. However, if more accurate determinations of protein concentration are needed, the bicinchoninic acid method of protein concentration determination may be more effective. Like the Lowry method of protein concentration determination, this method also involves the conversion of Cu^{2+} to Cu^{+} , but has the added advantage of much greater tolerance to interfering substances (Smith et al., 1985).

During biopanning, the total number of amplified phage particles stays approximately the same (Tables 3.3, 3.4). This implies that the ratio between the non-binding and binding phage changes with progressive cycles of biopanning (Konthur and Cramer, 2003). However, with each round of biopanning, phage particles with high affinity to the target protein but low efficiency in growth or infection are out-competed by phage particles with moderate affinity to the target protein but high effectivity in growth or elution (Kay et al., 2001; Konthur and Cramer, 2003). For this reason, the previous round of biopanning of Library A, namely Biopanning 3, was screened with PCR amplification and gel electrophoresis (section 3.2.4.1) in the hope of identifying non poly-Lys peptides that bind to PfAdoMetDC/ODC. Unfortunately, the *P. falciparum* cDNA insert size distribution of these phages was identical to those previously obtained with Biopanning 4, and thus it was assumed that these also encode for poly-Lys stretches and not further investigated. To verify that this distribution of cDNA insert sizes was indeed a result of the biopanning and not inherent in the original library, the original T7 library was screened as above. A much greater variety in size distribution of randomly chosen phage plaques was identified, with bands up to ~ 500 bp obtained. This correlates well with the original publication on the *P. falciparum* cDNA T7 library (Lauterbach et al., 2003) and implies that the results obtained were indeed due to the biopanning against recombinant PfAdoMetDC/ODC.

During biopanning, the washing step ensures that the non-binding phage is removed and thus leads to the enrichment of phage particles with affinity to the target protein. This implies that the wash buffer has to be carefully chosen to eliminate non-specific binding phage particles, while retaining the phage particles that binds to the bait protein. A too stringent wash buffer may lead to the enrichment of phage particles that have high affinity, but low selectivity to the bait protein (Willats, 2002). It was thought that the wash buffer (TBS, 0.5% v/v Tween-20) chosen for the creation of Library A may have been too stringent, leading to the enrichment of phage clones that bind with high affinity, but with poor selectivity to PfAdoMetDC/ODC. The concentration of detergent in the wash buffer can have a large effect, since while it should be high enough to reduce non-specific bait-prey and background (matrix-dependent) interactions, it should be low enough to maintain the specific interactions (Howell et al., 2006). In an effort to circumvent this problem, various different experimental strategies were followed (see Table 3.1), such as varying the Tween-20 and ionic concentrations of the wash buffer and blocking the bait protein with commercial poly-Lys. The exclusion of poly-Lys in the third round of biopanning during the creation of Library F was to ensure that phages that bind electrostatically to residual poly-Lys would not be obtained.

Following the first and second round of biopanning, the sizes of the inserts were verified by PCR amplification and gel electrophoretic analysis (section 3.2.4.1) (Fig 3.13). Based on these results, the modified experimental strategies were successful in circumventing the isolation of small inserts (similar to Library A) with sizes ranging from ~150 bp to ~800 bp. Phage clones from Libraries B-F (a total of 288 clones) were analysed after three rounds of biopanning and the *P. falciparum* cDNA inserts bigger than ~200 bp were chosen for further analysis. Sequencing of the *P. falciparum* cDNA inserts identified only one endogenous malarial peptide, derived from a putative Ebl-like protein. Considering that one in three of the cloned cDNA inserts should theoretically be in the correct reading frame, and 36 different clones were sequenced, ~12 in-frame sequences were expected. However, this is not what was obtained. These 36 clones led to the identification of only 13 unique *P. falciparum* cDNA inserts. This is probably due to the enrichment of these specific phage clones during the biopanning process. Of these, at least 4 should then have theoretically been endogenous proteins. However, only one endogenous malarial protein was obtained. Additionally, the non-native peptides were shorter than expected based on the sizes of the amplified cDNA inserts and only 4 encoded for peptides longer than 10 amino acids. The discrepancies between the size of the *P. falciparum* cDNA inserts and peptide lengths are due to the presence of stop codons that cause the termination of translation. However, this indicates that very few of the isolated phage encoded for peptides capable of binding to the bait protein since most contained only a few foreign amino acids on their coat

proteins. Chappel et al. has shown that during the initial amplification of a phage library, phage particles that do not produce and display the encoded cDNA inserts have a growth advantage. This has a direct effect on biopanning effectivity, due to the large number of non-productive phage particles with greater growth capabilities present (Chappel et al., 2004).

In November 2005, Douglas LaCount and co-workers published a protein interaction network of *P. falciparum* obtained from yeast Two-Hybrid screens in *S. cerevisiae* (LaCount et al., 2005). Amongst the identified interactions, they identified two hypothetical proteins that interact with PfAdoMetDC/ODC, namely PF10_0212 and MAL13P1.202. These two proteins were included in further bioinformatics analyses together with the peptides identified in this study. PF10_0212 is a ~53 kDa protein with no predicted transmembrane domains. It is expressed during the merozoite stage and has sequence similarity to several other malarial hypothetical proteins. The yeast Two-Hybrid study identified 31 other malarial interacting partners to this protein in addition to PfAdoMetDC/ODC. MAL13P1.202 is a 232 kDa hypothetical protein, with no transmembrane domains but several low-complexity regions. It has sequence similarity with several other Plasmodial hypothetical proteins as well as Smc domains, which is involved in cell division and chromosome partitioning. This protein was identified as a binding partner to 18 different Plasmodial proteins.

PFAO125c, a putative Ebl-1 like protein, is the only endogenous/native malarial protein identified by this study. Erythrocyte binding ligand 1 (EBL-1) is part of the *eb1* multigene family. These merozoite proteins bind to erythrocyte surface glycoproteins and are involved in invasion (Curtidor et al., 2005). It is expressed primarily during the merozoite stage, and has possible signal peptide and transmembrane regions. This protein also shows identity to the erythrocyte-binding ligand JESEBL/EBA-181. Gene ontology (GO) annotations indicate that this protein is an integral membrane protein involved in pathogenesis, with receptor activity. As such, this protein is probably involved in erythrocyte invasion. Domain analysis shows the presence of voltage-gated potassium channels and Duffy binding domains. However, this protein has been identified as an interacting partner to 12 other *P. falciparum* proteins by LaCount and co-workers (LaCount et al., 2005), which may imply that the binding to PfAdoMetDC/ODC is not specific. That study did not identify PfAdoMetDC/ODC as one of the binding partners of PFAO125c.

In conclusion, the fact that PFAO125c and PF10_0212 are expressed during the merozoite stage while PfAdoMetDC/ODC is expressed during the trophozoite stage, as well as the fact that PFAO125c, PF10_0212 and MAL13P1.202 seem to be promiscuous in binding to other proteins (according to the LaCount data), may imply that the binding of all three of these proteins to

PfAdoMetDC/ODC only occurs *in vitro* and does not have any biological relevance. Based on a genome wide computation model of the interactome, Date and co-workers generated a web-based service (plasmoMAP, <http://cbil.upenn.edu/cgi-bin/plasmomap/getPartners>) to identify possible protein interaction partners for a specific bait protein. According to their data, PfAdoMetDC/ODC have possible interactions with 147 other Plasmodial proteins. However, since no indication was given as to the fragment of prey protein responsible for the putative interaction, this set of data was not included in the search of peptide motifs binding to PfAdoMetDC/ODC (Fig 3.16). Neither PFAO125c, PF10_0212 nor MAL13P1.202 were identified by Date and co-workers as possible interaction partners for PfAdoMetDC/ODC (Date and Stoeckert Jr, 2006).

The process of biopanning with a random peptide library often leads to peptides with conserved consensus sequences, which can then be used as leads for synthetic peptide synthesis and further studies (Uchiyama et al., 2005). This consensus sequence is usually between five and eight amino acids long and can be utilised for the rational design of inhibitory drugs (Kay and Hamilton, 2001). The presence of consensus motifs in the peptides/proteins with affinity to PfAdoMetDC/ODC were investigated with the MEME Motif discovery tool (Bailey and Elkan, 1994). However, as shown in Fig 3.16, there is no single consensus sequence/motif that occurs in all the peptides. Only one motif (motif 9, Fig 3.16) occurs more than twice, but this motif is not very specific, with a high degree of variability.

Due to the presence of the *E. coli* chaperone proteins DnaK and GroEL after affinity purification of PfAdoMetDC/ODC, the specific binding of the affinity-selected phage to PfAdoMetDC/ODC and not to the *E. coli* proteins had to be verified (Fig 3.19).

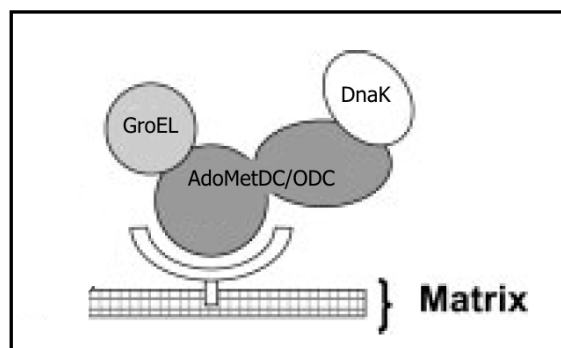


Figure 3.19: Possible sites of phage binding. Adapted from (Howell et al., 2006).

Due to the heterogeneous mixture of the affinity purified PfAdoMetDC/ODC, the phage particles could bind to either the recombinant malarial protein, or to the contaminating *E. coli* proteins.

This can be done by various methods such as BIAcore measurements, dot blot experiments and ELISA (Konthur and Crameri, 2003). Alternatively, a modified Western blot approach has been

described, where the bait proteins are separated by SDS-PAGE, transferred to a membrane and probed with phage particles. The position of the binding phage can then be determined using anti-phage antibodies (Li et al., 2002). Although the T7 Tail Fiber monoclonal antibody (Novagen, USA) that recognises the tail fiber protein of the T7 phage is available, the manufacturer specifically states that it is not suitable for Western blot analysis. As such, it was decided to verify the interactions using ELISA.

It was arbitrarily decided to screen only those phage clones that encoded a peptide longer than 10 amino acids on the capsid protein, namely BB7, CA3, CE8 and CG2 (CG2 encodes a fragment of the putative Ebl-1-like protein). Recombinant PfAdoMetDC/ODC and *E. coli* DnaK were expressed and used as the bait against which these phage clones were screened. Unfortunately, from Fig 3.18 it can be seen that all four phage clones give a higher signal of binding to *E. coli* DnaK than to PfAdoMetDC/ODC, indicating that the fusion peptides encoded on the capsid protein has affinity to the co-purified *E. coli* proteins rather than to the recombinant malarial protein. As such it was decided that it would be superfluous to test the affinity of these phages to GroEL. Due to the fact that the recombinant proteins used in protein-protein interaction analyses are routinely expressed in *E. coli*, the contamination of interaction studies by background proteins is unfortunately a common occurrence (Howell et al., 2006). Additionally, it is hypothesized that there is only about 4000-8000 distinct protein families in nature, with the associated redundancy in the basic structural motifs that it implies. This means that there could be interactions between proteins that do not occur in nature, merely due to the redundancy of the protein subdomains (Watt, 2006).

This implies that none of these peptides can be used as lead molecules for possible anti-malarial drug development. From Fig 3.12 it can be seen that for Library C, the levels of the full-length PfAdoMetDC/ODC used for the first biopanning appeared to be much less than that of the ~70 kDa band (consisting of DnaK and a fragmented product of PfAdoMetDC/ODC) and the 60 kDa GroEL. Although the concentration of PfAdoMetDC/ODC during the second and third rounds of biopanning were equal to or higher than the *E. coli* chaperone proteins (based on the intensity of the SDS-PAGE bands), it is feasible that the selection of affinity binders to DnaK and GroEL during the first round of biopanning led to the enrichment of mainly those phage clones. Although this was not the case with BB7, it is possible that due to the nature and function of the *E. coli* chaperone proteins, they have higher natural affinity to peptide partners and as such out-competed PfAdoMetDC/ODC as bait protein.

Chapter 4: Concluding discussion

Malaria is caused by the infection of humans with unicellular, eukaryotic protozoan parasites of the genus *Plasmodium* (Kirk, 2001). Malaria infection can lead to mortality, severe malaria, clinical malaria, or asymptomatic parasitemia, as well as several pregnancy-associated effects (Bremner, 2001). According to the WHO, more than 300 million severe cases of malaria infection occur worldwide, which results in more than a million deaths. However, Snow and colleagues have indicated that the actual number of clinical episodes of malaria may be as much as 50% higher (Snow et al., 2005). Due to the lack of an effective vaccine and escalating drug resistance, malaria is currently a greater problem than in any previous era (Kooij et al., 2006).

The development of new agents against malaria can be achieved both by targeting validated targets with novel strategies, thereby generating new drug candidates, and by investigating the biochemical and metabolic processes of the malaria parasite to identify new drug targets (Olliaro and Yuthavong, 1999). In the search for a new, physiologically active compound, one of the first steps is to discover a suitable drug target followed by the elucidation of this target enzyme, metabolic pathway or transport process properties and ultimately the design of an appropriate inhibitory ligand (Archakov et al., 2003). One approach in the drug target discovery process is the use of interaction analysis to find proteins that are either directly or indirectly involved in a specific metabolic pathway that has previously been identified as a viable drug target (Peltier et al., 2004). The inhibition of such interactions may then be used for disease treatment. The advantage of targeting a specific metabolic pathway through protein-protein interactions instead of the catalytic sites of its enzymes is that the active site of an enzyme often has high structural similarity to that of the human host, while there is greater structural variability in the protein-protein interfaces between different organisms. The diversity in the protein-protein interfaces of different organisms can lead to more effective differentiation between the parasite and host proteins. Resistance against chemotherapeutic agents is also often achieved by point mutations, which can have a small effect on the enzyme activity, but cause a decreased affinity to the chemotherapeutic agent. In contrast, in a specific organism, the important amino acids responsible for the protein-protein interface are often invariable and even one amino acid mutation can lead to the dissociation of the complex (Archakov et al., 2003). This implies that resistance to agents that target protein-protein interfaces should be slower to appear, since a functional mutation at both protein interfaces is necessary for effective resistance to occur (Buendía-Orozco et al., 2005).

Protein-protein interactions as drug targets in parasitic protozoa have been receiving growing attention, with increasing reports of non-active site based inhibitions of proteins. These range from anti-cancer applications (Fischer and Lane, 2004; Gadek and Nicholas, 2003; Vassilev et al., 2004) to targeting HIV (Schramm et al., 1996) and parasitic infections (Carrico et al., 2004; Ohkanda et al., 2004). There are several different methods that can be utilised for protein-protein interaction inhibition, such as the use of bifunctional blockers (Way, 2000), bioactive peptides or peptidomimetics (Cochran, 2000; Falciani et al., 2005; Meloen et al., 2004) or libraries of small planar aromatic compounds (Xu et al., 2006).

Recently, several protein-protein interaction analyses have been published that may aid in the design of mechanistically novel drugs that target Plasmodial protein-protein interactions. These interaction maps are compiled from a) Two-Hybrid analyses (LaCount et al., 2005), b) integration of experimental functional genomics and *in silico* data (Date and Stoeckert Jr, 2006) and c) the combination of known protein domain interactions, experimental protein interactions determinations and evolutionary conserved interactions in other organisms (Wuchty and Ipsaro, 2007). The large amount of work being done in the field of parasitic protein-protein interactions underscores the potential of exploiting these interactions for drug development.

Polyamines and their biosynthetic enzymes occur in increased concentrations in proliferating cells, which includes cancerous cells as well as parasitic organisms. As such, it is clear that the inhibition of polyamine metabolism is a rational approach for the development of anti-parasitic drugs (Birkholtz, 2002; Heby et al., 2003). In *P. falciparum*, a single open reading frame that encodes a bifunctional protein with both AdoMetDC and ODC activities uniquely facilitates polyamine synthesis (Müller et al., 2000). There are several differences between the Plasmodial and human rate-limiting enzymes that emphasize the potential this protein has as a drug target (Table 4.1).

Table 4.1: Comparison between the rate-limiting enzymes of human and *Plasmodium* polyamine biosynthesis.

Characteristic	Human polyamine biosynthetic enzymes	Plasmodial polyamine biosynthetic enzymes
Half-life	Short (15-35 min)	Longer than 2 hrs
Putrescine stimulation	AdoMetDC activity stimulated by putrescine	No putrescine stimulation of AdoMetDC activity Feedback regulation of ODC activity
Inhibition by Tris	Inhibits AdoMetDC activity	No Tris-mediated inhibition of AdoMetDC activity
Single or bifunctional arrangement	Two separate proteins	Single bifunctional peptide
Size	Comparable to other mammalian polyamine biosynthesis enzymes	Larger due to the presence of parasite specific inserts

Compiled from (Krause et al., 2000; Müller et al., 2001; Müller et al., 2000; Wells et al., 2006).

Since the bifunctional PfAdoMetDC/ODC encodes both rate-limiting enzymes in the polyamine pathway, inhibition of this enzyme should inhibit *Plasmodium* polyamine biosynthesis. The combined inhibition of parasitic polyamine biosynthesis and uptake should disrupt parasitic polyamine metabolism and can ultimately be used for disease treatment. This combined inhibition is necessary since it has been shown that some PfAdoMetDC/ODC inhibitors, such as DFMO, have a cytostatic rather than cytotoxic effect. It is thought that this is due to the uptake of polyamines by the parasite from the human host (Assaraf et al., 1987b; Müller et al., 2001). The bifunctional PfAdoMetDC/ODC has several parasite-specific inserts, and it has been suggested that they play a part in interactions with unknown regulatory proteins. Additionally, it has been shown that these stretches of amino acids are involved in various inter- and intra-domain interactions that are important for decarboxylase activity and bifunctional complex formation, which further emphasize their importance in protein-protein interactions (Birkholtz et al., 2004). The high degree of structural conservation between the active sites of the human and parasite AdoMetDC and ODC enzymes (Birkholtz et al., 2003; Wells et al., 2006), impedes the design of parasite-specific active site inhibitors. As such, the accumulating evidence for the importance of protein-protein interactions in the activities of the *Plasmodium* polyamine biosynthetic enzymes indicates that the inhibition of the bifunctional protein's protein-protein interactions is a viable alternative to active site based inhibition strategies. These protein-protein interactions refer to both the interdomain interactions as mediated by the parasite-specific interactions, as well as possible interactions with as yet unknown protein partners. This implies that the identification of the protein binding partners of the bifunctional PfAdoMetDC/ODC can be important for drug development. Additionally, the interfaces of oligomeric enzymes that are dependent on dimerization for activity, such as PfAdoMetDC/ODC, are viable targets for drug design. Therefore, any agent that can prevent said interaction may be used as a lead molecule for therapeutic applications (Pérez-Montfort et al., 2002), as was shown with malarial TIM (Singh et al., 2001).

However, since no crystal structure exists to date for this bifunctional enzyme and an *in silico* model of the heterotetrameric complex has not yet been created, direct design of molecules that disrupt the protein-protein interactions was not possible. It was thus attempted to optimise the heterologous expression and isolation of PfAdoMetDC/ODC to enable its utilization as bait in protein-protein interactions studies.

Bifunctional PfAdoMetDC/ODC was recombinantly expressed with a C-terminal *Strep*-tag II to allow affinity purification. Subsequent gel electrophoresis showed the presence of 3 contaminating proteins (~60 kDa, ~70 kDa and ~112 kDa) that co-elute with the ~330 kDa

heterotetrameric PfAdoMetDC/ODC. Western blot analysis showed that the ~60 kDa protein was not identified by the anti-*Strep*-Tag II antibody, indicating that it is of *E. coli* origin. In contrast, the ~112 kDa and ~70 kDa proteins were of heterologous origin with a *Strep*-tag II. The full-length bifunctional protein could not be purified from these co-eluting proteins by limiting hydrophobic interactions, TAP using both a His-tag and *Strep*-tag II for affinity selection or size-based purification strategies. These results indicate that the interactions between the contaminating proteins and the bifunctional protein is specific, leading to the formation of a protein complex larger than the expected ~330 kDa. The results obtained after TAP supports this hypothesis, since the contaminating fragments co-purified during the initial purification using IMAC via the His-tag (Fig 2.11). To verify this result, native PAGE analysis was performed, which showed that there was indeed a protein complex at ~600 kDa and another at ~400 kDa (Fig 2.16).

The heterologous origin of the ~ 112 kDa and ~ 70 kDa proteins, as indicated by the presence of the *Strep*-Tag II, suggested that these interacting proteins are smaller versions of the bifunctional protein. Western blot and MS analyses were performed to confirm this hypothesis. Explanations for the presence of smaller proteins include post-translational degradation, in-frame ribosomal slippage on mRNA secondary structures or false translation initiation at AUG codons downstream of the start codon. It was shown that while ribosomal slippage on mRNA secondary structures is responsible for a small fraction of contaminating peptides and post-translational degradation may account for the appearance of some background peptides, they are not responsible for the 3 major contaminating proteins. MS analysis showed that internal mRNA translation initiation sites account for two of the fragments, namely the ~112 kDa protein and a fraction of the ~70 kDa protein (Fig 2.20). The ~60 kDa and a fraction of the ~70 kDa protein were identified as *E. coli* chaperones produced due to the poor expression of the recombinant protein. This result is in agreement with the Western blots using anti-*Strep*-tag II antibody where the ~70 kDa band was strongly identified but not the ~60 kDa band. These results prove that it is unlikely that the protein can be purified to homogeneity using conventional means.

One way to prevent the over-induction of chaperone proteins is to make the translation of the PfAdoMetDC/ODC gene more *E. coli* amenable by the processes of codon optimisation and harmonization. In 1981 Toshimichi Ikemura noted that, in *E. coli*, abundant proteins are encoded for by codons corresponding to the majority of tRNAs. In contrast, those proteins that are encoded for by codons with low tRNA levels are expressed at much lower levels (Ikemura, 1981). This led to the dual processes of codon optimisation and codon harmonization. Codon

optimisation is the process where codons that are of a low frequency in the expression host are replaced by frequently used codons. This process will relieve the burden on the *E. coli* expression system, since the translation of the recombinant protein should be easier. However, in order to obtain higher levels of active, soluble recombinant protein, the gene will also have to be harmonized. This means that codons of low frequency usage in the malaria parasite are replaced with codons of low frequency usage in *E. coli*, and codons that are used frequently in malaria are replaced with codons that are frequently used in *E. coli*. By matching the translational procession *in vivo* and *in vitro*, correct folding of the protein is achieved (Kincaid et al., 2002). It has been shown that by adjusting *P. falciparum* merozoite proteins to mammalian codon usage (i.e. optimisation), four-fold higher expression could be obtained in mouse cells (Narum et al., 2001). This method has also been applied to the heterologous expression of *P. falciparum* proteins in *E. coli*, with mixed results. The gene optimisation of a multistage candidate vaccine, FALVAC-1, led to threefold higher expression in *E. coli* (Zhou et al., 2004). On the other hand, codon optimisation did not have any significant effect on the expression in *E. coli* of erythrocyte membrane protein I domains (Flick et al., 2004). It has also been shown that while a codon optimised *P. falciparum* gene for Liver-Stage antigen I led to a plasmid that was unstable, the codon harmonized construct led to high levels of protein expression in *E. coli* (Hillier et al., 2005).

It was decided to use the protein as is as bait in protein-protein interaction analyses, since more than 50 % of the protein eluate, namely the full-length protein, ~112 kDa protein and a part of the ~70 kDa protein are of PfAdoMetDC/ODC origin. However, this meant that any identified interactions would have to be strictly tested to ensure that the interaction is specific for PfAdoMetDC/ODC and not the co-purified chaperone proteins. It was decided to use a *P. falciparum* cDNA library cloned into the T7 lytic phage to identify peptide binding partners to PfAdoMetDC/ODC since these T7 phages are ideally suited for experimental conditions (Castagnoli et al., 2001). There are three possible types of results that could have been obtained through the use of such a library: Firstly, proteins that could have an interaction with PfAdoMetDC/ODC in the biological context due to co-expression at the correct location and lifecycle stage could have been identified. Secondly, non-native peptides originating from frameshifting events with affinity to PfAdoMetDC/ODC could have been obtained. Sequence alignment of such peptides could show conserved consensus regions that mediate the binding to PfAdoMetDC/ODC that can be used as possible lead sequences in drug development (Santonico et al., 2005). Lastly, fragments of PfAdoMetDC/ODC itself could have been obtained, which may be used to prevent dimerization of the protein, as was the case with Plasmodial TIM (Singh et al., 2001).

Following four rounds of biopanning, Library A, theoretically consisting of phages with affinity to PfAdoMetDC/ODC, was created. Subsequent sequence analysis showed that the phages did not contain *P. falciparum* cDNA inserts that encode for endogenous malarial protein fragments or even random peptides, but encoded stretches of Lys residues. Due to the positive nature of these phages, it is highly likely that they were isolated due to non-specific electrostatic interactions with PfAdoMetDC/ODC. During biopanning, the washing step ensures that the non-binding phage is removed and thus leads to the enrichment of phage particles with affinity to the target protein. This implies that the wash buffer has to be carefully chosen to eliminate non-selective binding phage particles, while retaining the phage particles that binds to the bait protein. A too stringent wash buffer may lead to the enrichment of phages that have high affinity, but low selectivity for the bait protein (Willats, 2002). In an effort to overcome this problem, various different experimental strategies were followed (see Table 3.1). Only the *P. falciparum* cDNA inserts bigger than ~200 bp were chosen for sequence analysis, which identified only 4 peptides longer than 10 amino acids. Of these, only one is an endogenous malarial peptide, derived from a putative Ebl-like protein. However, since this protein is expressed during a different stage of the Plasmodial lifecycle (merozoite stage as opposed to the trophozoite stage), it is unlikely that this interaction occurs *in vivo*. This phenomenon of false positives due to incorrect biological context unfortunately occurs often with both experimental and computational interaction analyses (Aloy and Russell, 2006).

The consensus sequence found in peptides are usually between five and eight amino acids long and can be utilised for the rational design of inhibitory drugs (Kay and Hamilton, 2001). The presence of consensus motifs in the peptides/proteins with affinity to PfAdoMetDC/ODC were investigated with the MEME Motif discovery tool (Bailey and Elkan, 1994). No consensus sequence could however be identified. This lack of consensus implies that it is unlikely that any of these sequences can be used for lead development. In addition, all four phage clones gave a signal of binding to *E. coli* DnaK as well as to the PfAdoMetDC/ODC eluate. This indicates that it is highly probable that the fusion peptides encoded on the capsid protein have affinity to the co-purified *E. coli* proteins rather than to the recombinant malarial protein.

There are several reasons that could explain why the study did not succeed in isolating phage particles that encode surface peptides specific for PfAdoMetDC/ODC. Considering that one in three of the cloned cDNA inserts should theoretically be in the correct reading frame, the 13 unique *P. falciparum* cDNA inserts that were obtained should have given at least 4 endogenous peptides. However, only one of these peptides was an endogenous malarial peptide. In addition, only 4 phages displaying peptides longer than 10 amino acids were obtained due to the high

prevalence of encoded stop codons. The high frequency of stop codons implies that very few of the phages encoded for peptides capable of binding to the bait protein, since most contained only a few foreign amino acids on their coat proteins. Chappel et al. has shown that during the initial amplification of a phage library, phage particles that do not produce and display the encoded cDNA inserts have a growth advantage. This has a direct effect on biopanning effectivity, due to the large number of non-productive phage particles with greater growth capabilities present (Chappel et al., 2004). As such, it is possible that the starting phage library was of poor quality, with very few phage particles actually displaying *Plasmodium* peptides. One possible explanation for the quality of the *P. falciparum* cDNA phage library is the method in which the mRNA was isolated (Lauterbach et al., 2003). Due to the A+T richness of the malarial genome, a poly-T column does not only isolate mRNA, but contaminating tRNA, rRNA and genomic DNA as well. These may lead to a reduction of protein encoding cDNA inserts in the library.

Although it was thought that the presence of the ~112 kDa and ~70 kDa N-terminally truncated fragments would not have a large effect in the interaction studies due to their PfAdoMetDC/ODC origin, the presence of the *E. coli* chaperone proteins clearly created problems. This implies that, at present, recombinant PfAdoMetDC/ODC cannot be used as bait in interaction analyses with a large variety of prey, due to the possible isolation of prey with affinity to the co-purified proteins.

Following completion of this study, it was attempted to increase the recombinant expression and subsequent purity of PfAdoMetDC/ODC by harmonizing approximately the first third of the gene to that of *E. coli* codon usage (results not shown). Although the silent mutation incorporated to remove the Shine Dalgarno site responsible for the ~112 kDa fragment did seem to decrease expression of this fragment, the overall expression and affinity purification of the protein were not significantly improved. Notably, the ~60 kDa and ~70 kDa fragments were still present. Higher protein levels with increased purity were however obtained when only the AdoMetDC domain was expressed from this construct. This implies that in order to obtain higher levels of pure, full-length protein, one may have to harmonize the entire gene. It is however possible that this expensive strategy will still not succeed in providing homogenous protein.

Alternatively, the use of a DnaK and GroEl deficient *E. coli* host may lead to the isolation of purer protein. This strategy would however require the co-expression of *P. falciparum* chaperone proteins to ensure correct folding of the bifunctional protein. Eukaryotic expression

systems, such as the baculovirus expression system or *Pichia pastoris* could also be tested to see if these systems provide pure, full-length PfAdoMetDC/ODC.

An alternative strategy might have been to use a combinatorial peptide library to identify binding peptides to PfAdoMetDC/ODC, which could have been used to identify lead sequences as well as possible native partners due to the concept of convergent evolution (Kay et al., 2000). Combinatorial peptide libraries have much greater diversity than a cDNA library, and are not influenced by the occurrence of a specific mRNA or the complexity involved in the expression of certain genome-encoded proteins, such as transmembrane regions (Rodi et al., 2001). Additionally, the high occurrence of stop-codons found in this study can be avoided by the careful design of the combinatorial ligands. However, the difficulties caused by the presence of the *E. coli* chaperone proteins would not have been avoided using this strategy, since there is a very large chance that peptides with affinity to these co-eluting proteins would be isolated. One method to circumvent this problem is to use the *in silico* data of Date and co-workers and Wuchty et al (Date and Stoeckert Jr, 2006; Wuchty and Ipsaro, 2007) as a starting point for more focused interaction studies. By testing just those proteins/peptides that have been previously identified as possible binding partners for PfAdoMetDC/ODC, through the use of techniques such as PCA or co-immunoprecipitation studies (Phizicky and Fields, 1995; Remy and Michnick, 2004), the isolation of interacting partners to the contaminating proteins may be avoided. This strategy could lead to the identification of biologically important interacting partners and/or specific protein motifs required for interaction with PfAdoMetDC/ODC that can be used for lead molecule development.

Alternatively, Two-Hybrid analysis such as the well-known yeast Two-Hybrid system could have been used for the identification of interacting proteins. This system does however have several drawbacks, such as the fact that the nuclear environment is not physiological for most proteins, while the chemical environment in phage display is more open to manipulation. Additionally, the proteins have to pass the nuclear membrane for the interaction to be detected. This method is also more time-consuming than phage display due to the longer life-cycle of the organism (Castagnoli et al., 2001; Rodi et al., 2001). Although LaCount and co-workers did use a yeast Two-Hybrid analysis to isolate two possible interaction partners to PfAdoMetDC/ODC (LaCount et al., 2005), it does not appear as if these interactions occur *in vivo* with a clear biological function. These proteins that were identified by the yeast Two-Hybrid analysis were promiscuous in binding and are also expressed during a different stage of the parasite lifecycle.

Since two independent experimental studies using different methodologies did not succeed in identifying interacting proteins to PfAdoMetDC/ODC with obvious biological function, it could be considered that PfAdoMetDC/ODC does not have protein binding partners *in vivo*. This is however extremely unlikely due to the highly regulated nature of polyamine metabolism. The activities and levels of the two rate-limiting enzymes in the polyamine pathway, ODC and AdoMetDC are controlled on the transcriptional, translational and post-translational levels (Müller et al., 2000). In humans, ODC is regulated by both negative and positive feedback regulation, as well as by the action of a polyamine-induced protein called antizyme (AZ). There are also distinct pathways for the retro-conversion of spermidine and spermine (Wallace et al., 2003). However, neither antizyme nor retro-conversion pathways have been found in *P. falciparum*. The bifunctional PfAdoMetDC/ODC also has a much longer half-life than its human counterparts, which means that its activities should be tightly controlled. However, to date, the regulation mechanisms of PfAdoMetDC/ODC have not been identified. Due to the absence of antizyme and retro-conversion pathways, it is highly possible that an as yet unknown protein or proteins regulate the activities of the bifunctional protein, and it is mainly due to technical difficulties that these regulating partners have not been identified. Certain protein-protein interactions are mediated by the posttranslational modifications (PTMs) that occur in eukaryotic cells. The interactions between cell-division cycle 4 protein and the substrate inhibitor of cyclin-dependent protein kinase-1; histone H3 and heterochromatin protein-1; and RNA polymerase II and its transcriptional regulators, are but a few that are all dependent on PTMs such as methylation, ubiquitination, phosphorylation or acetylation (Seet et al., 2006). It is possible that the interaction between PfAdoMetDC/ODC and a specific *in vivo* protein partner is dependent on an eukaryotic post-translational modification. If such were the case, this interaction would not have been identified in this study due to the use of a prokaryotic expression system. Protein-protein interactions can also be quite transient, (Kluger and Alagic, 2004), which makes the identification of interacting partners very difficult. It is also possible that PfAdoMetDC/ODC is regulated by the inhibition of translation by its cognate mRNA, as is the case with DHFR-TS (Zhang and Rathod, 2002). No sign of this type of regulation has yet been found.

In conclusion, while the targeting of parasitic protein-protein interactions for therapeutic intervention is a viable strategy, the pitfalls encountered in this study shows that it is not yet viable for the targeting of *Plasmodium* polyamine metabolism. Hopefully, with the advent of new technologies, this strategy may be revisited.

Summary

Due to the increasing resistance against the currently used antimalarial drugs, novel chemotherapeutic agents that target new metabolic pathways for the treatment of malarial infections are urgently needed. One approach to the drug discovery process is to use interaction analysis to find proteins that are involved in a specific metabolic pathway that has been identified as a drug target. Protein-protein interactions in such a pathway can be preferential targets since a) there is often greater structural variability in protein-protein interfaces, which can lead to more effective differentiation between the parasite and host proteins; and b) the important amino acids in a protein-protein interface are often conserved and even one amino acid mutation can lead to the dissociation of the complex, implying that resistance should be slower to appear.

Since polyamines and their biosynthetic enzymes occur in increased concentrations in rapidly proliferating cells, the inhibition of polyamine metabolism is a rational approach for the development of antiparasitic drugs. Polyamine synthesis in *P. falciparum* is uniquely facilitated by a single open reading frame that encodes both rate-limiting enzymes in the pathway, namely ornithine decarboxylase (ODC) and S-adenosylmethionine decarboxylase (AdoMetDC). The AdoMetDC/ODC domains are assembled in a heterotetrameric bifunctional protein complex of ~330 kDa. Inhibition of both decarboxylase activities is curative of murine malaria and indicates the viability of such strategies in malaria control. It was hypothesized that protein ligands to this enzyme can be utilized in targeting the polyamine biosynthetic pathway in a novel approach.

The bifunctional PfAdoMetDC/ODC was recombinantly expressed with a C-terminal *Strep*-tag-II to allow affinity purification. Subsequent gel electrophoresis analysis showed the presence of 3 contaminating proteins (~60 kDa, ~70 kDa and ~112 kDa) that co-elute with the ~330 kDa AdoMetDC/ODC. Efforts to purify the bifunctional protein to homogeneity included subcloning into a double-tagged vector for tandem affinity purification as well as size-exclusion HPLC. SDS-PAGE analysis of these indicated that separation of the four proteins was not successful, implicating the presence of strong protein-protein interactions. Western blot analysis showed that the ~112 kDa and ~70 kDa peptides were recombinantly produced with a C-terminal *Strep*-tag, indicating their heterologous origin. The ~60 kDa fragment was however not recognised by the tag-specific antibodies. This implies that this fragment is of *E. coli* origin. MS-analysis of the contaminating bands showed that the ~112 kDa peptide is an N-terminally truncated form of

the full-length protein, the ~70 kDa peptide is a mixture of N-terminally truncated recombinant protein and *E. coli* DnaK and the ~60 kDa peptide is *E. coli* GroEL.

A *P. falciparum* cDNA phage display library was used to identify peptide ligands to PfAdoMetDC/ODC. Of the peptides isolated through the biopanning process, only one was shown to occur *in vivo*. It could however not be conclusively shown that the isolated peptides bind to PfAdoMetDC/ODC and not to the co-eluting *E. coli* proteins. It is thought that while it is extremely likely that interacting protein partners to PfAdoMetDC/DOC exist, the available technologies are not sufficient to lead to the identification of such partners.

References

- Aloy, P., and R.B. Russell. 2006. Structural systems biology: modelling protein interactions. *Nature reviews*. 7:188-197.
- Altschul, S.F., W. Gish, W. Miller, E.W. Myers, and D.J. Lipman. 1990. Basic local alignment search tool. *J. Mol. Biol.* 215:413-410.
- Apic, G., T. Ignjatovic, S. Boyer, and R.B. Russell. 2005. Illuminating drug discovery with biological pathways. *FEBS Letters*. 579:1872-1877.
- Arav-Boger, R., and T.A. Shapiro. 2005. Molecular Mechanisms of Resistance in Antimalarial Chemotherapy: The Unmet Challenge. *Annu. Rev. Pharmacol. Toxicol.* 45:565-585.
- Archakov, A.I., V.M. Govorun, A.V. Dubanov, Y.D. Ivanov, A.V. Veselovsky, P. Lewi, and P. Janssen. 2003. Protein-protein interactions as a target for drugs in proteomics. *Proteomics*. 3:380-391.
- Arkin, M.R., and J.A. Wells. 2004. Small-molecule inhibitors of Protein-Protein interactions: Progressing towards the dream. *Nature reviews: Drug discovery*. 3:301-317.
- Assaraf, Y.G., L. Abu-Elheiga, D.T. Spira, H. Desser, and U. Bachrach. 1987a. Effect of polyamine depletion on macromolecular synthesis of the malaria parasite, *Plasmodium falciparum*, cultured in human erythrocytes. *Biochem. J.* 242:221-226.
- Assaraf, Y.G., J. Golenser, D.T. Spira, G. Messer, and U. Bachrach. 1987b. Cytostatic effect of DL- α -difluoromethylornithine against *Plasmodium falciparum* and its reversal by diamines and spermidine. *Parasitol Res.* 73:313-318.
- Azzazy, H.E., and W.E. Highsmith, Jr. 2002. Phage display technology: clinical applications and recent innovations. *Clinical Biochemistry*. 35:425-445.
- Baek, H., K. suk, Y. Kim, and S. Cha. 2002. An improved helper phage system for efficient isolation of specific antibody molecules in phage display. *Nucleic Acids Research*. 30:e18.
- Bahl, A., B. Brunk, R.L. Coppel, J. Crabtree, S.J. Diskin, M.J. Fraunholz, G.R. Grant, D. Gupta, R.L. Huestis, J.C. Kissenger, P. Labo, L. L., S.K. McWeeney, A.J. Milgram, D.S. Roos, J. Schug, and C.J. Stoeckert Jr. 2002. PlasmoDB: the *Plasmodium* genome resource. An integrated database providing tools for accessing, analyzing and mapping expressions and sequence data (both finished and unfinished). *Nucleic Acids Research*. 30:87-90.
- Bailey, T.L., and C. Elkan. 1994. Fitting a mixture model by expectation maximization to discover motifs in biopolymers. *Proceedings of the Second International Conference on Intelligent Systems for Molecular Biology*:28-36.
- Baneyx, F., and M. Mujacic. 2004. Recombinant protein folding and misfolding in *Escherichia coli*. *Nature Biotechnology*. 22:1399-1408.
- Bathurst, I., and C. Hentschel. 2006. Medicines for Malaria Venture: sustaining antimalarial drug development. *Trends in Parasitology*. 22:301-307.
- Birkholtz, L. 2002. Functional and Structural characterization of the unique bifunctional enzyme complex involved in the regulation of polyamine metabolism in *Plasmodium falciparum*. In Department of Biochemistry. University of Pretoria, Pretoria.
- Birkholtz, L., F. Joubert, A.W.H. Neitz, and A.I. Louw. 2003. Comparative properties of a Three-dimensional Model of *Plasmodium falciparum* Ornithine Decarboxylase. *Proteins:Structure, Function, and Genetics*. 50:464-473.
- Birkholtz, L., C. Wrenger, F. Joubert, G.A. Wells, R.D. Walter, and A.I. Louw. 2004. Parasite-specific inserts in the bifunctional S-adenosylmethionine decarboxylase/ornithine decarboxylase of *Plasmodium falciparum* modulate catalytic activities and domain interactions. *Biochem. J.* 377:439-448.
- Bitonti, A.J., J.A. Dumont, T.L. Bush, M.L. Edwards, D.M. Stemerick, P.P. McCann, and A. Sjoerdsma. 1989. Bis(benzyl)polyamine analogs inhibit the growth of chloroquine-resistant human malaria parasites (*Plasmodium falciparum*) *in vitro* and in combination with α -difluoromethylornithine cure murine malaria. *Proc. Natl.Acad.Sci.U.S.A.* 86:651-655.

- Bogan, A.A., and K.S. Thorn. 1998. Anatomy of Hot Spots in Protein Interfaces. *Journal of Molecular Biology*. 280:1-9.
- Bradbury, A.R.M., and J.D. Marks. 2004. Antibodies from phage antibody libraries. *Journal of Immunological Methods*. 290:29-49.
- Bradford, M.M. 1976. A rapid and sensitive method for the quantitation of microgram quantities of protein utilizing the principle of protein-dye binding. *Anal Biochem*. 72:248-254.
- Breman, J.G. 2001. The Ears Of The Hippopotamus: Manifestations, Determinants, and Estimates of the Malaria Burden. *Am. J. Trop. Med. Hyg.* 64:1-11.
- Breman, J.G., M.S. Alilio, and A. Mills. 2004. Conquering the intolerable burden of malaria: What's new, whats needed: a summary. *Am. J. Trop. Med. Hyg.* 71:1-15.
- Buckingham, S. 2004. Picking the Pockets of Protein-Protein Interactions. *In* Horizon Symposia-Charting chemical space. 1-4.
- Buendía-Orozco, J., A. Guerrero, and N. Pastor. 2005. Model of the TBP-TFIIB Complex from *Plasmodium falciparum*: Interface Analysis and Perspectives as a New Target for Antimalarial design. *Archives of Medical Research*. 36:317-330.
- Burger, P.B., L. Birkholtz, F. Joubert, N. Haider, R.D. Walter, and A.I. Louw. 2007. Structural and mechanistic insights into the action of *Plasmodium falciparum* spermidine synthase. *Bioorganic and Medicinal Chemistry*. 15:1628-1637.
- Carrico, D., J. Ohkanda, H. Kendrick, K. Yokayama, M.A. Blaskovich, C.J. Bucher, F.S. Buckner, W.C. Van Voorhis, D. Chakrabarti, S.L. Croft, M.H. Gelb, S.M. Sebt, and A.D. Hamilton. 2004. In vitro and in vivo antimalarial activity of peptidomimetic protein farnesyltransferase inhibitors with improved membrane permeability. *Bioorganic and Medicinal Chemistry*. 12:6517-6526.
- Casero, R.A., and P.M. Woster. 2001. Terminally Alkylated Polyamine Analogues as Chemotherapeutic Agents. *Journal of Medicinal Chemistry*. 44:1-26.
- Castagnoli, L., A. Zucconi, M. Quondam, M. Rossi, P. Vaccaro, S. Panni, S. Paoluzi, E. Santonico, L. Dente, and G. Cesareni. 2001. Alternative Bacteriophage Display Systems. *Combinatorial Chemistry & High Throughput Screening*. 4:121-133.
- Chappel, J.A., W.O. Rogers, S.L. Hoffman, and A.S. Kang. 2004. Molecular dissection of the human antibody response to the structural repeat epitope of *Plasmodium falciparum* sporozoite from a protected donor. *Malaria Journal*. 3.
- Clark, I., L.M. Alleva, A.C. Mills, and W.B. Cowden. 2004. Pathogenesis of Malaria and Clinically Similar Conditions. *Clinical Microbiology Reviews*. 17:509-539.
- Cochran, A.G. 2000. Antagonists of protein-protein interactions. *Chemistry and Biology*. 7:R85-R94.
- Cohen, S.S. 1998. A guide to the polyamines. Oxford University Press, Oxford.
- Coleman, C.S., B.A. Stanley, R. Viswanath, and A.E. Pegg. 1994. Rapid exchange of subunits of Mammalian Ornithine decarboxylase. *The Journal of Biological Chemistry*. 269:3155-3158.
- Condrón, B.G., J.F. Atkins, and R.F. Gesteland. 1991. Frameshifting in Gene 10 of Bacteriophage T7. *Journal of Bacteriology*. 173:6998-7003.
- Cox, F.E.G. 2002. History of Human Parasitology. *Clinical Microbiology Reviews*. 15:595-612.
- Curtidor, H., L.E. Rodríguez, M. Ocampo, R. López, J.E. García, J. Valbuena, R. Vera, Á. Puentes, M. Vanegas, and M.E. Patarroyo. 2005. Specific erythrocyte binding capacity and biological activity of *Plasmodium falciparum* erythrocyte binding ligand 1 (EBL-1)-derived peptides. *Protein Science*. 14:464-473.
- Das Gupta, R., T. Krause-Ihle, B. Bergmann, and I.B. Müller. 2005. 3-Aminoxy-1-Aminopropane and Derivatives Have an Antiproliferative Effect on Cultured *Plasmodium falciparum* by Decreasing Intracellular Polyamine concentrations. *Antimicrobial Agents and Chemotherapy*. 49:2857-2864.
- Date, S.V., and C.J. Stoeckert Jr. 2006. Computational modeling of the *Plasmodium falciparum* interactome reveals protein function on a genome-wide scale. *Genome Research*. 16:542-549.

- Davis, T.M.E., H.A. Karunajeewa, and K.F. Ilett. 2005. Artemisinin-based combination therapies for uncomplicated malaria. *MJA*. 182:181-185.
- Dellicour, S., S. Hall, D. Chandramohan, and B. Greenwood. 2007. The safety of artemisinins during pregnancy: a pressing question. *Malaria Journal*. 6:1-10.
- Eda, K., S. Eda, and I.W. Sherman. 2004. Identification of Peptides Targeting the Surface of *Plasmodium falciparum*-infected erythrocytes using a Phage Display Peptide Library. *Am. J. Trop. Med. Hyg.* 71:190-195.
- Edwards, G., and G.A. Biagini. 2006. Resisting resistance: dealing with the irrepressible problem of malaria. *British Journal of Clinical Pharmacology*. 61:690-693.
- Eisenberg, D., E.M. Marcotte, I. Xenarios, and T.O. Yeates. 2000. Protein function in the post-genomic era. *Nature*. 405:823-826.
- Ekstrom, J.L., I.I. Mathews, B.A. Stanley, A.E. Pegg, and S.E. Ealick. 1999. The crystal structure of human S-adenosylmethionine decarboxylase at 2.25 Å resolution reveals a novel fold. *Structure*. 7:583-595.
- Falciani, C., L. Lozzi, A. Pini, and L. Bracci. 2005. Bioactive Peptides from Libraries. *Chemistry and Biology*. 12:417-426.
- Fernández, L.A. 2004. Prokaryotic expression of antibodies and affibodies. *Current Opinion in Biotechnology*. 15:364-373.
- Fiedler, M., C. Horn, C. Bandtlow, M.E. Schwab, and A. Skerra. 2002. An engineered IN-1 F_{ab} fragment with improved affinity for the Nogo-A axonal growth inhibitor permits immunochemical detection and shows enhanced neutralizing activity. *Protein Engineering*. 15:931-941.
- Fischer, P.M., and D.P. Lane. 2004. Small-molecule inhibitors of the p53 suppressor HDM2: have protein-protein interactions come of age as drug targets? *Trends in Pharmacological Sciences*. 25:343-346.
- Flick, K., S. Ahuja, A. Chene, M.T. Bejarano, and Q. Chen. 2004. Optimized expression of *Plasmodium falciparum* erythrocyte membrane protein I domains in *Escherichia coli*. *Malaria Journal*. 3.
- Frevert, U. 2004. Sneaking in through the back entrance: the biology of malaria liver stages. *Trends in Parasitology*. 20:417-424.
- Gadek, T.R., and J.B. Nicholas. 2003. Small molecule antagonists of proteins. *Biochemical Pharmacology*. 65:1-8.
- Gandre, S., Z. Bercovich, and C. Kahana. 2002. Ornithine decarboxylase-antizyme is rapidly degraded through a mechanism that requires functional ubiquitin-dependant proteolytic activity. *Eur.J.Biochem*. 269:1316-1322.
- Gasteiger, E., A. Gattiker, C. Hoogland, I. Ivanyi, R.D. Appel, and A. Bairoch. 2003. ExpPASy: the proteomics server for in-depth protein knowledge and analysis. *Nucleic Acids Research*. 31:3784-3788.
- Gasteiger, E., C. Hoogland, A. Gattiker, S. Duvaud, M.R. Wilkins, R.D. Appel, and A. Bairoch. 2005. Protein Identification and Analysis Tools on the ExpPASy server. *In The Proteomics Handbook*. J.M. Walker, editor. Humana Press. 571-607.
- Ghosh, A., P. Srinivisan, E.G. Abraham, H. Fujioka, and M. Jacobs-Lorena. 2003. Molecular strategies to study *Plasmodium*-mosquito interactions. *Trends in Parasitology*. 19:94-101.
- Ghosh, A.K., L.A. Moreira, and M. Jacobs-Lorena. 2002. *Plasmodium*-mosquito interactions, phage display libraries and transgenic mosquitoes impaired for malaria transmission. *Insect Biochemistry and Molecular Biology*. 32:1325-1331.
- Ghosh, I., A.D. Hamilton, and L. Regan. 2000. Antiparallel Leucine Zipper-Directed Protein Reassembly: application to the Green Fluorescent Protein. *J. Am. Chem. Soc.* 122:5658-5659.
- Giannattasia, R.B., and B. Weisblum. 2000. Modulation of Erm methyltransferase Activity by peptides derived from Phage Display. *Antimicrobial Agents and Chemotherapy*. 44:1961-1963.
- Greenwood, B.M., K. Bojang, C.J.M. Whitty, and G.A.T. Targett. 2005. Malaria. *Lancet*. 365:1487-1498.

- Hafner, E., C. Tabor, and H. Tabor. 1979. Mutants of *Escherichia coli* that do not contain 1,4-diaminobutane (putrescine) or spermidine. *Journal of Biological Chemistry*. 254:12419-12426.
- Haider, N., M.-L. Eschbach, S. de Souza Dias, T.-W. Gilberger, R.D. Walter, and K. Lüersen. 2005. The spermidine synthase of the malaria parasite *Plasmodium falciparum*: Molecular and biochemical characterization of the polyamine synthesis enzyme. *Molecular & Biochemical Parasitology*. 142:224-236.
- Hall, T.A. 1999. BioEdit: A user-friendly biological sequence alignment editor and analysis program for Windows 95/98/NT. *Nucl.Acids. Symp. Ser.* 41:95-98.
- Hanahan, D., J. Jessee, and F.R. Bloom. 1991. Plasmid transformation of *Escherichia coli* and other bacteria. *In Methods in Enzymology*. Vol. 204. 63-114.
- Hartl, F.U., and M. Hayer-Hartl. 2002. Molecular Chaperones in the Cytosol: from Nascent Chain to Folded Protein. *Science*. 295:1852-1858.
- Heby, O., S.C. Roberts, and B. Ullman. 2003. Polyamine biosynthetic enzymes as drug targets in parasitic protozoa. *Biochemical Society Transactions*. 31:415-419.
- Heddi, A. 2002. Malaria pathogenesis: a jigsaw with an increasing number of pieces. *International Journal for Parasitology*. 32:1587-1598.
- Hillier, C.J., L.A. Ware, A. Barbosa, E. Angov, J.A. Lyon, D.G. Heppner, and D.E. Lanar. 2005. Process Development and Analysis of Liver-Stage Antigen 1, a Preerythrocyte-Stage Protein-Based Vaccine for *Plasmodium falciparum*. *Infection and Immunity*. 73:2109-2115.
- Hoess, R.H. 2001. Protein design and Phage display. *Chem. Rev.* 101:3205-3218.
- Hopkins, A.L., and C.R. Groom. 2002. The druggable genome. *Nature reviews*. 1:727-230.
- Houry, W.A. 2001. Chaperone-Assisted Protein Folding in the Cell Cytoplasm. *Current Protein and Peptide Science*. 2:227-244.
- Howell, J.M., T.L. Winstone, J.R. Coorsen, and R.J. Turner. 2006. An evaluation of *in vitro* protein-protein interaction techniques: Assessing contaminating background proteins. *Proteomics*. 6:2050-2069.
- Hyde, J.E. 2005. Drug-resistant malaria. *Trends in Parasitology*. 21:494-498.
- Ikemura, T. 1981. Correlation between the abundance of *Escherichia coli* transfer RNAs and the occurrence of the respective codons in its protein genes: A proposal for a synonymous codon choice that is optimal for the *E. coli* translational system. *Journal of Molecular Biology*. 151:389-409.
- Ito, T., K. Tashiro, S. Muta, R. Ozawa, T. Chiba, M. Nishizawa, K. Yamamoto, S. Kuhara, and Y. Sakaki. 2000. Toward a protein-protein interaction map of the budding yeast: A comprehensive system to examine two-hybrid interactions in all possible combinations between yeast proteins. *PNAS*. 97:1143-1147.
- Jambou, R., E. Legrand, M. Niang, N. Khim, P. Lim, B. Volney, M.T. Ekala, C. Bouchier, P. Esterre, T. Fandeur, and O. Mercereau-Puijalon. 2005. Resistance of *Plasmodium falciparum* field isolates to *in-vitro* artemether and point mutations of the SERCA-type PfATPase6. *Lancet*. 366:1960-1963.
- Jana, S., and J.K. Deb. 2005. Strategies for the efficient production of heterologous proteins in *Escherichia coli*. *Appl Microbiol Biotechnol*. 67:289-298.
- Jänne, J., L. Alhonen, M. Pietilä, and T.A. Keinänen. 2004. Genetic approaches to the cellular functions of polyamines in mammals. *Eur.J.Biochem*. 271:877-894.
- Joy, D.A., X. Feng, J. Mu, T. Furuya, K. Chotivanich, A.U. Krettli, M. Ho, A. Wang, N.J. White, E. Suh, P. Beerli, and X. Su. 2003. Early Origin and Recent Expansion of *Plasmodium falciparum*. *Science*. 300:318-321.
- Karlin, S., L. Brocchieri, A. Bergman, J. Mrazek, and A.J. Gentles. 2002. Amino acid runs in eukaryotic proteomes and disease associations. *Proc. Natl.Acad.Sci.U.S.A.* 99:333-338.
- Kay, B.K., and P.T. Hamilton. 2001. Identification of Enzyme Inhibitors from Phage-Displayed Combinatorial Peptide Libraries. *Combinatorial Chemistry & High Throughput Screening*. 4:535-543.

- Kay, B.K., J. Kasanov, S. Knight, and A. Kurakin. 2000. Convergent evolution with combinatorial peptides. *FEBS Letters*. 480:55-62.
- Kay, B.K., J. Kasanov, and M. Yamabhai. 2001. Screening Phage-displayed Combinatorial Peptide Libraries. *Methods*. 24:240-246.
- Keizer, D.W., L.A. Miles, F. Li, M. Nair, R.F. Anders, A.M. Coley, M. Foley, and R.S. Norton. 2003. Structures of Phage-Display peptides that Bind to the Malarial Surface protein, Apical Membrane Antigen 1, and Block Erythrocyte Invasion. *Biochemistry*. 42:9915-9923.
- Khan, S.M., and A.P. Waters. 2004. Malaria parasite transmission stages: an update. *Trends in Parasitology*. 20:575-580.
- Kim, K., and S.A. Lommel. 1998. Sequence Element Required for Efficient -1 Ribosomal frameshifting in Red Clover Necrotic Mosaic Dianthovirus. *Virology*. 250:50-59.
- Kincaid, R.L., E. Angov, and J.A. Lyon. 2002. Protein expression by codon harmonization and translational attenuation.
- Kirk, K. 2001. Membrane transport in the Malaria-Infected Erythrocyte. *Physiol Rev*. 81:495-537.
- Kluger, R., and A. Alagic. 2004. Chemical cross-linking and protein-protein interactions- a review with illustrative protocols. *Bioorganic Chemistry*. 32:451-472.
- Konthur, Z., and R. Crameri. 2003. High-throughput applications of phage display in proteomic analyses. *Targets*. 2:261-270.
- Kooij, T.W.A., C.J. Janse, and A.P. Waters. 2006. *Plasmodium* post-genomics: better the bug you know? *Nature reviews Microbiology*. 4:344-357.
- Krause, T., K. Lüersen, C. Wrenger, T.-W. Gilberger, S. Müller, and R.D. Walter. 2000. The ornithine decarboxylase domain of the bifunctional ornithine decarboxylase/S-adenosylmethionine decarboxylase of *Plasmodium falciparum*: recombinant expression and catalytic properties of two different constructs. *Biochem. J*. 352:287-292.
- Kremsner, P.G., and S. Krishna. 2004. Antimalarial combinations. *Lancet*. 364:285-294.
- Kriplani, U., and B.K. Kay. 2005. Selecting peptides for use in nanoscale materials using phage-displayed combinatorial peptide libraries. *Current Opinion in Biotechnology*. 16:470-475.
- LaCount, D.J., M. Vignali, R. Chettier, A. Phansalkar, R. Bell, J.R. Hesselberth, L.W. Schoenfeld, I. Ota, S. Sahasrabudhe, C. Kurschner, S. Fields, and R.E. Hughes. 2005. A protein interaction network of the malaria parasite *Plasmodium falciparum*. *Nature*. 438:103-107.
- Laemmli, U.K. 1970. Cleavage of structural proteins during the assembly of the head of bacteriophage T4. *Nature*. 227:680-685.
- Lanzillotti, R., and T.L. Coetzer. 2004. Myosin-like sequences in the malaria parasite *Plasmodium falciparum* bind human erythrocyte membrane protein 4.1. *hematologica*. 89:1168-1171.
- Lauterbach, S.B., R. Lanzillotti, and T.L. Coetzer. 2003. Construction and use of *Plasmodium falciparum* phage display libraries to identify host parasite interactions. *Malaria Journal*. 2.
- Legrain, P., J.L. Jestin, and V. Schächter. 2000. From the analysis of protein complexes to proteome-wide linkage maps. *Current Opinion in Biotechnology*. 11:402-407.
- Li, F., A. Dluzewski, A.M. Coley, A. Thomas, L. Tilley, R.F. Anders, and M. Foley. 2002. Phage-displayed Peptides Bind to the Malarial Protein Apical membrane Antigen-1 and Inhibit the Merozoite Invasion of Host Erythrocytes. *The Journal of Biological Chemistry*. 277:50303-50310.
- Lichty, J.J., J.L. Malecki, H.D. Agnew, D.J. Michelson-Horowitz, and S. Tan. 2005. Comparison of affinity tags for protein purification. *Protein Expression and Purification*. 41:98-105.
- Macreadie, I., H. Ginsburg, W. Sirawaraporn, and L. Tilley. 2000. Antimalarial Drug Development and New Targets. *Parasitology Today*. 16:438-444.
- Marchler-Bauer, A., and S.H. Bryant. 2004. CD-Search: protein domains annotations on the fly. *Nucleic Acids Research*. 32:327-331.
- Marton, L.J., and A.E. Pegg. 1995. Polyamines as targets for therapeutic intervention. *Annu. Rev. Pharmacol. Toxicol*. 35:55-91.
- Matuschewski, K. 2006. Vaccine development against malaria. *Current opinion in Immunology*. 18:449-457.

- Mehlin, C. 2005. Structure-Based Drug Discovery for *Plasmodium falciparum*. *Combinatorial Chemistry & High Throughput Screening*. 8:5-14.
- Mehlin, C., E. Boni, F.S. Buckner, L. Engel, T. Feist, M.H. Gelb, L. Haji, D. Kim, C. Liu, N. Mueller, P.J. Myler, J.T. Reddy, J.N. Sampson, E. Subramanian, W.C. Van Voorhis, E. Worthey, F. Zucker, and W.G.J. Hol. 2006. Heterologous expression of proteins from *Plasmodium falciparum*: Results from 1000 genes. *Molecular & Biochemical Parasitology*. 148:144-160.
- Meloan, R., P. Timmerman, and H. Langedijk. 2004. Bioactive peptides based on diversity libraries, supramolecular chemistry and rational design: A new class of peptide drugs. Introduction. *Molecular Diversity*. 8:57-59.
- Merril, C.R., D. Goldman, S.A. Sedman, and M.H. Ebert. 1981. Ultrasensitive stain for proteins in polyacrylamide gels shows regional variation in cerebrospinal fluid proteins. *Anal Biochem*. 72:248-254.
- Michelitsch, M.D., and J.S. Weissman. 2000. A census of glutamine/asparagine regions: Implications for their conserved function and the predictions of novel prions. *PNAS*. 97:11910-11915.
- Miller, L.H., D.I. Baruch, K. Marsh, and O.K. Doumbo. 2002. The pathogenic basis of malaria. *Nature*. 415:673-679.
- Molitor, I.M., S. Knöbel, C. Dang, T. Spielmann, A. Alléra, and G.M. König. 2004. Translation initiation factor eIF-5a from *Plasmodium falciparum*. *Molecular & Biochemical Parasitology*. 137:65-74.
- Mukhija, S., and B. Erni. 1997. Phage display selection of peptides against enzyme I of the phosphoenolpyruvate-sugar phosphotransferase system (PTS). *Molecular Microbiology*. 25:1159-1166.
- Mullen, L.M., S.P. Nair, J.H. Ward, A.N. Rycroft, and B. Henderson. 2006. Phage display in the study of infectious diseases. *Trends in Microbiology*. 14:141-147.
- Müller, S., G.H. Coombs, and R.D. Walter. 2001. Targeting polyamines of parasitic protozoa in chemotherapy. *Trends in Parasitology*. 17:242-249.
- Müller, S., A. Da'daras, K. Lüersen, C. Wrenger, R.D. Gupta, R. Madhubala, and R.D. Walter. 2000. In The Human Malaria Parasite *Plasmodium falciparum* Polyamines Are Synthesized by a Bifunctional Ornithine Decarboxylase, S-Adenosylmethionine Decarboxylase. *The Journal Of Biological Chemistry*. 275:8097-8102.
- Myers, D.P., I.K. Jackson, V.G. Ipe, G.E. Murphy, and M.A. Phillips. 2001. Long-Range Interactions in the Dimer Interface of Ornithine Decarboxylase Are Important for Enzyme function. *Biochemistry*. 40:13230-13236.
- Narum, D.L., S. Kumar, W.O. Rogers, S.R. Fuhrmann, H. Liang, M. Oakley, A. Taye, B.K.L. Sim, and S.L. Hoffman. 2001. Codon Optimization of Gene Fragments Encoding *Plasmodium falciparum* Merzoite Proteins Enhances DNA Vaccine Protein Expression and Immunogenicity in Mice. *Infection and Immunity*. 69:7250-7253.
- Neduva, V., R. Linding, I. Su-Angrand, A. Stark, F. de Masi, T.J. Gibson, J. Lewis, L. Serrano, and R.B. Russell. 2005. Systematic Discovery of New Recognition Peptides mediating Protein Interaction Networks. *PLOS Biology*. 3:1-10.
- Neuhoff, V., N. Arold, D. Taube, and W. Ehrhardt. 1988. Improved staining of proteins in polyacrylamide gels including isoelectric focusing gels with clear background at nanogram sensitivity using Coomassie Brilliant Blue G-250 and R-250. *Electrophoresis*. 9:255-262.
- Nirmalan, N. 2005. 2D Gel electrophoresis protocol optimised for *Plasmodium* samples, Pretoria.
- Nirmalan, N., P.F. Sims, and J.E. Hyde. 2004. Quantitative proteomics of the human malaria parasite *Plasmodium falciparum* and its application to studies of development and inhibition. *Molecular Microbiology*. 52:1187-1199.
- Oh, S.S., S. Voight, D. Fisher, S.J. Yi, P.J. LeRoy, L.H. Derick, S. Liu, and A.H. Chishti. 2000. *Plasmodium falciparum* erythrocyte membrane protein 1 is anchored to the actin-spectrin junction and knob-associated histidine-rich protein in the erythrocyte skeleton. *Molecular & Biochemical Parasitology*. 108:237-247.

- Ohkanda, J., F.S. Buckner, J.W. Lockman, K. Yokoyama, D. Carrico, R. Eastman, K. de Luca-Fradley, W. Davies, S.L. Croft, W.C. Van Voorhis, M.H. Gelb, S.M. Sebti, and A.D. Hamilton. 2004. Design and Synthesis of Peptidomimetic Protein Farnesyltransferase Inhibitors as Anti-*Trypanosoma brucei* Agents. *Journal of Medicinal Chemistry*. 47:432-445.
- Olliaro, P.L., and Y. Yuthavong. 1999. An Overview of Chemotherapeutic Targets for Antimalarial Drug Discovery. *Pharmacol. Ther.* 81:91-110.
- Osterman, A., N.V. Grishin, L.N. Kinch, and M.A. Phillips. 1994. Formation of Functional Cross-Species Heterodimers of Ornithine Decarboxylase. *Biochemistry*. 33:13662-13667.
- Pandey, K.C., S.X. Wang, P.S. Sijwali, A.L. Lau, J.H. McKerrow, and P.J. Rosenthal. 2005. The *Plasmodium falciparum* cysteine protease falcipain-2 captures its substrate, hemoglobin, via a unique motif. *PNAS*. 102:9138-9143.
- Paschke, M. 2006. Phage display systems and their applications. *Appl Microbiol Biotechnol*. 70:2-11.
- Pawson, T., and P. Nash. 2000. Protein-protein interactions define specificity in signal transduction. *Genes and development*. 14:1027-1047.
- Pécoul, B., P. Chirac, P. Trouiller, and J. Pinel. 1999. Access to Essential Drugs in Poor Countries. *JAMA*. 281:361-367.
- Peltier, J.M., S. Askovic, R.R. Becklin, C.L. Chepanoske, Y.J. Ho, V. Kery, S. Lai, T. Mujtaba, M. Pyne, P.B. Robbins, M. von Rechenberg, B. Richardson, J. Savage, P. Sheffield, S. Thompson, L. Weir, K. Widjaja, N. Xu, Y. Zhen, and J.J. Boniface. 2004. An integrated strategy for the discovery of drug-targets by the analysis of protein-protein interactions. *International Journal of Mass Spectrometry*. 238:119-130.
- Pérez-Montfort, R., M. Tuena de Gómez-Puyou, and A. Gómez-Puyou. 2002. The interfaces of Oligomeric Proteins as Targets for Drug Design against Enzymes from Parasites. *Current Topics in Medicinal Chemistry*. 2:457-470.
- Phizicky, E.M., and S. Fields. 1995. Protein-Protein Interactions: Methods for Detection and Analysis. *Microbiological Reviews*. 59:94-123.
- Piggott, A.M., and P. Karuso. 2004. Quality, not Quantity: The Role of Natural Products and Chemical Proteomics in Modern Drug Discovery. *Combinatorial Chemistry & High Throughput Screening*. 7:607-630.
- Pollina, E. 1996. Design and Synthesis of RGD Mimetics as Potent Inhibitors of Platelet Aggregation. *J. Undergrad. Sci.* 3:119-126.
- Preibisch, G., H. Ishihara, D. Tripiet, and M. Leineweber. 1988. Unexpected translation initiation within the coding region of eukaryotic genes expressed in *Escherichia coli*. *Gene*. 72:179-186.
- Rajotte, D., and Ruoslahti. 1999. Membrane Dipeptidase Is the Receptor for a Lung-targeting Peptide Identified by *in Vivo* Phage Display. *The Journal of Biological Chemistry*. 274:11593-11598.
- Remy, I., and S.W. Michnick. 2004. A cDNA library functional screening strategy based on fluorescent protein complementation assays to identify novel components of signaling pathways. *Methods*. 32:381-388.
- Rial, D.V., and E.A. Ceccarelli. 2002. Removal of DnaK contamination during fusion protein purifications. *Protein Expression and Purification*. 25:503-507.
- Richie, T.L., and A. Saul. 2002. Progress and challenges for malaria vaccines. *Nature*. 415:694-701.
- Ridley, R.G. 2002. Medical need, scientific opportunity and the drive for antimalarial drugs. *Nature*. 415:686-693.
- Ripka, A.S., and A.H. Rich. 1998. Peptidomimetic design. *Current Opinion in Chemical Biology*. 2:441-452.
- Roberts, M.W., and J.C. Rabinowitz. 1989. The Effect of *Escherichia coli* Ribosomal Protein S1 on the Translational Specificity of Bacterial Ribosomes. *The Journal of Biological Chemistry*. 264:2228-2235.

- Rodi, D.J., L. Makowski, and B.K. Kay. 2001. One from column A and two from column B: the benefits of phage display in molecular-recognition studies. *Current Opinion in Chemical Biology*. 6:92-96.
- Rosenberg, A., K. Griffen, F.W. Studier, M. McCormick, J.M. Berg, R. Novy, and R. Mierendorf. 1996. T7Select Phage Display System: A powerful new protein display system based on bacteriophage T7. *inNovations*. 6:1-6.
- Rost, B., G. Yachdav, and J. Liu. 2004. The PredictProtein Server. *Nucleic Acids Research*. 32:W3212-W326.
- Roux, S. 2006. Modulation of functional properties of bifunctional S-adenosylmethionine decarboxylase/Ornithine decarboxylase of *Plasmodium falciparum* by structural motifs in parasite-specific inserts. In Department of Biochemistry. University of Pretoria, Pretoria. 89.
- Sachs, J., and P. Malaney. 2002. The economic and social burden of malaria. *Nature*. 415:680-685.
- Sambrook, J., E.F. Fritsch, and T. Maniatis. 1989. Molecular cloning: A laboratory manual. Cold Spring Harbour Laboratory Press, Cold Spring Harbour.
- Santonico, E., L. Castagnoli, and G. Cesareni. 2005. Methods to reveal domain networks. *Drug Discovery Today*. 10:1111-1117.
- Schipper, R.G., L.C. Penning, and A.A.J. Verhofstad. 2000. Involvement of polyamines in apoptosis. Facts and controversies: effectors or protectors? *Cancer Biology*. 0:55-68.
- Schramm, H.J., J. Boetzel, J. Büttner, E. Fritsche, W. Göhring, E. Jaeger, S. König, O. Thumfart, T. Wenger, N.E. Nagel, and W. Schramm. 1996. The inhibition of human immunodeficiency virus proteases by 'interface peptides'. *Antiviral research*. 30:155-170.
- Seet, B.T., I. Dikic, M. Zhou, and T. Pawson. 2006. Reading protein modifications with interaction domains. *Nature reviews*. 7:473-483.
- Seiler, N., J.G. Delcros, and J.P. Moulinoux. 1996. Polyamine Transport in Mammalian Cells. An Update. *Int. J. Biochem. Cell Biol*. 28:843-861.
- Sherman, I.W. 1998. Malaria. ASM Press, Washington, D.C.
- Singh, G.S., B.R. Chandra, A. Bhattacharya, R.R. Akhouri, S.K. Singh, and A. Sharma. 2004. Hyper-expansion of asparagines correlates with an abundance of proteins with prion-like domains in *Plasmodium falciparum*. *Molecular & Biochemical Parasitology*. 137:307-319.
- Singh, S.K., K. Maithal, H. Balaram, and P. Balaram. 2001. Synthetic peptides as inactivators of multimeric enzymes: inhibition of *Plasmodium falciparum* triosephosphate isomerase by interface peptides. *FEBS Letters*. 501:19-23.
- Smith, G.P. 1985. Filamentous fusion phage: novel expression vectors that display cloned antigens on the virion surface. *Science*. 228:1315-1317.
- Smith, P.K., R.I. Krohn, G.T. Hermanson, A.K. Mallia, F.H. Gartner, M.D. Provenzano, E.K. Fujimoto, N.M. Goeke, B.J. Olson, and D.C. Klenk. 1985. Measurement of protein using bicinchoninic acid. *Anal Biochem*. 150:76-85.
- Snow, R.W., C.A. Guerra, A.M. Noor, H.Y. Myint, and S.I. Hay. 2005. The global distribution of clinical episodes of *Plasmodium falciparum* malaria. *Nature*. 434:214-217.
- Sobelewski, P., I. Gramaglia, J. Frangos, M. Intaglietta, and H.C. van der Heyde. 2005. Nitric oxide bioavailability in malaria. *Trends in Parasitology*. 21:415-422.
- Sørensen, H.P., and K.K. Mortensen. 2005. Soluble expression of recombinant proteins in the cytoplasm of *Escherichia coli*. *Microbial Cell Factories*. 4.
- Sowa, K.M.P., D.R. Cavanagh, A.M. Creasey, J. Raats, J. McBride, R. Sauerwein, W.F. Roeffen, and D.E. Arnot. 2001. Isolation of a monoclonal antibody from a malaria patient-derived phage display library recognising the Block 2 region of *Plasmodium falciparum* merozoite surface protein-1. *Molecular & Biochemical Parasitology*. 112:43-147.
- Su, X., J. Mu, and D.A. Joy. 2003. The "Malaria's Eve" hypothesis and the debate concerning the origin of the human malaria parasite *Plasmodium falciparum*. *Microbes and Infection*. 5:891-896.
- Su, X., Y. Wu, C.D. Sifri, and T.E. Wellems. 1996. Reduced extension temperatures required for PCR amplification of extremely A+T-rich DNA. *Nucleic Acids Research*. 24:1574-1575.

- Suthram, S., T. Sittler, and T. Ideker. 2005. The Plasmodium protein network diverges from those of other eukaryotes. *Nature*. 438:108-112.
- Szabo, A., T. Langer, H. Schroder, J. Flanagan, B. Bukau, and F.U. Hartl. 1994. The ATP hydrolysis dependent reaction cycle of the *Escherichia coli* Hsp70 system-DnaK, DnaJ and GrpE. *Proc. Natl.Acad.Sci.U.S.A.* 91:10345-10349.
- Szardenings, M. 2003. Phage display of Random Peptide Libraries: Applications, Limits and Potential. *Journal of Receptors and Signal Transduction*. 23:307-349.
- Thomas, T., and T.J. Thomas. 2001. Polyamines in cell growth and cell death: molecular mechanisms and therapeutic applications. *Cell Mol Life Sci*. 58:244-258.
- Turgut-Balik, D., D.K. Shoemark, K.M. Moreton, R.B. Sessions, and J.J. Holbrook. 2001. Overproduction of lactate dehydrogenase from *Plasmodium falciparum* opens a route to new antimalarials. *Biotechnology Letters*. 23:917-921.
- Turnbough Jr, C.L. 2003. Discovery of phage display peptide ligands for species-specific detection of *Bacillus* spores. *Journal of Microbiological Methods*. 53:263-271.
- Uchiyama, F., Y. Tanaka, Y. Minari, and N. Tokui. 2005. Designing Scaffolds of Peptides for Phage Display Libraries. *Journal of Bioscience and Bioengineering*. 99:448-456.
- van Dooren, G.G., L.M. Stimmler, and G.I. McFadden. 2006. Metabolic maps and functions of the *Plasmodium* mitochondrion. *FEMS Microbiol Rev*. 30:596-630.
- Vassilev, L.T., B.T. Vu, B. Craves, D. Carvajal, F. Podlaski, Z. Filipovic, N. Kong, U. Kammlott, C. Lukacs, C. Klein, N. Fotouhi, and E. Liu. 2004. *In vivo* Activation of the p53 Pathway by Small-Molecule Antagonists of MDM2. *Science*. 303:844-848.
- Vedadi, M., J. Lew, J. Artz, M. Amani, Y. Zhao, A. Dong, G.A. Wasney, M. Gao, T. Hills, S. Brokx, W. Qiu, S. Sharma, A. Diassiti, Z. Alam, M. Melone, A. Mulichak, A. Wernimont, J. Bray, P. Loppnau, O. Plotnikova, K. Newberry, E. Sundararajan, S. Houston, J. Walker, W. Tempel, A. Bochkarev, I. Kozieradzki, A. Edwards, C. Arrowsmith, D. Roos, K. Kain, and R. Hui. 2007. Genome-scale protein expression and structural biology of *Plasmodium falciparum* and related Apicomplexan organisms. *Molecular & Biochemical Parasitology*. 151:100-110.
- Vothknecht, U.C., and J. Soll. 2005. Chloroplast membrane transport: Interplay of prokaryotic and eukaryotic traits. *Gene*. 354:99-109.
- Wallace, H.M., and A.V. Fraser. 2003. Polyamine analogues as anticancer drugs. *Biochemical Society Transactions*. 31:393-396.
- Wallace, H.M., A.V. Fraser, and A. Hughes. 2003. A perspective of polyamine metabolism. *Biochem. J*. 376:1-14.
- Waller, K.L., B.M. Cooke, W. Nunomura, N. Mohandas, and R.L. Coppel. 1999. Mapping the Binding Domains involved in the Interaction between the *Plasmodium falciparum* Knob-associated Histidine-rich Protein (KHARP) and the Cytoadherence Ligand *P. falciparum* Erythrocyte Membrane Protein 1 (PfEMP1). *The Journal of Biological Chemistry*. 274:23808-23813.
- Walter, S., and J. Buchner. 2002. Molecular Chaperones-Cellular Machines for Protein Folding. *Angew. Chem. Int. Ed*. 41:1098-1113.
- Watt, P.M. 2006. Screening for peptide drugs from the natural repertoire of biodiverse protein folds. *Nature Biotechnology*. 24:177-183.
- Way, J.C. 2000. Covalent modification as a strategy to block protein-protein interactions with small-molecule drugs. *Current Opinion in Chemical Biology*. 4:40-46.
- Wells, G.A., L. Birkholtz, F. Joubert, R.D. Walter, and A.I. Louw. 2006. Novel properties of malarial *S*-adenosylomethionine decarboxylase as revealed by structural modelling. *Journal of Molecular Graphics and Modelling*. 24:307-318.
- Wiesner, J., R. Ortman, H. Jomaa, and M. Schlitzer. 2003. New Antimalarial Drugs. *Angew. Chem. Int. Ed*. 42:5274-5293.
- Willats, W.G.T. 2002. Phage display: practicalities and prospects. *Plant molecular Biology*. 50:837-854.
- Wilson, R.J.M. 2002. Progress with Parasite Plastids. *J. Mol. Biol*. 319:257-274.

- Wrenger, C., K. Lüersen, T. Krause, S. Müller, and R.D. Walter. 2001. The *Plasmodium falciparum* Bifunctional Ornithine Decarboxylase, S-Adenosyl-L-methionine Decarboxylase, Enables a Well Balanced Polyamine Synthesis without Domain-Domain interaction. *The Journal of Biological Chemistry*. 276:29651-29656.
- Wright, P.S., T.L. Byers, D.E. Cross-Doersen, P.P. McCann, and A.J. Bitonti. 1991. Irreversible inhibition of S-Adenosylmethionine Decarboxylase in *Plasmodium falciparum*-infected erythrocytes: Growth inhibition *in vitro*. *Biochemical Pharmacology*. 41:1713-1718.
- Wuchty, S., and J.J. Ipsaro. 2007. A Draft of Protein Interactions in the Malaria Parasite *P. falciparum*. *Journal of Proteome research*. 10.1021/pr0605769
- Xenarios, I., and D. Eisenberg. 2001. Protein interaction databases. *Current Opinion in Biotechnology*. 12:334-339.
- Xu, Y., J. Shi, N. Yamamoto, J.A. Moss, P.K. Vogt, and K.D. Janda. 2006. A credit-card library approach for disrupting protein-protein interactions. *Bioorganic and Medicinal Chemistry*. 14:2660-2673.
- Yeh, I., T. Hanekamp, S. Tsoka, P.D. Karp, and R.B. Altman. 2004. Computational Analysis of *Plasmodium falciparum* metabolism: Organizing Genomic Information to facilitate Drug Discovery. *Genome Research*. 14:917-924.
- Yin, H., and A.D. Hamilton. 2005. Strategies for Targeting Protein-Protein Interactions with Synthetic Agents. *Angew. Chem. Int. Ed.* 44:4130-4163.
- Young, J.A., and E.A. Winzeler. 2005. Using expression information to discover new drug and vaccine targets in the malaria parasite *Plasmodium falciparum*. *Pharmacogenomics*. 6:1-26.
- Zhang, K., and P.K. Rathod. 2002. Divergent Regulation of Dihydrofolate Reductase Between Malaria Parasite and Human Host. *Science*. 296:545-547.
- Zhou, Z., P. Schnake, L. Xiao, and A.A. Lal. 2004. Enhanced expression of a recombinant malaria candidate vaccine in *Escherichia coli* by codon optimization. *Protein Expression and Purification*. 34:87-94.

I. Appendix A

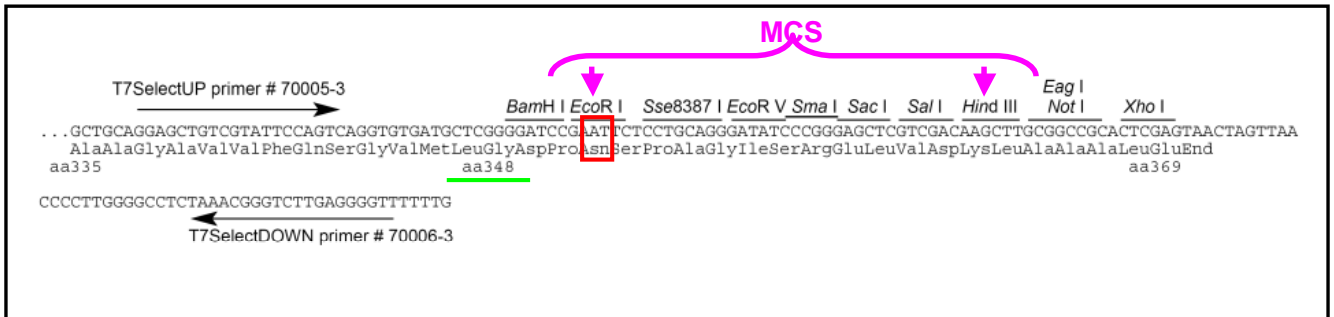


Figure I.1: T7Select 10-3b cloning region (Novagen, USA).

The multiple cloning sites with the restriction sites used for the cloning of the *P. falciparum* cDNA inserts (*EcoRI* and *HindIII*) are indicated in pink. The Asn, which should precede the in-frame cloning of the cDNA sequence, is indicated in red.

II. Appendix B: Screened phage clones

Table II.1: The various screened phage clones of the different libraries.

	RED (HindIII or EcoRI) (Eam 1140, Nde1, or Vsp1)	Large-Scale amplification	Large-scale amplification and cloned into pGem-T-easy	Sequenced
Library A				
AA10	X	X	X	X
AB5	X	X	X	X
AB8	X	X	X	X
AB12	X	X	X	X
AC5	X	X	X	X
AC8	X	X	X	X
AF2	X	X	X	X
Library B				
BA3	X	X		X
BB7	X X	X	X	X
Library C				
BP1 nr 4	X	X	X	X
CA3	X	X		X
CA9	X	X		X
CA11	X	X		X
CB8	X			
CB10	X	X		X
CB11	X			
CC1		X		X
CC2	X X	X		X
CC4	X X	X		X
CC5	X X		X	X
CC6	X X	X		X
CC8	X		X	X
CC11	X			
CD2	X X	X		X
CD4	X		X	X
CD7	X			
CD8	X			
CD10	X	X		X
CD11	X			
CE3	X X			
CE4	X X	X		X
CE5	X X	X		
CE8	X	X		X
CF1	X X	X		X
CF2	X X	X		X
CF7	X			
CG2	X		X	X
CG3	X X	X		X
CG5	X X			
CG8	X			
CH2	X X			
CH3	X X	X		X
CH6	X X	X		X
Library D				
none				
Library E				
EE8	X X	X		X
EF8	X X	X		X
EG8	X X		X	X
EG10	X X	X		
EH10	X X	X		X
EH11	X X	X		X
Library F				
FA2	X	X		
FA8	X		X	X
FA11	X X			
FB7	X	X		
FB8	X			X
FC8	X	X		X
FC12	X X	X	X	X
FD10	X X	X		X
FG10	X			